A Study of Observability-Enhanced Guidance Systems

by

George Estandy Hassoun
B.S., M.S.

A thesis submitted in fulfilment of the requirement for the degree of

Doctor of Philosophy

The University of Adelaide
Faculty of Engineering
Department of Electrical and Electronic Engineering

October 1995

ERRATUM

Page 3, line 6

Replace statement commencing with: "In a *two-radar command guidance ...*" by:

In a *two-radar command guidance,* one radar tracks the target while the other tracks the pursuer, and from this data guidance commands are calculated and communicated to the pursuer.

Page 82, line 8

Replace "the state $\hat{X}(k \mid k)$" by "the state estimate $\hat{X}(k \mid k)$, which is the estimated state at time k given the measurement at time k,".

Page 82, line 11

Replace "state" by "state estimate".

Page 111, equation (5.8)

Replace "X_f" by "R_f".

Replace "where X_f is the final state" by "where R_f is the final miss-distance given in terms of the final state vector X_f".

Page 113, equation (5.14)

Replace "X_f" by "R_f".

Page 118, equation (5.37)

Replace "X_{sf}" by "R_{sf}".

Page 137, line 6

Replace "line-of-sight" by "line-of-sight rate".

Page 148, Table 6.3

Replace the elements of the fourth column [$\hat{R}_f$ (ft)] by the corresponding elements of the fourth column of Table 6.5, page 163.

To

the silenced angel

who borrowed from her speaking days

to pay for

my unspoken words

Contents

Abstract

During the past decades, several research studies relating to modern navigation guidance systems have dealt with the design of advanced guidance algorithms. As the cost of modern guided systems is typically dominated by the seeker head, normally used for target tracking, these research efforts have focused on the possibility of using a simple seeker head - providing only bearing measurements - and compensating by the use of an advanced guidance algorithm. The present study falls within this class of research efforts, aiming at maximising the benefit of advanced computer technology, as it applies to guidance systems.

In a typical guidance system, the bearing-only-measurements are fed to a state estimator. Subsequently, the guidance law makes use of the state estimate to derive the control variable necessary to drive the pursuer towards its target. This approach is based on the separation principle which proposes to treat the controller (guidance law) and the state estimator separately and then combine them in cascade. However, when used alongside a conventional guidance law, such as proportional navigation, conventional state estimators such as the extended Kalman filter were shown to diverge towards the end of the intercept.

A different approach which has emerged recently suggests the design of the guidance law with the performance of the state estimator in mind. The resulting guidance law would not only seek accuracy and effectiveness, but it would also aim to increase the performance of the associated state estimator so that the estimation errors are minimised in the least squares sense. In this study, a novel guidance law dubbed *observable proportional navigation* belonging to the new approach is proposed. It

modifies proportional navigation in a simple but elegant way by incorporating a measure of observability in the control.

Depending on the nature of the noise and the state estimator used, several forms of this law could be considered. Two forms are explored in the current study, and applied to a two-dimensional missile-target system. In contrast to other guidance laws classified under the same approach, the solution of the new guidance law is given in closed form; a necessary limit on the coefficient of observability is derived; and the structure of the law is chosen to be simple and easy to implement. Simulation results substantiate the effective nature of the proposed law.

Declaration

This work contains no material which has been accepted for the award of any other degree or diploma in any university or other tertiary institution and, to the best of my knowledge and belief, contains no material previously published or written by another person, except where due reference has been made in the text.

I give consent to this copy of my thesis, when deposited in the University Library, being available for loan and photocopying.

SIGNED: DATE: ..... 11./10./05. .....

Acknowledgements

I would like to thank my supervisor Dr. C.C. Lim for the time and support he has given me during the course of this study. His valuable guidance and honest effort to steer the study in the right direction are all well appreciated.

I also thank Dr. M. Gibbard for taking a remarkable interest into this work, for supervising it during Dr. Lim's study leave, and for revising some of the written work.

My gratitudes go to Drs. C. Coleman, M. Pszczel and M. Evans for their support as the DSTO coordinators of this project and for their helpful suggestions and comments and their continued encouragement.

My appreciation goes to Dr. J. Speyer from the University of Texas at Austin, whose weathered insight into the topic at hand played an important role in the progress of this study. I also appreciate the assistance of Drs. K.L. Teo and L.S. Jennings from the University of Western Australia for their valuable input and interest in this study.

Finally, I would like to take this opportunity to thank the staff and students of the Department of Electrical and Electronic Engineering at the University of Adelaide for providing a pleasant and friendly atmosphere; I also salute the efforts of those of them working towards a more interactive postgraduate curriculum.

This research was supported by the University of Adelaide Scholarship, as well as by the DSTO Supplementary Scholarship. Both scholarships are greatfully acknowledged.

Publications

[1] G.E. Hassoun and C.C. Lim, "Maximum Information and Measurement Modifiability in Homing Missile Guidance", in 20^{th} *TTCP WTP-5 Symposium*, (DSTO, Salisbury), April 1992.

[2] G.E. Hassoun and C.C. Lim, "A Study of the Extended Kalman Filter's Performance in Bearing Only Measurement Problems", in *TTCP WTP5-KTA Meeting*, (DSTO, Salisbury), June 1993.

[3] G.E. Hassoun and C.C. Lim, "Advanced Guidance Control System Design for Homing Missiles with Bearings-Only-Measurements", *in IEEE International Conference on Industrial Technology*, (Guangzhou, China), December 1994.

[4] G.E. Hassoun and C.C. Lim, "Observability Enhanced Proportional Navigation for Homing Missiles with Bearings-Only-Measurements", to be submitted.

[5] G.E. Hassoun and C.C. Lim, "Maximum Information Guidance in Bearing-Only Measurement Systems", Technical Report, CTRL 94-1, The University of Adelaide, Department of Electrical and Electronic Engineering, March 1994.

[6] G.E. Hassoun and C.C. Lim, "Observable Proportional Navigation for Homing Missiles with Bearing-Only-Measurements", Technical Report, CTRL 94-3, The University of Adelaide, Department of Electrical and Electronic Engineering, August 1994.

Nomenclature

A	= System state matrix
A_c	= Closed loop state matrix
A_{M_X}, A_{M_Y}	= Pursuer acceleration components, $ft\ s^{-2}$
A_{T_X}, A_{T_Y}	= Target acceleration components, $ft\ s^{-2}$
A_n	= Pursuer normal acceleration, $ft\ s^{-2}$
A_s	= Sub-system state matrix
a	= Glint noise coefficient, $rad^2\ ft^2\ s$
B	= System control matrix
B_s	= Sub-system control matrix
b	= Thermal noise coefficient, $rad^2\ s$
C	= Measurement matrix
c	= Design parameter
D	= Residual matrix
$E(\cdot)$	= Expectation operator
e	= Heading error, rad
e_{a_T}	= Target acceleration estimation error, $ft\ s^{-2}$
e_p	= Position estimation error, ft
e_v	= Speed estimation error, $ft\ s^{-1}$
F_c	= Applied (or commanded) force
f	= Function operator
G	= Control gain
g	= Gravity constant, $ft\ s^{-2}$
H	= Measurement gradient matrix (in EKF)

H_p = Position part of measurement gradient matrix (in EKF)

h = Measurement matrix

I = Information matrix

I_n, 0_n = n-dimensional Identity and null matrices, respectively

J = Performance index (or objective function)

K = Estimator gain

M = Measurement gradient matrix (in MGEKF)

M_R = Solution to the Riccati equation

m = Mass of pursuer, Kg

N = Navigation constant (PNG)

N_1 = Navigation constant (AOPNG)

N_2 = Observability coefficient (AOPNG)

P = Error covariance matrix

P_s = State covariance matrix

Q = State weighting matrix

R = Pursuer-target range, ft

R_c = Control weighting matrix

R_f = Miss-distance, ft

R_X = State correlation matrix

S = System performance matrix

s = Normalised time

T, t = Time, s

t_0 = Initial time, s

t_f = Time-to-go, s

U, U_s, u = Control vectors

U_r, V_r = Relative speed components, $ft\ s^{-1}$

V, W, W_e = Noise spectral densities

V_c = Terminal speed, $ft\ s^{-1}$

V_M = Pursuer speed, $ft\ s^{-1}$

V_{r_X}, V_{r_Y} = Relative speed components, $ft\ s^{-1}$

V_T = Target speed, $ft\ s^{-1}$

v, w, ζ = White noise processes

v_r = Normalised speed

W_m = Weighting matrix

X = System state vector

X_f = Final system state vector

X_M, Y_M = Pursuer position components, ft

X_r, Y_r = Relative position components, ft

X_s = Sub-system state vector

X_T, Y_T = Target position components, ft

x = State perturbation/error vector

Z = Measurement vector

Z_f = Final state weighting matrix

z = Measurement perturbation vector

α = Non-dimensional normal acceleration

$\delta(\cdot)$ = Dirac delta function

Φ = State transition matrix

Φ_c = Closed loop transition matrix

ϕ = Target heading angle, rad

κ = Noise constant, ft^{-2}

λ = Target acceleration time constant

μ = Measure of observability

ν = Observability coefficient (in MOPNG)

Ω = Line-of-sight rotation angle, rad

ω = Observability coefficient

σ = Line-of-sight angle, rad

τ = Normalised time

θ = Pursuer heading angle, rad

ξ, η = Relative non-dimensional coordinates

$\hat{(\cdot)}$ = Estimation operator

List of Abbreviations

AOPNG	Additive Observable Proportional Navigation Guidance
BOMP	Bearing-Only-Measurement Problem
DCGL	Dual Control Guidance Law
EKF	Extended Kalman Filter
FIM	Fisher Information Matrix
LOS	Line-of-Sight
LQGL	Linear Quadratic Guidance Law
MGEKF	Modified Gain Extended Kalman Filter
MMT	Manned Maneuvering Target
MOPNG	Multiplicative Observable Proportional Navigation Guidance
OPNG	Observable Proportional Navigation Guidance
PNG	Proportional Navigation Guidance

List of Figures

List of Tables

Chapter 1

Introduction

Modern guided vehicles are typically equipped with guidance processors, considered to be their "brain", and destined to carry out two important functions [51]:

- Implementation of the necessary guidance algorithm, which together with the guidance law, aims to guide the vehicle towards its target.
- Assessment and evaluation of the performance of the guidance mission through the different phases of engagement.

The diagram presented by Lin [51] and partly reproduced in Figure 1.1 outlines the main components of the guidance algorithm. This algorithm can implement a *preset guidance* in which the trajectory to be followed by the pursuer is prestored, based on information obtained about the target before launch. For this type of guidance, it is not necessary to sense the motion of the target; the actual pursuer flight path is instead corrected if it is found to be different from the prestored profile [97].

In the same diagram (Figure 1.1), we see that an alternative to preset guidance that can be useful to intercept moving targets is *direct guidance*. In this type of guidance, the pursuer is provided with target information during the guidance phase, as well as in the pre-launch phase. At the heart of the direct guidance algorithm is the guidance law which makes use of the target information to issue the guidance

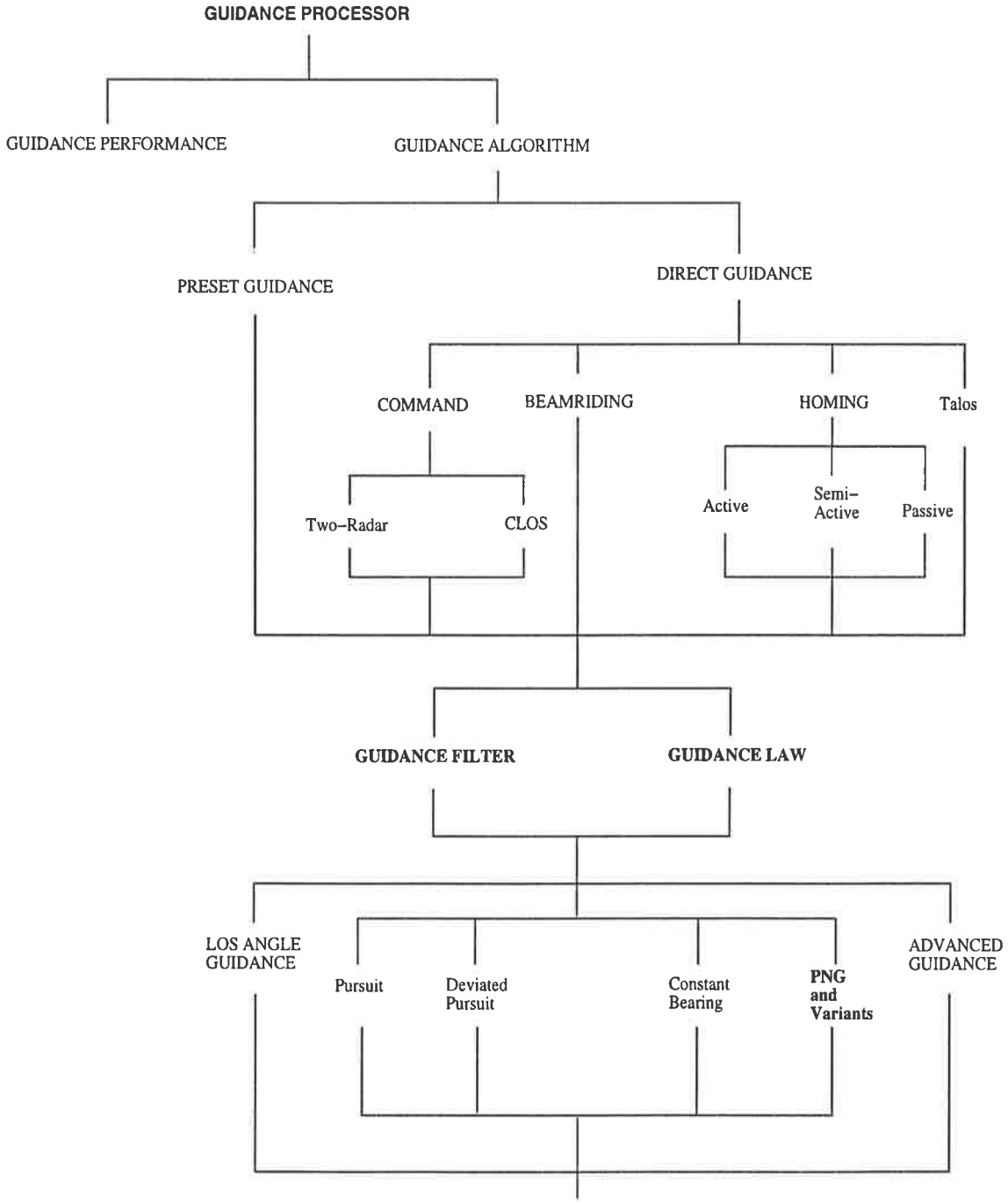

Figure 1.1: Functions of the guidance processor - Diagram based on Lin's book *Modern Navigation Guidance and Control Processing*

commands for the pursuer. Direct guidance includes command, beamriding and homing guidance.

In command guidance, the guidance task is achieved by generating electrical commands, outside the guided vehicle, based on the relative position between this vehicle and the target, and then transmitting those commands to an on-board sensor. It is possible to distinguish between two types of command guidance. In a *two-radar command guidance* one radar is used to track the target and another to track the guidance commands and send them to the pursuer. In a *command-to-line-of-sight guidance*, however, sometimes called *the three-point guidance* the pursuer approaches the target along the line joining the control point and the target.

In beamriding guidance, the aim is to guide the pursuer along a radar beam directed towards the target by a ground station, while in homing guidance, it is attempted to guide the pursuer towards the target based on signals reaching it from the target. If the homing guidance system transmits energy towards the target and recuperates the reflected signal, the homing is said to be active. It is called passive homing if the pursuer tracks a radiation characteristic emitted by the target itself. If however, the target is illuminated by a source located on a third platform (ground for example), the homing guidance is called semi-passive (or semi-active).

Other guidance algorithms are also possible, but for the purpose of this study, only passive homing is considered and more focus is given to the guidance law and the guidance filter, which work hand in hand to generate the control action and to filter out the unwanted noise. The global aim is to investigate advanced guidance algorithms on modern pursuers equipped with relatively simple passive seeker heads. It is envisaged to take advantage of the relatively low cost of modern processing capabilities to compensate for the *bearing-only-measurements* provided to the system designer, by this type of seeker heads.

The present study will emphasise two important areas: *the guidance law* typically designed to drive the pursuer to its destination in some optimal fashion, and the guidance filter or *the state estimator* designed to compensate for the poor measurements provided by the low-cost seeker. Both guidance law and state estimator are

the main building blocks of what is termed *the guidance system.*

1.1 Advanced Guidance Systems

The control of a pursuer tracking a moving target is, essentially, a guidance problem [105]. Given the initial conditions of the problem, the pursuer and the target dynamics, it is possible to find an optimum control effort and a corresponding optimal trajectory [41]. This assumes that the pursuer is equipped with "perfect" measurement devices to monitor the behaviour of the target. In actual advanced guidance systems, the measurements are noisy, which introduces another difficulty, namely the estimation of the true information, having access only to the noisy data. In this case, and assuming that the problem is linear, one could use the separation principle to treat each problem (*guidance* and *estimation*) separately. But, as we shall see later on, since the problem is not always linear, the separation principle ceases to be effective in many cases, and new ways to improve the guidance system performance prove to be necessary.

Concerning the guidance problem, several classes of guidance laws are noted. The degradation of most of them (e.g., proportional navigation) under conditions introducing large nonlinearities is identified as a current difficulty [105]. Another difficulty is shown to be related to the estimation problem. One of the most popular estimation algorithms, the extended Kalman filter, although highly effective in many applications was shown to diverge along proportional navigation, when provided with bearing-only-measurements [80].

In this study, several attempted solutions to the guidance and estimation problems are explored. Some are related to the guidance structure, others are linked to the filter structure, and a few are related to the overall control strategy. The following terminology will be used throughout this study:

- The **Guidance** law is the control scheme used to determine an appropriate trajectory to be followed in order to intercept the target.

- The **Estimation** algorithm is the process with which the state of the system is estimated in the case of noise corrupted dynamics and/or measurements.
- The **Control** strategy is the overall control technique used to manipulate both guidance and estimation in order to achieve the desired goal, e.g., the interception of the moving target in an optimal fashion.

In the following sections, some of the recent work relating to guidance systems will be reviewed and classified. On one hand, several guidance laws and techniques will be briefly described, on the other hand a historical overview of the development of several estimation techniques will be outlined, along with the main ideas motivating the development. In this, the relationship between guidance and estimation will be given particular attention, since it is believed that these two building blocks are mutually interactive and the design of one affects the other.

1.2 Guidance Problem

Guiding a moving object in space to intercept a specified target constitutes a relatively old problem probably dating back to the time of ancient seafarers [62]. Published treatments relevant to this topic did not however appear until the first half of this century with the attempts to study the kinematics of guided missiles [60, 88]. Some of the traditional guidance laws are still used today for the command of missiles pursuing targets having low levels of maneuverability. However, when it comes to targets having advanced characteristics, e.g., high maneuverability and smart sensing, the need is evident for more elaborate guidance laws. According to [62], those laws could be classified into several categories, some of which could be considered as *classical laws* while the others belong to the family of *modern laws*. Here is a brief look at some of them.

1.2.1 Line-of-Sight Angle Guidance

The missile flying under this law, considered to be a three-point guidance law, makes use of a "ground support" to track the target. The basic principle is to provide a missile normal velocity $V_{M\perp}$ proportional to the line-of-sight angular rate:

$$V_{M\perp} = R_{SM}\dot{\sigma}_{ST} \tag{1.1}$$

where
$V_{M\perp}$ is the magnitude of the missile normal velocity,
$\dot{\sigma}_{ST}$ is the magnitude of the line-of-sight angular rate (station to target), and
R_{SM} is the range from the ground station to the missile.

The line-of-sight angle guidance law is designated for two families of algorithms depending on the nature of its mechanisation: the command to line-of-sight guidance employs an "up-link to transmit guidance signals" from the ground station to the missile [62], while the beamrider attempts to guide the missile along an electro-optical beam generated by the ground station and directed at the target. Both families have high performance capabilities in terms of miss-distance but their associated low level of maneuverability and the cost of the ground support limit their usage.

1.2.2 Line-of-Sight Rate Guidance

This guidance law is similar in nature to the line-of-sight angle guidance, but is a two-point guidance between the missile and the target. It is more suitable for homing guidance algorithms rather than command to line-of-sight and beamrider algorithms which are best served through the line-of-sight angle guidance. The line-of-sight rate guidance could be subdivided into several guidance laws including pursuit, deviated pursuit, proportional navigation and constant bearing guidance. In the next paragraphs, two of these laws are briefly outlined.

Pursuit Guidance

Although simple in concept, this law does not require the support of a ground station. It attempts to keep the missile pointed at the target. There are two families of pursuit guidance laws: in the *attitude pursuit*, the missile tries to keep its centerline pointed at the target while in the *velocity pursuit*, the missile tries to align its velocity vector with the target. In this latter case the line-of-sight rate of rotation could be written as:

$$\dot{\sigma} = \frac{V_T - V_M}{R} \tag{1.2}$$

where
$\dot{\sigma}$ is the line-of-sight rate,
V_M and V_T are the missile and the target speeds, respectively, and
R is the range between target and missile.

The overall cost of this guidance law is less than that of the line-of-sight angle guidance. Its accuracy suffers however, more in the attitude pursuit than in the velocity pursuit. The maneuverability is still low although the reaction speed is higher than that associated with the line-of-sight angle guidance.

Proportional Navigation Guidance

Initially designed for intercept problems where missile and target have constant speeds, this law has its origins among the ancient sailors who noticed that a collision is most probable between two constant speed vessels which "maintain a constant relative bearing while closing in range" [62]. Due to its accuracy and relative ease of implementation, proportional navigation guidance (PNG) was widely used and investigated in an attempt to generalise its algorithm to the case of changing velocities. The same conclusion noticed in ancient times was confirmed in contemporary literature, e.g., "for constant velocity targets, intercept would almost always occur" [27, 62]. PNG's main characteristic is its attempt to null the line-of-sight rate by

adopting a missile heading angle rate proportional to the angular line-of-sight rate of change:

$$\dot{\theta} = N\dot{\sigma} \tag{1.3}$$

where
$\dot{\theta}$ is the rate of the missile flight path angle,
$\dot{\sigma}$ is the rate of the line-of-sight angle, and
N is the navigation ratio gain.

Given that the missile acceleration superiority over the target is at least fivefold to assure intercept [59], the performance of this law in terms of miss-distance is largely greater than that of the pursuit guidance laws and close enough to the accuracy of the line-of-sight angle guidance laws. Although most literature deal with a two-dimensional PNG, it was shown that a three-dimensional development is also possible [1]. However the most critical limitation of the PNG remains the constant velocities requirement and the apparent non-adaptability to the case of maneuvering targets.

1.2.3 Linear Quadratic Guidance

Known also under the name of *optimal linear guidance*, the linear quadratic guidance law (LQGL) was influenced by the success of optimal control theory. Since the 1960's many engineers tried to adopt optimisation techniques to tackle the missile intercept problem. Two of the most influential methods were linear quadratic regulation and its dual analog: Kalman filtering.

The general optimisation problem consists of the minimisation of a cost functional which, in the case of the missile problem, includes a term on the final time and a term on the control effort. More precisely, the optimisation is formulated as:

$$\min_{U(\cdot)} E\{J\} = E\left\{X'(t_f)QX(t_f) + \int_{t_0}^{t_f} U'(t)R_cU(t)dt\right\} \tag{1.4}$$

subject to the stochastic system equation:

$$\dot{X}(t) = AX(t) + BU(t) + Gw(t) \tag{1.5}$$

where

t_0 is the initial time,
t_f is the final time,
$E(\cdot)$ is the expectation operator,
Q and R_c are weighting matrices,
X is the state (X' its transpose),
U is the control vector, and
w is a white Gaussian noise process.

This guidance law necessitates an on-board microcomputer but achieves high performance levels in terms of miss-distance (better performance than the PNG), flexibility (ease of implementation of a constraint) and adaptability to target maneuvering. In fact PNG can be shown to be a special case of the linear quadratic guidance law [16, 38].

The performance of the LQGL however, is highly dependent on the estimation of the "time-to-go". This was identified as one of the main limitations of the algorithm. Typically, the range and the range rate between the target and the missile (pursuer) are needed in order to estimate the time-to-go, but those measurements are usually corrupted with noise. Other problems include sensitivity to initial conditions and selection of the weighting matrices.

1.2.4 Other Guidance Schemes

In addition to the guidance laws mentioned so far, there is a set of other guidance laws varying widely in terms of concept and implementation. Some of these laws deal with simple ad-hoc controllers, while some others are concerned with special applications of the optimisation theory, differential games in particular [23].

Explicit guidance laws for the pitch steering of an ascent rocket were formulated in [89], where the time-to-go needs to be estimated as in the case of the linear quadratic guidance law. In [65], near-optimum guidance laws were proposed based on a method of successive approximations similar to quasilinearisation [62]. Dynamic programming was used in [18] to solve for a minimum control effort trajectory, and a complete solution to the dynamic programming problem was given.

The near-optimum solution of a differential game was dealt with in [5] through a successive linearisation of a two-point boundary value problem. This scheme was later applied to an air-to-air missile guidance problem in [66] and showed improved performance over proportional navigation.

Many other guidance schemes fall within this family [62], and some are of particular relevance to our present study. The work of Casler [17] for example examined ways of introducing line-of-sight angle perturbations with the view of minimising the variance of key guidance parameters.

1.3 Estimation Problem

Now that some of the main guidance schemes are explored, we turn to the estimation problem and overview some of the most popular estimation techniques.

Since the formulation of the *least squares method* by Gauss, which was prompted by astronomical studies carried out towards the end of the 18th century [77], several scientists have attempted to work on the estimation problem as it relates to the motion of comets. In 1806, the French scientist Legendre invented the tech-

nique independently and published it in his work "Nouvelles méthodes pour la détermination des orbites des comètes".

But it was not until this century that the estimation theory received another boost with the "explosion" of the so called *Kalman filtering* in the early 1960's. This latest algorithm could be regarded as a recursive solution to the least squares problem posed some 170 years before. According to [77], one of the few differences between the least squares algorithm and the Kalman algorithm is the fact that the latter allows for the state to change with time. The real merit of the Kalman algorithm, however, is its adaptability to digital computer implementation and its generalisable approach.

In many applications, especially those related to the estimation of orbit trajectory, the system dynamics and the measurements are nonlinear in nature. Kalman theory could be extended to accommodate these applications by linearising the relevant equations and accounting for the linearisation procedure in the filter recursive equations. This fact gives birth to the so called *extended Kalman filter* [44].

1.3.1 Extended Kalman Filter

This filter - to be studied in Chapter 4 - proves to be effective for a good number of applications. When applied to tracking manned maneuvering targets (MMT) for example, the extended Kalman filter (EKF) resulted in a performance superior to that of simpler filters such as least squares filters (although this is not true if the MMT is not maneuvering!) [75]. Nevertheless, several problems related to the EKF were reported, perhaps the most common of them is the *filter divergence* along a path provided by the proportional navigation guidance law. This problem was shown not to be due to the filter structure, it was rather linked to the errors introduced by the linear approximation and initialisation associated with the algorithm. In the case of bearing-only-measurements, it was suggested that the interaction of bearing and range inflicts "premature covariance collapse" which causes filter instability [2]. Several alternative techniques were suggested to improve the stability

of the filter. A few of them are outlined in the following sections.

1.3.2 Pseudolinear Tracking Filter

In order to avoid the divergence associated with the linearisation and initialisation techniques adopted in the EKF formulation, several ad-hoc modifications were proposed [91]. The filter termed *pseudolinear tracking filter* introduces a modification on the covariance initialisation, then decouples the covariance computations from the estimated state vector, by replacing the measured bearings with the so called *pseudolinear measurement residuals* [2]. In this manner, the pseudolinear tracking filter prevents the feedback and amplification of solution errors and therefore achieves "convergence to the complete solution" [53]. However, although stable and simple to implement, the pseudolinear tracking filter proved to generate biased range estimates when noisy measurements are involved. A closed form of the bias error was derived and shown to be geometry dependent [4]. On the other hand, for applications where bearing rates are high or measurement noise is low the estimates provided by the pseudolinear tracking filter proved to be quite adequate.

1.3.3 Coordinate Transformation Based Filters

Since the convergence and optimality of the standard Kalman filter is proved for linear systems, it follows that the problematic convergence of the EKF is certainly linked to the nonlinearities of the systems dynamics and/or those of the measurements. Consequently, it was attempted to alter those nonlinearities so as to reduce their effects on the performance of the overall system. One of the early ideas along this line suggested the use of a coordinate system in which the system and measurements equations are linear. The use of the EKF in a cartesian coordinate system was compared to its use in a "range-direction-cosine" coordinate system [54]. Less error and less bias were obtained with the new coordinate system. Similar success was reported later on when a coordinate transformation of the state and measurements to a modified polar reference frame led to the formulation of a "stable and

asymptotically unbiased " EKF, namely the *modified polar coordinate filter* [3].

The coordinate system transformation proved to be useful even in the case of the so called *nonlinear filters*, which will be seen in section 1.3.5. A polar coordinate transformation was introduced in [9] "at measurement times". The performance of the resulting *polar coordinate filter* proved to be superior to that of the cartesian-system-based EKF.

Although the new trend in changing reference frames eliminated the divergence problem, the resulting filters were far from optimal, unlike their linear counterparts. In fact, the coordinate transformation was shown to increase filter stability "at the expense of optimality" [98]. As a consequence, a "stability measure" was introduced to guide the designer in the usually ad-hoc selection process of the new frame [98].

1.3.4 Modified Gain Extended Kalman Filter

In the design of the extended Kalman filters, three problems were apparent: *stability, bias*, and *optimality*. The attempts to solve those problems were based on ad-hoc techniques of linearisation and coordinate system selection. The modified gain extended Kalman filter (MGEKF), proposed in 1983, attempted to solve the first two of those problems in a more formal way.

Global stability had been shown for the pseudolinear tracking observer when applied to a special class of nonlinear measurements [81]. In addition, it was suggested in [90] to use a constant gain with the extended Kalman observer, in order to obtain a *stochasticly stable* observer. This was called the constant gain extended Kalman observer [72]. However, both of those two design ideas had their drawbacks when used in a noisy environment: the first showed range bias as mentioned earlier, and the second proved to be too slow to use in real time applications.

The concept upon which the MGEKF is built, is based on the attempt to eliminate the drawbacks of the pseudolinear tracking observer and the constant gain extended Kalman observer, while maintaining their benefits. MGEKF proposes to use a modified gain with the extended Kalman observer when it is applied to a special class

of nonlinear functions called "modifiable functions". The resulting modified gain extended Kalman observer was extended to the case of noisy systems and the gain algorithm was altered so that the derived gains depend only on past measurements. A subsequent analysis of the resulting filter showed global stability and its performance when applied to the bearing-only-measurement problem (BOMP) proved to be superior to the performance of both extended Kalman filter and pseudolinear tracking filter. The superiority of MGEKF over EKF will be verified during the course of the present study.

1.3.5 Nonlinear Filters

Most of the filters discussed so far could be grouped under the umbrella of the *modified extended Kalman filters.* Motivated by the fact that the Kalman filter was shown to be optimum in the case of linear dynamics and linear measurements, many authors tried to extend the Kalman filter methodology to the nonlinear case after simply linearising the appropriate equations. The different variations of this family of filters is only due to the different methods dealing with the linearisation and optimisation schemes.

Another way of dealing with this question is to approach it as a pure nonlinear filtering problem. *Nonlinear filtering theory* is a field of its own. Developed by Stratonovich, Kushner and Wonham and grouped by Ho, Lee and Jazwinski, this field relies heavily on probabilistic and stochastic notions such as the *maximum likelihood estimation* method, the *conditional probability density function*, etc [44]. Filters based on this theory could be classified as *nonlinear filters* (as opposed to the modified extended Kalman filters). They range from the *iterative filters* to the *second order filters* [54], including the *finite-dimensional filters* of Sorenson and Stuberrud and the *moment sequences filter* of Kushner [8]. The polar coordinate filter encountered in section 1.3.3 is a nonlinear filter in which the *conditional modes* of the conditional probability density function are preserved in the transformation.

Although "it is not known how the statistics of the conditional probability density

function relate to the extended Kalman filter" [8], it was shown that, at least for a scalar problem, none of the second-order filters has better performance than the EKF [73]. In this context, the so called *assumed density filter* tried to estimate the *conditional mode* of the conditional probability density function as opposed to its *conditional mean* adopted in a large number of nonlinear filters. When applied to the homing missile intercept problem using a six-degree-of-freedom simulation program, the assumed density filter showed a slight negative bias but it outperformed the EKF during most of the flight.

The nonlinear filters are the last of the estimation techniques briefly outlined in this introduction. Now we turn our attention to the control strategy which sets up the mode of interaction between guidance and estimation.

1.4 Control Strategy

In order to achieve the overall aim of the guidance problem, it is clear that two challenging objectives need to be met at the same time: enhancing Kalman filter stability and performance, on one hand, and achieving target intercept, on the other. In most of the existing literature dealing with the missile guidance problem using bearing-only-measurements, the control strategy adopted takes advantage of the *separation principle* "in the sense of Witsenhausen" [85]. This principle validates the independence between guidance and estimation. Consequently, over a certain period of time, it was almost customary to work on the improvement of the filter, implement the resulting estimation algorithm in cascade with a guidance law then analyse the performance of the overall control system. Although correct, this strategy is now proving to be inadequate and a new approach to the control problem is slowly emerging. In the following, it is attempted to briefly outline the historic origins of the separation principle, point out one of the important problems associated with its use for guidance systems (namely the observability criterion), and finally broadly present the new trend in control strategy.

1.4.1 Separation Principle

Theorem 1.1 *(Separation Theorem) The minimal expected error in controlling a stochastic linear system is obtained by choosing the control gain matrix as the solution of the corresponding deterministic optimum control problem and the observer gain matrix as the optimum gain for the corresponding Kalman filter [25].*

The first idea hinging on the separation principle goes back to 1956 when an econometrician (H. A. Simon) was studying the problem of *dynamic programming* under uncertainty [74]. He stated that, even in the case of uncertainty of future variables, one can transform the problem into one of dynamic programming by simply replacing the first-period "certain" values by their unconditional expectations. The next set of action could be based on the information available from the first one and so on. This was termed the *certainty equivalence* principle and it was suggested that it is only true when the performance criterion is quadratic.

This idea was extended to the field of control theory when Joseph and Tou [46] showed, only one year after Kalman's solution to the optimal observer (and estimator) problem [48], that even in the case of uncertainty of the state, one can transform the problem into one of "optimal observer" by simply working with the state expectation rather than the "certain" state. A similar formulation was also given for the optimal control problem and the two were combined to form the so called "separation principle". It wasn't until 1963 that the idea took its current generalised form under the name of "separation theorem" when Gunckel and Franklin showed that for generalised linear systems, the resulting compensator derived from the combination of the optimum controller and the optimum filter is optimum itself [42]. Up to that stage, the formulation covered discrete systems only. But later that decade, it was extended to the case of continuous systems, and was shown to be valid under general conditions, not only under the quadratic performance assumption [99].

1.4.2 Observability Criterion

For linear, noise-free systems the separation theorem provides satisfactory results. It is well known that an optimal controller and an optimal observer, combined in cascade, result in an optimal overall compensator, for the above mentioned class of systems. When applied to linear noisy systems, however, the theorem remains applicable to an optimal controller and an optimal estimator placed in cascade if the system is observable. When it comes to nonlinear systems though, the notion of *optimal filter* is not existent in general. It was only hoped that by extending the Kalman methodology one would come up with an optimal filter for certain classes of nonlinear systems. This intuition proved to be misleading. The divergence problem of the EKF, the bias problem of the pseudolinear tracking filter, the overdamping problem of the constant gain extend Kalman filter are all proofs of this misconception. Note however that our bearing-only-measurement problem (BOMP) - to be defined in the next chapter - is not only a nonlinear problem but also a noisy one. As the observability requirement is vital in the linear case, it is natural not to disregard it in the nonlinear case. The question is how to incorporate observability into the system design in such a way that we can have a trackable solution. This question, which is at the centre of our present study, led a few authors to tackle the observability question of systems with bearing-only-measurements.

One of the earliest works along this line is that of Nardone and Aidala [58]. In the analysis of bearing-only-measurement systems, necessary and sufficient conditions on "own-ship motion" were established in order to insure observability of a constant velocity target. It was shown that, even when the bearing rate is nonzero, certain types of maneuvers remain unobservable, contrary to some previous assumptions. This work was extended to the three-dimensional target tracking problem in [30]. In parallel to these studies, the same problem was treated from a different angle and generalised in [63]. It was then extended to the case of a three-dimensional maneuvering target problem [64]. More recently, the maneuvering limitations of a fixed-wing target aircraft were used to identify specific scenarios resulting in the loss of observability [36]. Initialisation guidelines designed to avoid unobservability

were also provided.

1.4.3 Maximum Information Guidance

The observability criterion was the motivation behind which a new approach to system guidance was recently attempted. While most conventional optimal methods try to optimise time and control effort only, the new approach optimises a measure on system observability. Since the information on observability is best contained in the *observability gramian*, the trace of this matrix was adopted in the work of [80] as a performance index to be maximised. More interestingly, since the dynamics of the BOMP problem are linear, in a cartesian coordinate, and the measurements nonlinear, the "maximum information" matrix is nothing but the so called "Fisher information matrix", which under the conditions of the present problem could be obtained in an "elegant" closed form to be explored in Chapter 3. The resulting "maximum information trajectory" was fed to an EKF and its performance compared to that of a *proportional navigation trajectory.* It was found that, even for large initial estimation errors, the behaviour of the EKF along the maximum information guidance path is satisfactory while it diverges along the PNG path [80]. A subsequent application of this guidance law on a two-dimensional BOMP in which target and missile have constant velocity showed that as the observability information content increases the final time and the control effort increase [41]. This obviously contradicts the objectives of conventional optimal guidance laws.

1.4.4 Dual Control Guidance

The conception of the non-conventional maximum information guidance law has paved the way for the creation of a new research area in guidance systems. The aim of the new trend is to identify the advantages of observability and its usefulness to the overall guidance problem, in the light of the latest developments in filter design. Since the MGEKF was considered "a breakthrough in guidance filter development" [85], it was tested along a maximum information guidance trajectory and its per-

formance compared to the EKF performance. The results were in favour of the MGEKF [83].

Consequently, it became apparent that the conventional approach of designing the guidance law and the filter algorithm separately, then combining them in cascade, according to the separation principle, was not completely adequate. Designing the guidance law with the filter requirements in mind and designing the filter algorithm with the guidance objective in mind, sounded like the new viable alternative. Since there seems to be a conflict between the "conventional" and the "new", a tradeoff seemed inevitable. This formed the basis of the so called "dual control" design.

The dual control concept is still at its early stage of development, and certainly needs much study. Although many ad-hoc algorithms could be classified as falling in the class of dual controllers, "the structure of the (dual) controller is not well understood" [85]. As an example of an ad-hoc application seemingly possessing the dual control property, the MGEKF was used in [40] along a trajectory determined by adding to the classical quadratic performance index an additional factor proportional to the final time (since observability seems to increase with the final time). The resulting dual control guidance law was shown to perform better than the more conventional linear quadratic guidance law (section 1.2.3), in terms of estimation errors.

It is believed that the developments related to the maximum information guidance are one significant step towards the overall aim of the dual control concept. One problem that remains to be addressed is the design of an algorithm for the accurate determination of the time-to-go (which is critical in the problem formulation). One other problem is the determination of the observability coefficient. This is still "more of an art than a science" [62]. The present research study addresses the above two problems, among others, and attempts to find alternative solutions.

1.5 Dual Control Theory

Dual control guidance and maximum information guidance, considered in the previous sections, have their origins in what is termed *"dual control theory"* initiated by Feldbaum [22] and developed further by other authors [10, 11, 94, 95].

According to this theory, there are two problems to be solved simultaneously by the "controlling device" [22]:

- Clarification of the properties and the state of the controlled plant, on the basis of the information fed into it.
- Determination of the steps necessary for successful control, on the basis of the properties discovered in the plant.

According to the same theory, optimal systems could be divided into three types:

- Optimal systems having complete or the maximum information possible about the controlled plant. For this type of systems, considered through *dynamic programming* [12], dual control is not necessary, since all (or the maximum possible) information needed is available.
- Optimal systems having incomplete information about the plant and independent or passive accumulation of information in the control. For this type of systems, considered in [12, 56, 68] dual control is impossible because "the information is accumulated by means of observation alone, and the rate of its accumulation does not depend on the strategy of the controlling device" [22].
- Optimal systems having incomplete information about the plant and active accumulation of the information in the control process. For this type of systems, dual control, consisting of studying actions as well as directing actions, is both useful and possible.

For the purpose of dual control theory an *optimal system* is defined as follows:

Definition 1.1 *An optimal system is a system for which the average risk, i.e., the mathematical expectation of the overall loss function, is minimal [22].*

Theoretically, dynamic programming is used to derive an optimal control sequence, in the sense defined above, using the important notion of information state and the principle of optimality [6, 12]. This leads to a stochastic dynamic programming equation.

But the solution to the stochastic dynamic programming equation requires the availability of the conditional density which is usually infinite dimensional. In addition, the dimension of the information state grows linearly with the quantisation number. A third difficulty in applying the dual control theory is the practical impossibility to store the control associated with each information state. These difficulties are the result of the so-called the *curse of dimensionality.*

One alternative approach, suggested in [95], makes use of the "wide-sense property" [20] to reduce the dimension of the information state and solve the dual control problem, although in a sub-optimal fashion. It consists of:

- Approximating the information state such that its dimension stays finite.
- Approximating the optimal cost-to-go associated with each information state.
- Computing the control value on-line.

The Subsequent application of dynamic programming leads to an expression of the optimal cost consisting of the control cost and the estimation cost. This expression is called the *"dual cost"* [11].

In this thesis, it will not be dealt with the dual control theory in its widest sense. However, the essence of duality is present through the attempt to optimise control and estimation simultaneously.

1.6 Thesis Significance and Purpose

With the recent advances in computer technology, the dual control guidance approach (section 1.4.4) is assuming significant importance. Unlike the separation principle (section 1.4.1), dual control guidance carries the potential of combining the advantages of conventional control laws, such as proportional navigation, with those of more advanced concepts such as maximum information [41]. It promises, therefore, to effectively use relatively simple seeker heads - providing bearing-only-measurements - and compensating with the use of an elaborate, observability-enhanced guidance algorithm.

Much work has been carried out to understand and analyse the characteristics of observability-enhanced guidance laws [39, 80, 83, 85]. However, existing studies do not provide closed-form expressions for these newly emerging laws, nor do they provide a systematic way of selecting the observability coefficient - a critical step in the application of the resulting guidance law. In addition, the present observability-enhanced guidance laws rely on the problematic estimation of the time-to-go and they also lack simplicity and ease of implementation when used on-line in a closed-loop setting.

In this thesis, a novel guidance law dubbed *observable proportional navigation* is proposed. While this law is simple and easy to implement, it belongs to the dual control guidance approach in the sense that it incorporates a measure of observability into the control prescribed by proportional navigation. Two distinct forms of this guidance law are considered, based on the nature of the associated noise and state estimator. Closed-form solutions of the new guidance law are given and necessary limits on the coefficient of observability are determined. Both forms of the new law are applied to a two-dimensional missile-target bearing-only-measurement problem and the corresponding simulations substantiate the effectiveness of the proposed law.

To pave the way for the introduction of observable proportional navigation, this thesis includes a brief, but self-contained study of conventional guidance laws, pop-

ular state estimators and existing observability-enhanced guidance laws, as they apply to two-dimensional bearing-only-measurement problems.

1.7 Thesis Structure

In the chapters to follow, the guidance system is dissected into its main building blocks: guidance law, state estimator, flight control system, pursuer and target dynamics, and measurement sensor [71]. Each element, except the flight control system, is then considered separately and in conjunction with the others. The guidance law and the state estimator are given special attention, since the interaction between these two blocks is central to the understanding of the present work.

Proportional navigation is discussed in the next chapter, as one of the most used guidance laws. Its origins, rationale and role in the guidance loop are analysed and illustrated step by step for the two-dimensional case. PNG is also applied to maneuvering and non-maneuvering targets. The main features of PNG are highlighted and its limitations pinpointed, paving the way for the introduction of the state estimator.

As an alternative to PNG, the maximum information guidance law is introduced in the third chapter. Using control parametrisation as a numerical tool, this guidance law is derived and compared to proportional navigation. The approach followed to present this guidance law is purely deterministic, since the objective is essentially to derive the trajectories and control efforts under maximum information guidance and compare them to those under PNG. Control parametrisation is also compared to the shooting method and the advantages of using the former method are noted.

In the fourth chapter, the state estimator is introduced. The extended Kalman filter is first derived and several variants of the EKF are then explored including the iterated extended Kalman filter, the iterated linear filter-smoother, and the modified gain extended Kalman filter. Simulation studies of the extended Kalman filter along a trajectory provided by proportional navigation illustrate the filter

divergence problem towards the end of the pursuer-target engagement.

The dual control guidance law is addressed in the fifth chapter. The very important idea of guidance law *mechanisability* is stressed and, as a direct consequence, a mechanisable guidance law, the linear quadratic guidance law is described first. Using a similar formulation, the dual control guidance law is then analysed and the expressions of its coefficients derived. DCGL is then applied to a two-dimensional bearing-only-measurement problem and compared to the LQGL. Characteristics and shortcomings are also outlined.

In the sixth chapter, a new guidance law is presented and developed in two distinct forms. In both forms, dubbed *additive observable proportional navigation* (AOPNG) and *multiplicative observable proportional navigation* (MOPNG), it is proposed to *maintain* rather than *maximise* system observability in the same way proportional navigation attempts to *maintain* constant line-of-sight angle. The new guidance law conserves the simplicity and ease of implementation of PNG while adding an additional feature related to filter observability. Closed form solutions of the law are derived, and necessary conditions for effective intercept are established. Monte-Carlo simulations enable the comparison of the new law with PNG.

Finally, the last chapter summarises the diverse messages of this study, highlighting the contributions and suggesting future research directions.

Chapter 2

Proportional Navigation Guidance

As mentioned in the introduction, this study will specifically focus on the guidance law, as a major function of the guidance processor. Since the aim of the guidance law is to issue the control effort necessary to drive the pursuer to intercept the target, its role is considered pivotal for the success of the overall guidance system.

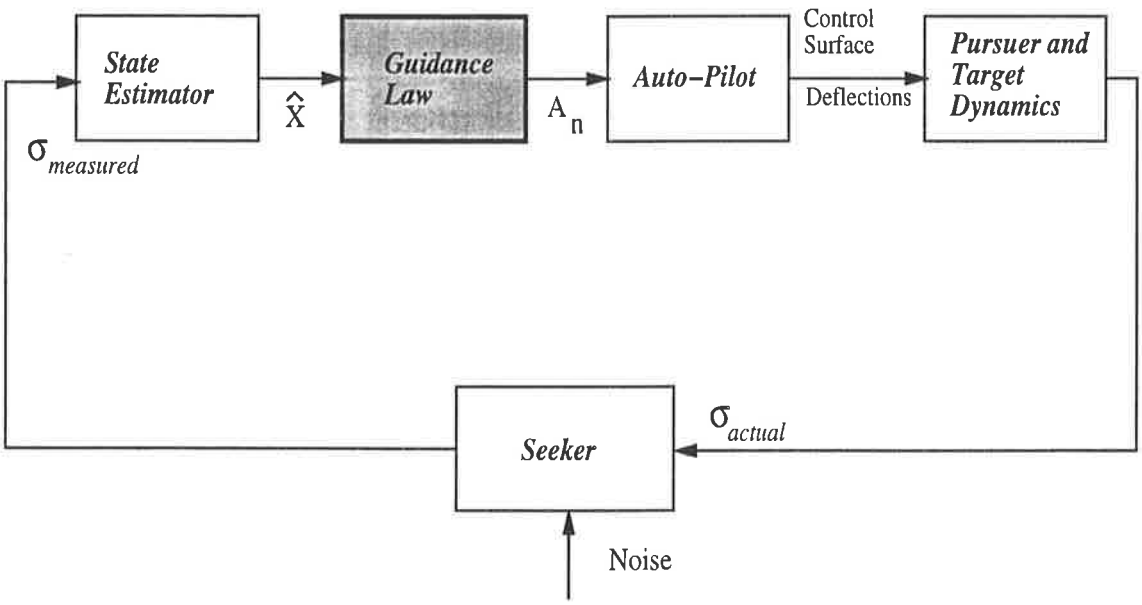

Figure 2.1: Closed loop guidance - the guidance law

In general, the guidance law utilises the state representing the pursuer-target system or the state estimate originating in the state estimator (see Figure 2.1), as its input. The state estimator itself is fed by the passive seeker head, whose sensor tracks the relative pursuer-target trajectory, which results from the action of the commanded control effort on the automatic pilot.

For the purpose of our study, low cost passive seekers are used for the homing pursuer. These will provide bearing-only-measurements such as target elevation or azimuth. The absence of range information makes the guidance task relatively hard for the guidance law, which will attempt to achieve its goal with limited information. Among all guidance laws mentioned in Chapter 1, this study will focus on proportional navigation guidance (PNG) whose simplicity and ease of implementation will be used to our advantage.

Since its proposal at the beginning of this century, PNG has received a good deal of attention due to its effectiveness and simplicity. The optimality of this guidance law was later established by showing that it could be interpreted as a particular case of the more general quadratic optimal control theory [16].

Four methods of implementation of the two-dimensional PNG will be explored in the following sections. The first method demonstrates the ease of implementation of PNG and its formulation is based on the pursuer speed. In contrast, the second method is based on the terminal speed and is relatively more popular. The third method is a particular case of the second one and its simplified form leads to the derivation of closed form solutions providing a valuable insight into the characteristics of PNG. Finally, the last method is the implementation of proportional navigation as a special case of the linear quadratic guidance law, indirectly demonstrating its optimality.

In order to analyse PNG two approaches are used in this thesis. In the *deterministic approach*, the coordinates and velocities of the pursuer-target system, as well as the measurements are considered noise-free and no state estimator is used. In the *stochastic approach*, the system and/or the measurements are considered riddled with noise and uncertainty, and a state estimator is used. In the present chapter

and the following one, we focus on the deterministic approach, leaving the stochastic approach to Chapters 4, 5, and 6.

2.1 Guidance Problem Formulation

The deterministic approach to the guidance problem takes the form of a generally nonlinear relative pursuer-target dynamics model, in which pursuer and target are considered to be point-masses moving at constant speeds for simplicity. For the two-dimensional case (Figure 2.2), the guidance dynamics model could be written as:

$$\begin{aligned} \dot{X}_r &= V_T cos\phi - V_M cos\theta \\ \dot{Y}_r &= V_T sin\phi - V_M sin\theta \\ \dot{\theta} &= \frac{A_n}{V_M} \end{aligned} \tag{2.1}$$

where X_r and Y_r are the relative coordinates of the pursuer-target system:

$$\begin{aligned} X_r &= X_T - X_M \\ Y_r &= Y_T - Y_M \end{aligned} \tag{2.2}$$

V_M and V_T are the pursuer and target speeds, respectively; θ and ϕ the pursuer and target heading angles, respectively; and A_n the pursuer normal acceleration under which action the pursuer is expected to follow the target until intercept. Note that (2.1) will be referred to as the *guidance model* in this study.

The two major limitations of the problem are essentially in the control (A_n is limited to a certain maximum magnitude), and the type of measurement, which, in the two-dimensional case, reduces to the elevation (or azimuth):

$$\sigma = \arctan \frac{Y_r}{X_r} \tag{2.3}$$

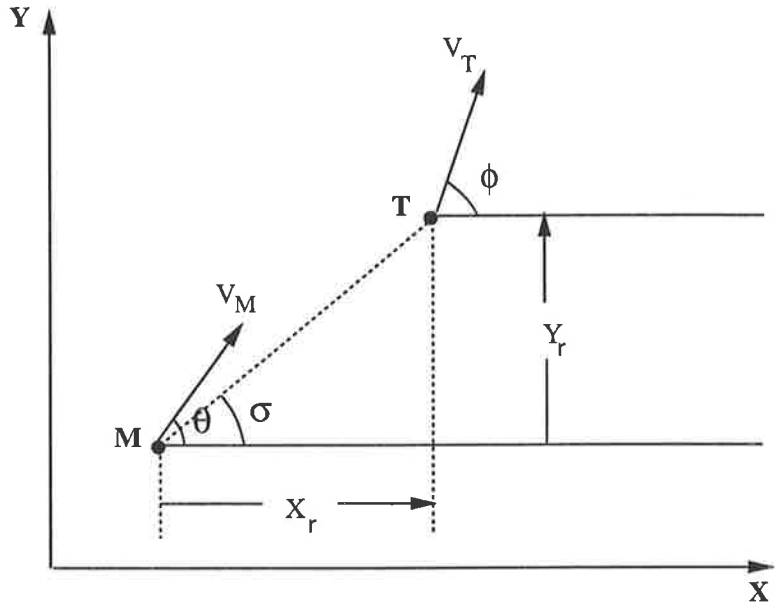

Figure 2.2: Two-dimensional pursuer-target geometry

The initial conditions of the problem can be assumed known and they are obtainable from the carrying aircraft before launch:

$$t_0 = 0 \quad X_{r0} = R_0 \quad Y_{r0} = 0 \quad \theta_0 = 0 \tag{2.4}$$

The final conditions or the problem constraints are defined by the requirement to intercept the target.

$$X_{rf} = 0 \quad Y_{rf} = 0 \tag{2.5}$$

Since the time of intercept is not known in advance, nor the pursuer heading angle at the final time, they are taken in the optimisation problem as:

$$t_f = free \quad \theta_f = free \tag{2.6}$$

however, in many cases, the time of intercept is estimated initially and during the engagement and used in the derivation of the control history.

Generally speaking, the guidance problem consists of finding this control history subject to the initial and final conditions, so that a certain engagement criteria, (time, cost, etc.) is optimised.

To illustrate the different guidance laws used in this study, several engagement scenarios are being used, the most common of them is one where the pursuer is moving towards its target with a constant speed $V_M = 1600ft\ s^{-1}$ while the target is moving away from the pursuer with a heading angle $\phi = 30°$ and a speed of $V_T = 800ft\ s^{-1}$ (see Figure 2.2). Other scenarios are also considered to illustrate the validity of the guidance scheme over a range of situations.

2.2 Pure Proportional Navigation

We consider the basic two-dimensional guidance model described by (2.1) in the previous section.

In order to guide the pursuer in its pursuit of the target, Guelman's proportional navigation, commonly referred to as *pure proportional navigation* proposes to apply a normal acceleration (normal to the pursuer velocity) proportional to the rate of change of the line-of-sight angle [27, 28, 29]. If the pursuer speed, V_M is constant, it could be used in the formulation of the law, as follows:

$$A_n = NV_M\dot{\sigma} \tag{2.7}$$

where N, called the navigation constant, determines how responsive the guidance is. This constant plays a vital role in the success of the interception mission, as we shall see in section 2.4.

Since the guidance law is considered deterministic here, the line-of-sight angle measured by the passive seeker could be described by (2.3), which if differentiated and replaced in (2.7), leads to an expression of the control variable, A_n, in terms of the relative coordinates:

$$\begin{aligned} A_n &= NV_M \frac{1}{1+(\frac{Y_r}{X_r})^2}\left(\frac{\dot{Y}_r}{X_r} - \frac{\dot{X}_r Y_r}{X_r^2}\right) \\ &= NV_M \frac{X_r\dot{Y}_r - Y_r\dot{X}_r}{X_r^2 + Y_r^2} \end{aligned} \tag{2.8}$$

Using (2.8) in (2.1), we obtain the following:

$$\begin{aligned} \dot{X}_r &= V_T cos\phi - V_M cos\theta \\ \dot{Y}_r &= V_T sin\phi - V_M sin\theta \\ \dot{\theta} &= \frac{N}{X_r^2 + Y_r^2}[V_T(sin\phi X_r - cos\phi Y_r) - V_M(sin\theta Y_r - cos\theta Y_r)] \end{aligned} \tag{2.9}$$

Figure 2.3 shows the target and pursuer trajectories described by the above system, as well as the corresponding normal acceleration histories, for several values of the navigation constant N. These results are obtained by sequentially solving (2.10) until the miss-distance reaches a minimal value. Note that the adopted scenario is similar to that mentioned in section 2.1 and the pursuer is initially pointing towards the target.

Definition 2.1 *The miss-distance defined at any time, t, is the distance between pursuer and target that would result if guidance were terminated at the time t.*

It is readily seen that the pursuer trajectory generated by proportional navigation, gradually aligns itself with the target trajectory and approaches a straight line as N becomes large. The corresponding normal acceleration starts from an initial relatively high value and gradually decreases until reaching zero. This trend is true with mostly high values of N. Eventually, N reaches a limit where the dimension of the normal acceleration becomes impractical. On the other hand, if N decreases steadily a limit is reached where the normal acceleration is practically constant. These, as well as other features, will be analytically explained in the next sections.

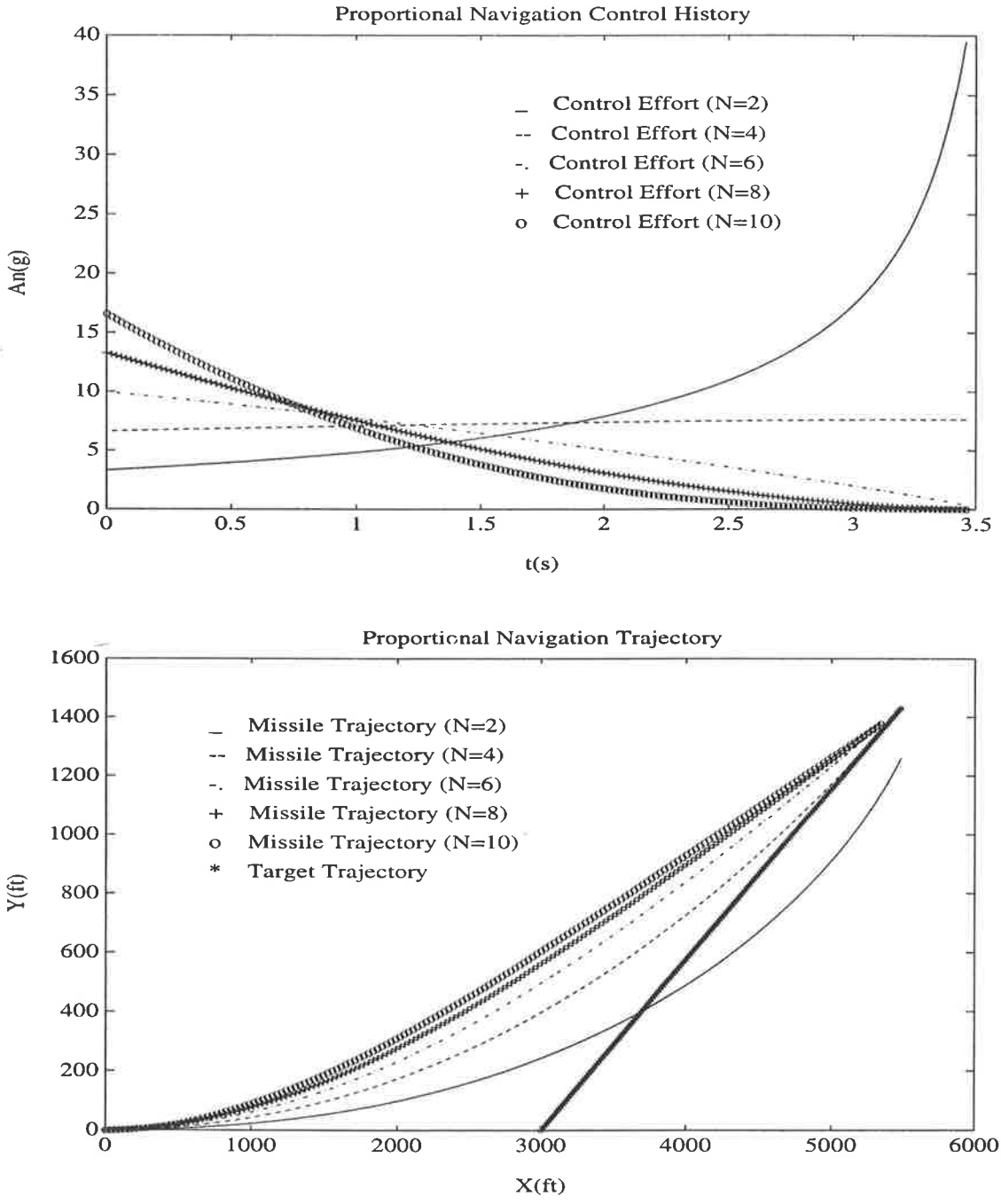

Figure 2.3: Pure proportional navigation trajectories and control histories

2.3 True Proportional Navigation

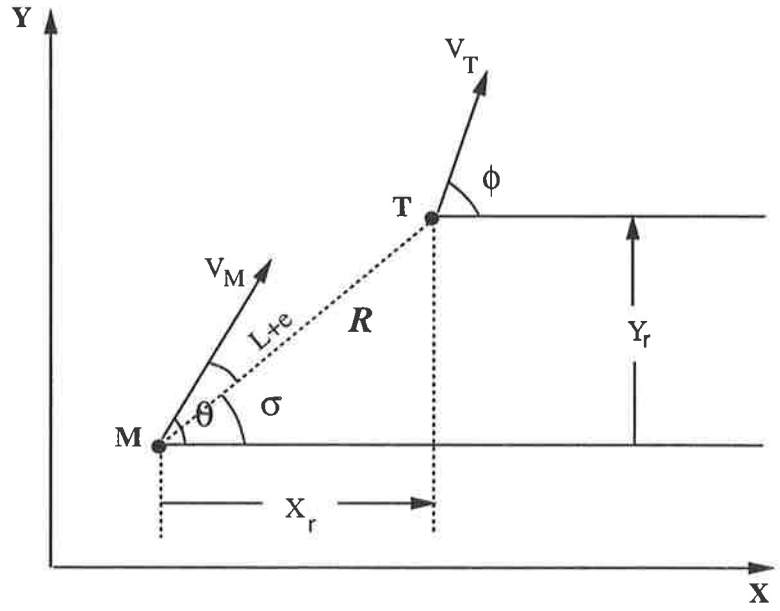

Figure 2.4: Two-dimensional pursuer-target engagement geometry

In true proportional navigation, the control effort is taken to be the acceleration normal to the line-of-sight (see Figure 2.4). Its magnitude is taken to be proportional to:

1. the rate of the line-of-sight angle, $\dot{\sigma}$, and
2. the range rate, $\dot{R}$.

The direction of this normal acceleration, A_n, is chosen so that it attempts to compensate for the effect of the changing variables:

$$A_n = -N\dot{R}\dot{\sigma} \tag{2.10}$$

where N, is the navigation constant.

The logic behind this law is therefore intuitively simple. The faster the lateral change (line-of-sight angle) or the faster the longitudinal change (range) the higher is the applied normal acceleration in a direction that counteracts the lateral and/or

the longitudinal change, respectively. This concept continually applies until the range itself becomes minimal.

2.3.1 Two-Dimensional Engagement

We consider an engagement scenario as illustrated by Figure 2.4, and outlined in section 2.1. The range, R, between the pursuer and the target is given by:

$$R^2 = X_r^2 + Y_r^2 \tag{2.11}$$

where X_r and Y_r, the relative coordinates in the inertial coordinate system are defined in section 2.1.

In order to take up the case where the pursuer initial heading angle is not defined, we slightly deviate from the initial conditions given in section 2.1. In this case, starting from well defined initial positions for the pursuer (X_{M_0}, Y_{M_0}) and the target (X_{T_0}, Y_{T_0}) and a known initial target heading angle, ϕ_0, we can proceed to define the initial pursuer heading angle, θ_0 (see Figure 2.4). Part of this angle is the line-of-sight angle itself, the other part is called the *lead angle* and is denoted by L in Figure 2.4. In fact, since a pursuer employing proportional navigation is not fired at the target but is fired in a direction to lead the target [105], this angle is the theoretical angle between the pursuer velocity vector and the line-of-sight, and could be obtained by applying the law of sines to the *collision triangle.*

Definition 2.2 *A collision triangle is the triangle made by the line-of-sight between the pursuer and the target, and the pursuer and target velocity vectors, when those velocities lead the pursuer to intercept the target, without any further control action.*

Finally, an arbitrary heading error "e" could be considered to provide the following expression of the pursuer heading angle:

$$\theta = \sigma + sin^{-1}\frac{V_T sin(\phi + \sigma)}{V_M} + e \tag{2.12}$$

Having the initial relative coordinates and heading angles available, the components of the initial relative speed could be derived by simple inspection of the engagement geometry, i.e.,

$$\begin{aligned} V_{r_x}(t) &= -V_T cos\phi - V_M cos\theta \\ V_{r_y}(t) &= V_T sin\phi - V_M sin\theta \end{aligned} \tag{2.13}$$

2.3.2 Algorithm

From (2.3) we conclude that the rate of the line-of-sight angle is given by:

$$\dot{\sigma} = \frac{X_r V_{r_y} - Y_r V_{r_x}}{R^2} \tag{2.14}$$

and that the range rate is:

$$\dot{R} = \frac{X_r V_{r_x} + Y_r V_{r_y}}{R} \tag{2.15}$$

Given the initial conditions and a chosen navigation constant, it is possible to apply the guidance law described by (2.10) and generate the corresponding trajectory and control effort history. The following algorithm summarises the steps needed:

Step 1: Using the initial conditions and (2.10), compute the corresponding normal acceleration, A_n.

Step 2: Integrate the line-of-sight rate and use the resulting line-of-sight angle to project A_n along the X and Y axes.

Step 3: Integrate the normal acceleration components to generate the pursuer speed components. Reintegrate to generate the pursuer position components.

Step 4: If the target is not maneuvering, integrate its speed to provide its position.

Step 5: If the target is maneuvering, calculate the rate of its heading angle given the value of its acceleration, then integrate and use the result to determine the target position.

Step 6: Repeat steps 1 to 5 until the pursuer-target range becomes minimal, i.e., the range rate reaches zero.

2.3.3 Simulation

The procedure described above was translated to a Matlab routine similar to the Fortran program found in [105] and simulated for a target travelling initially away from the pursuer and a pursuer-target scenario in which $\phi = 30°$, $V_M = 1600\ ft\ s^{-1}$, and $V_T = 800\ ft\ s^{-1}$. The pursuer and target trajectories as well as the normal acceleration histories were recorded in Figure 2.5, for several values of the proportional navigation constant, N.

We note that for $N = 2$, 3, and 4, intercept occurs around 3.5 seconds after the beginning of the engagement. Higher the value of N, more responsive the pursuer trajectory, higher the initial control and lower the final one. For $N = 1$ however, close intercept does not occur and the control variable increases significantly towards the end of the engagement unlike the control variable corresponding to higher values of N. $N = 2$ provides a critical behaviour of the control, which proves to be about constant during the whole period of the engagement. In section 2.4, the dependence of the pursuer trajectory and the control effort on the navigation constant is analysed further.

The same routine was tested with a target travelling initially towards the pursuer with a heading angle $\phi = 0°$. Both have the same speeds as above but the target is maneuvering away from the pursuer with a constant acceleration of $3g$, where g is the acceleration of gravity (Figure 2.6). The simulation shows that intercept

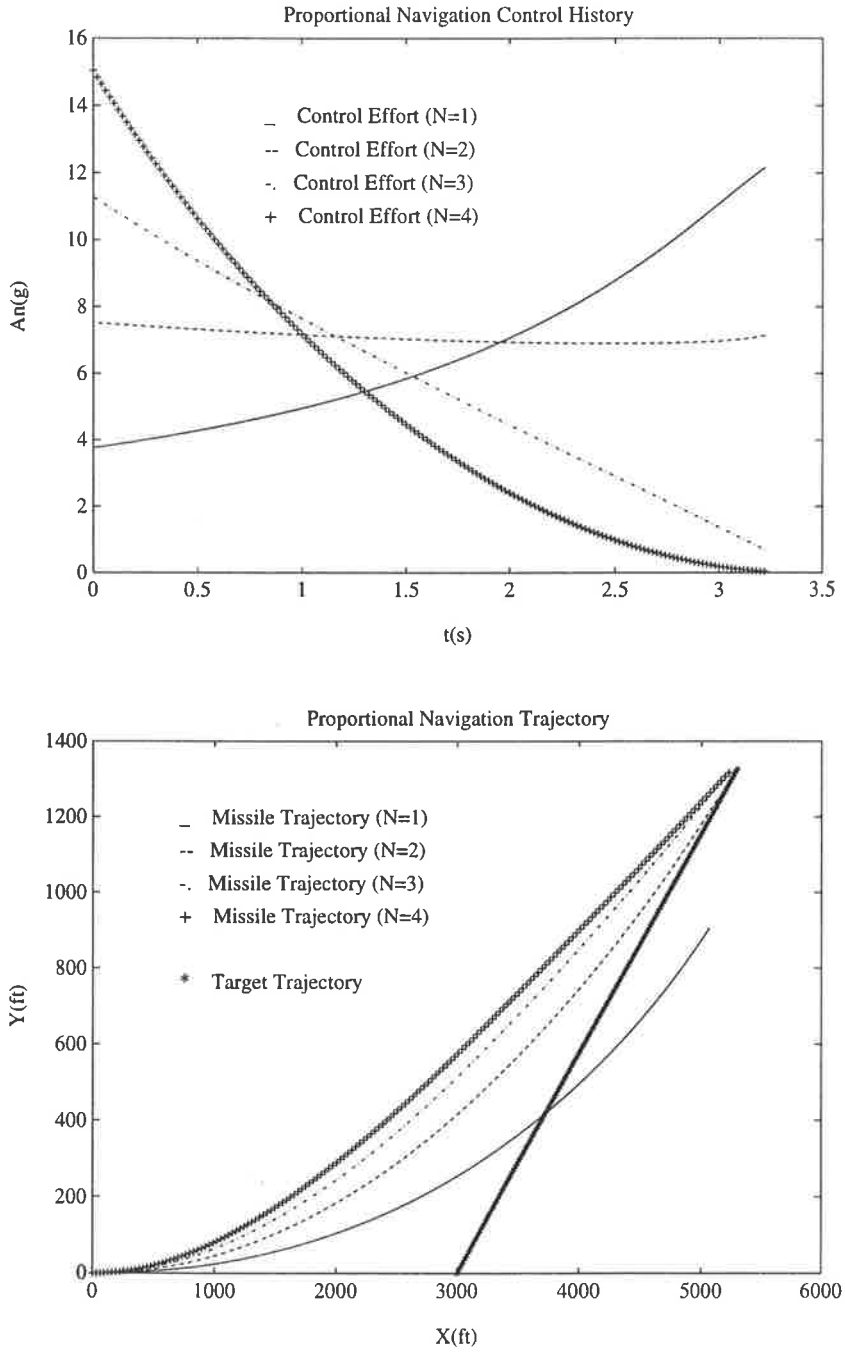

Figure 2.5: True proportional navigation trajectories and control histories

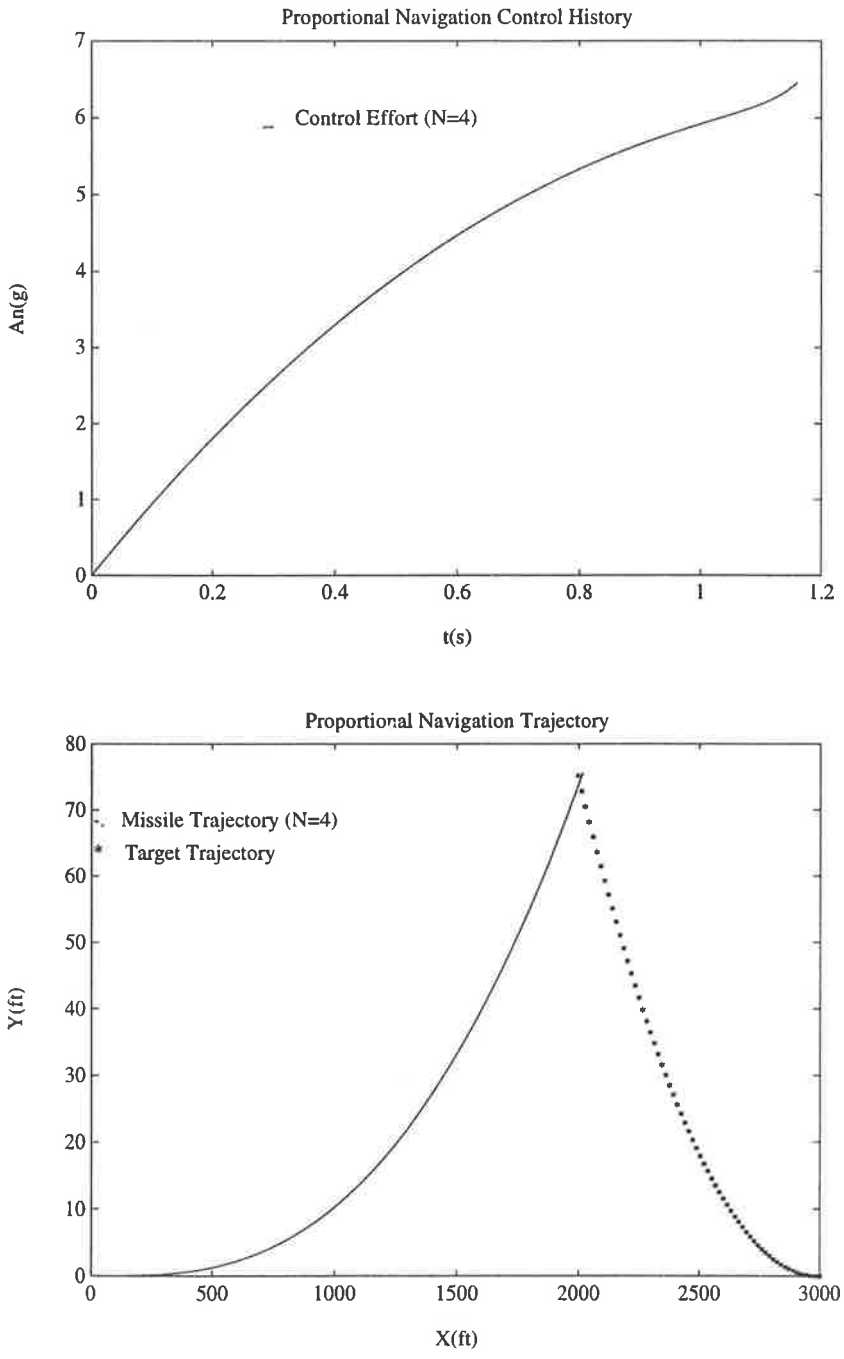

Figure 2.6: True proportional navigation applied to a maneuvering target

occurs just over one second from the start of the engagement, but the applied control increases gradually, while maintaining a reasonable limit of about $6g$.

In order to better understand the behaviour of the PNG driven pursuer described herein, it is useful to further simplify the guidance law under consideration and attempt to analyse the resulting simplified equations. This is the subject of the next section.

2.4 Simplified Proportional Navigation

The value of the navigation constant is crucial in the determination of the intercept behaviour. It would be interesting to uncover the relationship between this constant and the control effort, or the pursuer trajectory, so that a better understanding of the proportional navigation law would be achieved. Since this problem is nonlinear in nature certain linearisation or approximation is necessary. Also, instead of working with cartesian coordinates, we use the polar coordinates system in which the computations can be simplified.

2.4.1 Polar Engagement Dynamics

In [57] the pursuer-target engagement geometry is represented in a polar coordinate system. This system provides a valuable insight into the characteristics of proportional navigation, with no great computational hardship.

The range, in this coordinate system, is represented by a vector directed along the line-of-sight ($\vec{j}$ axis) towards the pursuer (see Figure 2.7).

$$\vec{R} = R\vec{j} \tag{2.16}$$

Since the line-of-sight angle is changing with time, the rotation of the line-of-sight could be represented by a vector along the $\vec{k}$ axis, defined by:

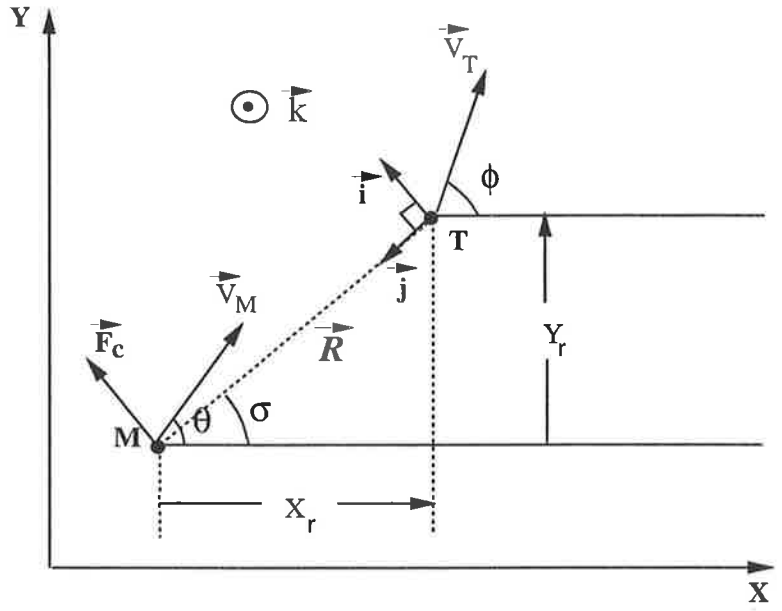

Figure 2.7: Two-dimensional polar engagement geometry

$$\vec{\Omega} = \dot{\sigma}\vec{k} \tag{2.17}$$

It is proposed to derive the expression of the relative acceleration by consecutive derivation of the range vector. The relative speed vector is derived by differentiating (2.16), taking into account the rotating nature of the vector $\vec{j}$.

$$\begin{aligned} \frac{d\vec{R}}{dt} &= \dot{R}\vec{j} + \vec{\Omega} \times \vec{R} \\ &= \dot{R}\vec{j} - R\dot{\sigma}\vec{i} \end{aligned} \tag{2.18}$$

Differentiating the relative speed results in the expression of the relative acceleration vector:

$$\begin{aligned} \frac{d^2\vec{R}}{dt^2} &= \ddot{R}\vec{j} - \dot{R}\dot{\sigma}\vec{i} - R\ddot{\sigma}\vec{i} + \vec{\Omega} \times \frac{d\vec{R}}{dt} \\ &= (\ddot{R} - R\dot{\sigma}^2)\vec{j} - (R\ddot{\sigma} + 2\dot{R}\dot{\sigma})\vec{i} \end{aligned} \tag{2.19}$$

As mentioned in the previous section, the only acceleration applied to the pursuer-target system is normal to the line-of-sight, e.g., along the $\vec{i}$ axis. This leaves us with the following equations:

$$\frac{F_c}{m} = -(R\ddot{\sigma} + 2\dot{R}\dot{\sigma}) \tag{2.20}$$

$$0 = (\ddot{R} - R\dot{\sigma}^2) \tag{2.21}$$

where F_c is the applied force normal to the line-of-sight, and m is the mass of the pursuer.

Equations (2.20) and (2.21) are called the equations of motion of the pursuer-target system.

2.4.2 Closed Form Expressions

As suggested by its form and behaviour (equation 2.7 and Figure 2.5),one of the aims of proportional navigation is to continuously push the line-of-sight angle rate towards zero. It is therefore reasonable to assume that the second order magnitude of the line-of-sight angle rate, $\dot{\sigma}^2$, is negligible. Applied to (2.21), this assumption leads to conclude that the derivative of the range magnitude is constant.

$$\dot{R} = constant \tag{2.22}$$

By definition, the *terminal speed* is written as:

$$\dot{R} \equiv -V_c \tag{2.23}$$

which means that the terminal speed for this type of proportional navigation is constant.

Note from (2.13) that this assumption amounts to the case where the heading angles are small (head-on or tail chase engagements [105]). In this case the terminal speed

would be nothing but the difference between the pursuer and target speeds in the case of a tail chase, and their sum in the case of a head-on. Furthermore, the proportional navigation law becomes proportional only to the line-of-sight rate:

$$\frac{F_c}{m} = NV_c\dot{\sigma} \tag{2.24}$$

Replacing (2.24) in (2.20), we get:

$$R\ddot{\sigma} + (N-2)V_c\dot{\sigma} = 0 \tag{2.25}$$

At this stage, it is advantageous to define another important quantity, namely the *time-to-go*, t_f.

Definition 2.3 *The time-to-go, t_f, defined at any time, t, elapsed since the start of the engagement, is the time remaining before the presumed intercept occurs.*

It follows that:

$$t_f = \frac{R}{V_c} \equiv \frac{R_0}{V_c} - t \tag{2.26}$$

where R_0 is the pursuer-target initial range.

Taking (2.26) into consideration, the differential equation (2.25) could be readily solved to yield:

$$\dot{\sigma} = (\frac{t_f}{t_{f_0}})^{N-2}\dot{\sigma}_0 \tag{2.27}$$

where $\dot{\sigma}_0$ is the initial line-of-sight angle rate and t_{f_0} the initial time-to-go, i.e., the time-to-go from the beginning of engagement until intercept. Differentiating (2.27):

$$\ddot{\sigma} = (N-2)\frac{t_f^{N-3}}{t_{f_0}^{N-2}}\dot{\sigma}_0 \tag{2.28}$$

In this context, the *miss-distance* defined earlier in section 2.2, can be written as:

$$\begin{aligned} R_f &\simeq R\, t_f\, \dot{\sigma} \\ &= V_c\, t_f^2\, \dot{\sigma} = \frac{R^2 \dot{\sigma}}{V_c} \end{aligned} \tag{2.29}$$

Finally, using the expression of $\dot{\sigma}$ (2.27) in (2.29), we get the following closed form expression of the miss-distance in terms of the time-to-go:

$$R_f = R_{f_0}(\frac{t_f}{t_{f_0}})^N \tag{2.30}$$

where t_{f_0} is the initial miss-distance.

2.4.3 Important Characteristics

Given (2.27), (2.28) and (2.30), it is possible to deduce some important characteristics that apply to the simplified proportional navigation problem, which would still apply to the true PNG problem under small angle approximations. Note that in the above equations, we can define the following initial quantities:

$$\begin{aligned} \dot{\sigma}_0 &= \frac{R_{f_0} V_c}{R_0^2} \\ t_{f_0} &= \frac{R_0}{V_c} \end{aligned} \tag{2.31}$$

Four important characteristics are noted from (2.27) and (2.28):

- When the proportional navigation constant, N, is less than 2, (2.27) suggests that the line-of-sight rate, and therefore the applied acceleration becomes very large towards the end of intercept, when $t_f \to 0$.
- When $N = 2$, however, the same equation shows that the normal acceleration becomes constant.

- In the case where the value of N is between 2 and 3, (2.28) shows that the pursuer angular acceleration, and therefore the pursuer torque becomes very large near intercept.

- If N is equal or larger than 3 the system behaves well in the sense of providing a control force and torque which converge to 0 towards the end of the intercept. In practice, the value of N is usually taken between 3 and 6 [105].

We could also note from (2.30), that higher N is, quicker is the homing. Note that all characteristics deduced from the closed form expressions were noticed, to a certain degree of approximation, in the simulations presented in the previous sections (see Figure 2.5).

N.B.: It is interesting to note that since the terminal speed V_c is assumed to be constant, the simplified or "linearised" proportional navigation [67] could be defined in several different forms while retaining the same characteristics. In section 2.2 for example, instead of using the terminal speed in the guidance law, the pursuer speed, V_M, was used (see (2.7)) and the normal acceleration is taken to be normal to the pursuer velocity vector which is parallel, in this case to the line-of-sight:

$$\frac{F_c}{m} = NV_M\dot{\sigma} \tag{2.32}$$

That law was simulated for different values of N (see Figure 2.3). Those simulations could easily be "translated" into one which corresponds to our present simplified definition (based on V_c) by noting that:

$$NV_c\dot{\sigma} = N_pV_M\dot{\sigma} \tag{2.33}$$

where, for the purpose of this note, N is the navigation constant under the simplified proportional navigation, while N_p is the navigation constant under the pure proportional navigation. This means that:

$$N_p = \frac{V_M}{V_c} N \tag{2.34}$$

In the case of the simulation in question, $V_c = V_M - V_T = \frac{V_M}{2}$, which leads us to deduce that: $N_p = 2N$. Under these conditions, the simulations could be redrawn in terms of the simplified proportional navigation constant, N (see Figure 2.8).

2.5 Optimal Proportional Navigation

In addition to the three previous definitions, proportional navigation could be defined as a perturbation guidance law about a minimal control effort trajectory [41]. This classification allows to present proportional navigation as a standard optimal control problem.

2.5.1 Problem Statement

Given the system dynamics (2.1) and the initial conditions (2.4), the optimal proportional navigation problem consists of finding the normal acceleration history, $A_n(t)$, which minimises the performance index:

$$J = \int_{t_0}^{t_f} A_n^2(t) dt \tag{2.35}$$

subject to the final constraints of zero miss-distance specified in (2.5).

One way to solve this optimisation problem is to use a numerical optimisation technique. The following section describes one such technique.

2.5.2 Control Parametrisation - MISER3

There are several numerical techniques belonging to the field of mathematical programming that could be used to solve the proportional navigation optimisation

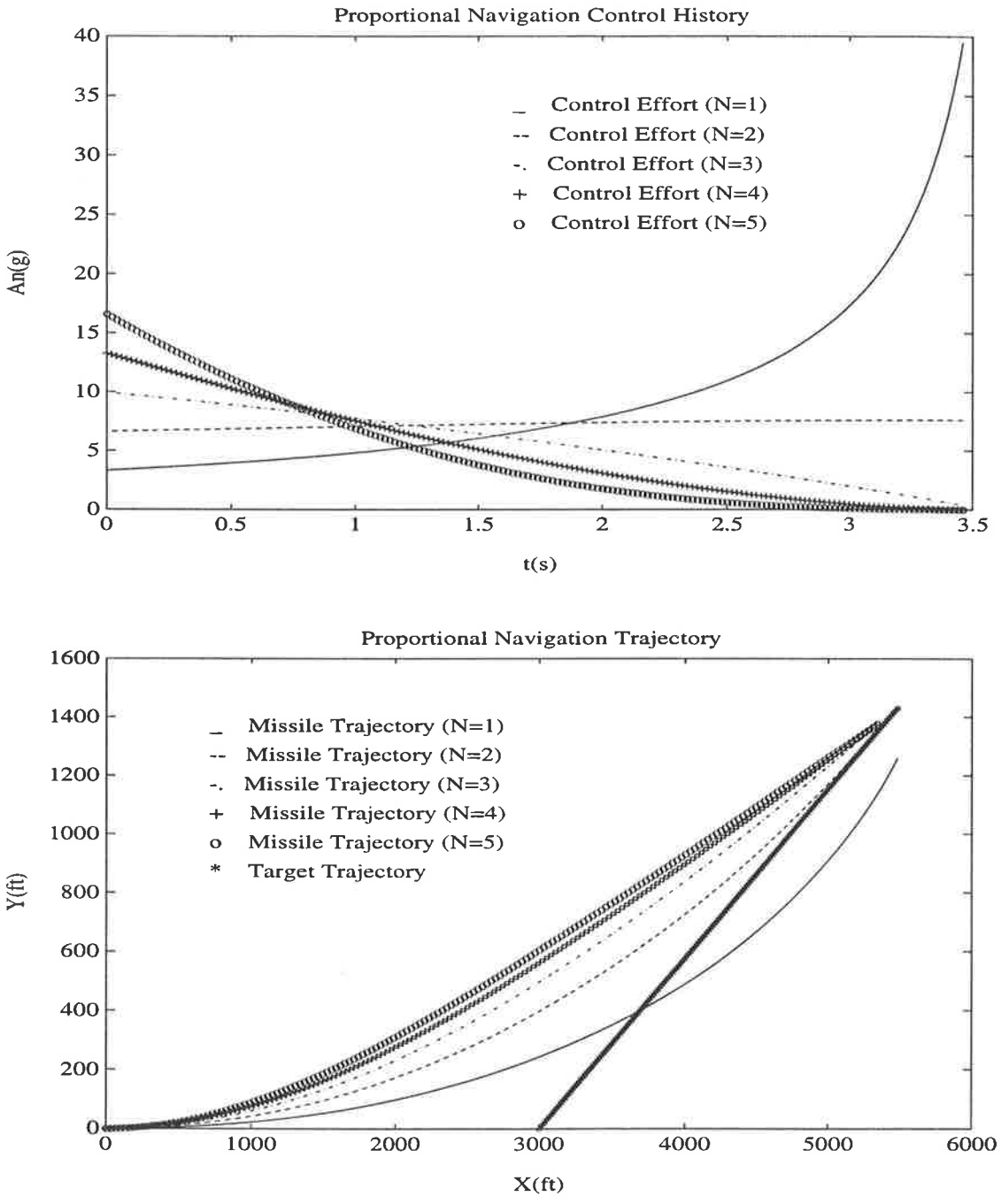

Figure 2.8: Pure proportional navigation based on the navigation constant of the simplified proportional navigation

problem. The iterative shooting method is one such technique that was used in [41] and [83] to solve the two-point boundary value problem. In essence this method assumes a set of values, called Lagrange multipliers, as initial guesses and solves the two-point boundary value problem until reaching the terminal point ("shooting" at the target terminal point). The difference between the resulting terminal conditions and the specified ones are then used to reinitialise the Lagrange multipliers. The shooting method is highly useful but its effectiveness can suffer under numerically sensitive problems [69].

In the present study, a technique based on the concept of *control parametrisation* is used and implemented through a software programme called MISER3 [45]. This software has been used successfully to solve numerous engineering constrained optimisation problems [92].

The main idea behind the concept of control parametrisation is the approximation of each control component $u_i(t)$ in the system by a zero-th order spline function defined on a set of knots $t_0 \leq t_j^i \leq t_f$. In other words, each control component could be written as:

$$u_i(t) = \sum_{j=1}^{k_i} \sigma_{ij} \chi_{ij}(t) \tag{2.36}$$

where i is an index referring to the specific control component:

$$i = 1, \cdots, n_c \tag{2.37}$$

n_c is the maximum number of control components; k_i is the maximum number of subintervals defined for the control component u_i in the time interval; σ_{ij} is a basis parameter corresponding to the j^{th} subinterval; χ_{ij} is an indicator function defined as follows:

$$\chi_{ij}(t) = \begin{cases} 1, & t_{j-1}^i \leq t \leq t_j^i \\ 0, & \text{otherwise} \end{cases} \tag{2.38}$$

Generally speaking, the optimisation problem consists of finding the optimal state trajectory, given n_c continuous control components and n_z discrete system parameters, subject to the system dynamics and n_g equality and inequality constraints. By following the discretisation procedure described above, this problem is approximated by that of finding the optimal state trajectory, given $n_p = \sum_{i=1}^{n_c} k_i + n_z$ discrete parameters, the same dynamics and the same constraints. The latter problem is recognised as a standard nonlinearly constrained mathematical programming problem and is solved using well known methods in the calculus of variations.

One of the innovations of MISER3 is the formulation of the performance index and the constraints in the same standard canonical form. Given the system dynamics:

$$\dot{x} = f(t, x(t), u(t), z) \tag{2.39}$$

where $f(\cdot)$ is a nonlinear function of t the time, $x(t)$ the state vector, $u(t)$ the control vector and z the system parameter vector. Under MISER3 the performance index takes the form:

$$G_0(u, z) = \Phi_0(x(t_f), z) + \int_{t_0}^{t_f} g_0(t, x, u, z)dt \tag{2.40}$$

and the constraints the form:

$$G_k(u, z) = \Phi_k(x(\tau_k), z) + \int_{t_0}^{\tau_k} g_k(t, x, u, z)dt \begin{matrix} = \\ \geq \end{matrix} 0 \tag{2.41}$$

where k is an integer between 1 and n_g.

To use MISER3, it is necessary to transform the problem in hand into the formulation given above. A differentiation of the functions involved f, g_0, g_k, etc. with respect to the state components, the control components and the system parameters, is also necessary. For more information on how to use MISER3, the reader is referred to the work of Jennings et al. [45].

2.5.3 Simulation

We first proceed to transform the previously stated problem into a non-dimensional one, in which the unknown initial time-to-go, t_{f_0}, which is denoted hereinafter as t_f for simplicity, is transformed into a system parameter, z. The following variable transformation is adopted:

$$\begin{aligned} \tau &= \frac{t}{t_f} \\ x_1 &= X_r \\ x_2 &= Y_r \\ x_3 &= \theta \\ v_r &= \frac{V_M}{V_T} \\ u_1 &= \frac{A_n}{V_M^2} \\ z_1 &= V_M t_f \end{aligned} \tag{2.42}$$

The problem becomes that of minimising the following performance index:

$$J = \frac{1}{2}\int_0^1 z_1 u_1^2 d\tau \tag{2.43}$$

subject to the system dynamics:

$$\begin{aligned} \dot{x_1} \equiv f_1 &= z_1 \cdot (\frac{cos\phi}{v_r} - cosx_3) \\ \dot{x_2} \equiv f_2 &= z_1 \cdot (\frac{sin\phi}{v_r} - sinx_3) \\ \dot{x_3} \equiv f_3 &= z_1 \cdot u_1, \end{aligned} \tag{2.44}$$

under the initial conditions:

$$\tau_0 = 0 \quad x_{10} = R_0 \quad x_{20} = 0 \quad x_{30} = 0 \tag{2.45}$$

and the final (desired) conditions:

$$\tau_f = 1 \quad x_{1f} = 0 \quad x_{2f} = 0 \tag{2.46}$$

Note that we could identify the function g_0 defined in (2.40) as:

$$g_0 = \frac{1}{2} z_1 u_1^2$$

while the non-zero elements of the gradients necessary to carry out MISER3 computations are as follows:

$$\begin{aligned} \frac{\partial g_0}{\partial u_1} &= z_1 u_1 \\ \frac{\partial f_1}{\partial x_3} &= z_1 sin x_3 \\ \frac{\partial f_2}{\partial x_3} &= -z_1 cos x_3. \end{aligned} \tag{2.47}$$

The system described above was simulated using MISER3 for the same scenario used in [41], namely for $\phi = 30°$, $V_T = 1000\ ft\ s^{-1}$, $V_M = 1300\ ft\ s^{-1}$, and $R_0 = 3000\ ft$. One single difference was adopted though; it relates to the pursuer initial heading angle which was taken to be $\theta = 0$, in line with the intuitive practice of the human pilot.

The simulation results are plotted in Figure 2.9. Characteristically, we can see that the normal acceleration prescribed by the optimal PNG decreases with time until reaching a value close to zero, while the corresponding pursuer trajectory follows a corrective action, starting from the initial heading angle and, aligning the pursuer with the target path.

2.6 Summary

In this chapter, we have focussed on the proportional navigation guidance law for homing interceptors, equipped with passive bearing-only-measurement seekers. As a significant function of the guidance processor, the guidance law plays a major role

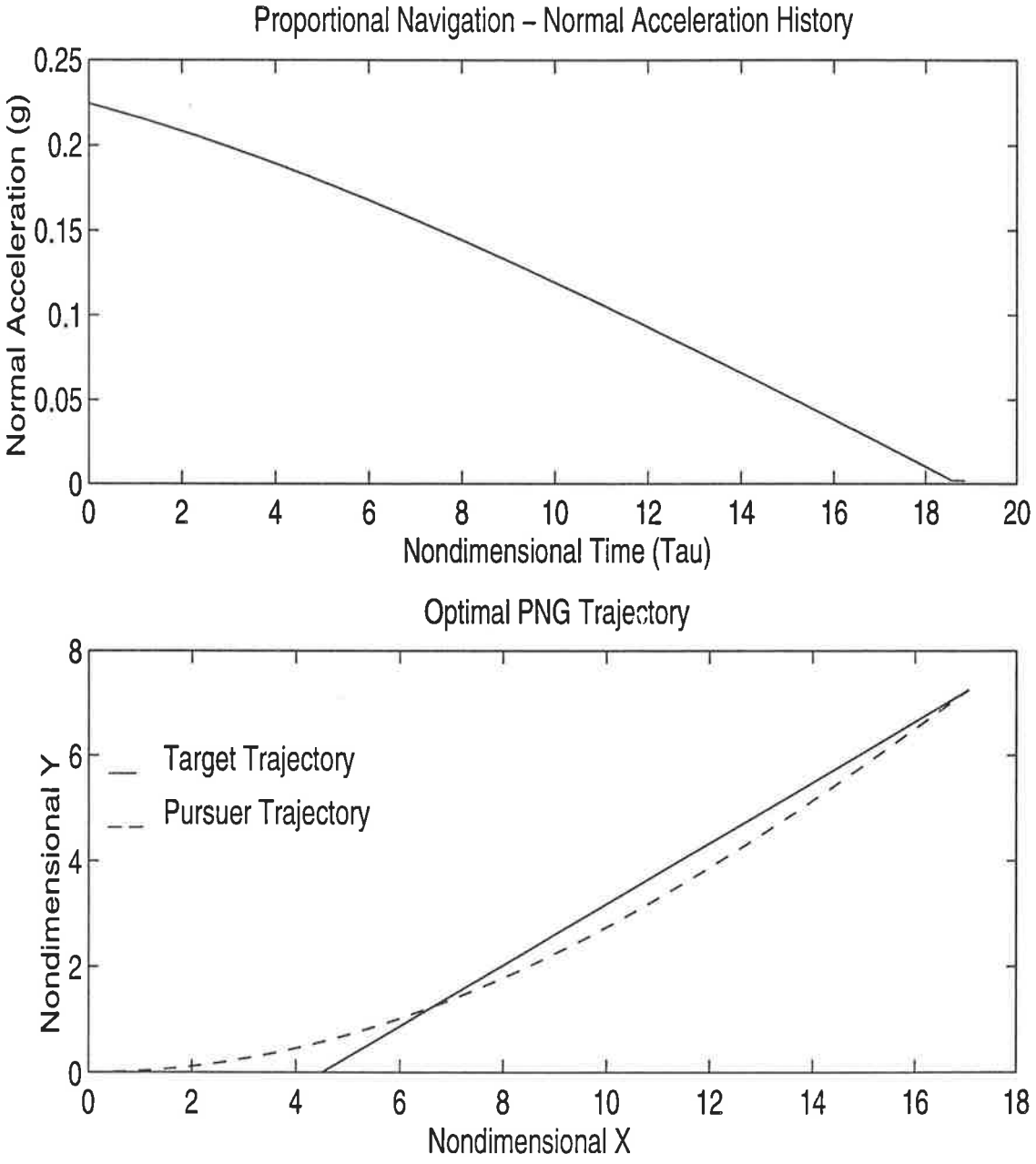

Figure 2.9: Optimal PNG trajectory and control history

in the way in which the interceptor is guided to intercept its target. Among all the known guidance laws, proportional navigation guidance (PNG) received the prime attention, due to its effectiveness and ease of implementation.

These advantages were illustrated through four different methods applied, in a deterministic setting, on a two-dimensional model. In the pure PNG the normal acceleration applied to the pursuer is taken to be proportional to the line-of-sight angle rate, in addition to the pursuer speed. The law, simulated using an integration technique reveals the main features of proportional navigation guidance, namely a control effort profile decreasing with time for high values of the navigation constant and increasing in time for small value of the navigation constant. The corrective nature of the PNG trajectory was evident in the simulation.

In the true proportional navigation method, the prescribed normal acceleration, which is proportional to the line-of-sight angle rate and to the terminal speed, was applied to a non-maneuvering as well as a maneuvering target. The simulation was conducted, starting from the initial conditions of the pursuer-target system and arriving at the generation of the normal acceleration in terms of the available data. The general features of proportional navigation, relating to the control effort and the induced trajectory were shown to be conserved.

True proportional navigation is simplified in the third method to allow for the derivation of analytical closed form solutions of PNG's equations of motion. Those solutions allow for the analytical interpretation of the features of PNG encountered in the previous two methods. Many important notions such as the miss-distance and the time-to-go were formally defined and the reasons for the inappropriateness of high values as well as low values of the navigation constant were revealed and a practical range on this constant was justified.

Finally, under the name *optimal proportional navigation*, we have included the formulation of PNG as an optimisation problem, taking advantage of the fact that PNG is a perturbation around a minimal control effort trajectory. The optimisation problem was solved using a software package, MISER3, based on control parametrisation. The introduction of MISER3, as an alternative to other calculus

of variation methods, was very significant because it will allow us to extend the PNG problem paving the way for the development of other guidance laws such as the one we will see in the next chapter.

Chapter 3

Maximum Information Guidance

One of the proportional navigation implementation methods presented in the previous chapter, namely *optimal proportional navigation*, is based on the modern optimal control theory. In general terms, this theory seeks to optimise a *performance index*, over an appropriate control range. The optimisation algorithm is typically based on Hamilton-Lagrange method when an analytical solution is possible. However, when the complexity of the system model does not allow for the existence of an analytical solution, numerical methods stemming from the theory of the calculus of variations are usually used.

In the linear quadratic optimal control problem, the performance measures contained in the performance index are generally composed of one or more of three quadratic measures, namely a measure on the state of the system, a measure on the control effort, and a measure on time. Optimising one or more of these measures produces satisfying results when the problem is considered to be deterministic. As shown in the previous chapter, *optimal proportional navigation* could be considered an optimisation algorithm where only control effort is optimised and produces satisfying results for the two-dimensional bearing-only-measurement problem (BOMP), if no noise is taken into consideration.

However, when the measurement noise enters into play, or when the modelling of the system dynamics is considered to be an inaccurate representation of the real system,

the above deterministic approach proves to be inadequate [52, 80]. In this case, a state estimator is needed to filter out the measurement noise and to provide state estimates. If the state estimator is used in cascade with the traditional PNG, it had been shown that it would suffer from a divergence problem, although the method is motivated by the separation principle for linear systems. The main reason behind the filter divergence problem was attributed to the lack of filter observability [80].

In this chapter, the structure of optimal proportional navigation is utilised as the framework for deriving an observability-enhanced guidance law. This law consists of adding to the optimal PNG performance index a measure of filter observability and then optimising this index in the same way control effort is optimised in optimal PNG. The rationale of this observability-enhanced guidance law, as it is applied here, is double-edged: although the measure of observability is defined in a stochastic setting in which the measurement is noisy, the guidance law itself is applied in a deterministic setting, as was the case with PNG in Chapter 2. It could be argued that our present objective is to simply examine first the characteristics of the law endowed with observability criteria. Therefore, it is permissible to recur to this double-edged approach, eliminating the need for a filter in the loop, at least in a first approach.

Three types of measures of observability are defined, all based on the Fisher information matrix which is derived using the duality theorem and the dual interplay between optimal regulation and optimal estimation. One of these measures is then used in an optimisation algorithm based on control parametrisation (section 2.5.2) and applied to the two-dimensional bearing-only-measurement problem (BOMP), to illustrate the general characteristics of the observability-enhanced guidance law, namely those related to the control history and the pursuer trajectory, as compared to the characteristics of proportional navigation.

3.1 Optimal Regulation and Optimal Estimation

The observability of linear noise-free systems has been known since the 1960's to be an indication of the link and accessibility between the measurements and the state of the system. For these systems, the observability matrix is well known as a signal quantising system observability in the same way the controllability matrix is a signal quantising system controllability. For noisy measurement systems however, the observability gramian is pinpointed instead, as an observability-related signal in which some indication of the measurement noise is taken into consideration.

In the following, the observability gramian is derived using the concept of duality between controllability and observability (and therefore optimisation and estimation) for a special class of stochastic systems where the measurements only are noisy. For this type of systems, it could be shown that the observability gramian is the inverse of the error covariance matrix and is called the Fisher information matrix.

In order to justify the use of the Fisher information matrix as a novel tool in the formulation of optimisation algorithms, it is useful to derive this matrix and define its relationship to the observability of noisy systems. In this context, we use the existing theory related to linear continuous systems and extend the results to systems with nonlinear measurements.

Roughly, the dual control concept consists of *blending* the requirements of the estimation algorithm into the design of the optimisation algorithm as if a common factor exists between optimisation and estimation. This idea is not completely new. In fact, upon laying down the foundations of modern control theory, Kalman realised the existence of a duality property between the optimum estimation problem and the optimum regulation problem. He defined a *duality concept* between the two problems and pointed out their similarities [48]. Kalman also derived the *duality theorem* which states that under several duality relations these two problems are equivalent [50].

Theorem 3.1 *(Duality Theorem) The optimal control problem and the optimal estimation problem are dual of each other in the following sense:*

Let $\tau \geq 0$. Replace every matrix $X(t) = X(t_0 + \tau)$ in the equations of the optimal estimation problem by $\hat{X}'(t) = \hat{X}'(T-t)$, where T is the discretisation period. Then one has the equations of the optimal control problem. Conversely, replace every matrix $\hat{X}(T - \tau)$ in the equations of the optimal control problem by $X'(t_0 + \tau)$. Then one has the equations of the optimal estimation problem [48].

Although differing in purpose, the duality theorem and the dual control seem to have a common ground. It is still true that "the physical significance of the duality is intriguing", but it is also true that "the duality theorem offers a powerful tool for developing the theory..." [48].

In the following sections, the Fisher information matrix, which plays an important role in the dual control concept, is derived by using the principles drawn from the duality theorem. The derivation is mainly based on the information contained in [24].

3.1.1 Linear Quadratic Regulator

Consider the linear dynamic system:

$$\dot{X}(t) = AX(t) + BU(t) \tag{3.1}$$

where the control law is proposed to be linear:

$$U(t) = -GX(t) \tag{3.2}$$

where G is a constant gain vector.

The closed loop equation could be written as:

$$\dot{X} = (A - BG)X \equiv A_c X \tag{3.3}$$

and the closed loop solution in terms of the transition matrix $\Phi_c(\tau, t)$ between the present time t and any instant τ is:

$$X(\tau) = \Phi_c(\tau, t)X(t) \tag{3.4}$$

The linear quadratic regulator problem consists of finding the gain, G_{opt}, which optimises the performance criterion, defined between two arbitrary time instants t and T, as:

$$J = \int_t^T [X'(\tau)QX(\tau) + U'(\tau)R_c U(\tau)]d\tau \tag{3.5}$$

where Q is a positive semi-definite state weighting matrix and R_c a positive definite control weighting matrix, while the superscript $'$ denotes the transpose.

Using (3.2) in (3.5), the performance index becomes:

$$J = \int_t^T X'(\tau)L(\tau)X(\tau)d\tau \tag{3.6}$$

where

$$L(\tau) = Q + G'R_c G$$

With (3.4) we have:

$$J = X'(t)S(t, T)X(t) \tag{3.7}$$

where

$$S(t, T) = \int_t^T \Phi_c'(\tau, t)L(\tau)\Phi_c(\tau, t)d\tau \tag{3.8}$$

is a symmetric matrix, which we will call *system performance matrix.*

Finally, the derivatives of (3.6) and (3.7) are obtained and equated to yield:

$$-\dot{S} = SA_c + A_c'S + L, \quad S(T,T) = 0 \tag{3.9}$$

This differential equation and its solution in (3.8) play an important role in optimal regulation and optimal estimation.

Assuming that a gain G_{opt} exists such that the performance index V is minimised, there would correspond to it a matrix S_{opt} which satisfies the differential equation (3.9). Any other gain G and any corresponding matrix S could be written as:

$$G = G_{opt} + H$$

$$S = S_{opt} + D$$

By substituting S and S_{opt} into (3.9) and subtracting the resulting equations from each other, we derive a differential equation to be satisfied by the "residual" matrix D, namely:

$$-\dot{D} = DA_c + A_c'D + (G_{opt}'R_c - S_{opt}B)H + H'(R_cG_{opt} - B'S_{opt}) + H'R_cH \tag{3.10}$$

This equation is of the same form given by (3.9) with the matrix L given by the last three terms. On the other hand, an optimal gain produces, by definition, a minimum performance index:

$$X'S_{opt}X \leq X'(S_{opt} + D)X = X'S_{opt}X + X'DX$$

This means that D has to be at least positive semi-definite. This condition is only satisfied if:

$$G_{opt} = R_c^{-1}B'S_{opt} \tag{3.11}$$

where S_{opt} satisfies (3.9) with the control gain replaced by the expression of G_{opt}:

$$-\dot{S}_{opt} = S_{opt}A + A'S_{opt} - S_{opt}BR_c^{-1}B'S_{opt} + Q \tag{3.12}$$

This is the matrix Riccati equation. It also plays an important role in the linear regulation theory and its dual discipline.

3.1.2 Linear Stochastic Estimator

Consider the system dynamics as:

$$\dot{X} = FX + w, \quad given \quad X(0) \tag{3.13}$$

and the observations (measurements) as:

$$Y = CX + v \tag{3.14}$$

where v and w are Gaussian uncorrelated zero mean white noise having the positive definite functions V and W as spectral densities, respectively:

$$E\{w(\tau)w'(\xi)\} = W(\tau)\delta(\tau - \xi) \tag{3.15}$$

$$E\{v(\tau)v'(\xi)\} = V(\tau)\delta(\tau - \xi) \tag{3.16}$$

$$E\{v(\tau)w'(\xi)\} = 0 \quad \forall\tau, \xi \tag{3.17}$$

The solution of (3.13) in terms of the transition matrix could be written as:

$$X(t) = \Phi(t, t_0)X(t_0) + \int_{t_0}^{t} \Phi(t, \tau)w(\tau)d\tau \tag{3.18}$$

The state correlation matrix could be written as:

$$R_X(t,\tau) = E\{X(t)X'(\tau)\} = \Phi(t,t_0)E\{X(t_0)X'(t_0)\}\Phi'(t,t_0) + \int_{t_0}^{t}\int_{t_0}^{\tau}\Phi(t,\tau)E\{w(\tau)w'(\xi)\}\Phi'(\tau,\xi)d\xi d\tau \tag{3.19}$$

Given the initial state covariance matrix $P_s(t_0) = E\{X(t_0)X'(t_0)\}$ we could write the correlation matrix, for $\tau \geq t$, after a few manipulations:

$$R_X(t,\tau) = P_s(t)\Phi'(\tau,t) \tag{3.20}$$

where $P_s(t)$ is called the *state covariance matrix*, and is given by:

$$P_s(t) = R_X(t,t) = \Phi(t,t_0)P_s(t_0)\Phi'(t,t_0) + \int_{t_0}^{t}\Phi(t,\tau)W\Phi'(t,\tau)d\tau \tag{3.21}$$

By comparing the state covariance matrix given by (3.21) to the system performance matrix given by (3.8), and taking into consideration the distinctions due to the integration limits and to the duality relations [47], we could apply the duality principle and deduce that $P_s(t)$ is a solution to the following differential equation:

$$\dot{P}_s = P_sF' + FP_s + W, \quad given \quad P_s(t_0) \tag{3.22}$$

This equation is comparable to (3.9) corresponding to the linear quadratic regulator problem.

If we now consider a system similar to (3.13), to which an input $U(t)$ is applied and an output $Y(t)$ is extracted, we undertake to find an estimate $\hat{X}$ of the state X having the dynamics:

$$\dot{\hat{X}} = F\hat{X} + K(Y - C\hat{X}) + BU(t) \tag{3.23}$$

It is possible to obtain the dynamics of the error function $x = X - \hat{X}$:

$$\dot{x} = F_c x + \zeta \tag{3.24}$$

where

$$F_c \equiv F - KC$$

and ζ is the error noise with a spectral density W_e given by:

$$W_e = W + KVK'$$

By comparing the dynamics of the error to the dynamics given by (3.13), we could write an equation similar to (3.22) but in terms of the error covariance matrix:

$$\dot{P} = F_c P + P F_c' + W_e, \quad given \quad P(t_0) \tag{3.25}$$

It becomes therefore clear that the problem of finding the optimal gain K_{opt}, which minimises the error covariance matrix P, could be reduced to a linear regulator problem, using the duality theorem. The expressions of the optimal estimation gain and its corresponding differential equation (to be satisfied by the error covariance matrix), could be deduced from (3.11) and (3.12) after taking into consideration the duality relations. We thus have:

$$K_{opt} = P_{opt} C' V^{-1} \tag{3.26}$$

and

$$\dot{P}_{opt}^{-1} = P_{opt} A' + A P_{opt} - P_{opt} C' V^{-1} C P_{opt} + W \tag{3.27}$$

It is from this last differential equation that the Fisher information matrix is derived.

3.2 Fisher Information Matrix

The above results could be extended to stochastic linear systems associated with nonlinear measurements. Instead of the process given by (3.13) and its associated measurements defined by (3.14), let us consider the following process and associated nonlinear measurements:

$$\dot{X} = FX + BU + w \tag{3.28}$$

$$Y = \sigma(X) + v \tag{3.29}$$

where w and v are two Gaussian white noise vectors having two positive definite functions W and V for spectral densities, respectively, and $\sigma(X)$ is a nonlinear function of X.

Given an *optimised control history* $U(t)$, it is generally possible to find a *nominal* path, X_N which verifies the deterministic form of (3.28), namely:

$$\dot{X}_N = FX_N + BU \tag{3.30}$$

If we could verify that the measurement perturbations around the nominal trajectory are "small" enough, we could linearise those perturbations around this trajectory using Taylor's series expansion to the first order term. That is:

$$Y = \sigma(X_N) + \frac{\partial \sigma}{\partial X}|_{X=X_N}(X - X_N) + v \tag{3.31}$$

Let:

$$x = X - X_N \tag{3.32}$$

$$y = Y - \sigma(X_N) \tag{3.33}$$

Subtracting (3.30) from (3.28) and manipulating (3.31):

$$\dot{x} = Fx + w \tag{3.34}$$

$$y = H(X_N)x + v \tag{3.35}$$

where

$$H(X_N) \equiv \frac{\partial \sigma}{\partial X} |_{X=X_N} \tag{3.36}$$

Note that the determination of the *optimised control variable* is normally performed by an optimisation algorithm. Once determined, it is used in the state estimation algorithm by following one of the linear optimal estimation algorithms as described by (3.23). This procedure which extends the estimation technique from linear to nonlinear systems is known as *extended state estimation* or *extended filtering.*

Considering the propagation equation of the error covariance matrix, namely (3.27), replacing P_{opt} by P for convenience, and using the linearised form of the measurements (3.35), we have:

$$\dot{P}^{-1} = PA' + AP - PH'(X_N)V^{-1}H(X_N)P + W \tag{3.37}$$

For a noise free process ($W = 0$), (3.37) can be transformed using a matrix identity: $\dot{P}^{-1} = -P^{-1}\dot{P}P^{-1}$, into a form similar to that given by (3.9) in P^{-1}:

$$-\dot{P}^{-1} = P^{-1}A + A'P^{-1} - H'(X_N)V^{-1}(X_N)H(X_N) \tag{3.38}$$

Its solution is given by (cf (3.8) with $T \equiv t_0$):

$$I = P^{-1} = \int_{t_0}^{t} \Phi' H'(X_N)V^{-1}H(X_N)\Phi d\tau \tag{3.39}$$

This is known as the "Fisher information matrix" [41, 55, 80].

Lemma 3.1 *For a system described by (3.34) and (3.35), for which no process noise is considered and the additive measurement noise is white and Gaussian, the Fisher information matrix which represents the amount of information in the system, is given by the inverse of the covariance matrix.*

Kalman [47, 49] showed that a dynamical system described by (3.34) and (3.35) is completely observable if, and only if, the information matrix given by (3.39) is positive definite [44]. Based on this result, we could establish a close link between system observability and the Fisher information matrix, which is subsequently called the *observability gramian* [25].

Theorem 3.1 *(Observability theorem) A system is observable if and only if the matrix defined by (3.39) is nonsingular for* $t > t_0$.

This matrix is called the observability gramian.

It is on this link between system observability and the observability gramian that the crux of the present study is built. In other terms, if we could quantify system observability by defining a certain measure on observability, it would be possible to maximise it through the performance index used in the optimisation algorithm. Note that this performance index is similar to the one given by (3.5), since the optimisation algorithm could be seen as a nonlinear counterpart of the (linear) optimal regulation problem (section 3.1).

This clears the way for the definition of the measure of observability based on the observability gramian. Any possible norm of the observability gramian is an acceptable measure as long as it could be written under the integral form given by (3.5). Since the observability gramian is itself an integral, it is necessary that the envisaged norm accommodates the integration operation in an acceptable fashion. In the next section, several candidate norms are defined and one of them is adopted in the last section.

3.2.1 Maximum Information - The Hilbert Norm

A possible definition of the observability measure could be deduced upon realising that maximising some measure of the Fisher information matrix can be translated into minimising the Hilbert (or spectral) norm of the error covariance matrix (see (3.39)). This procedure amounts to maximising the minimum eigenvalue of the information matrix [83]. In the two-dimensional bearing-only-measurement problem (BOMP), the corresponding performance index, relative to the position part of the information matrix, could be written as:

$$J = \lambda_{min} I_2 = \frac{1}{2}[(I_{11} + I_{22}) - \sqrt{(I_{11} + I_{22})^2 - 4(I_{11}I_{22} - I_{12}I_{21})}] \tag{3.40}$$

where:

$$\begin{aligned} H_1 &= -\frac{Y_r}{X_r^2 + Y_r^2} \\ H_2 &= \frac{X_r}{X_r^2 + Y_r^2} \end{aligned} \tag{3.41}$$

$$\begin{aligned} I_{11} &= \int_{t_0}^{t_f} H_1(X_N) V^{-1} H_1(X_N) dt \\ I_{22} &= \int_{t_0}^{t_f} H_2(X_N) V^{-1} H_2(X_N) dt \\ I_{12} &= \int_{t_0}^{t_f} H_1(X_N) V^{-1} H_2(X_N) dt \\ I_{21} &= \int_{t_0}^{t_f} H_2(X_N) V^{-1} H_1(X_N) dt \end{aligned} \tag{3.42}$$

and X_r and Y_r are the relative position coordinates between the pursuer and the target.

The measure (3.40) was used in [40] to generate an observability-enhanced trajectory. This measure cannot be accommodated, however, by the control parametrisation technique (section 2.5.2), since this technique only allows for performance indices of the form encountered in (2.40). It is clearly seen that (3.40) is not

amenable to the standard canonical form of MISER3 because the square root does not commute with the integral operation and because the product of integrals is not equal to the integral of products. This is in line with the reason behind the rejection in [80] of the determinant as an allowable measure of observability due to the non-commutability of the product and integral operations.

3.2.2 Maximum Information - The Trace

One alternative choice of the observability measure is the trace of the Fisher information matrix [80]. Unlike the determinant operation, the trace commutes with the integration operation, making it possible to define a performance index of the form given by (2.40).

In order to reduce the amount of computations involved to determine the performance index, it is possible to partition the problem into several parts (position, velocity, and acceleration), and determine the trace of the most relevant part (position). In the two-dimensional BOMP example, the above procedure leads to the following definition of a performance index providing a measure on maximum information (or maximum observability):

$$J = I_{11} + I_{22} \tag{3.43}$$

where I_{11} and I_{22} are given by (3.42).

The index described by (3.43) could be written under the form (Appendix A):

$$J = \int_{t_0}^{t_f} \frac{dt}{1 + \kappa(X_r^2 + Y_r^2)} \tag{3.44}$$

where κ is a constant dependent on the noise model (equivalent to the constant c in [80]).

3.2.3 Maximum Information - The b-norm

In the following, we introduce a new measure of observability which makes use of all the elements of the information matrix.

Let us consider the sum of the absolute values of all the elements of an $n \times n$ matrix A. This sum could be shown to be a norm on the matrix A.

Theorem 3.1 *Given a matrix $A \in \mathbb{R}^{n \times n}$, where $n \in \mathbb{N}$, the sum ot the absolute values of all the elements of A is a norm of A.*

For a proof of the above theorem, see Appendix A. This norm is hereafter called *"the b-norm"*.

The fact that all the elements of the matrix are involved in the b-norm (as opposed to only the diagonal elements in the trace) leads to believe that its optimisation should bring about several additional advantages. The interactions between cross diagonal elements are taken into consideration with this norm, which should have an important effect on the nature of the optimised information.

In order to derive the expression of the b-norm of the information matrix, let us consider the expression of the information matrix relating to the two-dimensional bearing-only-measurement problem, defined along the entire engagement trajectory (cf. equation 3.39):

$$I = \int_{t_0}^{t_f} \Phi' H' V^{-1} H \Phi d\tau \tag{3.45}$$

As we shall see in the next chapter, the transition matrix Φ for the two-dimensional BOMP takes the following form (see also [31, 83]):

$$\Phi(t_{k+1}, t_k) = \begin{bmatrix} 1 & 0 & f_1 & 0 & f_4 & 0 \\ 0 & 1 & 0 & f_1 & 0 & f_4 \\ 0 & 0 & 1 & 0 & f_3 & 0 \\ 0 & 0 & 0 & 1 & 0 & f_3 \\ 0 & 0 & 0 & 0 & f_2 & 0 \\ 0 & 0 & 0 & 0 & 0 & f_2 \end{bmatrix} \tag{3.46}$$

where:

$$\begin{aligned} f_1 &\equiv t_{k+1} - t_k \\ f_2 &= e^{-\lambda f_1} \\ f_3 &= \frac{1}{\lambda}(1 - e^{-\lambda f_1}) \\ f_4 &= \frac{1}{\lambda^2}(e^{-\lambda f_1} + \lambda f_1 - 1) \end{aligned} \tag{3.47}$$

while the measurement gradient vector H has the form:

$$H = [H_1 \quad H_2 \quad 0 \quad 0 \quad 0 \quad 0] \tag{3.48}$$

where the components H_1 and H_2 are given by (3.41), while the measurement noise spectral density has the form:

$$V = \frac{a}{X_r^2 + Y_r^2} + b \tag{3.49}$$

where a and b are two constants characterising the measurement noise.

Consequently, it is possible, due to the explicit form of the above expressions, to obtain a closed form expression of the b-norm of the information matrix I (see Appendix A), namely:

$$J_I = \int_{t_0}^{t_f} \frac{(1 + \frac{2|X_r Y_r|}{R^2})(1 + t + \mid e^{-t} + t - 1 \mid)^2}{a + bR^2} dt \tag{3.50}$$

where $R^2 = X_r^2 + Y_r^2$.

In general terms, although the measure (3.50) is relatively complex and not quadratic (and is not therefore amenable to a closed form solution as a linear quadratic optimal control problem as we shall see in Chapter 5), it could be easily put under the canonical form of MISER3 (2.40). It is therefore acceptable as a performance index in a control parametrisation optimisation scheme, in addition to being a more comprehensive measure than the trace.

3.3 Maximum Information Characteristics

In the following, it is envisaged to use one of the previously mentioned measures of observability, namely the trace (of the position part) of the fisher information matrix (section 3.2.2), in an optimisation algorithm similar to the one used in the previous chapter for proportional navigation. Since the setting is still purely deterministic, our purpose will not be to test the overall guidance performance, rather it is meant as a preliminary simulation aiming to compare the general characteristics of an observability-enhanced guidance law to the "observability-deprived" PNG.

Let us consider the two-dimensional guidance model dynamics for the BOMP problem (2.1), presented in Chapter 2 (see Figure 2.2), namely:

$$\begin{aligned} \dot{X}_r &= V_T cos\phi - V_M cos\theta \\ \dot{Y}_r &= V_T sin\phi - V_M sin\theta \\ \dot{\theta} &= \frac{A_n}{V_M} \end{aligned} \tag{3.51}$$

Given the initial conditions (2.4), namely:

$$t_0 = 0 \quad X_{r0} = R_0 \quad Y_{r0} = 0 \quad \theta_0 = 0 \tag{3.52}$$

and the final (desired) conditions (2.5) and (2.6):

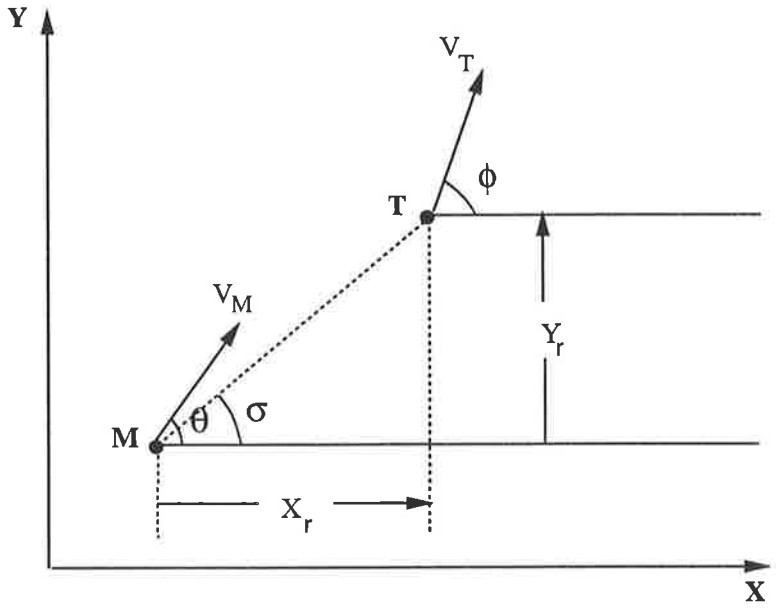

Figure 3.1: Geometry of the two-dimensional BOMP

$$t_f = free \quad X_{rf} = 0 \quad Y_{rf} = 0 \quad \theta_f = free \tag{3.53}$$

We proceed to define a performance index composed of two terms. The first one is derived from (3.44), and the second is a classical control effort term:

$$J = \frac{1-\omega}{2}\int_{t_0}^{t_f} A_n^2 dt - \omega \int_{t_0}^{t_f} \frac{dt}{1+\kappa(X_r^2+Y_r^2)} \tag{3.54}$$

where ω is an observability weighting coefficient such that: $0 \leq \omega \leq 1$.

Note that when $\omega = 0$ the problem is a standard control effort optimisation which is equivalent to a proportional navigation guidance law, while if $\omega = 1$ the problem is a maximum information guidance law.

Under these circumstances, the problem is formulated in a fashion suitable for implementation on MISER3, and the results of the simulation are recorded for $\phi = 30°$, $V_T = 1000\ ft\ s^{-1}$, $V_M = 1300\ ft\ s^{-1}$, $\kappa = 22.5 \times 10^{-7}\ ft^{-2}$ and $R_0 = 3000\ ft$.

3.3.1 Problem Formulation

In [41] the dynamics model (2.1), the initial (2.4) and final conditions (2.5) and (2.6), as well as the performance index (3.54) are transformed into a non-dimensional model via the following variable transformation:

$$\begin{aligned} \tau &= \sqrt{\kappa} V_M t \\ \xi &= \sqrt{\kappa} X_r \\ \eta &= \sqrt{\kappa} Y_r \\ v_r &= \frac{V_M}{V_T} \\ \alpha &= \frac{A_n}{\sqrt{\kappa} V_M^2} \\ \rho &= \sqrt{\kappa} R \end{aligned} \tag{3.55}$$

The problem becomes that of minimising (optimising) the following performance index:

$$J = \frac{1-\omega}{2} \int_{\tau_0}^{\tau_f} \alpha^2 d\tau - \omega \int_{\tau_0}^{\tau_f} \frac{d\tau}{1+\xi^2+\eta^2} \tag{3.56}$$

subject to the system dynamics:

$$\begin{aligned} \dot{\xi} &= \frac{cos\phi}{v_r} - cos\theta \\ \dot{\eta} &= \frac{sin\phi}{v_r} - sin\theta \\ \dot{\theta} &= \alpha \end{aligned} \tag{3.57}$$

and the initial and final conditions, respectively:

$$\tau_0 = 0 \quad \xi_0 = \rho_0 \quad \eta_0 = 0 \quad \theta_0 = 0 \tag{3.58}$$

$$\tau_f = free \quad \xi_f = 0 \quad \eta_f = 0 \tag{3.59}$$

We transform the non-dimensional model above into the standard canonical form of MISER3 (2.40) and (2.41) by adopting the following transformations:

$$\begin{aligned} s &= \frac{\tau}{\tau_f} \\ x_1 &= \xi \\ x_2 &= \eta \\ x_3 &= \theta \\ u_1 &= \alpha \\ z_1 &= \tau_f \end{aligned}$$

The system dynamics take the form:

$$\begin{aligned} \dot{x_1} \equiv f_1 &= z_1 \cdot (\frac{cos\phi}{v_r} - cosx_3) \\ \dot{x_2} \equiv f_2 &= z_1 \cdot (\frac{sin\phi}{v_r} - sinx_3) \\ \dot{x_3} \equiv f_3 &= z_1 \cdot u_1 \end{aligned} \tag{3.60}$$

under the initial conditions:

$$s_0 = 0 \quad x_{10} = \rho_0 \quad x_{20} = 0 \quad x_{30} = 0 \tag{3.61}$$

and the final (desired) conditions:

$$s_f = 1 \quad x_{1f} = 0 \quad x_{2f} = 0 \tag{3.62}$$

while the performance index becomes:

$$J = \frac{1-\omega}{2} \int_0^1 z_1 u_1^2 ds - \omega \int_0^1 \frac{z_1}{1 + x_1^2 + x_2^2} ds \tag{3.63}$$

Note that we could identify the function g_0 in (2.40) as:

$$g_0 = \frac{1-\omega}{2} z_1 u_1^2 - \omega \frac{z_1}{1+x_1^2+x_2^2}$$

while the non-zero elements of the gradients necessary to carry out MISER3 computations are as follows:

$$\begin{aligned}
\frac{\partial g_0}{\partial x_1} &= \frac{2\omega z_1 x_1}{(1+x_1^2+x_2^2)^2} \\
\frac{\partial g_0}{\partial x_2} &= \frac{2\omega z_1 x_2}{(1+x_1^2+x_2^2)^2} \\
\frac{\partial g_0}{\partial u_1} &= (1-\omega) z_1 u_1 \\
\frac{\partial f_1}{\partial x_3} &= z_1 sin x_3 \\
\frac{\partial f_2}{\partial x_3} &= -z_1 cos x_3.
\end{aligned} \tag{3.64}$$

3.3.2 Simulation Results

The system described above, its initial and final conditions and the performance index, J, were processed through the standard version of MISER3 (section 2.5.2) for increasing values of ω. The number of knots chosen was 64 which is sufficient to generate effective control, and the range of control effort was made practically infinite ($\pm 10^{20}$). The results of the simulations are plotted in Figure 3.2. This figure shows the trajectories of the target and missile, as well as the normal acceleration histories for different observability weighting coefficients ω ranging from 0 to 0.24. Higher values of ω proved to lead MISER3 to diverge due to intergration failure. This was also observed by other investigators using different computational methods [41].

The numerical informations obtained from Figure 3.2 are summarised in Table 3.1 which includes the minimum performance index J_{min} reached for each observability coefficient ω, as well as the time-to-go t_f, and the maximum normal acceleration A_{nMax}. The amount of information I_{tot}, represented by the integrated weighted

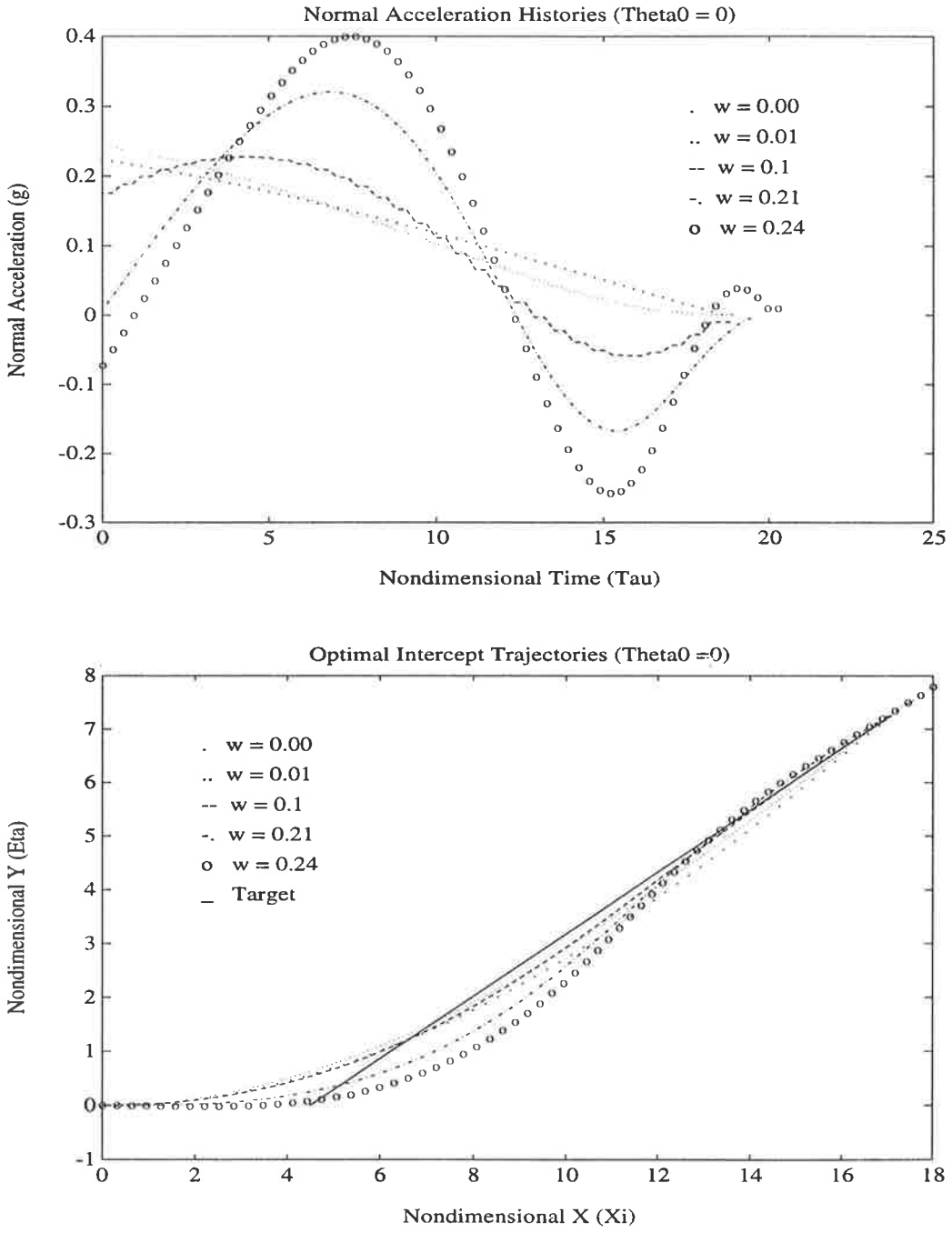

Figure 3.2: Observability-enhanced guidance law

ω	J_{min}	$t_f(s)$	$A_{nMax}(g)$	I_{tot}
0	.0128	9.6757	.2247	0
.01	-.0450	9.5847	.2437	.0570
.1	-.5689	9.6476	.2274	.5698
.21	-1.2141	10.0491	.3204	1.1584
.24	-1.3918	10.3937	.3995	1.1967

Table 3.1: Observability-enhanced guidance law - numerical results

trace of the Fisher information matrix is also recorded.

It is noted that as the observability coefficient ω increases, the information content appears to increase at the expense of a longer time-to-go and a larger maximum control variable. On the other hand, as the guidance law moves away from "proportional navigation" towards "maximum information", the control history becomes oscillatory with increasing frequency while the corresponding pursuer trajectory tends to approach a tail chase. These results agree with those obtained in [41] and tend to characterise the optimisation algorithms in which the observability information content is taken into consideration.

3.4 Summary

In this chapter, an observability-enhanced guidance law is explored. Similar in form to the *optimal proportional navigation*, seen in Chapter 2, this law, proposed by [41] and called maximum information guidance seeks to optimise observability in addition to control effort, which is solely optimised in optimal PNG. Although the motivation behind maximum information guidance is stochastic in nature, the setting in which it is *tested* herein is deterministic. Control parametrisation (MISER3) and constrained optimisation are used the same way they were used in Chapter 2. The only difference lies in the definition of the performance index which, in the case of maximum information, is a measure of system observability.

Three measures of system observability were defined, all based on the Fisher information matrix. This matrix, called the observability gramian for the noisy measurement systems at hand, is first derived for linear systems using the duality relations between controllability and observability. The definition is then extended to the case of nonlinear measurement systems which is the case for our bearing-only-measurements. The relationship between Fisher information matrix and system observability was particularly emphasised based on Kalman's theorem [47, 49].

The first candidate measure of observability was taken to be the position part of the Fisher information matrix Hilbert (or spectral) norm. The derivation of this norm is possible and although it was previously used to define one form of the maximum information guidance, it is not amenable to the canonical form of the performance index used by MISER3.

The second explored measure of observability was the trace (of the position part) of the Fisher information matrix. Although this measure does not exactly represent information on the interactions of all combinations of the state components (diagonal elements only), it represents a sizable amount of the information needed and offers, in addition, a viable alternative to be used with control parametrisation as an optimisation tool. Since the trace operation is commutative with the integral operation, the resulting performance index can take the standard canonical form of MISER3.

The third and last candidate measure of observability was the b-norm of the Fisher information matrix. It consists of the sum of the absolute values of all its elements. This sum was first proved to be a norm, then derived in closed form for the two-dimensional BOMP problem. Although complex to handle, this norm is amenable to MISER3 formulation and includes all combinations of information contained in the Fisher information matrix.

In the last section of this chapter, the maximum information guidance law, based on the trace of the information matrix, was simulated and compared to proportional navigation. The performance index of the corresponding optimal law is made of two parts weighted by an observability coefficient. The first part represents the

PNG contribution and the second part the observability contribution. Depending on the value of the observability coefficient, the resulting law could be purely PNG or maximum information. Practically, it was possible to induce a certain amount of observability into the proportional navigation guidance law, but not a maximum amount. The reasons are linked to computational difficulty and to the fact that the "amount" of observability is limited depending on the geometry of the problem. Nevertheless, even with a partially informed guidance law, the effects of adding observability were clear. They mainly materialised in a shorter miss-distance, at an expense of a longer time-to-go and higher and oscillatory control history.

From a guidance point of view, better accuracy is therefore achieved but the running cost is higher. In addition, since adding observability leads to an oscillatory tail chase trajectory, it is concluded that the line-of-sight angle is not nulled in the shortest possible time, as is done with PNG. Instead, the trajectory is modulated while intercept is achieved at the same time. In the following chapter, these benefits of observability-enhanced guidance laws will be revisited in a stochastic setting.

Chapter 4

State Estimator

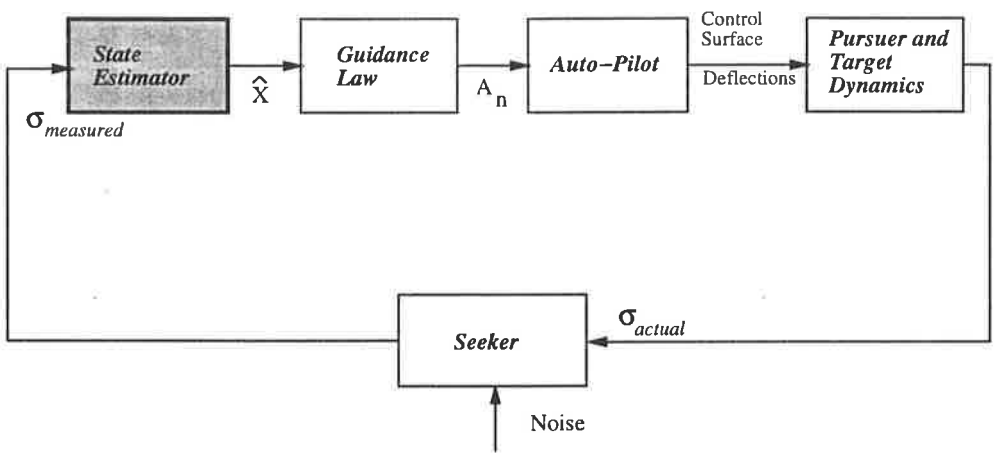

Figure 4.1: Closed loop guidance - the state estimator

In the previous two chapters, the guidance law was considered in a purely deterministic setting. Either proportional navigation or maximum information was taken to be the guidance law according to which the pursuer seeks to reach the moving target assuming that the relative dynamics between pursuer and target are known and that the seeker measurements are accurate. Although this type of deterministic analysis is permissible, since it allows to study the main characteristics of the guidance law, it does not faithfully portray the real problem where noise and uncertainties are present. Both types of perturbations add another dimension to the problem, and pose an additional challenge to the system designer.

Modelling errors are almost always existent and measurements are generally noisy

especially when the seeker used is low cost and the corresponding measurements are bearing-only. Consequently, there is a need for a state estimator in the guidance loop (Figure 4.1), whose role is to filter out, as much as possible, the noise and disturbances and recuperate the true relative state of the system, so that it could be used effectively in the guidance law. One objective of this chapter is to analyse the state estimator, especially the extended Kalman filter (EKF), and to explore some of its variants such as the modified gain extended Kalman filter and the iterative extended Kalman filters. Another objective is to apply the EKF to the missile guidance problem in a bid to illustrate its divergence problem, along a proportional navigation trajectory.

In the development of the maximum information guidance law in Chapter 3, the main motivation behind the design of an observability-enhanced guidance law was introduced. This motivation was identified as the divergence of the extended Kalman filter, when used along a trajectory provided by proportional navigation. In this chapter, we are going to "witness" more explicitly the divergence problem through the application of the extended Kalman filter to the two-dimensional BOMP problem considered in the last two chapters.

The performance of the EKF along PNG will also be compared to its performance along a trajectory provided by the maximum information guidance law. Although both laws are not given, here, as an explicit function of the state vector (control parametrisation and MISER3 are used to derive the normal acceleration in both guidance laws), we can clearly get a more realistic feel of the advantages and features of an observability-enhanced guidance law. Shorter miss-distance, higher normal acceleration and longer time-to-go are all apparent. In addition, the state estimation errors are compared between PNG and maximum information. The lower estimation errors associated with maximum information guidance coupled with the lower final miss-distance provide a glimpse of the achievement of a dual objective. This type of "dual control" will be dealt with separately in the next chapter.

In addition to the extended Kalman filter and its iterative variants, a more recent type of extended Kalman filter called the modified gain extended Kalman filter

will be explored. This state estimator takes advantage of the special form of the bearing-only-measurements available in the two-dimensional BOMP, to modify the formulation of the extended Kalman filter resulting in improved estimation performance.

4.1 Extended Kalman Filter

We have seen in Chapter 2 that bearing as well as range measurements are needed to compute the commanded pursuer acceleration when the guidance law is proportional navigation. If the on-board seeker provides only bearing information, e.g., line-of-sight angle σ, and if this information is noisy, which is the case in passive seekers, then an estimation technique is necessary to rectify any modeling uncertainty (absence of range) or reduce any measurement noise.

This technique, in the form of a Kalman filter [7, 44, 78], attempts to recuperate the system state (position, speed, etc.) by using the noisy measurements and the pursuer normal accelerations as they are prescribed by the guidance law (see Figure 4.1). Furthermore, since the measurements are nonlinear, the standard Kalman filter - optimal for linear systems - could not be used. One possible alternative is to linearise the measurements and "extend" the filter so that an algorithm similar to the standard Kalman filter could be used.

The guidance system whose state needs to be estimated could be written, in general, under the following continuous form:

$$\dot{X}(t) = AX(t) + BU(t) \tag{4.1}$$

$$Z(t) = \sigma(X(t)) + v(t) \tag{4.2}$$

where the state vector $X \in \mathbb{R}^n$, the measurement σ is a nonlinear function of the state and $v(t)$ is a Gaussian uncorrelated white noise whose spectral density is represented by the positive definite function denoted by V (see (3.16)).

Suppose that we generate by some suitable means a reference (or nominal) trajectory satisfying:

$$\dot{X}_N(t) = AX_N(t) + BU(t), \quad given \ X_N(t_0) \tag{4.3}$$

for $t \geq t_0$, where the nominal state vector X_N is close to the real state vector X.

We define the following state and measurement perturbations:

$$\begin{aligned} x(t) &= X(t) - X_N(t) \\ z(t) &= Z(t) - Z_N(t) \end{aligned} \tag{4.4}$$

where $Z_N(t) = \sigma(X_N(t))$ is the measurement along the nominal trajectory.

If we subtract (4.3) from (4.1) and expand (4.2) in Taylor's series around $X_N(t)$, we get:

$$\begin{aligned} \dot{x}(t) &= Ax(t) \\ z(t) &= \left.\frac{\partial \sigma}{\partial X}\right|_{X=X_N} x(t) + v(t) \end{aligned} \tag{4.5}$$

Discretising:

$$\begin{aligned} x_{k+1} &= \Phi(k+1,k)x_k, \quad given \ x_0 \\ z_k &= M(t_k, X_{N_{t_k}})x_k + v_k \end{aligned} \tag{4.6}$$

where $x_0 = \hat{X}_0 - X_N(t_0)$, $\hat{X}_0$ being the initial state estimate and,

$$M(t_k, X_{N_{t_k}}) = \left.\frac{\partial \sigma_i}{\partial X_j}\right|_{X=X_N(t_k)} \tag{4.7}$$

the measurement gradient.

We note that (4.6) are similar in form to the system and measurements equations of a standard Kalman filter, with the difference that the measurement matrix is not a constant matrix. We could therefore follow one of the various approaches to derive the standard Kalman filter algorithm [25].

However, it is important to realise that while the standard Kalman filter is applied to the state X of the system at hand, the Kalman filter developed herein for nonlinear measurements applies to the state perturbation x. Once the state perturbation has been calculated, at a certain time, the state $\hat{X}(k \mid k)$ could be deduced, if the choice of the nominal trajectory is well defined:

$$\hat{X}(k \mid k) = X_N(k) + \hat{x}(k \mid k) \tag{4.8}$$

which leads to the calculation of the forward state $\hat{X}(k+1 \mid k)$, by using the discretised solutions to the state and measurement equations (4.1) and (4.2), namely:

$$X_{k+1} = \Phi(k+1,k)X_k + \Gamma(k+1,k)U_k \tag{4.9}$$

$$Z_k = \sigma(X_k,k) + v_k \tag{4.10}$$

where the vector $\Gamma(k+1,k)$ is given by:

$$\Gamma(k+1,k) = \int_{t_k}^{t_{k+1}} \Phi(t_{k+1},\tau)B(\tau)d\tau \tag{4.11}$$

and derived explicitly in Appendix B. Note from (4.8) and (4.4) that:

$$\tilde{X}(k \mid k) \equiv X(k) - \hat{X}(k \mid k) = x(k) - \hat{x}(k \mid k) \equiv \tilde{x}(k \mid k) \tag{4.12}$$

which means that the state estimation error is equivalent to the state perturbation estimation error, and therefore their respective covariance matrices are the same:

$$P(k \mid k) = cov\{\tilde{X}(k \mid k)\} = cov\{\tilde{x}(k \mid k)\} \tag{4.13}$$

We deduce from the above that the choice of the nominal trajectory is very critical to the performance of the resulting filter. If this trajectory is generated off-line independently of the filter, the resulting filter is called the *linearised Kalman filter.* However, if this nominal trajectory is calculated on-line as indicated in the following section, the resulting filter is called the *extended Kalman filter* [15].

4.1.1 Choice of the Nominal Trajectory

As stated in [44], "the obvious choice of the reference trajectory is made (initially) with $X_N(t_0) = \hat{X}(t_0)$, the prior estimate of the state", in that case, we deduce from (4.8) that:

$$\hat{x}(t_0 \mid t_0) = 0 \tag{4.14}$$

and in view of the expression of the predicted state in the standard Kalman filter algorithm [25], applied to system (4.9), we can write:

$$\hat{x}(t_1 \mid t_0) = 0 \tag{4.15}$$

We can linearise subsequently about the estimated state vector $\hat{X}(t_1 \mid t_1)$. By (4.8), we conclude again:

$$\hat{x}(t_1 \mid t_1) = 0 \tag{4.16}$$

In a similar fashion, it is possible to determine that, between observations, the best estimate of the perturbation is null [44]:

$$\hat{x}(t \mid t_k) = 0 \tag{4.17}$$

for $t_k \leq t \leq t_{k+1} \quad \forall k$.

As a result, the best estimate of the state, between observations, is the nominal state provided by (4.3):

$$\hat{X}(k+1 \mid k) = \Phi(k+1 \mid k)\hat{X}(k \mid k) + \Gamma(k+1,k)U(k) \tag{4.18}$$

In the extended Kalman filter, the linearisation is therefore performed around the trajectory defined by (4.18). This is the essential feature of the EKF [82]. On the other hand, the remark, concerning the null perturbation estimate between observations, modifies the expression of the estimated state vector in the standard Kalman filter [25] to become:

$$\hat{X}(k+1 \mid k+1) = \hat{X}(k+1 \mid k) + K(k+1)[Z_{k+1} - \sigma(\hat{X}(k+1 \mid k)] \tag{4.19}$$

4.1.2 Algorithm

The extended Kalman filter algorithm follows the same steps of the numerous methods used to derive the standard Kalman filter algorithm, based on the state equation (4.1) and the measurement equation (4.2) and taking into consideration the equivalence satisfied by the covariance matrix in (4.13), in addition to the choice of the nominal trajectory. Upon carrying out suitable initialisation and given the input U and the measurement spectral density V, this algorithm consists of the following steps [25, 44]:

Step 1: Store the filter state $[\hat{X}(k \mid k),\ P(k \mid k)]$

Step 2: Calculate the predicted state:
$$\hat{X}(k+1 \mid k) = \Phi(k+1,k)\hat{X}(k \mid k) + \Gamma(k+1,k)U(k)$$

Step 3: Calculate the predicted error covariance:
$$P(k+1 \mid k) = \Phi(k+1,k)P(k \mid k)\Phi'(k+1,k)$$

Step 4: Derive the filter gain:

$$K(k+1) = P(k+1 \mid k)M'[MP(k+1 \mid k)M' + V(k+1)]^{-1}$$

Step 5: Compute the estimated state vector:

$$\hat{X}(k+1 \mid k+1) = \hat{X}(k+1 \mid k) + K(k+1)[Z_{k+1} - \sigma(\hat{X}(k+1 \mid k))]$$

Step 6: Deduce the updated error covariance:

$$P(k+1 \mid k+1) = [I - K(k+1)M]P(k+1 \mid k)$$
$$[I - K(k+1)M]' + K(k+1)V(k+1)K'(k+1)$$

Step 7: Set $k = k+1$ and return to step 1.

Note that in the above, $M \equiv M(k+1, \hat{X}(k+1 \mid k))$.

On the other hand, it is noted that the standard Kalman filter algorithm could readily be deduced from the above algorithm, by replacing the nonlinear expression of the measurement by its linear counterpart.

4.2 Modified Gain Extended Kalman Filter

As an alternative to the extended Kalman filter, it is possible to design a Kalman filter that takes advantage of the special form of the nonlinear measurements. In [4], it was shown that the bearing-only-measurement equation (4.2) could be expressed in a linear form as a function of the state. This result led to the formulation of a new guidance filter structure. The linear form of the measurement equation is the following:

$$(\sin\sigma)X_r - (\cos\sigma)Y_r = 0 \tag{4.20}$$

which can be verified by substitution of the equation defining the expression of the line-of-sight angle (2.3).

In a matrix form, the equation is expressed as:

$$HX = 0 \tag{4.21}$$

where:

$$X = [X_r \;\; Y_r \;\; U_r \;\; V_r \;\; A_{T_X} \;\; A_{T_Y}]' \tag{4.22}$$

and:

$$H = [\sin\sigma(X) \;\; -\cos\sigma(X) \;\; 0 \;\; 0 \;\; 0 \;\; 0] \tag{4.23}$$

Song & Speyer [76] use this measurement equation to develop a special Kalman filter called the modified gain extended Kalman filter. It is shown in [76] that the extended Kalman filter algorithm could still be used but with the measurement gradient H replaced by the "modifiable gain" G in the expression of the Kalman gain (step 4). G is defined as:

$$\sigma_k(X) - \sigma_k(X_N) = G_k(\sigma_k(X), X_N) \cdot (X - X_N) \tag{4.24}$$

where X and X_N are any two n-dimensional real vectors: $X \in \mathbb{R}^n$ and $X_N \in \mathbb{R}^n$.

Definition 4.1 *A time varying function σ_k: $\mathbb{R}^n \rightarrow \mathbb{R}^q$ is modifiable if there exists a $q \times n$ time varying matrix of functions G_k: $\mathbb{R}^q \times \mathbb{R}^n \rightarrow \mathbb{R}^q$, so that for any X, X_N $\in \mathbb{R}^n$ and $k \in Z_+$ (nonnegative integer), the relation (4.24) is verified.*

We note that if $\sigma(X)$ of (4.24) approaches $\sigma(X_N)$, then the vector G reduces to H and the MGEKF algorithm becomes equivalent to that of the extended Kalman filter. However, if $\sigma(X)$ is replaced by the *true* measurement Z, given by (4.2), the performance of the resulting algorithm has been shown to be superior to that of the extended Kalman filter [83].

For the two-dimensional guidance system, it is possible to derive the expression of the modified gain in terms of the line-of-sight angle σ and the relative coordinates X_r and Y_r [76]:

$$G = -D\frac{\eta}{\alpha}H \tag{4.25}$$

where

$$\begin{aligned} D &= \frac{1}{\cos\sigma X_{r_N} + \sin\sigma Y_{r_N}} \\ \alpha &= \tan\eta = \frac{Y_r X_{r_N} - X_r Y_{r_N}}{X_r X_{r_N} + Y_r Y_{r_N}} \\ \eta &= \sigma(X) - \sigma(X_N) \\ H &= [\sin\sigma(X) \quad -\cos\sigma(X) \quad 0 \quad 0 \quad 0 \quad 0] \end{aligned}$$

Recently, it has been shown in [26] that, when the angle η is sufficiently small, the expression of the modified gain could be simplified to the form:

$$\begin{aligned} G &= -DH \\ &= \frac{[\sin\sigma(X) \quad -\cos\sigma(X) \quad 0 \quad 0 \quad 0 \quad 0]}{\cos\sigma X_{r_N} + \sin\sigma Y_{r_N}} \end{aligned} \tag{4.26}$$

This simplified form avoids the numerical difficulties arising from a very small denominator obtained when the two measurements $\sigma(X)$ and $\sigma(X_N)$ approach the same value.

4.3 Iterative Kalman Filters

The use of iterative Kalman filters for guidance systems was suggested in [21] as one of 10 different approaches to the target tracking problem using bearing-only-measurements. Those theoretical approaches were designed to form the basis of a

simulation study aimed at achieving the best possible tracking performance. Around the same time, one form of the iterated extended Kalman filter (both rectangular and spherical) was used in [84] in a comparative study of the performance of several filters. The concurrent guidance law that was used, however, was the biased proportional navigation. As we shall see, those filters offer another alternative to the EKF, basically trading performance for time.

The main motivation behind the design of iterative filters is well related to the adequate choice of the nominal trajectory around which the system is linearised. In the linearisation procedure of a nonlinear estimation problem, the nominal trajectory has to satisfy the deterministic part of the process dynamics and it has to be at the same time *close enough* to the true trajectory. In the extended Kalman filter, the nominal trajectory is chosen to be equal to the best estimate between observations. In the following, two alternative approaches are briefly explored from a theoretical point of view. The iterative filters were applied in [34] to the two-dimensional BOMP problem and their performance compared to that of the EKF. They both exhibited less estimation errors than the EKF for most of the pursuer-target engagement within 2 to 3 local iterations.

4.3.1 Iterated Extended Kalman Filter

The assumption adopted in the extended Kalman filter that between observations, the nominal state is the best estimate of the state is a simplifying one. Let us consider the expression of the estimated state perturbation vector:

$$\hat{x}(k+1 \mid k+1) = \hat{x}(k+1 \mid k) + K(k+1) \cdot [z_{k+1} - M \cdot \hat{x}(k+1 \mid k)]$$

where, by definition:

$$\hat{x}(k+1 \mid k+1) = \hat{X}(k+1 \mid k+1) - \hat{X}(k+1 \mid k) \tag{4.27}$$

$$z_{k+1} = Z_{k+1} - \sigma(\hat{X}(k+1 \mid k), k+1) \tag{4.28}$$

This assumption leads to the expression of the estimated state vector in step 5 of section 4.1.2.

(4.27) is the direct result of the application of the standard Kalman filter algorithm to the linearised form of the deviation between the nonlinear filter trajectory and the nominal (or reference) trajectory [44].

The above assumption might well be true around the beginning of the estimation process, but usually ceases to be accurate in later stages. The iterated extended Kalman filter proposes a remedy to this deficiency by firstly calculating the state estimate based on this same assumption, then recalculating it based on the assumption that the difference between the best estimate and the nominal trajectory, between observations, is equal to the difference between the newly calculated estimate and the estimate between observations. This process is repeated until the variation in the new estimate becomes negligible. In this case, the new state estimate, denoted as η, will be given by the iterator:

$$\begin{aligned} \eta_{i+1} &= \hat{X}(k+1 \mid k) + K(k+1) \cdot [Z_{k+1} - \sigma(\eta_i, k+1) \\ &\quad -M \cdot \{\hat{X}(k+1 \mid k) - \eta_i\}] \end{aligned} \tag{4.29}$$

where i denotes the iteration number.

The iterations start by taking $\eta_1 = \hat{X}(k+1 \mid k)$, and proceed to update the value of η. It can be seen that the measurement gradient, in those iterations multiplies a factor that was assumed null in the EKF. It is, therefore expected that the iterated extended Kalman filter reduces the effect of measurements nonlinearities, especially when these nonlinearities are significant [19].

4.3.2 Iterated Linear Filter-Smoother

This filter uses an iterative procedure to enhance the estimation, not only beyond time t_{k+1} but also between observations (in the interval t_k to t_{k+1}) [44], thus allowing

theoretically for a better performance. Starting from an initial guess for the state variable, ξ_i ($\xi_1 = \hat{X}(k \mid k)$), the algorithm calculates the nominal point based on the (generally nonlinear) state equation. The estimate between observations $\hat{X}(k+1 \mid k)$ is calculated using that nominal point:

$$\hat{X}(k+1 \mid k) = X_N(k+1, \xi_i) + \Phi(k+1, k; \xi_i)[\hat{X}(k \mid k) - \xi_i] \tag{4.30}$$

The algorithm of the iterated extended Kalman filter (section 4.3.1) is then used once to calculate a better estimate η_{i+1} of the state vector $\hat{X}(k+1 \mid k+1)$, which is smoothed back to time t_k, using a linearised smoother to generate a better estimate of ξ_i:

$$\xi_{i+1} = \hat{X}(k \mid k) S(k; \xi_i)[\eta_{i+1} - \hat{X}(k+1 \mid k)] \tag{4.31}$$

where $S(k; \xi_i) = P(k \mid k)\Phi'(k+1, k; \xi_i)P^{-1}(k+1 \mid k)$.

At this stage the whole procedure is repeated, starting from the calculation of the nominal point. The iterations are terminated once the smoothed value, ξ_i, stops changing significantly.

As we can see, an additional feature of this filter lies in the calculation of the nominal point using the process nonlinear model. The benefit is therefore more obvious where the nonlinearities are in the process. (See [44] for a more accurate description of this filter).

4.4 Simulations and Results

In this section, we apply the extended Kalman filter to the two-dimensional bearing-only-measurement problem. Since the formulation of the extended Kalman filter (section 4.1) assumes a linear filter model, it is necessary to find an alternative to the nonlinear guidance model, presented in section 2.1.

4.4.1 Filter Model

The linear continuous model used to describe the relative motion between the pursuer and the target assumes that the target acceleration is a first-order Gauss-Markov process [80, 96]:

$$\begin{aligned} \dot{X}_r &= U_r \\ \dot{Y}_r &= V_r \\ \dot{U}_r &= A_{T_X} - A_{M_X} \\ \dot{V}_r &= A_{T_Y} - A_{M_Y} \\ \dot{A}_{T_X} &= -\lambda_{T_X} A_{T_X} + w_X \\ \dot{A}_{T_Y} &= -\lambda_{T_Y} A_{T_Y} + w_Y \end{aligned} \tag{4.32}$$

where X_r and Y_r are the relative coordinates as in the guidance model (2.1), U_r and V_r the relative speed components, A_{T_X} and A_{T_Y} the target acceleration components and A_{M_X} and A_{M_Y} the pursuer (missile) acceleration components. In addition, λ_{T_X} and λ_{T_Y} are the acceleration components time constants and w_X and w_Y are two zero-mean Gaussian white noise processes.

This model could be described by (4.1) where:

$$\begin{aligned} X &= [X_r \; Y_r \; U_r \; V_r \; A_{T_X} \; A_{T_Y}]' \\ U &= [A_{M_X} \; A_{M_Y}]' \\ A &= \begin{bmatrix} 0 & 0 & 1 & 0 & 0 & 0 \\ 0 & 0 & 0 & 1 & 0 & 0 \\ 0 & 0 & 0 & 0 & 1 & 0 \\ 0 & 0 & 0 & 0 & 0 & 1 \\ 0 & 0 & 0 & 0 & -\lambda_{T_X} & 0 \\ 0 & 0 & 0 & 0 & 0 & -\lambda_{T_Y} \end{bmatrix} \end{aligned} \tag{4.33}$$

$$B = \begin{bmatrix} 0 & 0 \\ 0 & 0 \\ -1 & 0 \\ 0 & -1 \\ 0 & 0 \\ 0 & 0 \end{bmatrix}$$

which could be discretised to provide:

$$X_{k+1} = \Phi(k+1,k)X_k + \Gamma(k+1,k)U_k \tag{4.34}$$

where the transition matrix Φ is given by [96] (see Appendix B):

$$\Phi(k+1,k) = \begin{bmatrix} 1 & 0 & f_1 & 0 & f_4 & 0 \\ 0 & 1 & 0 & f_1 & 0 & f_4 \\ 0 & 0 & 1 & 0 & f_3 & 0 \\ 0 & 0 & 0 & 1 & 0 & f_3 \\ 0 & 0 & 0 & 0 & f_2 & 0 \\ 0 & 0 & 0 & 0 & 0 & f_2 \end{bmatrix} \tag{4.35}$$

$$\begin{aligned} f_1 &= t(k+1) - t(k) \\ f_2 &= e^{-\lambda f_1} \\ f_3 &= \frac{1}{\lambda}(1 - e^{-\lambda f_1}) \\ f_4 &= \frac{1}{\lambda^2}(e^{-\lambda f_1} + \lambda f_1 - 1) \end{aligned} \tag{4.36}$$

λ being the target maneuver time constant (assumed the same in the X and Y directions) [80], while the matrix Γ is given by (Appendix B):

$$\Gamma(k+1,k) = \begin{bmatrix} -\frac{f_1^2}{2} & 0 & -f_1 & 0 & 0 & 0 \\ 0 & -\frac{f_1^2}{2} & 0 & -f_1 & 0 & 0 \end{bmatrix}' \tag{4.37}$$

and the line-of-sight measurement satisfies the form given by (4.2) in which:

$$\sigma(X) = \arctan \frac{Y_r}{X_r} \tag{4.38}$$

and where the spectral density, V, of the noise, v, is given by (3.49), namely:

$$V = \frac{a}{R^2} + b \tag{4.39}$$

R being the target-pursuer range and a and b the glint and thermal noise coefficients respectively, having for values [96]:

$$\begin{aligned} a &= 0.25\ rad^2 ft^2 s \\ b &= 56.25 \times 10^{-8}\ rad^2 s \end{aligned}$$

4.4.2 Simulations

Adopting a pursuer-target engagement scenario where $V_M = 1600\ ft\ s^{-1}$, $V_T = 800\ ft\ s^{-1}$ and $\phi = 30°$, we have simulated the extended Kalman filter and noted its performance through the calculation of the following estimation errors:

$$\begin{aligned} e_p &= \frac{1}{n}\sqrt{[\sum_{i=1}^{n}(X_{rN_i} - \hat{X}_{r_i})]^2 + [\sum_{i=1}^{n}(Y_{rN_i} - \hat{Y}_{r_i})]^2} \\ e_v &= \frac{1}{n}\sqrt{[\sum_{i=1}^{n}(U_{rN_i} - \hat{U}_{r_i})]^2 + [\sum_{i=1}^{n}(V_{rN_i} - \hat{V}_{r_i})]^2} \\ e_{aT} &= \frac{1}{n}\sqrt{[\sum_{i=1}^{n}(A_{TX_{Ni}} - \hat{A}_{T_{Xi}})]^2 + [\sum_{i=1}^{n}(A_{TY_{Ni}} - \hat{A}_{T_{Yi}})]^2} \end{aligned} \tag{4.40}$$

where e_p, e_v and e_{aT} are the position, speed and target acceleration estimation errors, respectively. The subscript N denotes the *nominal value*. The number n represents how many times the simulation was run under the same conditions. In our case 10 Monte-Carlo runs were carried out for each set of initial conditions, in line with the number of runs adopted in [80, 83].

Two types of nominal trajectories (more accurately speaking, their corresponding control effort histories) were fed to the filter. Both were obtained by an optimisation technique using MISER3 (section 2.5.2). The first minimises control effort only, and is therefore equivalent to proportional navigation (see Chapter 2), the second optimises the trace of the (position part) of the Fisher information matrix and is therefore, by definition, the maximum information guidance law (see Chapter 3). We note that those trajectories were fed off-line to the filter, in all the simulations performed.

Four sets of simulations were conducted with the EKF as the filter of choice. In a fifth set however, the performance of the modified gain extended Kalman filter (section 4.2) was compared, through the estimation errors cited above (4.40), to that of the EKF with the aim of exploring any possible benefit due solely to the filter. With the same goal in mind, two iterative filters (section 4.3.1) were used in two additional sets of simulations. In the last three sets of simulations proportional navigation was the guidance law of choice.

4.4.3 Results

As indicated by Figures 4.2 to 4.5, the filter clearly diverges under proportional navigation for all four cases of initial conditions (position and/or speed errors draft away from zero). This filter divergence is at the origin of the present research study. Since it is attributed to a lack of filter observability towards the end of the engagement, this divergence is the motivation behind the attempt to implement "more observability" into the filter, while still trying to achieve the aim of the guidance law [76]. The same figures indicate that the maximum information guidance law, outperforms proportional navigation especially towards the end of the engagement where the observability ingredient is most needed.

This outperformance is not the same for all engagement scenarios (Figure 4.3) and is more pronounced with the position components of the filter state vector than with other state components, which is to be expected since only the position part

of the Fisher information matrix is considered in the calculation of the observability measure.

When the modified gain extended Kalman filter is used along proportional navigation (Figure 4.6), one can notice some performance improvement over the case where EKF is used although signs of performance deterioration still exist towards the end of the intercept. The same improvement is noticeable when the iterative extended Kalman filter (Figure 4.7) and the iterated linear filter-smoother (Figure 4.8) are used although more in the position component than in the speed and target acceleration components. It is also noticed that the time-to-go shortens when the iterative filters are used compared to the case where the extended Kalman filter is used, while this time-to-go remains approximately the same with the modified gain extended Kalman filter.

4.4.4 Initialisation Issues

In our simulations, it was taken care of the fact that the filter model is equivalent to the guidance model presented in Chapter 2 (section 2.1). This is done by equating the position, speed, and acceleration corresponding to each of the two models. As a result of this operation (see Appendix B), the following conditions are imposed on the filter, in order for the two models to be equivalent:

$$
\begin{aligned}
A_{M_X} &= -A_n \cos\theta \\
A_{M_Y} &= A_n \sin\theta \\
U_r^f(0) &= V_T \cos\phi - V_M \cos\theta_0 \\
V_r^f(0) &= V_T \sin\phi - V_M \sin\theta_0 \\
X_r^f(0) &= X_r^g(0) \\
Y_r^f(0) &= Y_r^g(0) \\
A_{T_X}(0) &= 0 \\
A_{T_Y}(0) &= 0
\end{aligned}
$$

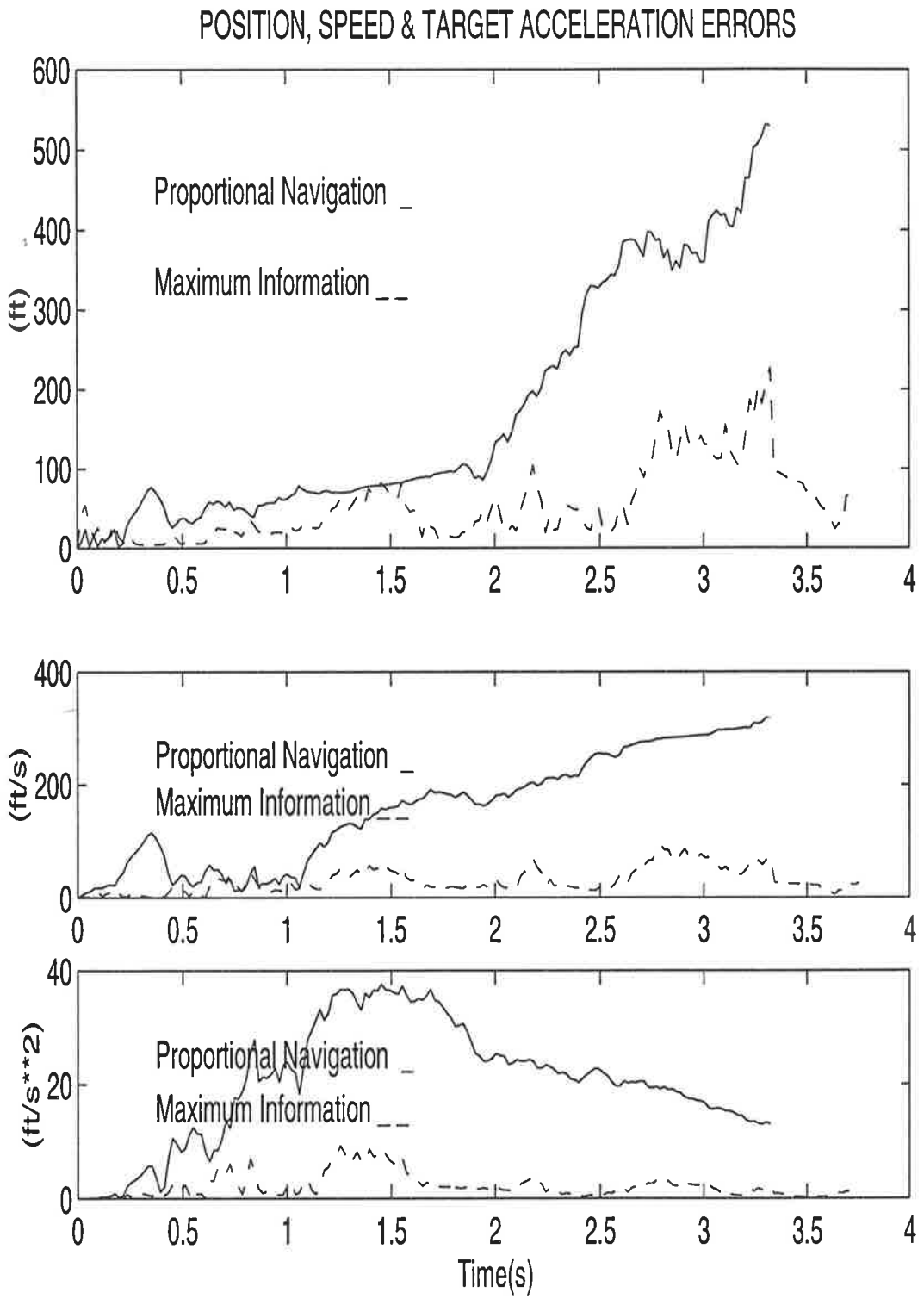

Figure 4.2: Position, speed and target acceleration errors of the EKF for no initial errors

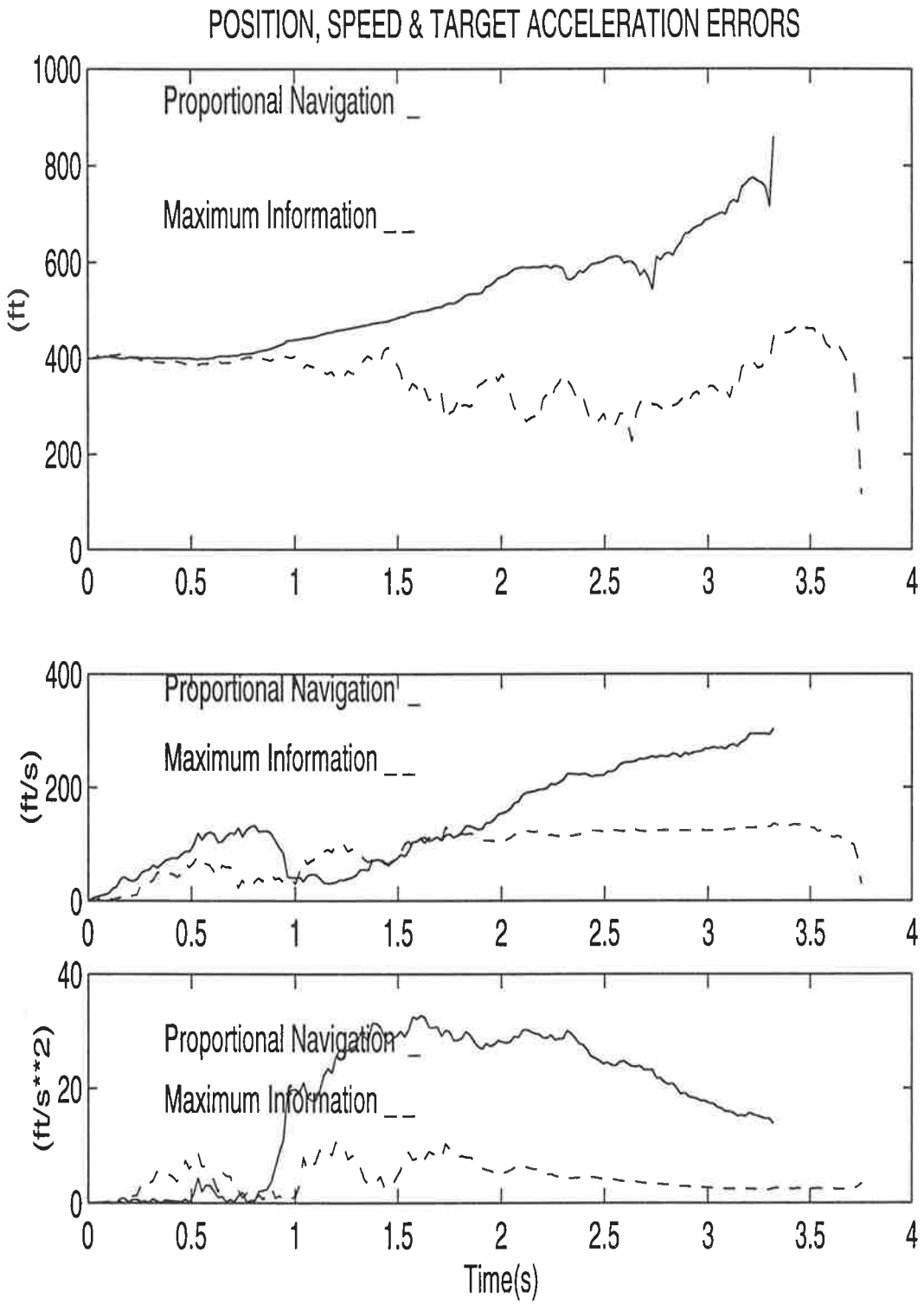

Figure 4.3: Position, speed and target acceleration errors of the EKF for an initial position error of 400 ft

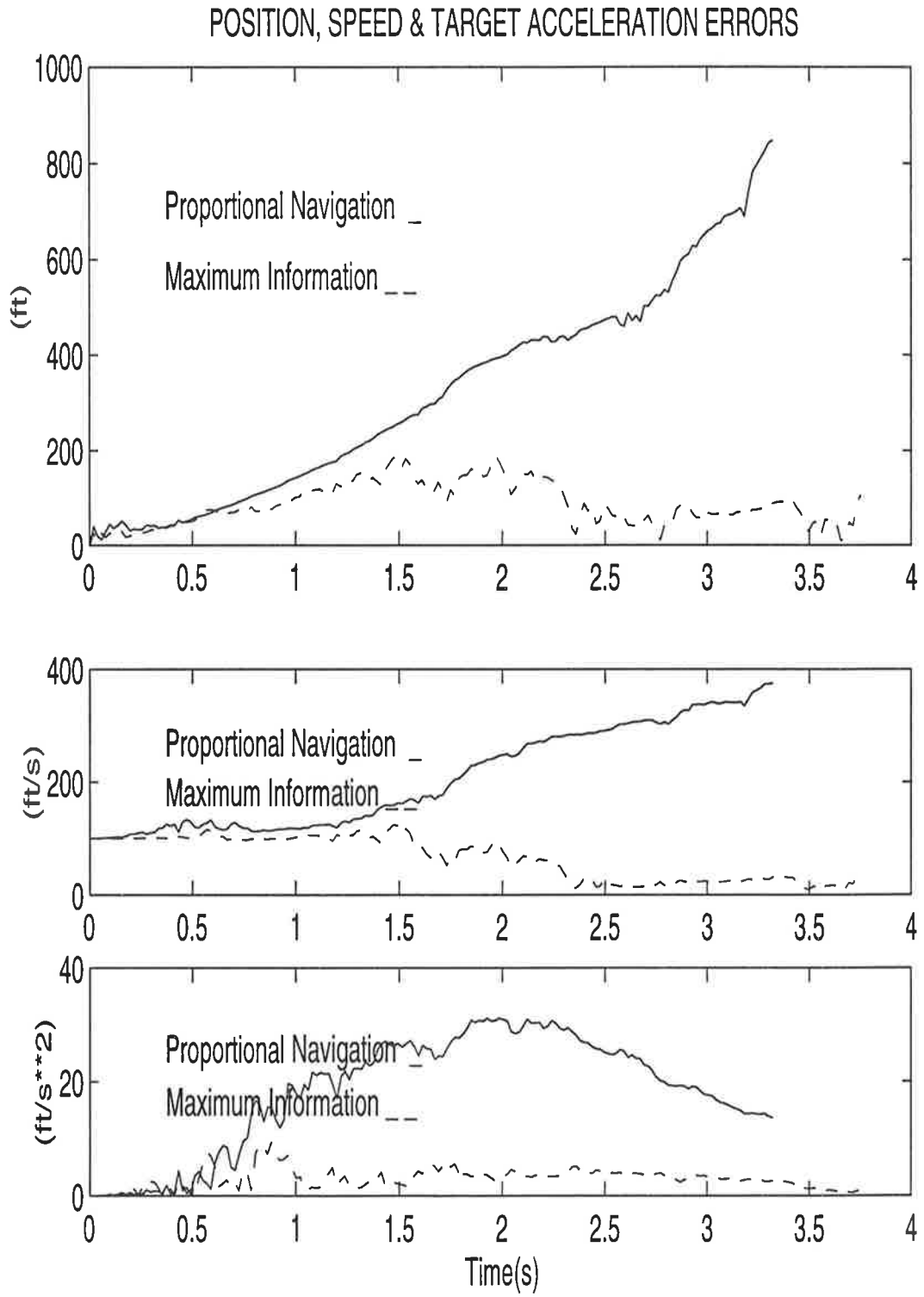

Figure 4.4: Position, speed and target acceleration errors of the EKF for an initial speed error of 100 $ft\ s^{-1}$

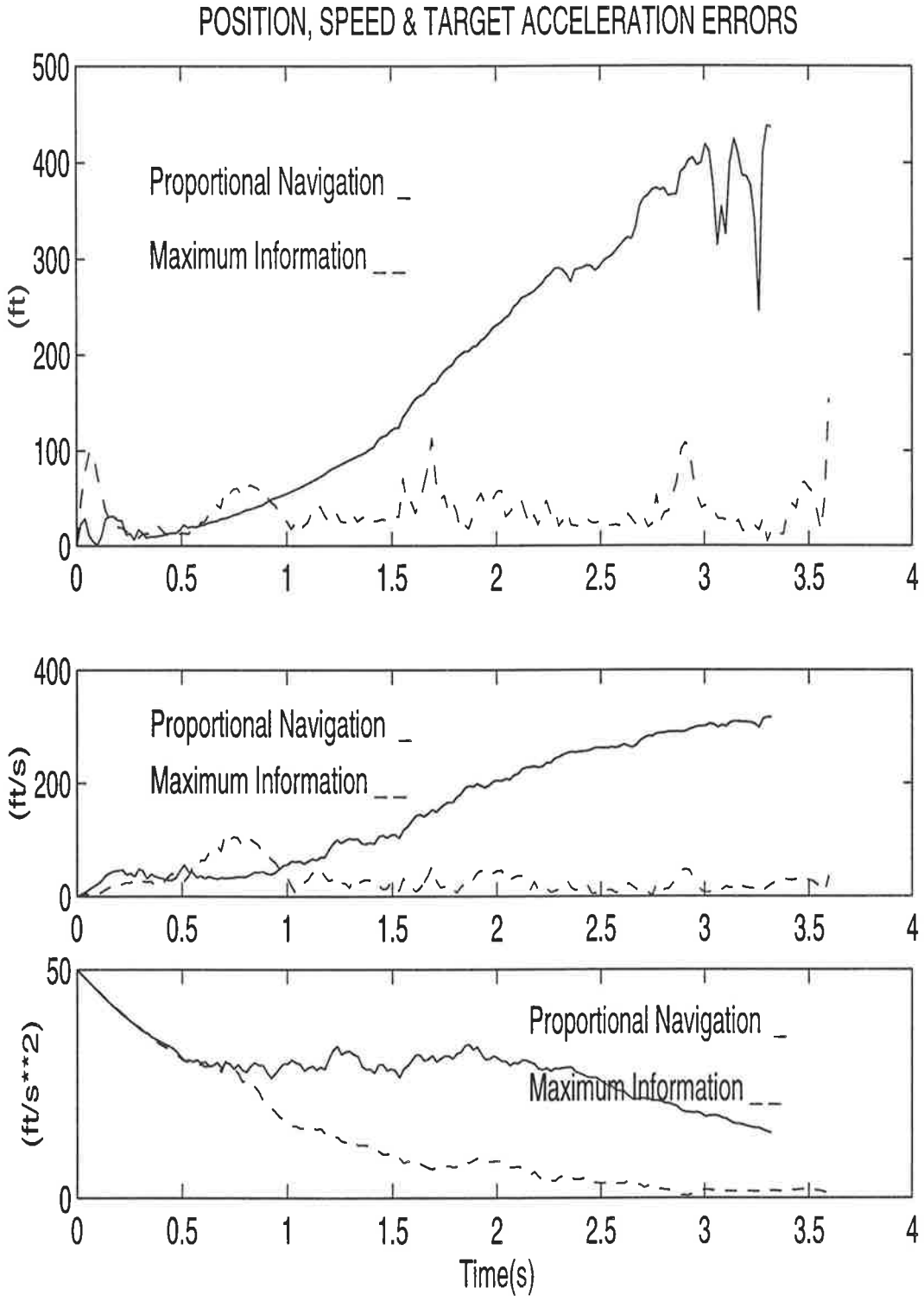

Figure 4.5: Position, speed and target acceleration errors of the EKF for an initial target acceleration error of 50 $ft\ s^{-2}$

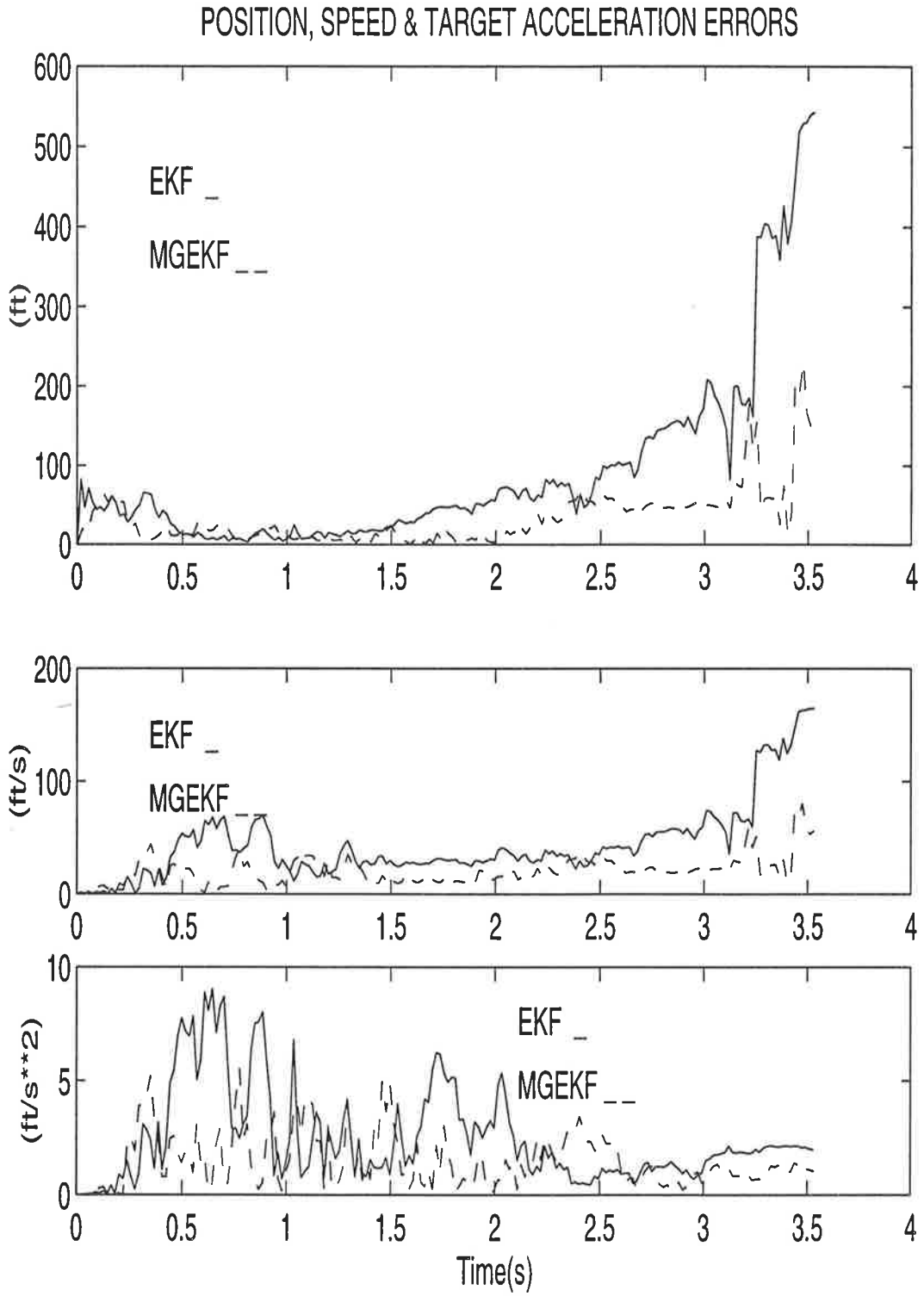

Figure 4.6: Position, speed and target acceleration errors of the MGEKF for no initial estimation errors

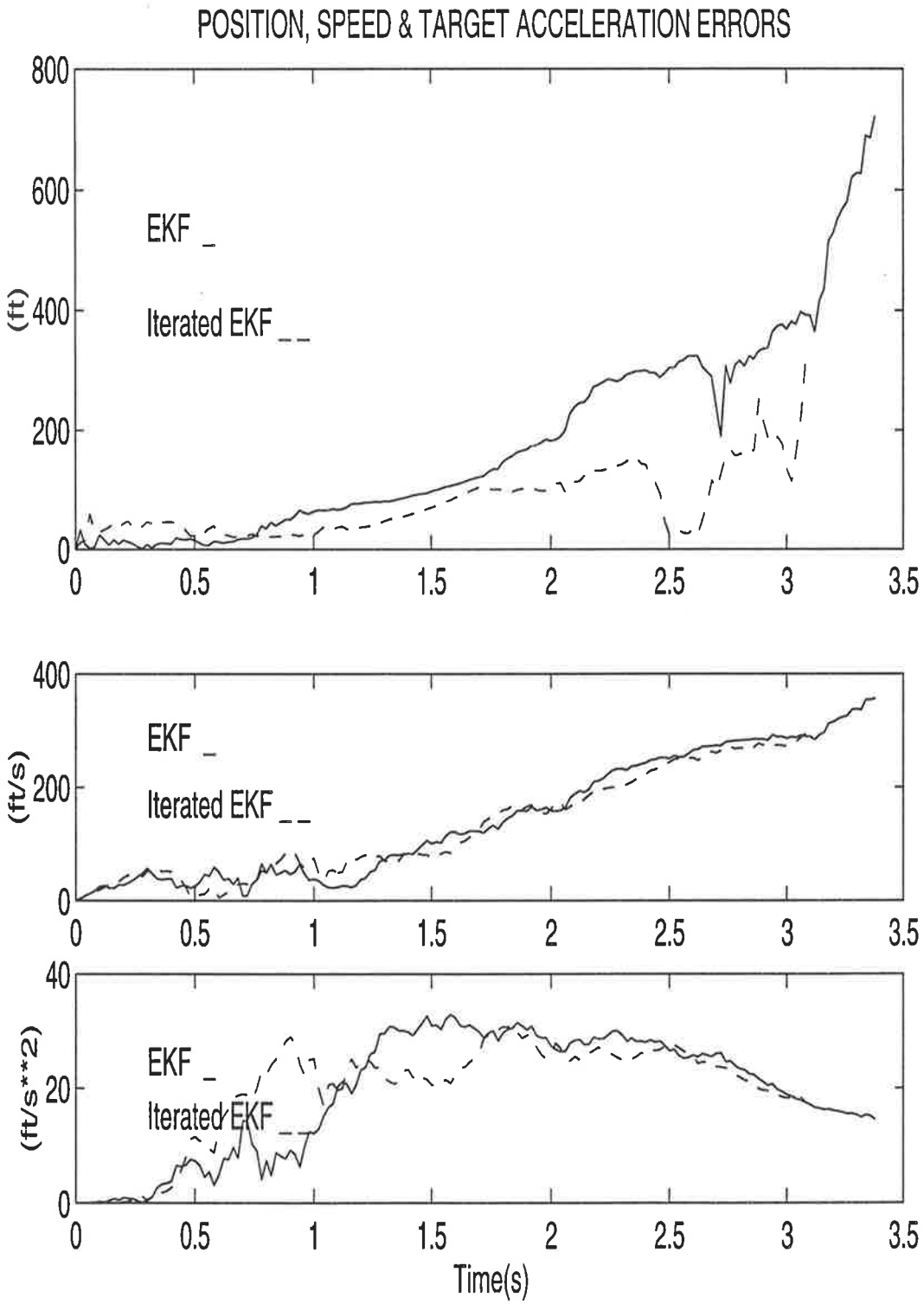

Figure 4.7: Position, speed and target acceleration errors of the iterated extended Kalman filter for no initial estimation errors

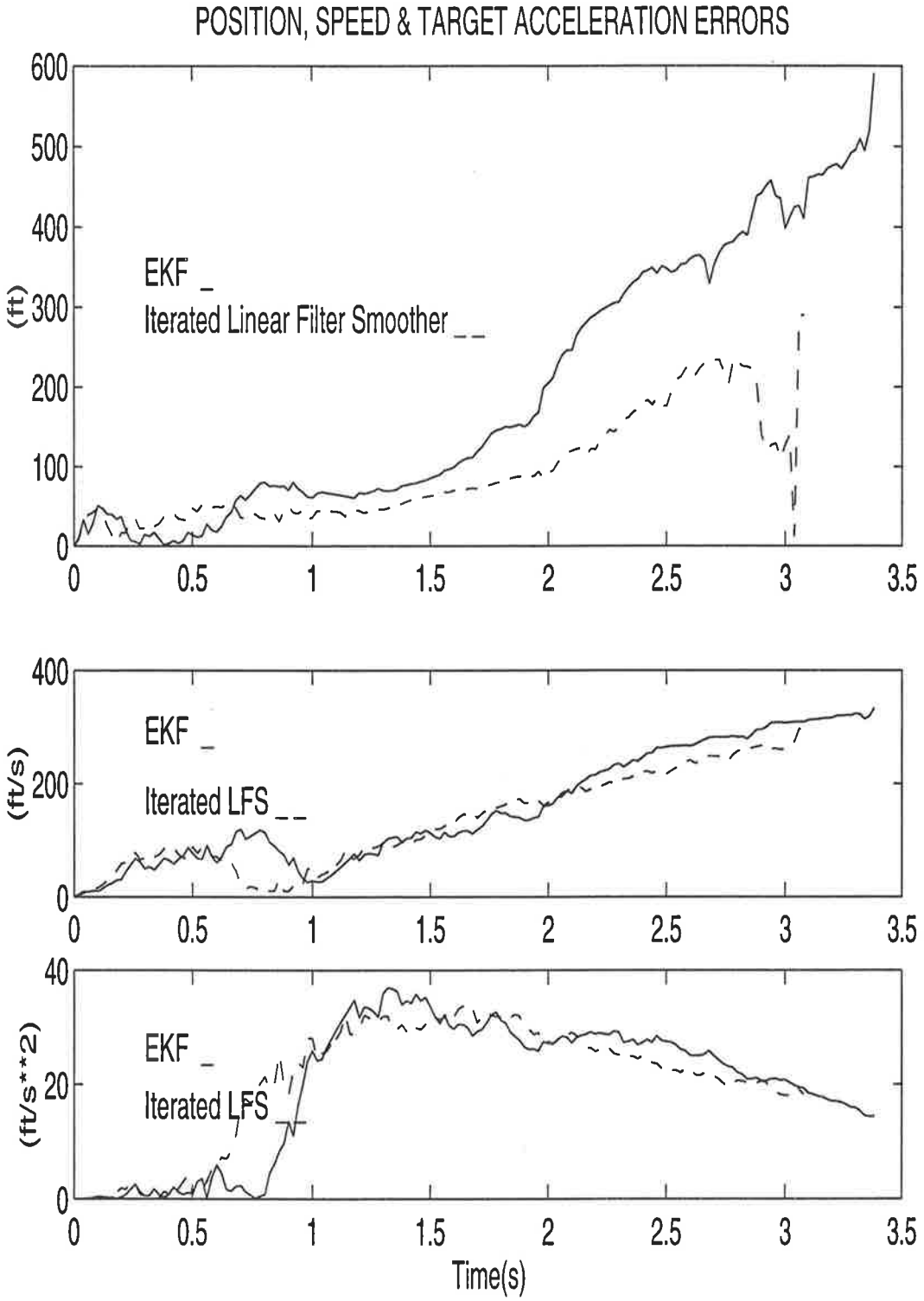

Figure 4.8: Position, speed and target acceleration errors of the iterated linear filter-smoother for no initial estimation errors

where the superscript f refers to the filter model where the superscript g refers to the guidance model.

One appropriate way to verify the equivalence of the guidance and filter models is to assume, in the above simulations, that the pursuer trajectory is known at all times, and plot the target trajectory as it is provided by the guidance and the filter, respectively.

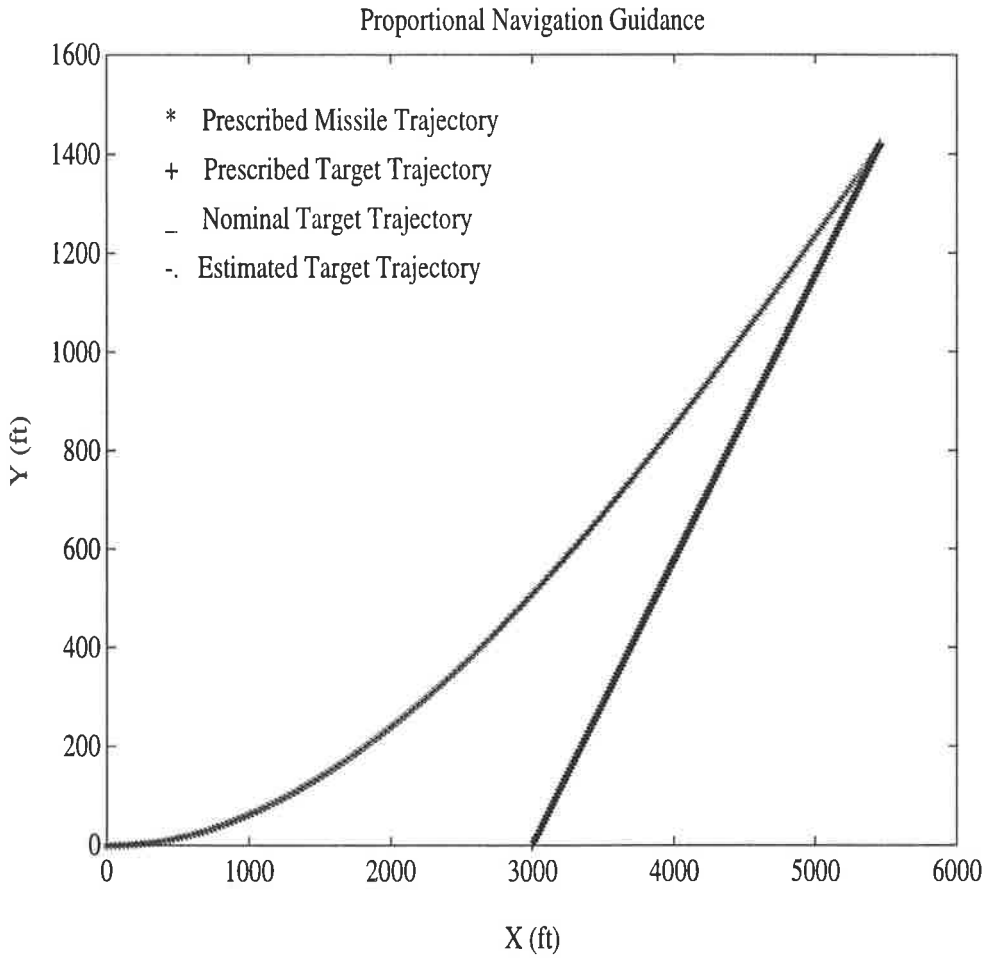

Figure 4.9: Engagement trajectories as provided by the guidance and the filter models respectively - proportional navigation guidance

This procedure was performed in Figure 4.9 for the proportional navigation guidance, and in Figure 4.10 for the maximum information guidance, taking the same scenario considered in the previous section. Both plots show that the prescribed trajectories, e.g., the ones provided by the guidance laws, and their corresponding

nominal trajectories, e.g., the ones provided by the filter model, are almost identical.

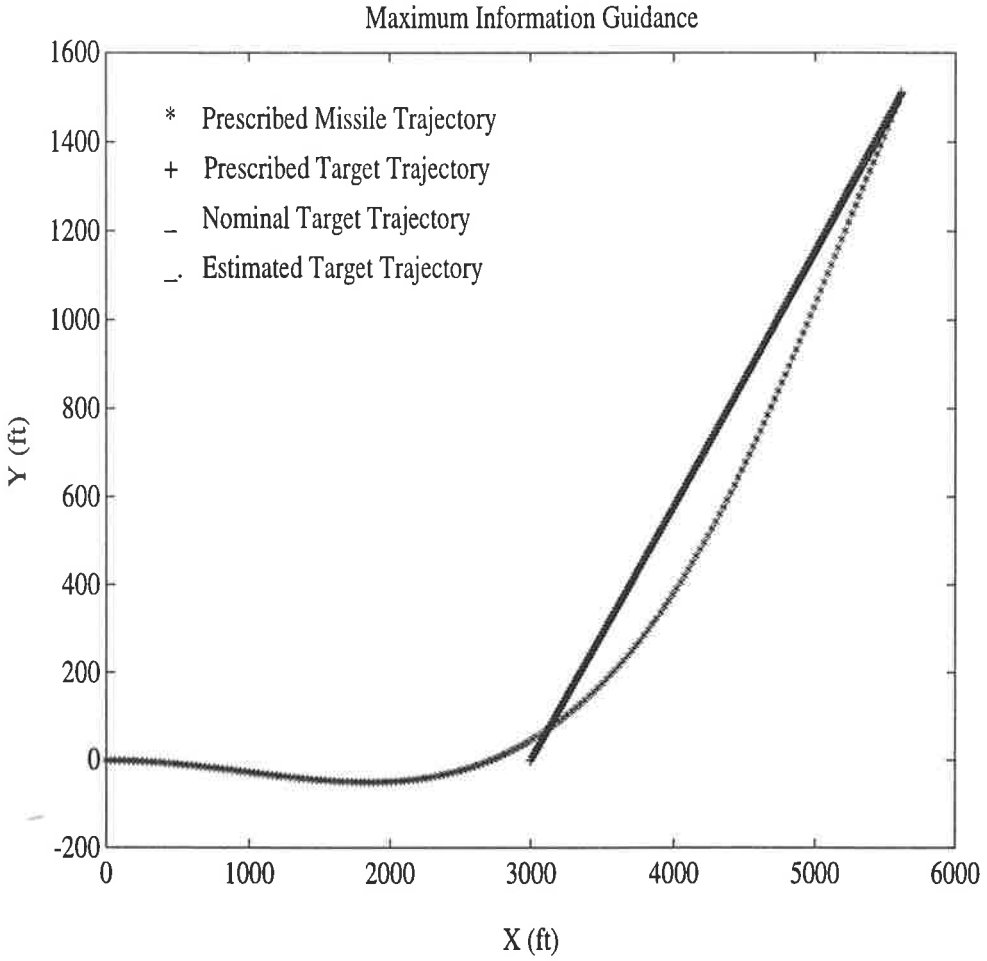

Figure 4.10: Engagement trajectories as provided by the guidance and the filter models respectively - maximum information guidance

4.5 Summary

This chapter presents the bearing-only-measurement problem from a stochastic point of view. The importance of the stochastic approach lies in the fact that the whole idea of observability enhancement gravitates around the divergence of the state estimator, when the guidance law used in conjunction with the Kalman filter is proportional navigation. While the overall problem is stochastic in the sense that the measurements feeding the Kalman filter are noisy, the guidance law is still

generated off-line, through an optimisation tool (MISER3).

The system model used in this chapter was taken to be different from the guidance model presented in Chapter 2. A linear model was chosen here to accommodate the formulation of the extended Kalman filter. However, the implication that this model needs to be equivalent to the guidance model meant that certain initial conditions were imposed on the filter state.

As the bearing measurements are nonlinear, it was natural to use the extended Kalman filter (EKF) as the preferred state estimator. In the derivation of the EKF, the issues related to the choice of the nominal trajectory were given special consideration. The difference between the EKF and the linearised Kalman filter [33] was specifically emphasised as being essentially related to the difference between a batch nominal trajectory and an on-line trajectory.

One way to enhance the performance of the extended Kalman filter, from a purely estimation point of view, is obtained by carrying out local iterations between each step of the filter and the other. This is performed through the iterative extended Kalman filters. The first such filter to be considered, the iterated extended Kalman filter (IEKF), calculates more accurately the difference between the state estimate and its nominal counterpart, between observations. The second, the iterated linear filter-smoother (ILFS), uses the IEKF first, and smoothes the estimate back to provide a better estimate, especially when the nonlinearities are in the system dynamics.

The simulations of the EKF along proportional navigation illustrated the well documented divergence of the filter. Its simulations along maximum information revealed higher guidance performance in terms of estimation errors on position, speed and target acceleration for various initial conditions. Since the observability measure of the maximum information guidance law was formulated based on the position part only of the Fisher information matrix, the outperformance of the EKF appeared the most in the position estimation errors, regardless of the nature of the initial estimation errors.

Now that we have illustrated the Kalman filter divergence problem, in addition to a possible solution, it is time to introduce more realism into the guidance system by making use of an on-line guidance law, as opposed to using an off-line optimisation tool. This is the subject of the next chapter.

Chapter 5

Dual Control Guidance

Control parametrisation and other general optimisation techniques offer elegant and useful solutions to problems such as the bearing-only-measurement problem where the time-to-go is unknown apriori, the imposed final restrictions are stringent and the variables to be optimised are not well defined. In the analysis stage, when the intent is to uncover the characteristics of a new performance index, the use of the above techniques is well justified. However, when implemented in the guidance loop, these techniques do not result in a "mechanisable" guidance law [40, 86], in the sense of providing, on-line, a control variable that is an explicit function of the state estimate vector issued by the Kalman filter. Rather, these techniques offer the possibility of deriving the control variable off-line, and typically storing it in the form of a look-up table to be used by the state estimator. While this is useful for analysis purposes, it stops short of facilitating the implementation task. Among the reasons behind this difficulty are the very broad and general approach of the general optimisation techniques, and the lack of access to the time-to-go. In this chapter, we narrow down the general optimisation technique, adopt an estimated version of the time-to-go and restrict the problem to linear and quadratic systems that could be solved and *mechanised* through the standard linear quadratic optimisation technique.

On one hand, the standard linear quadratic approach allows for the definition of the

linear quadratic guidance law (LQGL), based on the optimisation of control effort in addition to the final state. The definition of this law illustrates the benefits of this approach which are quite significant. The resulting closed form of the law and the linearity of the gain expression simplify the computational task of the processor in charge of the guidance algorithm, giving it a remarkable flexibility. In addition, the linear quadratic guidance law proves to be a general guidance law with a broader scope than traditional guidance laws such as proportional navigation. In fact LQGL reduces to proportional navigation for a particular value of its design parameter [16].

On the other hand, the linear quadratic optimisation technique provides a most appropriate tool to accommodate the idea of dual control, as applied to bearing-only-measurement problems. For this type of problems, dual control stipulates to take into consideration the inherent interaction between guidance and state estimation, as opposed to handling each task independently in line with the separation principle. This interaction could best be served by feeding the state estimate, instead of the true state to the guidance law. Since the control provided by the linear quadratic guidance law is an explicit function of the state, the dual control concept could be accommodated by replacing the true state, in its expression, by the estimated state provided by the Kalman filter.

This idea, by itself, relates more to the separation principle [99] rather than to the probabilistic dual control theory described in [22] or the wide-sense dual control of [95] (section 1.5). However, if we consider the fact that the state estimate is obtained using a nominal trajectory derived by optimising a measure of observability of the state estimate, and that this state estimate is used, on-line, in the derivation of the nominal trajectory, we would then appreciate the significance of the "dual control" concept which tends to blend the aims of control and estimation in the guidance loop.

Hence, the dual control guidance law (DCGL) is formulated. Although more complex analytically due to the additional information on observability, it is presented in the same simple form as the LQGL and its derivation follows the same procedure. In addition to being designed for stochastic systems, DCGL enjoys several features

including observability and mechanisability. In addition, the control coefficients are derived analytically which ensures ease of implementation. As we shall see however, several limitations are still present in DCGL, including the necessity to estimate the time-to-go, the limited structure and the ad-hoc way of choosing its associated observability coefficient.

Among the appealing benefits of both quadratic guidance laws is their ability to be easily implemented in a closed loop linking the state estimator to the guidance law. This feature constitutes a departure from previous works such as the ones described in Chapters 3 and 4. Whereas in those works the performance of the state estimator was analysed based on the assumption that the guidance law is independent of the state estimate, the quadratic guidance laws described herein have the ability to establish a continuous closed-loop link between the state estimator and the guidance law. Due to this link the guidance laws are considered *mechanisable* [40, 86].

Definition 5.1 *The term* mechanisability *of a guidance law refers to the ability to apply the guidance law on-line, along with the state estimator in the guidance loop. Consequently, a guidance law is mechanisable when the control variable is given as an explicit function of the state variables.*

Another modification to the approach followed in previous work is the adoption of the same model for the guidance law and the state estimator. In Chapter 4, the point was made that the guidance and filter models should be equivalent and steps were taken to ensure this equivalence. In the present work, the nonlinear guidance model is discarded altogether and replaced by the linear filter model. In addition to making the linear optimisation study feasible, this modification enables the simulation of simple maneuvering targets. Two target maneuver models will be considered, the Gauss-Markov model and the circular model.

In the following section, the LQGL problem is formulated and solved. The DCGL is then formulated and solved in section 5.2, while in the last section, both laws are simulated, applied to three different scenarios and their estimation and guidance performances compared.

5.1 Linear Quadratic Guidance Law

More recently developed than proportional navigation [16], this guidance law is based on the idea of minimising a performance index consisting of a combination of control effort and final miss-distance. One of its advantages is that it reduces to proportional navigation for a particular value of its design parameter. It also provides more insight into the significance of the role of guidance in striking a balance between final miss-distance and control effort minimisation.

5.1.1 Minimising Control Effort

As described in [40], the system at hand is composed of the relative pursuer-target position, the relative speed and the target acceleration model (see Chapter 4). In the two-dimensional space this system could be represented by (4.1) namely:

$$\dot{X}(t) = AX(t) + BU(t) \tag{5.1}$$

where X, U, A and B are the components of the state vector, the control vector, the state matrix, and the control matrix, respectively, as defined in (4.34), namely:

$$X = [X_r \; Y_r \; U_r \; V_r \; A_{TX} \; A_{TY}]' \tag{5.2}$$

$$U = [A_{MX} \; A_{MY}]' \tag{5.3}$$

$$A = \begin{bmatrix} 0 & 0 & 1 & 0 & 0 & 0 \\ 0 & 0 & 0 & 1 & 0 & 0 \\ 0 & 0 & 0 & 0 & 1 & 0 \\ 0 & 0 & 0 & 0 & 0 & 1 \\ 0 & 0 & 0 & 0 & -\lambda & 0 \\ 0 & 0 & 0 & 0 & 0 & -\lambda \end{bmatrix} \tag{5.4}$$

$$B = \begin{bmatrix} 0 & 0 \\ 0 & 0 \\ -1 & 0 \\ 0 & -1 \\ 0 & 0 \\ 0 & 0 \end{bmatrix} \tag{5.5}$$

where the target acceleration time constants are considered the same in the X and Y directions. Given some prescribed initial conditions:

$$t_0 \ , \ X_0 \tag{5.6}$$

and a prescribed final time:

$$t_f \tag{5.7}$$

the linear quadratic guidance law proposes to solve the guidance problem by minimising the following performance index:

$$J = \frac{c}{2} X_f^2 + \frac{1}{2} \int_{t_0}^{t_f} U(t)^2 dt \tag{5.8}$$

where X_f is the final state, $U(t)$ the control variable and c a constant design parameter. The minimisation procedure is subject to a linear form of the control variable:

$$U(t) = C(t)X(t) \tag{5.9}$$

where $C(t)$ is the control gain matrix.

The performance index (5.8) aims at minimising the control effort with a penalty on the final miss-distance. The system model (5.1) is the same as what was dubbed *the*

filter model as opposed to *the guidance model* in Chapter 4 and [34]. There, the point was made that particular care should be taken to insure the equivalence between the two models since they represent the same system. In line with that point, only one system model is used in the present study for both guidance and filtering. This formulation allows the problem to be split into two separate problems, due to the symmetry of the system model geometry in the X and Y directions [40]. Each of the two problems could be formulated as follows:

Given the following sub-system:

$$\dot{X}_s(t) = A_s X_s(t) + B_s U_s(t) \tag{5.10}$$

where

X_s is the sub-system state vector given by:

$$X_s = [X_r \; U_r \; A_{TX}]' \tag{5.11}$$

U_s the sub-system control variable, equal to the X (or Y) component of the pursuer normal acceleration A_{MX} (or A_{MY}, respectively).

A_s the sub-system state matrix:

$$A_s = \begin{bmatrix} 0 & 1 & 0 \\ 0 & 0 & 1 \\ 0 & 0 & -\lambda \end{bmatrix} \tag{5.12}$$

and B_s the sub-system control matrix:

$$B_s = \begin{bmatrix} 0 \\ -1 \\ 0 \end{bmatrix} \tag{5.13}$$

The prescribed initial conditions are:

$$t_0, \quad X_{s0}$$

and the prescribed final time:

$$t_f$$

It is proposed to minimise the performance index:

$$J = \frac{c}{2} X_{s_f}^2 + \frac{1}{2} \int_{t_0}^{t_f} U_s(t)^2 dt \tag{5.14}$$

such as the control variable assumes a linear form similar to (5.9):

$$U_s(t) = C_s(t) X_s(t) \tag{5.15}$$

5.1.2 Derivation

The problem described above is similar to the general optimum control problem with terminal penalty, described in [25]. The performance index (5.8) could take the form:

$$J = \int_{t_0}^{t_f} [X_s' Q X_s + U_s' R_c U_s] dt + X_{s_f}' Z X_{s_f} \tag{5.16}$$

where $Q = 0_3$, $R_c = \frac{1}{2}$, and Z is given by:

$$Z = \begin{bmatrix} \frac{c}{2} & 0 & 0 \\ 0 & 0 & 0 \\ 0 & 0 & 0 \end{bmatrix} \tag{5.17}$$

The solution can therefore be given in the linear form of (5.15), where the sub-system gain matrix $C_s(t) \in \mathbb{R}^3$ has the form [25]:

$$C_s(t) = R_c^{-1} B_s' M_R(t) \tag{5.18}$$

the matrix $M_R(t)$ is the solution to the Riccati equation:

$$-\dot{M}_R = M_R A_s + A_s' M_R - M_R B_s R_c^{-1} B_s' M_R + Q \tag{5.19}$$

with the final condition:

$$M_R(t_f) = Z \tag{5.20}$$

The solution of the Riccati equation (5.19) could be decomposed in the following manner [25]:

$$M_R = P L^{-1} \tag{5.21}$$

where the matrices P and L satisfy the following differential equations:

$$\dot{P} = -QL - A_s' P; \qquad P(t_f) = Z \tag{5.22}$$

$$\dot{L} = A_s L - B_s R_c^{-1} B_s' P; \qquad L(t_f) = I \tag{5.23}$$

By solving the two differential equations (5.22) and (5.23) (see Appendix C) and calculating the expression of the matrix $C_s(t)$ from (5.18) we obtain the following closed form expression:

$$C_s(\tau) = [\frac{N}{\tau^2} \quad \frac{N}{\tau} \quad \frac{N(e^{-\lambda\tau} + \lambda\tau - 1)}{(\lambda\tau)^2}] \tag{5.24}$$

where N is the navigation ratio:

$$N = \frac{3c\tau^3}{c\tau^3 + 3} \tag{5.25}$$

and τ the time-to-go at time t:

$$\tau = t_f - t \tag{5.26}$$

We can now account for the second similar symmetrical problem (section 5.1.1), in order to derive the six-dimensional control gain matrix $C(t)$ given in (5.9). We clearly see that when the weighting constant c is sufficiently large, the linear quadratic guidance law reduces to proportional navigation with a navigation constant $N = 3$ [16]. This is in tune with the conclusion drawn in Chapter 2 limiting N to values equal or greater than 3 (section 2.4.3).

N.B.: Note that while the time-to-go is denoted by t_f in Chapter 2, it is represented by τ in this chapter for simplicity. Here, t_f refers to the initial time-to-go, identified by t_{f_0} in Chapter 2.

5.2 Dual Control Guidance Law

The bearing-only-measurement system could basically be seen as a nonlinear stochastic system. It is well known that in such systems the overall control task can have a dual effect [11, 17]. It could be considered to be composed of two parts: an estimator and a feedback regulator. In fact "the optimal control has an interesting property. The control will not only try to drive the output to its desired value ... (but also) will improve the state estimate and the future controls" [7]. This duality property was sought in [39, 40, 80] through the characteristics of the Fisher information matrix. It was believed that adding a measure of observability to classical guidance laws would enhance the estimation properties as well as achieving the guidance objective of minimum miss-distance. Three different measures of the observability gramian were examined in Chapter 3. In the following, the trace of the observability gramian is re-examined from a slightly different perspective.

5.2.1 Trace of the Observability Gramian

Given a noise-free system (5.1) and a nonlinear measurement perturbed by Gaussian white noise, the observability gramian (3.39) could be written as:

$$I = \int_{t_0}^{t_f} \Phi' H' V^{-1} H \Phi dt \tag{5.27}$$

where Φ is the system transition matrix, H the measurement gradient, V the spectral density of its associated noise, t_0 the initial time of engagement and t_f its final time.

The transition matrix of system (5.1) could be derived in closed form [31]:

$$\Phi(k+1,k) = \begin{bmatrix} I_2 & f_1 I_2 & \frac{e^{-\lambda f_1}+\lambda f_1 - 1}{\lambda^2} I_2 \\ 0_2 & I_2 & -\frac{e^{-\lambda f_1}-1}{\lambda} I_2 \\ 0_2 & 0_2 & e^{-\lambda f_1} I_2 \end{bmatrix} \tag{5.28}$$

where $f_1 \equiv t(k+1) - t(k)$ is the time increment and λ the target maneuver time constant [80].

On the other hand, the expression of the only line-of-sight measurement is given by (4.38), namely:

$$Z(t) = \arctan \frac{Y_r}{X_r} + v(t) \tag{5.29}$$

Its gradient vector could therefore be written as:

$$H = [sin\theta \;\; cos\theta \;\; 0 \;\; 0 \;\; 0 \;\; 0] \tag{5.30}$$

while the measurement noise $v(t)$ is white and Gaussian. Its spectral density V assumes, in what follows, the following form:

$$V = R^{-2} \tag{5.31}$$

where R is the range between the target and the pursuer.

Note that this form is a simplified version of the noise spectral density adopted in Chapter 4 (4.39).

Also, in a general problem formulation, it is desirable to multiply the observability gramian by a weighting matrix, W_m, chosen in the following as:

$$W_m = \begin{bmatrix} w_1 I_2 & 0_2 & 0_2 \\ 0_2 & w_2 I_2 & 0_2 \\ 0_2 & 0_2 & w_3 I_2 \end{bmatrix} \tag{5.32}$$

where I_2 is the two-dimensional identity matrix.

It is therefore possible to define a performance index made out of the weighted observability gramian as:

$$J = tr\left[W_m \int_{t_0}^{t_f} \Phi' H' V^{-1} H \Phi dt\right] \tag{5.33}$$

Given the commutativity of the trace and integral operations on one hand, and the commutativity and associativity of the trace and matrix product operations on the other hand, it is possible to write (5.33) as:

$$J = \int_{t_0}^{t_f} tr\left\{[H' V^{-1} H][\Phi W_m \Phi']\right\} dt \tag{5.34}$$

From the expressions of H and V we could derive the expression of the performance index J:

$$J = 2\int_{t_0}^{t_f} R^2[w_1 + w_2 f_1^2 + \frac{w_3}{\lambda^4}(e^{-\lambda f_1} + \lambda f_1 - 1)^2]dt \tag{5.35}$$

This expression provides a simple means to maximise observability in the system.

5.2.2 Maximising Observability

To simplify the problem, the weighting coefficients w_2 and w_3 are taken to be zero. This leaves the performance index (5.35) with just the position weighting coefficient w_1, which will be denoted by ω:

$$\frac{J}{2} = -\omega \int_{t_0}^{t_f} R^2 dt \tag{5.36}$$

Optimising this performance index would mean optimising the information on the observability of the position component of the system. Note that a minus sign was added to account for the fact that optimal control problems seek to *minimise* the performance index while our objective is to *maximise* observability.

Finally, the dual control guidance law attempts to blend the concepts of maximum observability and minimum control effort, by simply blending the two performance indices (5.8) and (5.36) into a single one:

$$J = \frac{c}{2} X_f^2 + \frac{1}{2} \int_{t_0}^{t_f} (U(t)^2 - \omega R^2) dt \tag{5.37}$$

Consequently, the problem of the dual control guidance law simply becomes that of minimising the performance index (5.37), for the system described by (5.1), subject to the initial and final conditions described by (5.6) and (5.7), respectively.

5.2.3 Derivation

The solution to the dual control guidance law follows the same procedure carried out to solve the linear quadratic guidance law (section 5.1.2). The problem is subdivided into two different problems described each by a sub-system as in (5.10) for which the corresponding performance index satisfies the general form (5.16). The expressions of the matrices A_s, B_s, R_c and Z are the same, but the expression of Q in this case becomes:

$$Q = \begin{bmatrix} \frac{\varepsilon}{2} & 0 & 0 \\ 0 & 0 & 0 \\ 0 & 0 & 0 \end{bmatrix} \tag{5.38}$$

The dual control of each sub-system could, also in this case, be given under the linear form (5.15), where the matrix C_s is given by (5.18) whose solution amounts to solving the two differential equations (5.22) and (5.23). In this case however, the additional complexity of the problem complicates the inversion of the matrix L, due to the relative complexity of its elements. The control gain matrix is not given, therefore, in a closed form as is the case with the LQGL, instead it is given in terms of the elements, P_{ij} and L_{ij} $(i, j = 1, \cdots, 3)$ of the two matrices P and L, solutions of (5.22) and (5.23), respectively.

$$C_s = [C_1 \;\; C_2 \;\; C_3] \tag{5.39}$$

where

$$\begin{aligned} C_1 &= P_{21}L_{11}^{-1} + P_{22}L_{21}^{-1} + P_{23}L_{31}^{-1} \\ C_2 &= P_{21}L_{12}^{-1} + P_{22}L_{22}^{-1} + P_{23}L_{32}^{-1} \\ C_3 &= P_{21}L_{13}^{-1} + P_{22}L_{23}^{-1} + P_{23}L_{33}^{-1} \end{aligned}$$

The expressions of the elements of the matrices P and L are given in Appendix C. Note that, as in the LQGL case, once the elements of C_s are determined, the control gain matrix $C(t)$ in (5.9) is deduced by accounting for the second similar sub-system (see section 5.1.1).

5.3 Simulations and Results

The two guidance laws LQGL (section 5.1) and DCGL (section 5.2) were applied to a two-dimensional bearing-only-measurement problem depicted in Figure 5.1.

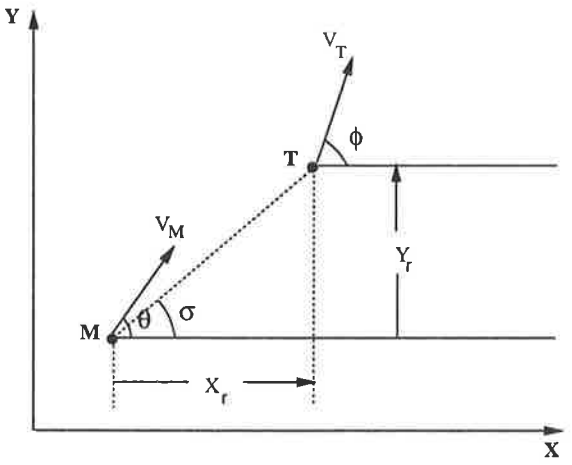

Figure 5.1: Two-dimensional engagement geometry

Three engagement scenarios were simulated, in which the pursuer and target speeds were considered constant throughout the engagement. The profile of the target acceleration as well as the target heading angle were different for each scenario.

5.3.1 Simulations

Both guidance laws were mechanised along the extended Kalman filter (see section 4.1), in a closed loop setting (see Figure 4.1). The design parameter c in the LQGL was taken to be high enough ($c = 10^4$) to approximate proportional navigation, while the weighting factor ω in the DCGL was taken to be equal to 0.03 s^{-4}.

The measurement as well as its noise (5.29) are illustrated in Figure 5.2 for one of the engagement scenarios. In the first of the three examined scenarios, the target is moving at a constant heading angle (equal to 30°) with no acceleration. In the second scenario, the target pulls an initial acceleration of $9g$ in each of the $-X$ and Y directions. Each component of this acceleration decreases exponentially with time with a maneuverability time constant $\lambda = 1$ (see Figure 5.3). In the third scenario, the target pulls a constant normal acceleration of $9g$ resulting therefore in a circular trajectory.

The simulations were recorded in two sets of graphs. In the first set (Figures 5.4,

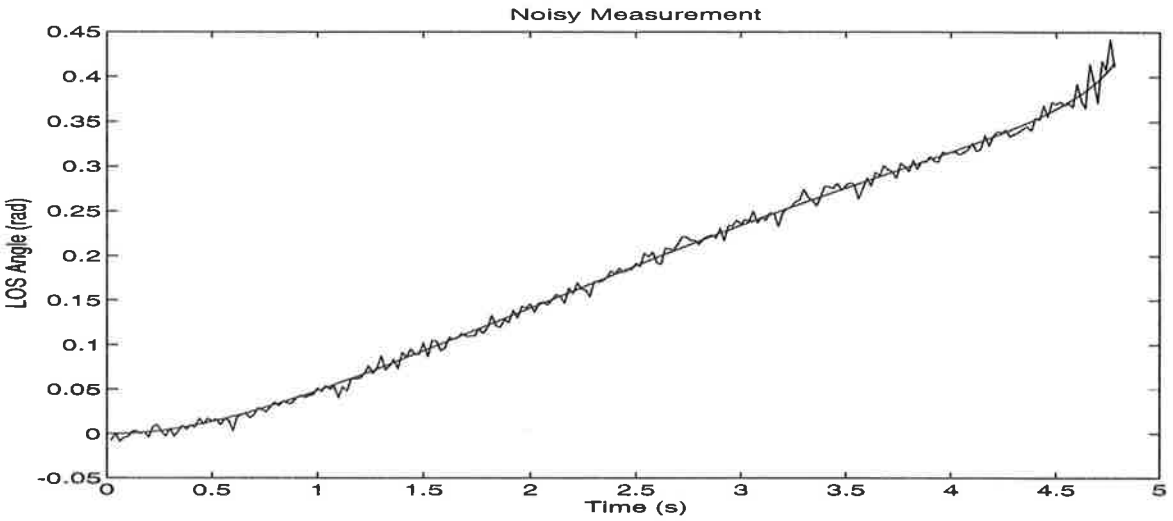

Figure 5.2: Typical noisy measurement for the first engagement scenario

5.6, 5.8, 5.10), the average state estimation errors over 50 Monte-Carlo runs were plotted in terms of the engagement time. These errors are defined in exactly the same way as in Chapter 4 (equation 4.40). The second set of graphs (Figures 5.5, 5.7, 5.9, 5.11) depicts the pursuer and target true trajectories as well as the target estimated trajectory, assuming that the pursuer trajectory is accessible through the use of on-board accelerometers [39, 76, 83].

On the other hand, two tables were compiled in Table 5.1 and Table 5.2. They contain the average final miss-distances and times-to-go over the 50 Monte-Carlo runs for the LQGL and the DCGL. In Table 5.1, this data was computed based on the estimated variables, while in Table 5.2 the calculations were based on the true variables.

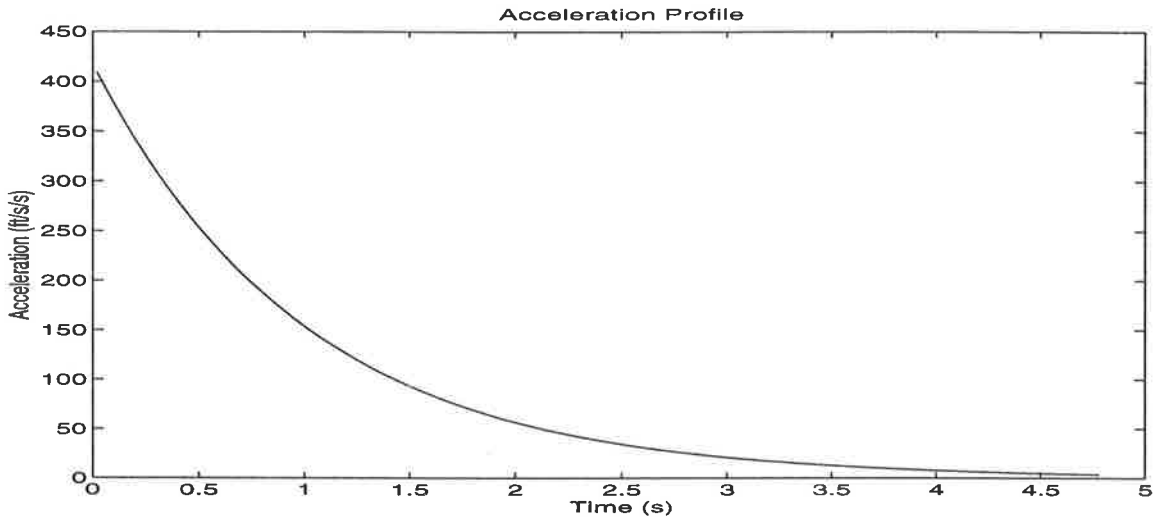

Figure 5.3: Acceleration profile for the second engagement scenario

5.3.2 Comments

In the first scenario (Figures 5.4 and 5.5), both LQGL and DCGL perform reasonably well in terms of position and speed errors during most of the engagement. However, the position error and to a lesser extent the speed error of the LQGL degrade drastically during the last phase of the engagment, while the DCGL errors remain within a reasonable range. This difference in the performance tends to be more pronounced towards the final instants of the engagement, and it could be easily seen by comparing the estimated target trajectories in Figure 5.5. In this figure, it is noted that DCGL causes the pursuer to maneuver slightly around the target trajectory, instead of going straight to its destination.

The simulations relating to the second scenario (Figures 5.6 and 5.7) suggest the

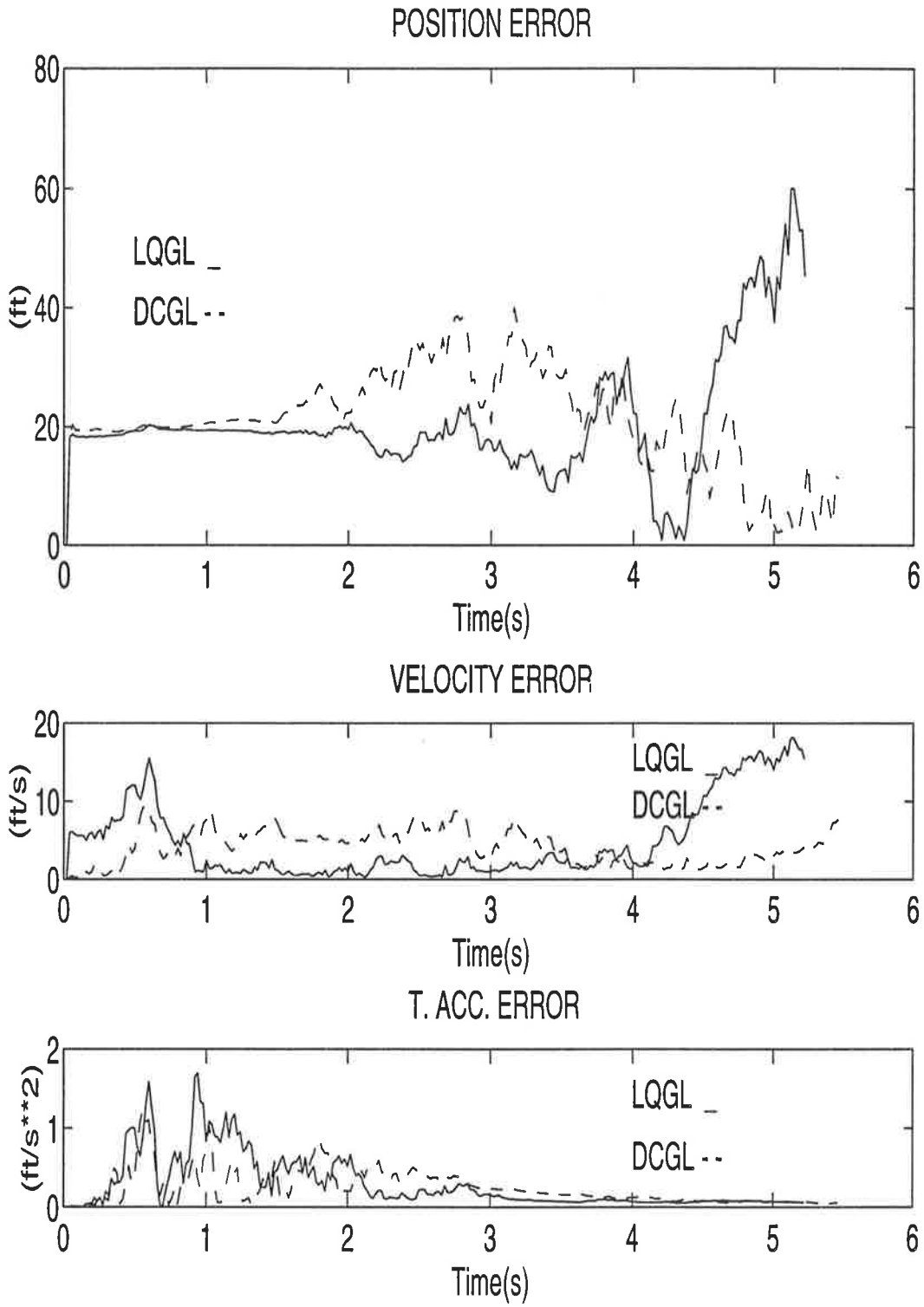

Figure 5.4: State estimation errors for scenario 1

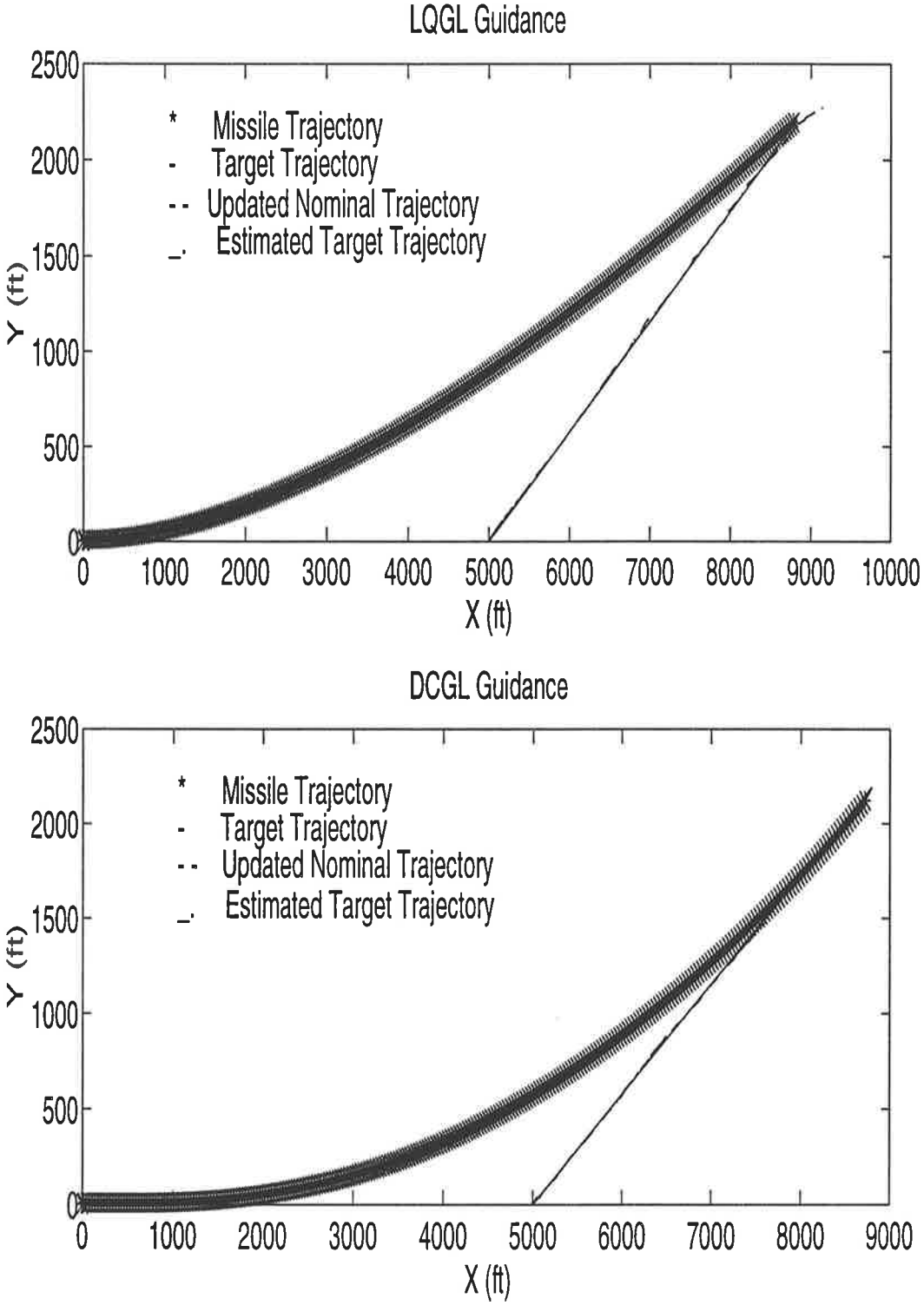

Figure 5.5: Pursuer and target trajectories for scenario 1

same conclusions as those related to the first, namely that the DCGL outperforms the LQGL towards the end of the engagement, in terms of position errors. This is to be expected since although the target is maneuvering at the beginning of the engagement, its acceleration decreases exponentially until it emulates the behaviour of the non-maneuvering target. It is to be noted however that the final time-to-go is less than that of the non-maneuvering target since the acceleration tends to reduce the range between pursuer and target. We also note the surge in target acceleration error at the beginning of the engagement, in line with the high initial value of target acceleration. This error decreases gradually with time. On the other hand, if we compare the pursuer and target trajectories for both LQGL and DCGL we notice that the DCGL final miss-distance is not negligible, although the shape of the trajectory suggests that intercept is not far away. This error in the miss-distance could be attributed to our inaccurate scheme of estimating the time-to-go (range divided by range rate), rather than to a lack of observability. Although other methods of time-to-go estimation could be used (see for example [93]), this simplified method was adopted to avoid further complexity in the problem.

The third scenario presents the biggest challenge to both guidance laws. In fact neither one converges to an acceptable final miss-distance, but the study of their respective behaviour sheds some light on the nature of the problem of handling maneuvering targets. By examining Figures 5.8 and 5.9, we could immediately see that the performance of both guidance laws in terms of position error remains acceptable for the first few seconds after the start of the engagement (about 2 seconds), at which time the estimated target trajectory departs from its true one, then tries to converge again. However, it was noticed that when the target heading angle approaches 90° the performance diverges drastically. For that reason, we have limited the simulation of this scenario to a heading angle less than 90°, in an attempt to analyse this "departure" phenomenon. It is noticed that for this limited scenario, the DCGL has better convergence criteria than the LQGL, in the sense that it attempts to follow the true target trajectory instead of the estimated one.

But, as outlined in the introduction, perhaps some of the most interesting results of the present study is the importance of the approach adopted here to study the

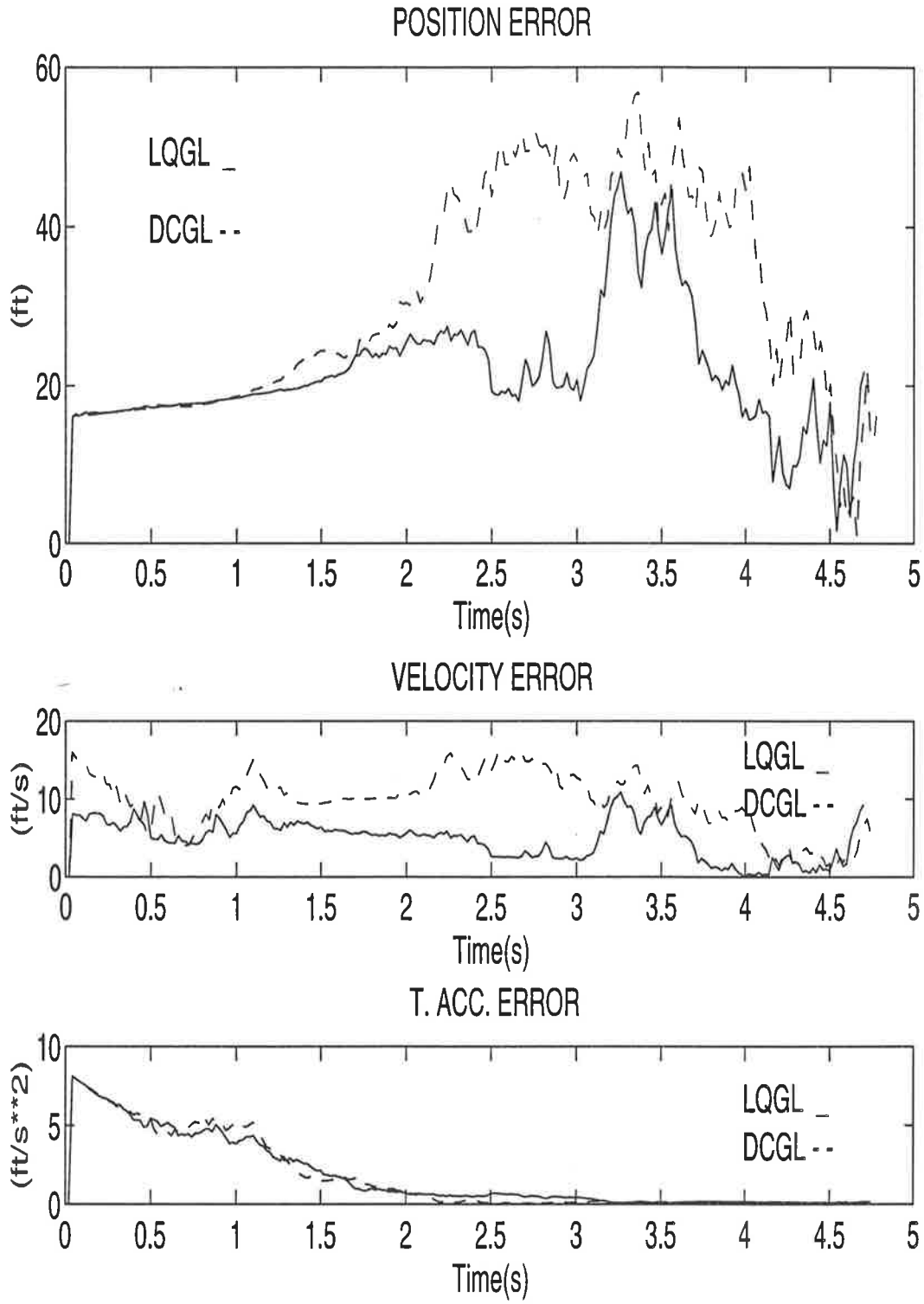

Figure 5.6: State estimation errors for scenario 2

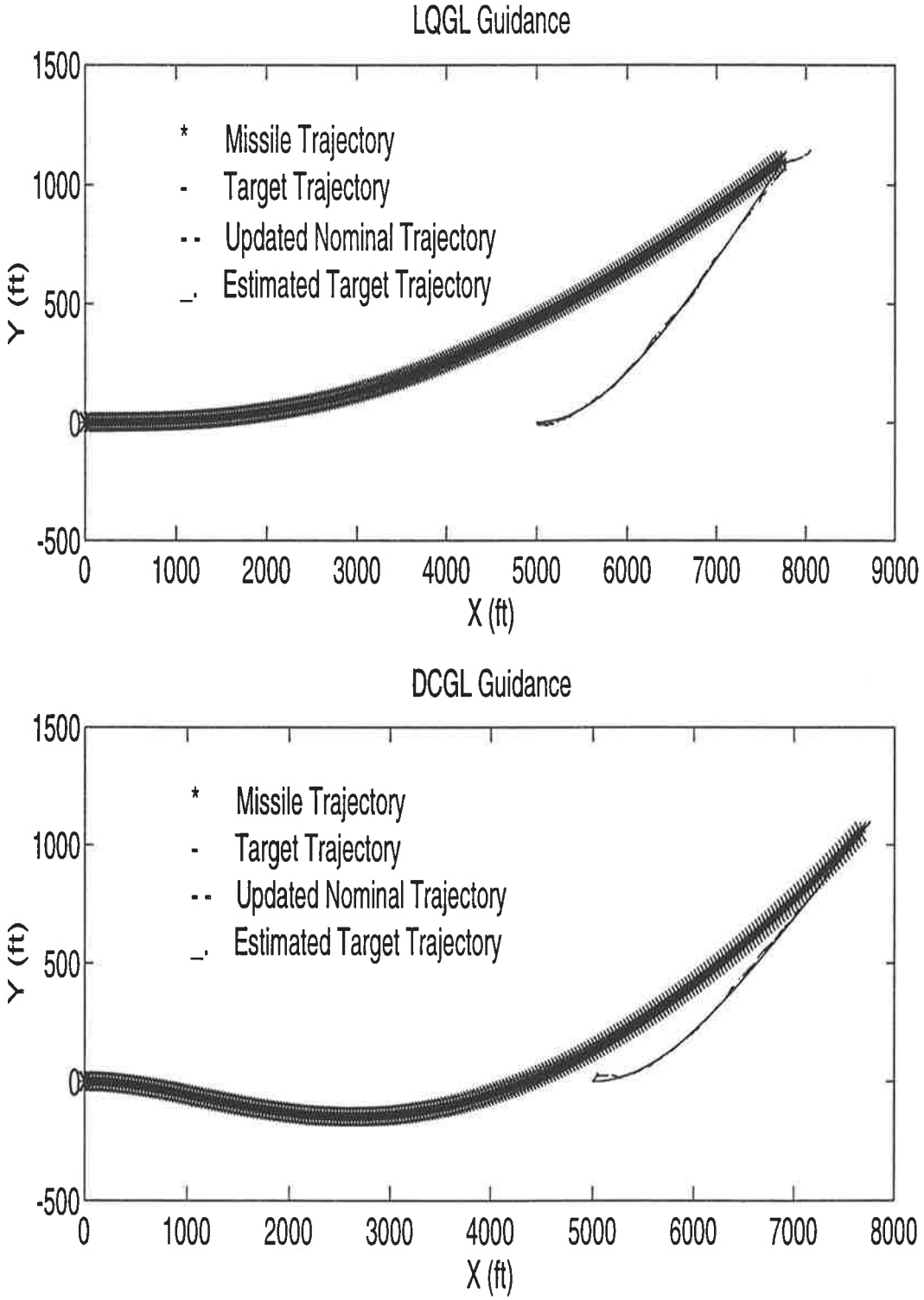

Figure 5.7: Pursuer and target trajectories for scenario 2

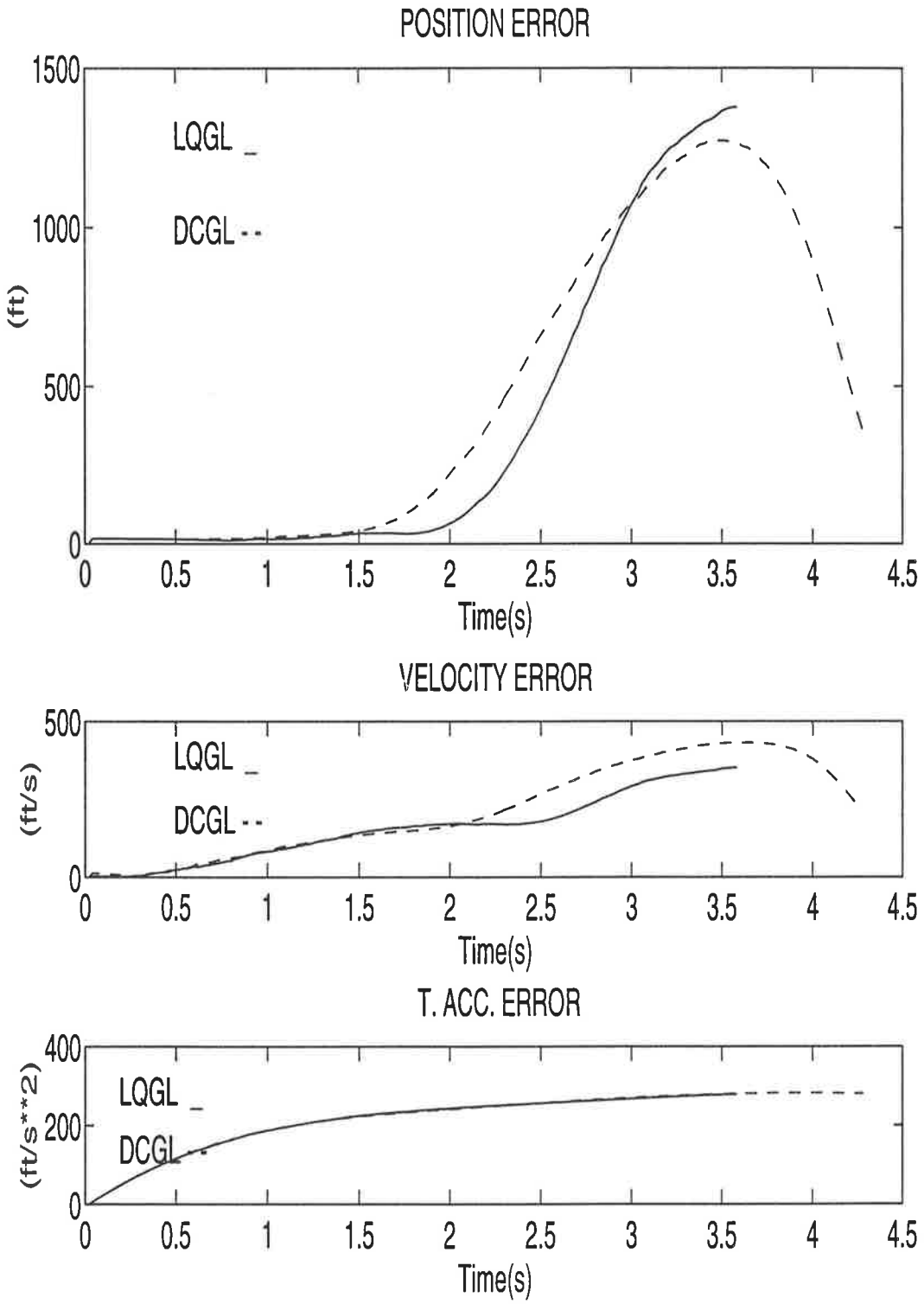

Figure 5.8: State estimation errors for scenario 3

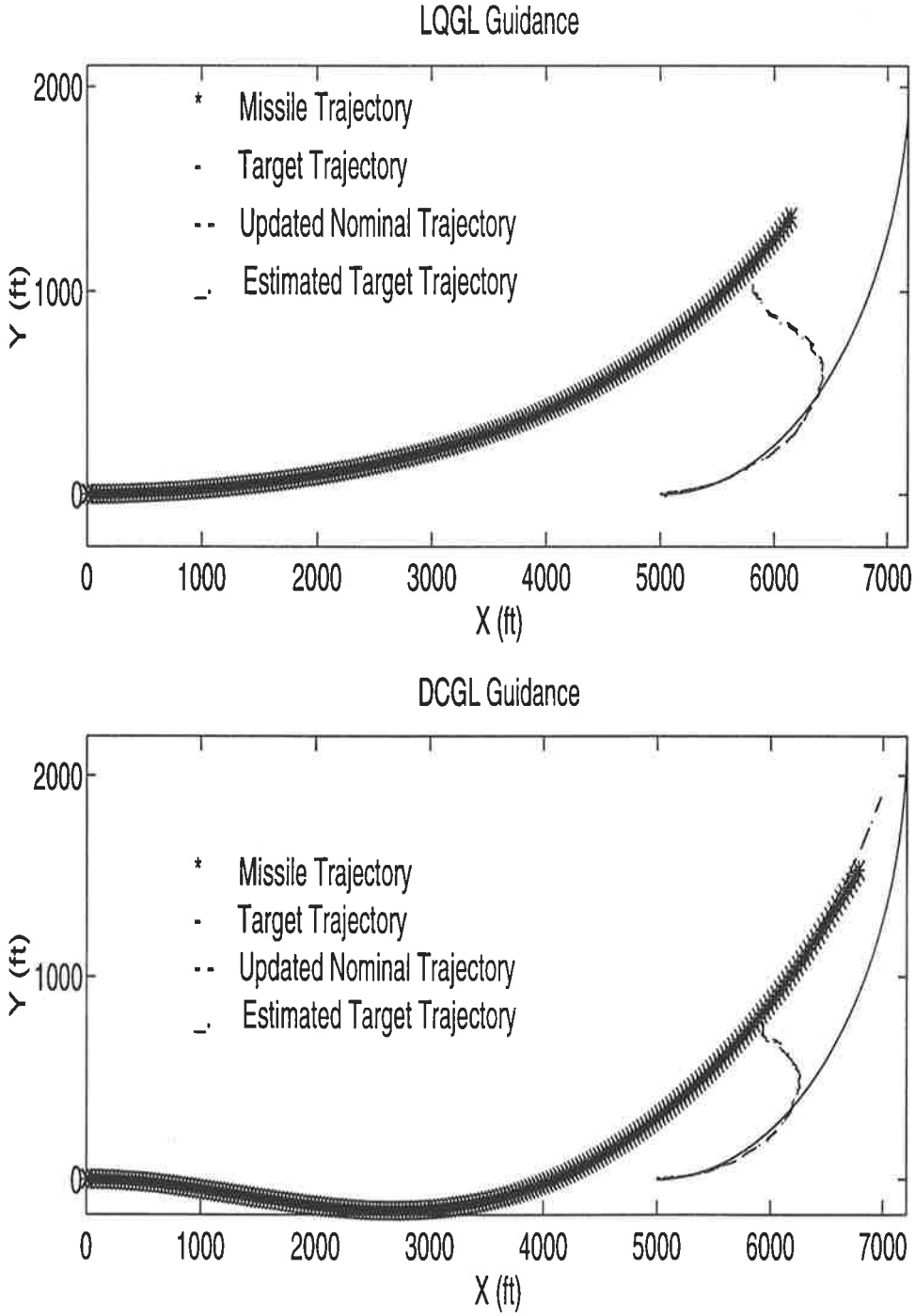

Figure 5.9: Pursuer and target trajectories for scenario 3

guidance laws in addition to the importance of their *mechanisability*. In an open-loop approach, the practice is to feed the true state (or its corresponding normal acceleration) to the guidance law, in order to study the filter performance. That is what was done in the simulations represented in Figures (5.10) and (5.11) and in the fourth rows of Tables (5.1) and (5.2) (scenario entitled 3a). In these simulations, the true state of the engagement with a circularly maneuvering target (scenario 3) were used by the guidance law. The final position estimation errors were found far less than the errors obtained when the state estimate were fed to the Kalman filter. The importance of this point lies in the fact that working with a non-mechanisable law can be misleading by suggesting favourable filter performance while the true performance is far from being so.

Finally, the data contained in Tables 5.1 and 5.2 summarise in a quantitative form the simulation results portrayed in the above figures. Table 5.1 contains the miss-distances and the times-to-go for both guidance laws as they are estimated by the Kalman filter, while Table 5.2 contains the true miss-distances and times-to-go as they are prescribed by the guidance laws. Table 5.1 allows for the comparison of LQGL and DCGL in the presence of the state estimator, while Table 5.2 allows for the observation of the effect of the state estimator (by comparing with Table 5.1). It is noted that DCGL presents a significant miss-distance improvement over LQGL for the first two scenarios, however the times-to-go for both guidance laws appear to be quite close. This is quite contradictory with the preliminary study performed on maximum information (Chapter 3), which suggested that the miss-distance improves on behalf of a longer time-to-go. This could be explained in part by the fact that our time-to-go in the linear quadratic guidance is specified by the problem while in the previous study the time-to-go was taken to be a free parameter. On the other hand, it could be argued that the time lost by DCGL during the first part of the engagement is regained during the last part of the engagement where the LQGL finds it difficult to observe the target and satisfy the homing criterion. On the other hand, it is readily seen that the data contained in Table 5.2 differ sometimes substantially from their estimated counterparts contained in Table 5.1, more so for LQGL than for DCGL. However, the trend of shorter DCGL

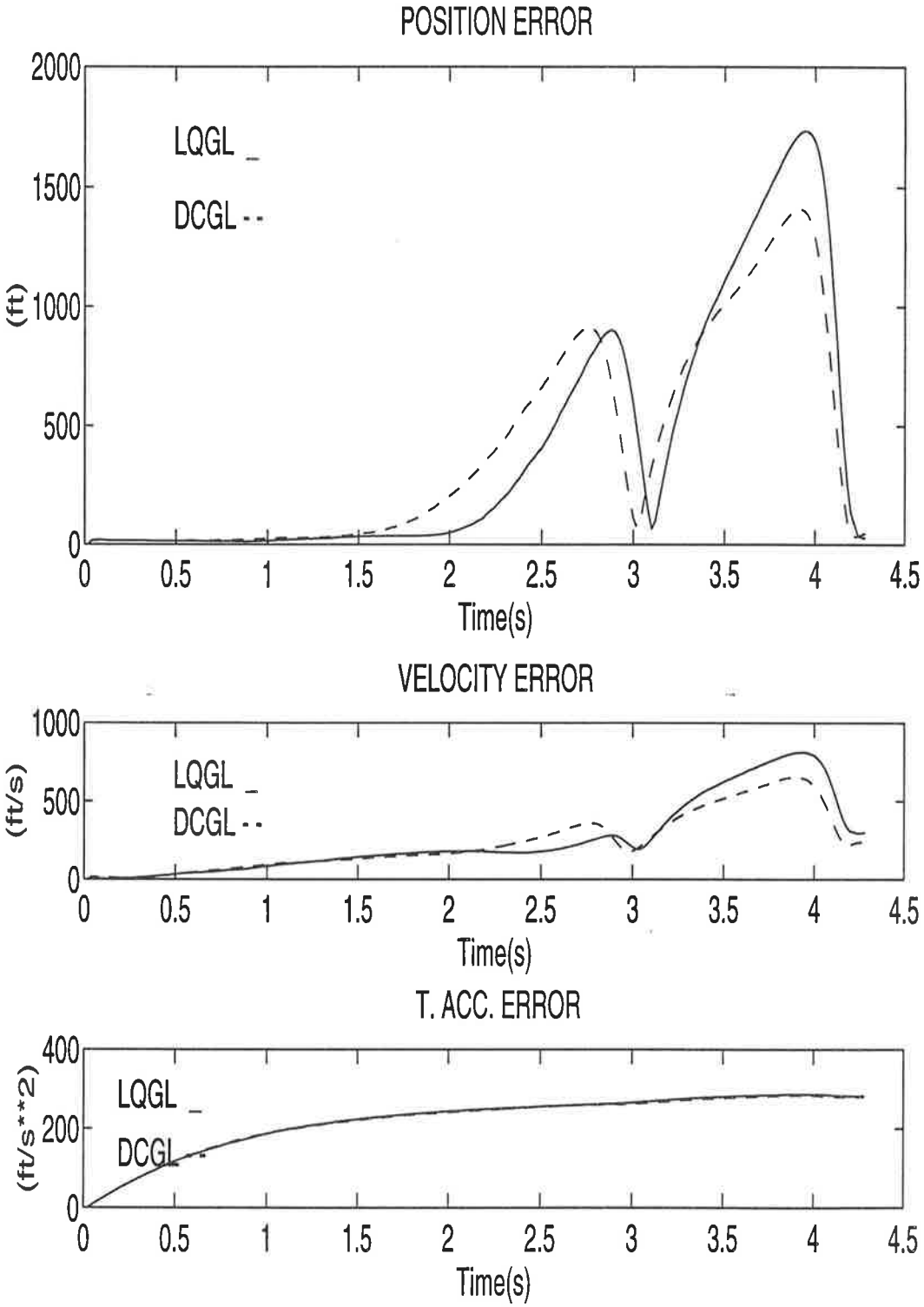

Figure 5.10: State estimation errors for scenario 3 - True state components are used

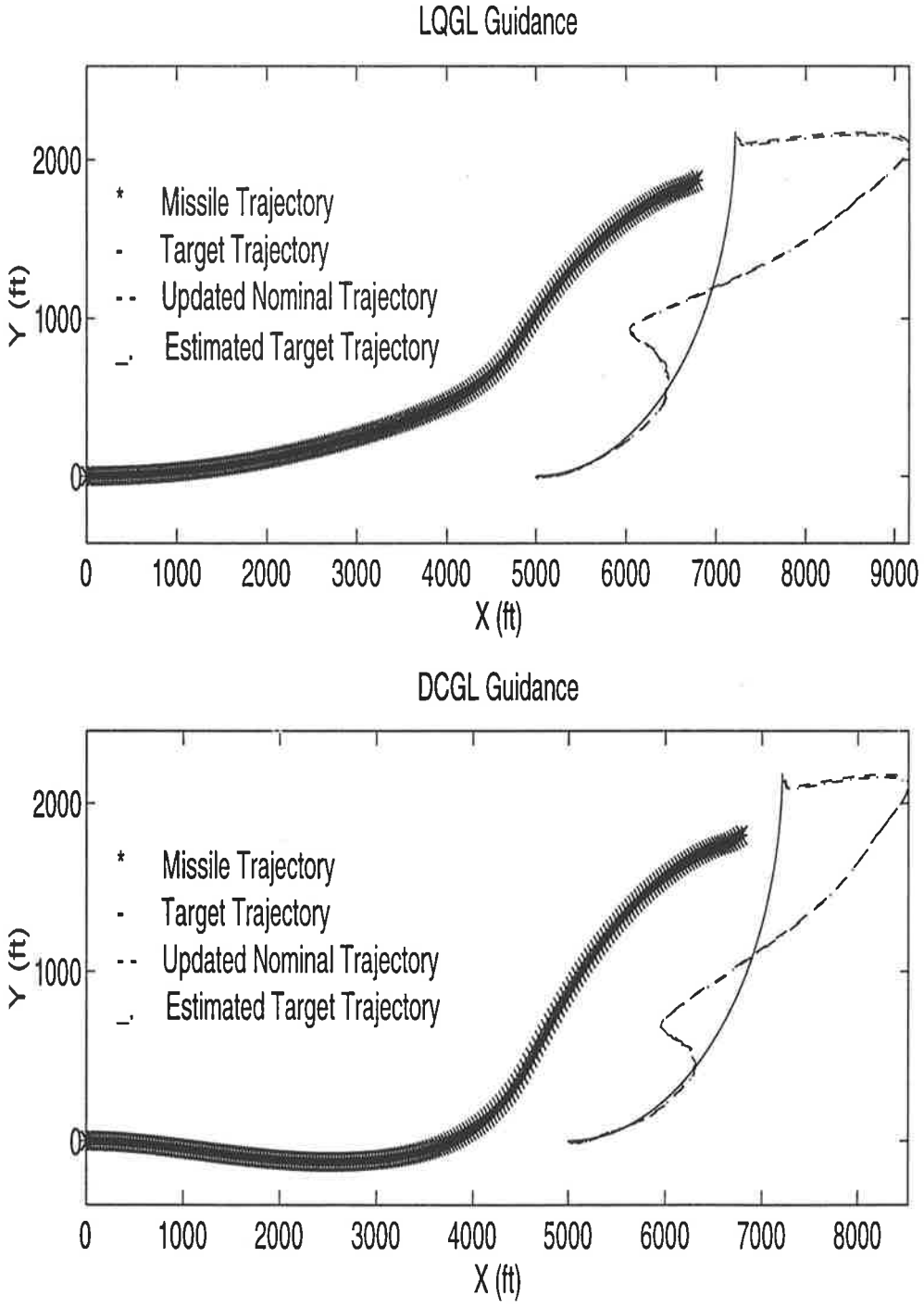

Figure 5.11: Pursuer and target trajectories for scenario 3 - True state components are used

Scenario	LQGL		DCGL	
	$\hat{R}_f\ (ft)$	$\hat{t}_f\ (s)$	$\hat{R}_f\ (ft)$	$\hat{t}_f\ (s)$
1	98.15	5.75	74.24	5.48
2	243.4	4.92	74.78	4.83
3	116.78	3.60	421.29	4.28
3a	476.64	4.28	497.42	4.28

Table 5.1: Average estimated data for 50 Monte-Carlo runs

Scenario	LQGL		DCGL	
	$R_f\ (ft)$	$t_f\ (s)$	$R_f\ (ft)$	$t_f\ (s)$
1	311.76	5.46	68.10	5.48
2	136.10	4.38	62.36	4.38
3	1493.8	3.90	731.20	4.28
3a	490.41	4.28	542.63	4.28

Table 5.2: Average true data for 50 Monte-Carlo runs

miss-distance appears to be conserved for the first and second scenario. The data related to the third scenario are to be interpreted from a different perspective. As a matter of fact, our state estimator is not designed to handle circularly rotating targets and the problems appearing around the target heading angle of 90° prevent the filter convergence. However, it seemed informative to simulate this case in order to acquire better insight into the problem at hand and to graphically compare the LQGL and DCGL performances.

5.4 Summary

In this chapter, the dual control guidance law (DCGL) is introduced as an alternative to the non-mechanisable maximum information guidance law (Chapter 3).

Since DCGL could be considered as an "extension" to the linear quadratic guidance law (LQGL) this latter law was studied first. Both guidance laws consider a simple linear engagement model whose transition matrix could be easily obtained in closed form. They also assume the same given initial conditions and prescribed final time. The difference between the two laws lies only in the definition of the performance index to be optimised.

The linear quadratic guidance law (LQGL) attempts to minimise the control effort along the engagement trajectory and the miss-distance at the final time. Due to the simplicity of the engagement dynamics, this law could be formulated in closed form leading to a linear expression of the control in terms of the state. It is shown that the resulting control gain depends on the time-to-go and the design parameter weighting the final miss-distance in the performance index. It is also noted that when the value of this design parameter increases, LQGL approaches proportional navigation guidance.

The dual control guidance law, on the other hand, adds a measure of observability to the elements of the LQGL performance index. Not only does it attempt to minimise control effort along the engagement trajectory, but it also tries to maximise observability at the same time. The control could also be obtained analytically in this case (but not in final closed form), however it is more complex and depends on the observability coefficient, in addition to the time-to-go and the design parameter weighting the miss-distance.

A straight forward application of both guidance laws on the two-dimensional bearing-only-measurement problem allowed us to identify one problem encountered with proportional navigation along the extended Kalman filter, namely the divergence of the estimation towards the end of the engagement. A possible remedy is to use the DCGL which offers better performance in terms of less miss-distance and small estimation errors for non-maneuvering and maneuvering targets possessing a Gaussian acceleration model.

Among the most important contributions of the analysis carried out in this chapter, is the approach to the guidance problem. The fact that both guidance laws are

provided as an explicit function of the state variables is very significant since it allows to close the guidance loop. This approach is in line with the dual control concept which stipulates that the interaction between the state estimator and the guidance law has significant repercussions on the overall performance of the state estimator. Allowing the state estimator and the guidance law to interact, even at the testing stage is therefore crucial and represents a distinctive departure from previous approaches (Chapters 2, 3 and 4).

Another contribution of the present approach is the ability to simulate maneuvering targets. Instead of adopting two different models for the guidance and the filter, the so called *filter model* [34] was adopted for both guidance and filtering. Although simple and linear, this model provides the benefit of simulating maneuvering targets since it accounts for the target acceleration. The non-maneuvering and "exponentially maneuvering" targets are covered by this model by just accommodating the initial conditions. The "circularly maneuvering" target, however, is not accounted for by the model. Nevertheless, it was simulated in an attempt to study the performance of the state estimator and to compare the behaviour of the two guidance laws in the case of unexpected target maneuvers.

Finally, this study allowed us to sense the importance of the estimation of the time-to-go. Accurately estimating the time-to-go is crucial for the success of LQGL and DCGL. This is perhaps due to the nature of the linear quadratic optimal control problem which inherently assumes a known final time. As we saw in the simulation, the difficulty in estimating the time-to-go is less critical for the DCGL than for the LQGL since the former guidance law seems to better align the pursuer with the target trajectories especially in light of the speed superiority of the pursuer. However, a more pressing problem of the DCGL seems to be the choice of the observability weighting coefficient. One of the observations that surfaced, as a result of the simulations carried out in the present study, leads to the conclusion that, for each engagement scenario, there seems to exist an optimal observability weighting coefficient, beyond which the filter performance deteriorates. The choice of this coefficient was made by trial and error, and although it is possible to choose a "safe" observability coefficient for several possible scenarios, it would be desirable

to identify a more structured selection procedure or to formulate the problem so that it does not include an observability coefficient. The issues of the time-to-go and the observability coefficient are two of the limitations of DCGL. They will both be addressed in the next chapter, which proposes a guidance law where the estimate of the time-to-go is not needed and a where a necessary condition on the existence of the observability coefficient is established.

Chapter 6

Observable Proportional Navigation

While the features of proportional navigation, including its effectiveness and ease of implementation are attractive, the Kalman filter divergence problem along the proportional navigation trajectory remains a very limiting impediment. This problem was and still is at the origin of several efforts aiming at designing observability-enhanced guidance laws. In these laws, the objective is not only to null the line-of-sight but also to maximise a certain measure of observability deemed essential for the guidance law to succeed.

Several observability-enhanced guidance laws were analysed in this study. They all optimise certain measures of system observability along with the measure on control effort optimised in proportional navigation. Some of these laws, such as maximum information guidance (Chapter 3), are not mechanisable, while others, such as the dual control guidance (Chapter 4), are mechanisable in the guidance loop. The observability-enhanced guidance laws, typically based on the Fisher information matrix, have provided significant improvements in convergence characteristics for the associated state estimators and resulted in shorter final miss-distances in comparison with proportional navigation at the expense of longer times-to-go. However, these observability-enhanced guidance laws featured several limitations such as com-

plexity, necessity to constantly estimate the time-to-go, in addition to the ad-hoc way of selecting their respective coefficients of observability.

In this chapter, a new observability-enhanced guidance law for homing missiles is presented. As does the dual control guidance law, the new law aims to blend the effectiveness of proportional navigation guidance with the observability of maximum information guidance, while offering the additional feature of mechanisability. But since this new law makes use of the conventional form of proportional navigation (2.10), as opposed to its optimal quadratic form (2.35), used in the dual control guidance law, it retains the simplicity and ease of implementation of proportional navigation guidance while still being responsive to the change in the amount of information on observability of the guidance system.

The *observable proportional navigation guidance law* (OPNG), presented here, addresses the major limitations of the previously proposed observability-enhanced guidance laws. It basically introduces a new term representing the rate of the observability information into the expression of proportional navigation. In the same way that PNG attempts to *maintain* a constant line-of-sight angle by driving the normal acceleration proportionally to the line-of-sight rate, the new guidance law attempts to *maintain* a "constant observability" by driving the normal acceleration proportionally to the "rate of observability". Unlike the dual control guidance law, the observable proportional navigation guidance law does not attempt to *maximise* observability, it rather aims to *maintain* it, in line with the established fact that the observability deterioration occurs only towards the end of the engagement [96].

Both maximum information guidance (Chapter 3) and dual control guidance (Chapter 4) attempt to maximise observability regardless of the initial level of observability. The ensuing problems of both guidance laws, i.e., selection of the observability coefficient, estimation of the time-to-go, non-existence of a closed form solutions, etc., limit the effectiveness of these observability-enhanced guidance laws. The newly proposed observable proportional navigation attempts to address these limitations, at the expense of relaxing the observability requirement. In other words, starting from an observable initial scenario [36], if we can solve some of the limita-

tions mentioned above, while maintaining the initial satisfactory level of observability, we would have contributed to the ultimate solution of this guidance problem.

Depending on the form of the applied normal acceleration, one can formulate several forms of the observable proportional navigation guidance law that can potentially achieve its stated aim. Two forms of the observable proportional navigation guidance law were analysed in this chapter. The *additive* OPNG adds an observability term to the expression of PNG, and the *multiplicative* OPNG multiplies this term by the expression of PNG. For these two variants of OPNG, closed form solutions of the proposed guidance law are given in terms of the relative range and the coefficient of observability, for two distinct noise models. In addition, necessary bounds on the observability coefficient are established in terms of the initial conditions.

In both cases, the law is simple and mechanisable along the corresponding filter, and, unlike DCGL, does not rely on the continuous estimation of the time-to-go. Several Monte-Carlo simulations of the law in both forms, are applied to a two-dimensional guidance system. They show that, within a close range of the necessary bounds on the observability coefficient, the state estimator exhibits better estimation performance under the new law than under proportional navigation. The end-result is manifested in shorter final miss-distances at the expense of longer times-to-go and higher control efforts.

6.1 Observable Proportional Navigation Guidance Law

Given the pursuer-target dynamics either in the form of the guidance model (2.1) or in the form of its equivalent filter model (4.32), the observable proportional navigation guidance law (OPNG) prescribes, in general, a pursuer normal acceleration A_n as a function of the rate of an appropriate measure on system observability $\dot{\mu}$ [32]:

$$A_n = f(\dot{\mu}) \tag{6.1}$$

The expression of μ is based on the Fisher information matrix, as in the case of the DCGL, and can take one of the forms of the observability measures encountered in Chapter 3. As we can see from (3.39), this expression depends on the filter used alongside the guidance law, through the measurement (or pseudo-measurement) gradient, as well as on the noise model, through the noise spectral density. In addition, the dependence function f can take several possible forms. In the following, we consider two distinct forms of this function along with two different forms of noise and filter models, respectively.

6.2 Additive Observable Proportional Navigation

6.2.1 Expression

In this law, the function $f(\cdot)$, that defines the dependence of the guidance law on system observability, is additive. It contains the original expression of the PNG normal acceleration and a novel term relating to the rate of an observability measure, μ:

$$A_n = -N_1 \dot{R}\dot{\sigma} - N_2 \dot{R}\dot{\mu} \tag{6.2}$$

where N_1 is the (proportional) navigation constant and N_2 is the (additional) observability coefficient reflecting the amount of observability in the law.

There is an apparent similarity between the form of the expression of AOPNG and the biased proportional navigation outlined in [14, 103]. But while the constant bias term in the latter guidance law tends to directly rectify the line-of-sight angle rate in the expression of the guidance law, the variable observability measure in

the AOPNG is more concerned with the associated state estimator. Not only does AOPNG *react* to the change in range and line-of-sight along the intercept trajectory, but also to the change of observability in the state estimator. It is intended to induce a modulation of the proportional navigation trajectory by the new additive term reflecting observability. Note that, while range and line-of-sight angle are two geometrical, directly measurable quantities, observability as such is not directly measurable. Yet in certain cases, its rate could be derived in terms of the state components, as we have seen in Chapter 3 (3.44).

In the AOPNG, $\dot{\mu}$ is taken to be the rate of the trace of the Fisher information matrix [80]. For bearing-only-measurements induced by glint noise only, the spectral density of the noise (4.39) takes the form:

$$V = \frac{a}{R^2} \tag{6.3}$$

where R is the range between the pursuer and the target and a the glint noise coefficient.

Assuming that the filter used is the MGEKF (section 4.2), we could derive from (3.39) the rate of the trace of the position part of the Fisher information matrix, μ, in the same fashion as (5.35) was derived in Chapter 5. We obtain:

$$\dot{\mu} = \frac{R^2}{a} \tag{6.4}$$

6.2.2 Closed Form Solution

In this section, we solve the equations of motion of the guidance system in the polar coordinate system (see (2.20), (2.21) and [57]), as they apply to the additive observable proportional navigation guidance law:

$$\ddot{R} - R\dot{\sigma}^2 = 0 \tag{6.5}$$

$$R\ddot{\sigma} + 2\dot{R}\dot{\sigma} = N_1\dot{R}\dot{\sigma} + \frac{N_2}{a}\dot{R}R^2 \tag{6.6}$$

If we multiply (6.6) by $\frac{R}{\dot{R}}$, we get:

$$R^2\frac{\ddot{\sigma}}{\dot{R}} + 2R\dot{\sigma} = N_1R\dot{\sigma} + \frac{N_2}{a}R^3 \tag{6.7}$$

As in [104], let us define the massless angular momentum of the pursuer relative to the target as:

$$h = R^2\dot{\sigma} \tag{6.8}$$

then we could write (6.7) as:

$$\frac{dh}{dR} - N_1\frac{h}{R} = \frac{N_2}{a}R^3 \tag{6.9}$$

This is a first order ordinary differential equation whose solution takes the form [87]:

$$hR^{-N_1} = \int_{t_0}^{t_f}\frac{N_2}{a}R^{3-N_1}dR + C \tag{6.10}$$

where C is an integration constant dependent on the initial conditions.

If $N_1 \neq 4$

In the case where $N_1 \neq 4$ we could write:

$$hR^{-N_1} = \frac{N_2R^{4-N_1}}{a(4-N_1)} + C \tag{6.11}$$

Using the initial conditions (namely $\dot{\sigma} = \dot{\sigma}_0$ when $R = R_0$) and the definition of the massless angular momentum (6.8), we deduce the expression of the line-of-sight rate:

$$\dot{\sigma} = \dot{\sigma}_0(\frac{R}{R_0})^{N_1-2} + \frac{N_2}{a(4-N_1)}R^2\left[1-(\frac{R}{R_0})^{N_1-4}\right] \tag{6.12}$$

Now we can use the expression of $\dot{\sigma}$ into (6.5):

$$\ddot{R} = R\dot{\sigma}^2 = R_0{\dot{\sigma_0}}^2(\frac{R}{R_0})\left\{(\frac{R}{R_0})^{N_1-2} + m(\frac{R}{R_0})^2\left[1-(\frac{R}{R_0})^{N_1-4}\right]\right\} \tag{6.13}$$

where $m = \frac{N_2 R_0^2}{a(4-N_1)\dot{\sigma_0}}$.

Equation (6.13) can then be integrated to yield:

$$\begin{aligned}\dot{R}^2 &= R_0^2\dot{\sigma}_0^2\left[\frac{m^2}{3}(\frac{R}{R_0})^6 + \frac{4m(1-m)}{N_1+2}(\frac{R}{R_0})^{N_1+2} + \frac{1-2m+m^2}{N_1-1}(\frac{R}{R_0})^{2(N_1-1)}\right] \\ &+\dot{R}_0^2 - R_0^2\dot{\sigma}_0^2\left[\frac{m^2}{3} + \frac{4m(1-m)}{N_1+2} + \frac{(1-m)^2}{N_1-1}\right]\end{aligned} \tag{6.14}$$

If $N_1 = 4$

In this case, a similar procedure to the one described in the previous section leads to the following expressions for the rates of the line-of-sight angle and the range:

$$\dot{\sigma} = \dot{\sigma}_0(\frac{R}{R_0})^2 + \frac{N_2}{a}R^2 ln(\frac{R}{R_0}) \tag{6.15}$$

$$\begin{aligned}\dot{R}^2 &= R_0^2{\dot{\sigma}_0}^2\left\{\frac{1}{3}(\frac{R}{R_0})^6 + \frac{2}{3}m(4-N_1)\left[(\frac{R}{R_0})^6(ln(\frac{R}{R_0}) - \frac{1}{6})\right]\right. \\ &\left.+\frac{1}{3}(4-N_1)^2m^2\left[(\frac{R}{R_0})^6(ln^2(\frac{R}{R_0}) - \frac{1}{3}ln(\frac{R}{R_0}) + \frac{1}{18})\right]\right\} + \dot{R}_0^2 \\ &-\frac{1}{3}\left[1 - \frac{m(4-N_1)}{3} + \frac{m^2(4-N_1)^2}{18}\right]\end{aligned} \tag{6.16}$$

We see that the expressions of the range rate and the line-of-sight angle rate are derivable in closed form which can help deduce the theoretical characteristics of the new guidance law.

Lemma 6.1 *When implemented in conjunction with the modified gain extended Kalman filter, and a passive seeker providing bearing-only-measurements corrupted with glint noise only, the additive observable proportional navigation guidance law defined by (6.2) and applied to the two-dimensional pursuer-target intercept problem defined by (6.5, 6.6), has closed form solutions in (6.12) and (6.13) if the navigation constant $N_1 \neq 4$, and in (6.15) and (6.17) if the navigation constant $N_1 = 4$.*

6.2.3 Characteristics

It is noted from (6.12) that the line-of-sight rate reduces to that of proportional navigation when $N_2 = 0$. For $N_2 \neq 0$ however, the line-of-sight rate approaches zero, as in the case of proportional navigation, but it is modulated by an additional factor. It is also possible to verify that, for constant range rate, the restriction on the navigation constant N_1 is the same as the one imposed in the case of proportional navigation (namely $N_1 > 2$) in order to avoid an infinite normal acceleration.

For illustration purposes, let us take the case where $N_1 = 3$. From (6.12) we have:

$$\frac{\dot{\sigma}}{\dot{\sigma}_0} = m(\frac{R}{R_0})^2 + (1-m)\frac{R}{R_0} \tag{6.17}$$

where $m = \frac{N_2 R_0^2}{a(4-N_1)\dot{\sigma}_0}$.

Figure 6.1 shows this relationship with different values of m.

It clearly reveals that proportional navigation ($m = 0$) nulls the line-of-sight rate linearly, while observable proportional navigation modulates the dependence between the line-of-sight rate and the range, while still nulling the line-of-sight rate, at the end of the engagement.

In addition, from (6.13) we can write:

$$\frac{\dot{R}}{\dot{R}_0} = \left\{1 + \frac{1}{A^2}\left\{\frac{m^2}{3}[(\frac{R}{R_0})^6 - 1] + \frac{4}{5}m(1-m)[(\frac{R}{R_0})^5 - 1]\right.\right.$$

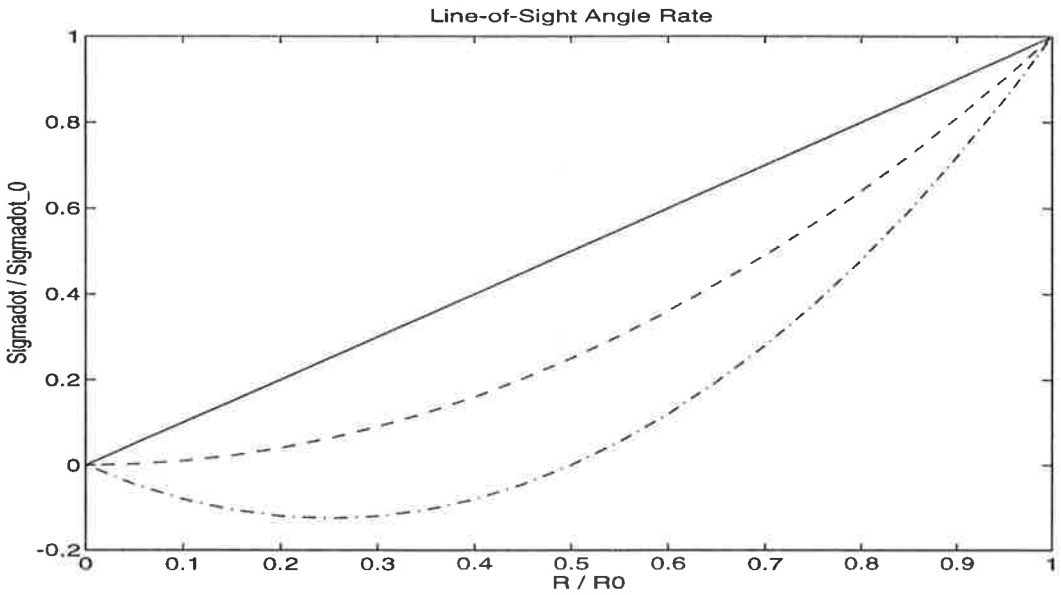

Figure 6.1: Line-of-sight angle rate vs range for $m = 0$ (solid line); $m = 1$ (dashed) and $m = 2$ (dash-dotted)

$$+\frac{1}{2}(m-1)^2[(\frac{R}{R_0})^4 - 1]\Big\}\Big\}^{\frac{1}{2}} \tag{6.18}$$

which is plotted in Figure 6.2. Note that $A = \frac{\dot{R}_0}{R_0\dot{\sigma}_0}$ as defined in [103].

Given (6.17) and (6.18), it is possible to determine the conditions for an effective intercept, i.e., an intercept "with a finite acceleration and with a finite time of duration" [101]. Those conditions allow us to determine a necessary condition on the observability coefficient, N_2, for the intercept to be effective, for the case where $N_1 \neq 4$, namely:

$$N_2 \leq \frac{9}{2}a\frac{\dot{\sigma}_0}{R_0^2}(N_1-2)\frac{-1+\sqrt{1-\frac{4}{27}\frac{(N_1-4)(N_1+2)}{(N_1-2)^2}}}{N_1-4} \tag{6.19}$$

However, for the case where $N_1 = 4$ a more careful study reveals that an effective intercept in the sense defined in [101] is not possible and therefore it is excluded.

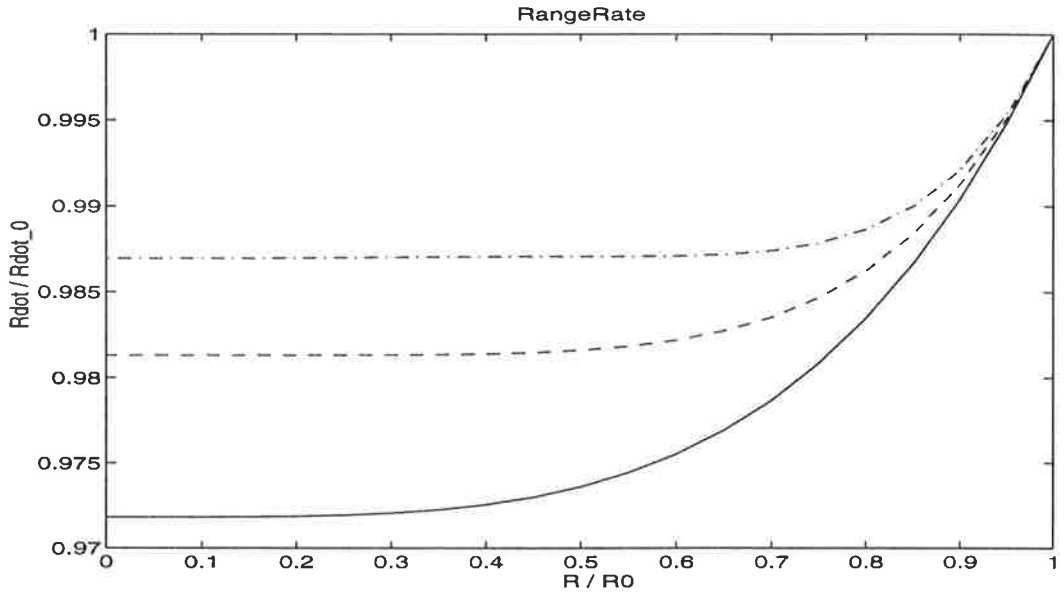

Figure 6.2: Range rate vs range for $m = 0$ (solid line); $m = 1$ (dashed) and $m = 2$ (dash-dotted)

6.2.4 Simulation

In order to test the behaviour of the additive observable proportional navigation guidance law, its performance was analysed against the performance of proportional navigation for three different scenarios outlined in Table 6.1. The state estimator used for both guidance laws was the modified gain extended Kalman filter, and the measurement noise was made of a glint component only, having a spectral density of the form outlined in (6.3), where the glint coefficient a is given by:

$$a = 0.25 rad^2 ft^2 \ s \tag{6.20}$$

We note that in the three different scenarios, the initial distance separating pursuer from target is the same and is equal to 3000 ft. In addition, the navigation constant N_1 was taken to be equal to 3 in all three cases. On the other hand, the maximum values of the observability coefficient $N_{2_{max}}$ were deduced from (6.19) and used to choose the actual adopted values of N_2. Both N_2 and $N_{2_{max}}$ are listed in Table 6.2.

Scenario	$V_M\ (ft\ s^{-1})$	$V_T\ (ft\ s^{-1})$	$\phi_0\ (o)$
1	1600	800	30
2	1600	800	45
3	1600	1000	30

Table 6.1: Three pursuer-target scenarios

Scenario	$N_{2max}\ (10^{-8})$	$N_2\ (10^{-8})$
1	3.77	1
2	5.48	0.9
3	4.84	1

Table 6.2: Observability coefficients for three different scenarios

Two different types of performance criteria were compared between proportional navigation and additive observable proportional navigation. On one hand, the estimation of the final miss-distance and the final time-to-go were recorded, and on the other, the estimation errors on position, speed, and target acceleration were plotted along the intercept trajectory. These estimation errors are defined as in (4.40), namely:

$$\begin{aligned} e_p &= \frac{1}{n}\sqrt{[\sum_{i=1}^{n}(X_{ri}-\hat{X}_{r_i})]^2+[\sum_{i=1}^{n}(Y_{ri}-\hat{Y}_{r_i})]^2} \\ e_v &= \frac{1}{n}\sqrt{[\sum_{i=1}^{n}(U_{ri}-\hat{U}_{r_i})]^2+[\sum_{i=1}^{n}(V_{ri}-\hat{V}_{r_i})]^2} \\ e_{aT} &= \frac{1}{n}\sqrt{[\sum_{i=1}^{n}(A_{TX_i}-\hat{A}_{TX_i})]^2+[\sum_{i=1}^{n}(A_{TY_i}-\hat{A}_{TY_i})]^2} \end{aligned} \tag{6.21}$$

where n denotes the number of Monte-Carlo runs, which was 50 in our simulations, and the subscript N, denoting the nominal value in (4.40), is eliminated here to simplify the equations.

The average estimated miss-distances and times-to-go for the 50 Monte-Carlo runs

Scenario	Additive OPNG		True PNG	
	$\hat{R}_f\ (ft)$	$\hat{t}_f\ (s)$	$\hat{R}_f\ (ft)$	$\hat{t}_f\ (s)$
1	39.64	3.98	225.04	3.58
2	39.57	4.78	2118.70	3.32
3	97.12	5.67	1091.90	4.72

Table 6.3: Comparative miss-distances and times-to-go for PNG and additive observable PNG

are recorded in Table 6.3. They show a clear advantage in using the additive observable proportional navigation guidance law, in terms of estimated miss-distances at the expense of a longer estimated times-to-go. The trend is consistent for the three different scenarios considered.

For illustration purposes, the position, speed and target estimation errors are shown in Figure 6.3, Figure 6.4 and Figure 6.5 which show a lower estimation error for AOPNG, especially towards the end of the intercept where proportional navigation shows a great amount of unpredictability. The corresponding pursuer trajectories shown in Figure 6.6, Figure 6.7 and Figure 6.8, respectively, present a certain amount of oscillatory maneuvering before reaching the target.

In order to test the sensitivity of AOPNG to variations in the glint coefficient a, the simulations above were repeated with different values of a reaching up to 25 % of its value mentioned in (6.20). The same general features mentioned above were recorded, which highlights the robustness of AOPNG to variations in the design parameters.

All of the above simulations correspond to three scenarios covered by the analysis of the observable proportional navigation guidance which led to the derivation of the closed form solution and the necessary bound on the observability coefficient. In Figures 6.9 and 6.10 however, an additional scenario was explored in which the target is maneuvering with an acceleration of the form given in (4.34) where the

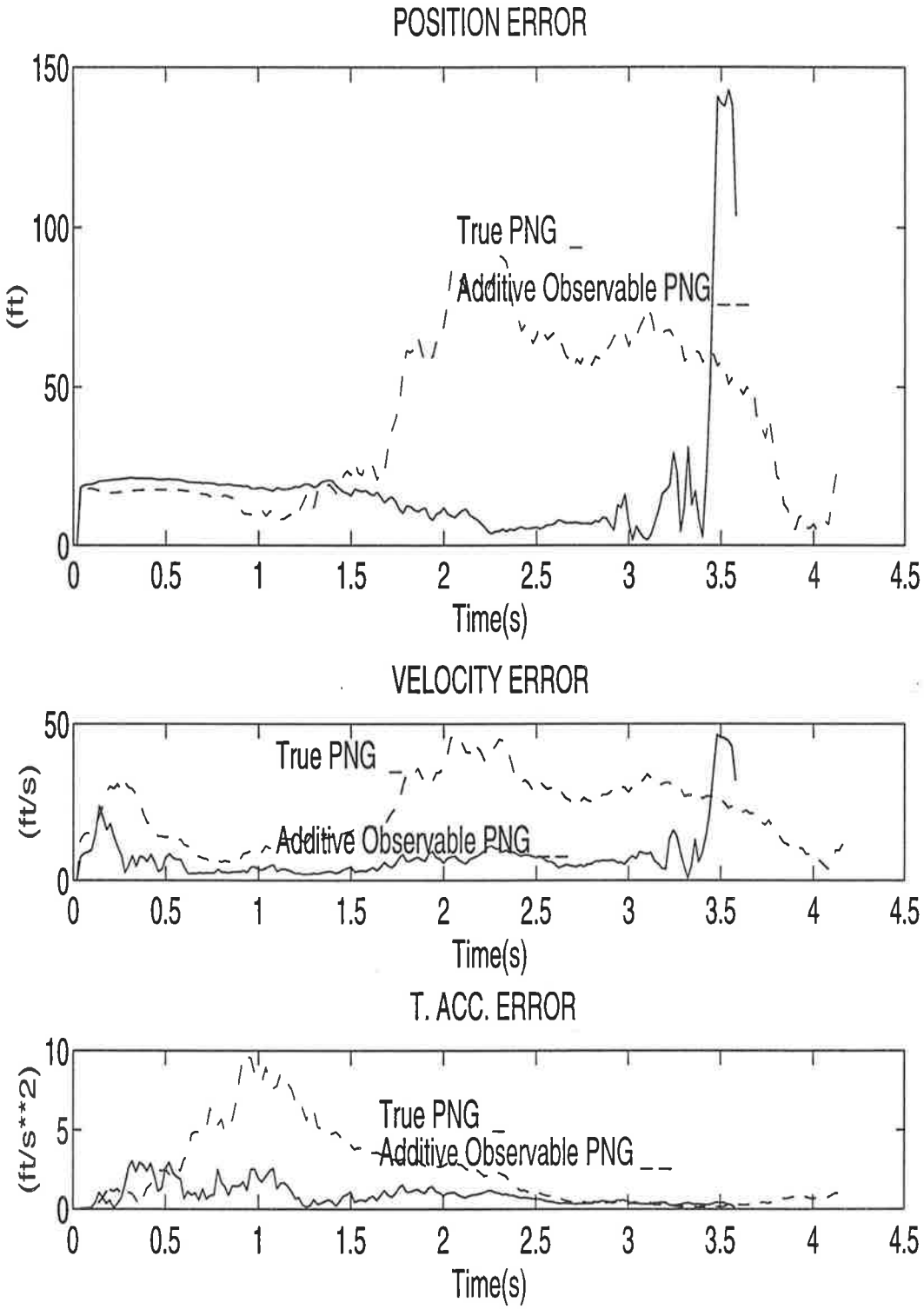

Figure 6.3: Estimation errors for scenario 1

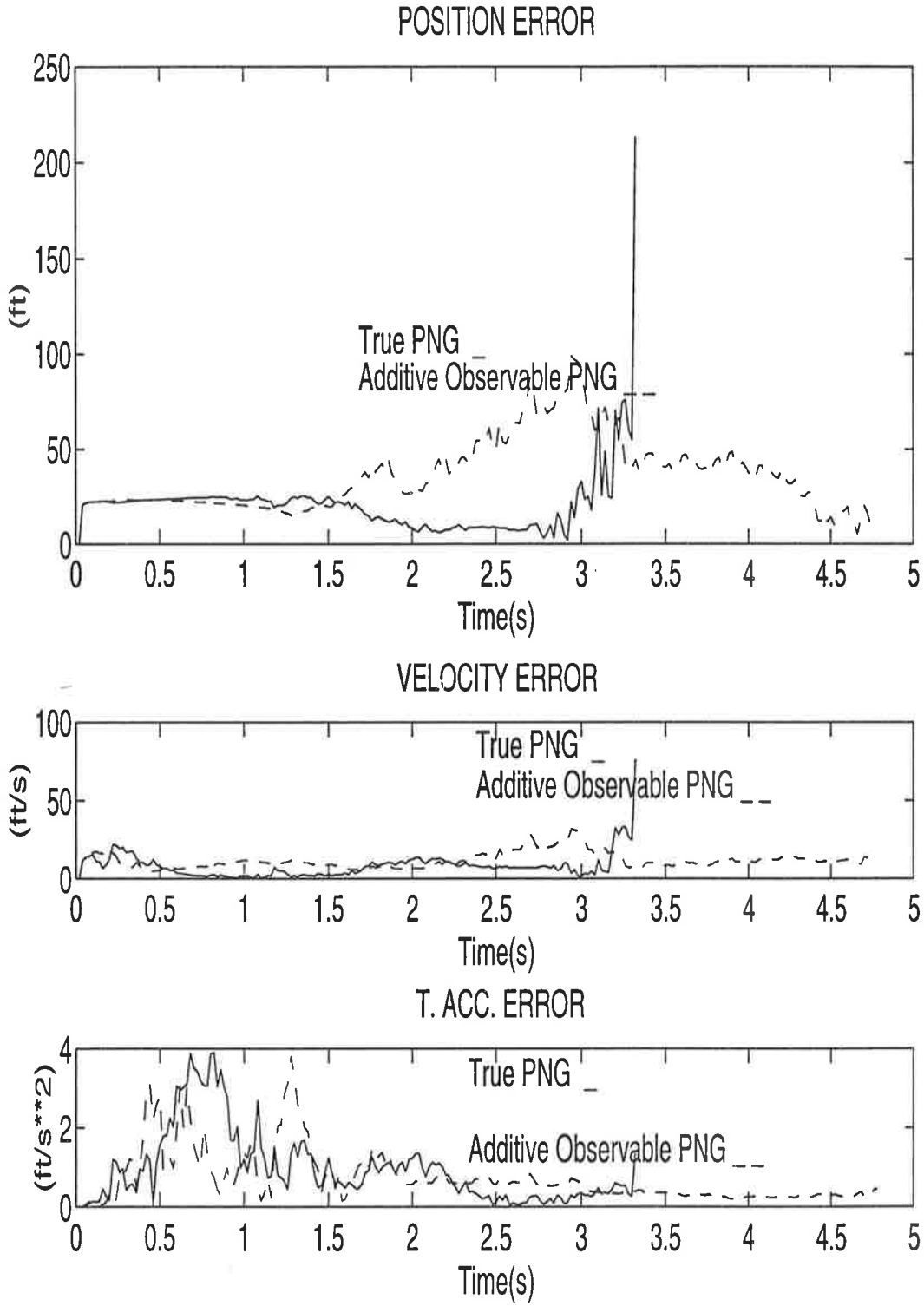

Figure 6.4: Estimation errors for scenario 2

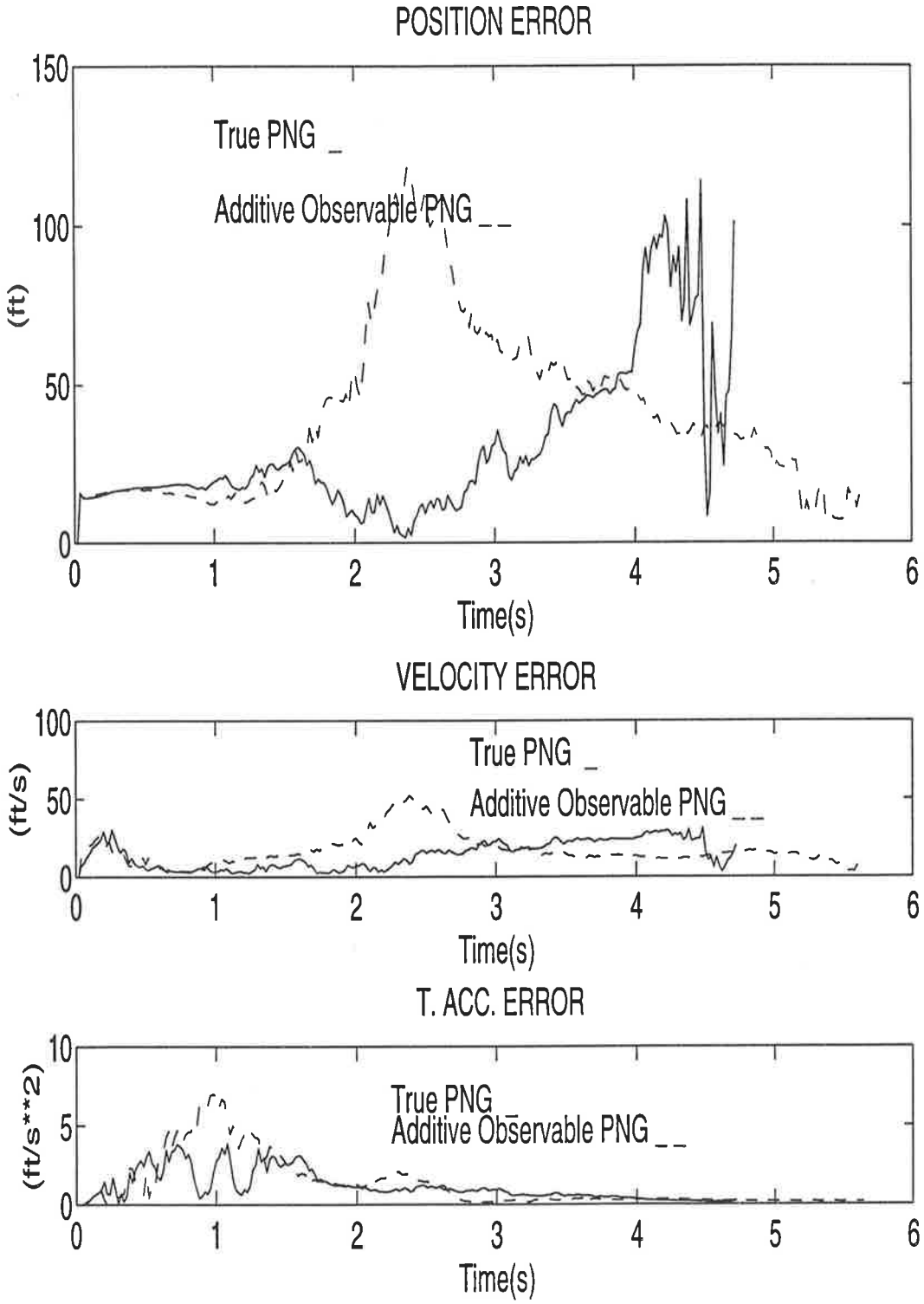

Figure 6.5: Estimation errors for scenario 3

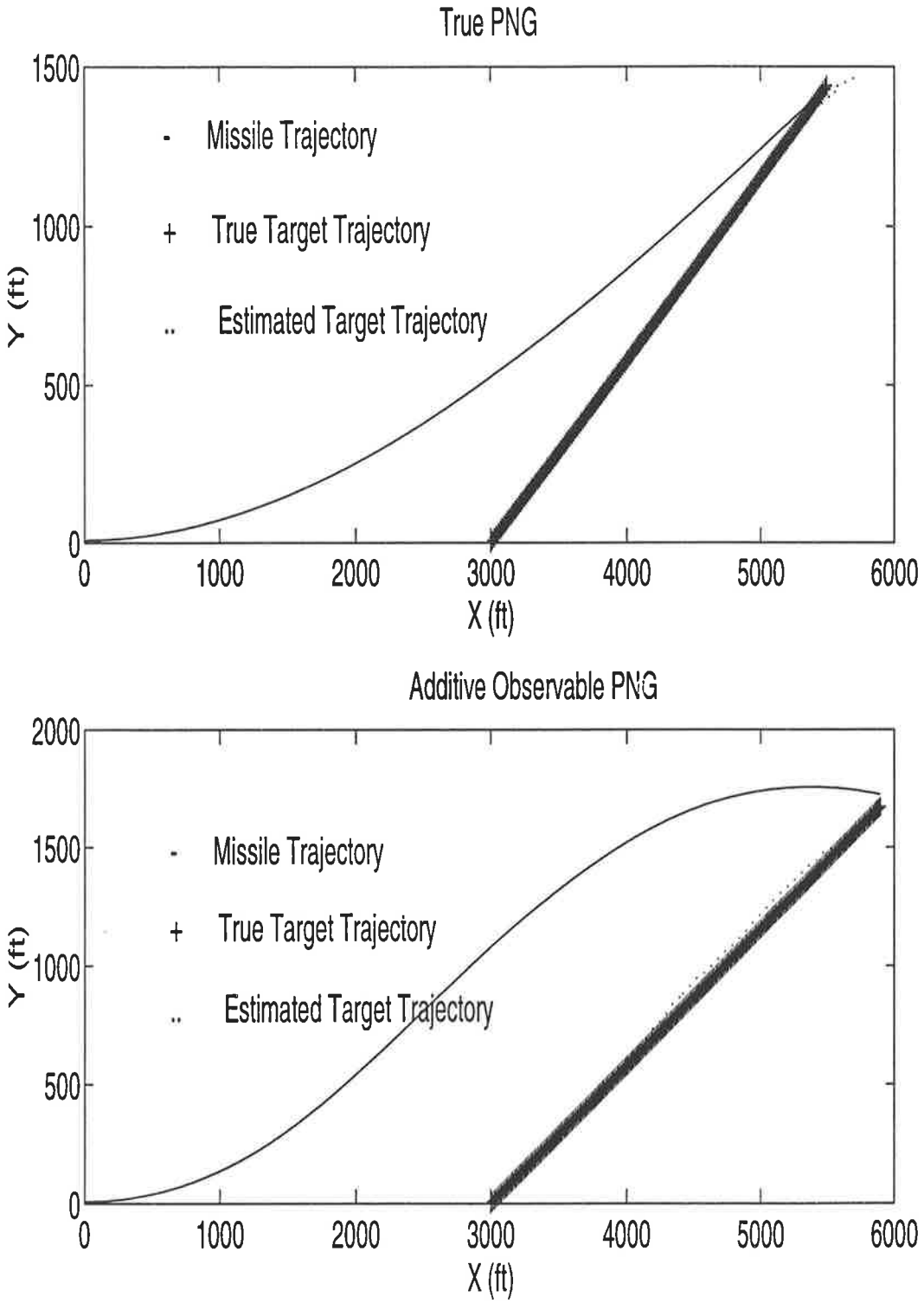

Figure 6.6: Pursuer and target trajectories for scenario 1

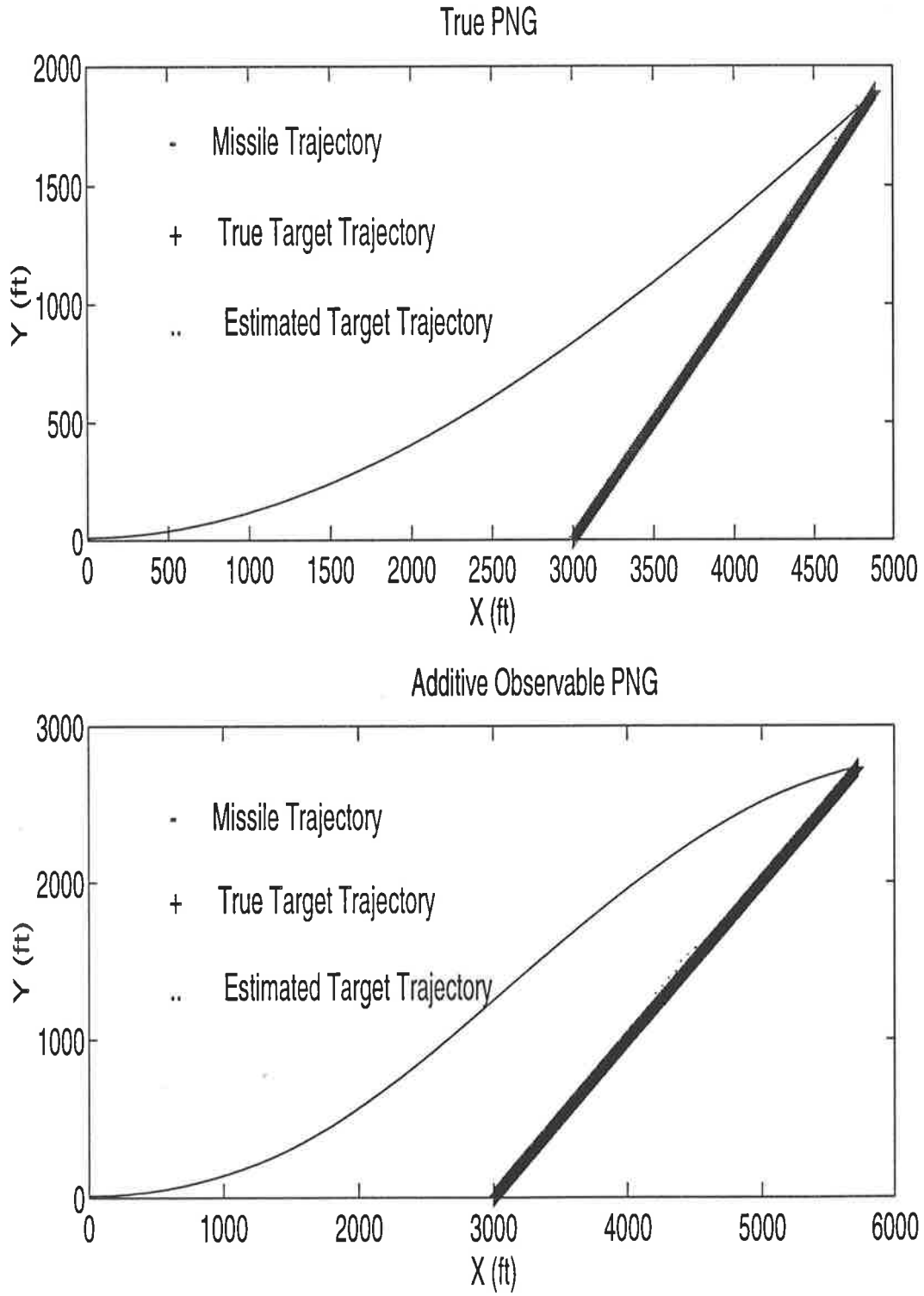

Figure 6.7: Pursuer and target trajectories for scenario 2

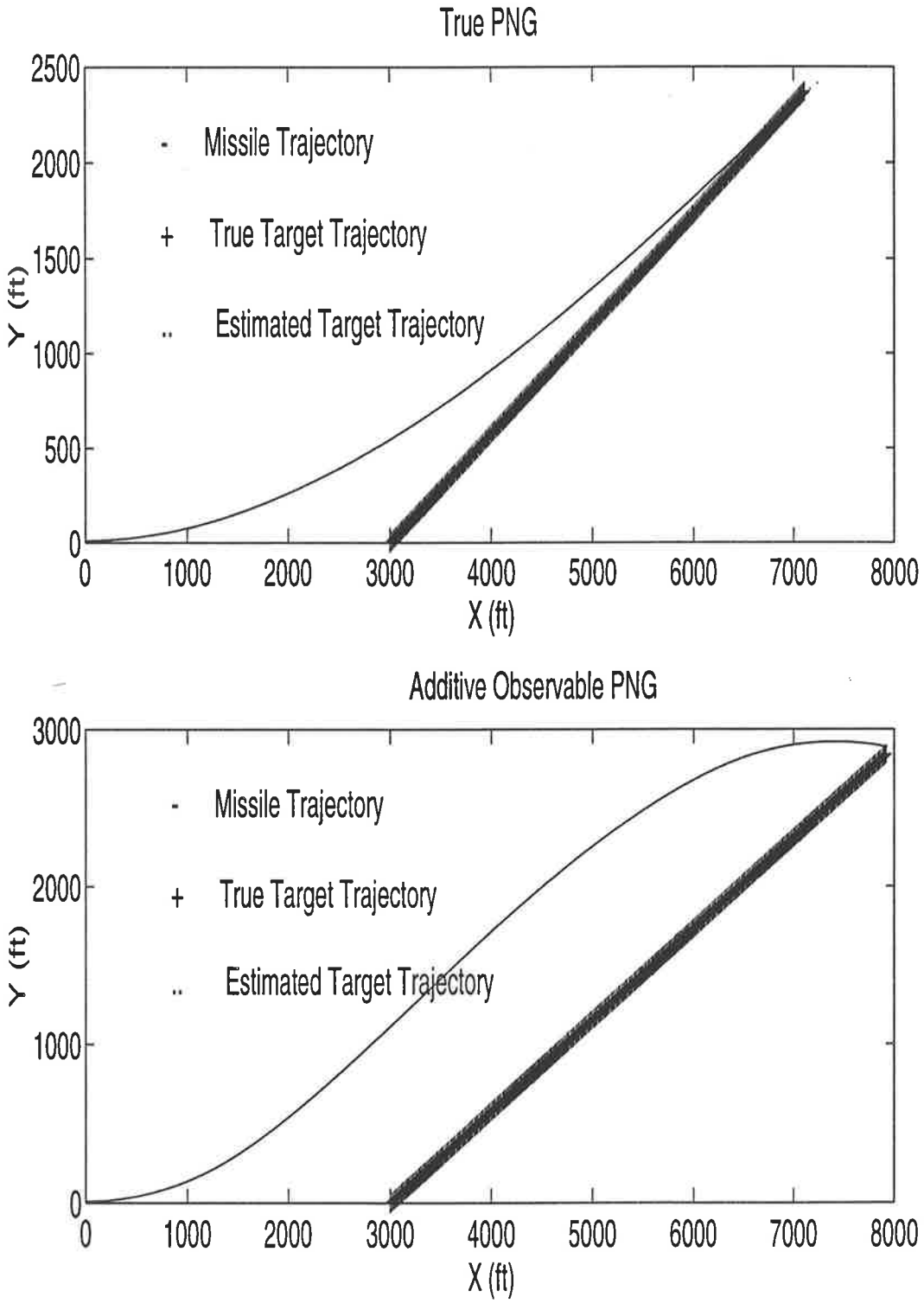

Figure 6.8: Pursuer and target trajectories for scenario 3

initial X and Y components of the target acceleration are $-9g$ and $9g$, respectively. The simulations clearly show that AOPNG performance is still better than that of the PNG towards the intercept although the choice of the observability coefficient in this case is not obvious since no necessary bound on that coefficient was determined. The oscillatory nature of the observable trajectory is specifically noted in contrast with the smooth proportional navigation trajectory.

6.3 Multiplicative Observable Proportional Navigation

6.3.1 Expression

In this law, the function $f(\cdot)$ of (6.1), that defines the dependence of the guidance law on system observability, is chosen to be multiplicative. It multiplies the expression of the PNG normal acceleration by the rate of the measure of observability, μ:

$$A_n = -N\dot{R}\dot{\sigma}\dot{\mu} \tag{6.22}$$

where $\dot{\mu}$ is the rate of the trace of the Fisher information matrix.

Once again, the intention is to modulate proportional navigation by a term reflecting system observability. The normal acceleration reacts simultaneously to a combination of factors, including observability. However, the *reaction* to these factors, in this case, is lumped together instead of being separated into two terms as in AOPNG. The guidance law is therefore expected to strike a certain balance between the factors involved.

The bearing-only-measurements are supposed, in this case, to be corrupted by thermal noise only. The corresponding spectral density (4.39) takes therefore the form:

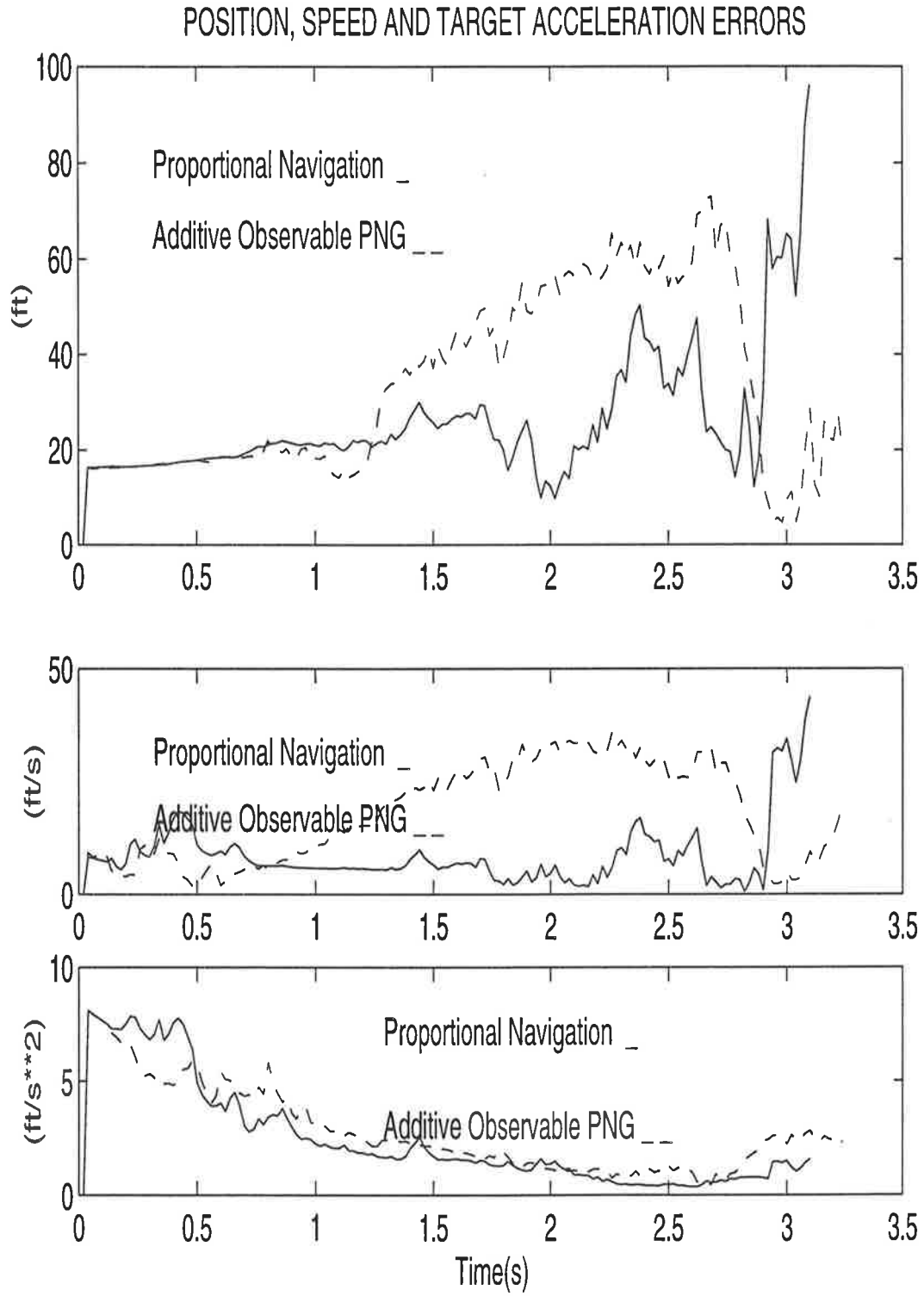

Figure 6.9: Estimation errors for the maneuvering target case - Additive observable PNG

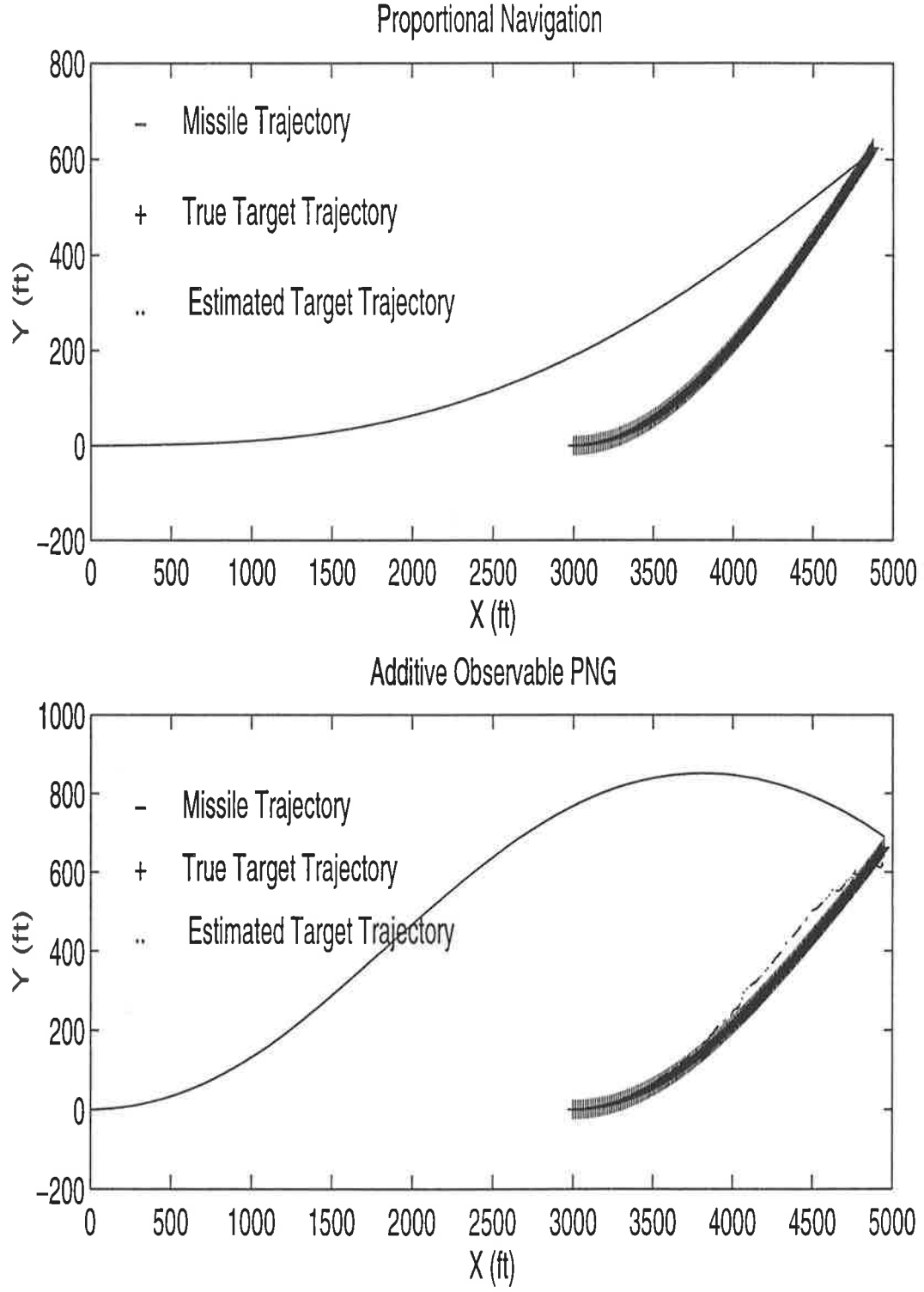

Figure 6.10: Pursuer and target trajectories for the maneuvering target case - Additive observable PNG

$$V = b \tag{6.23}$$

where b is the thermal noise coefficient.

On the other hand, the Kalman filter used for this law is the EKF (section 4.1). The reason behind the selective choice of the Kalman filter as well as the type of noise is to allow for a simplified closed form solution to the problem. This will become clearer in the next section.

The rate of the trace of the position part of the Fisher information matrix could be derived from (3.39) and (6.23), resulting in:

$$\dot{\mu} = \frac{1}{bR^2} \tag{6.24}$$

Closed Form Solution

The equations of motion (2.20) and (2.21) of the guidance system, as they apply to the multiplicative observable proportional navigation guidance law, have the following expressions in the polar coordinate system:

$$\ddot{R} - R\dot{\sigma}^2 = 0 \tag{6.25}$$

$$R\ddot{\sigma} + 2\dot{R}\dot{\sigma} = \nu\frac{\dot{R}\dot{\sigma}}{R^2} \tag{6.26}$$

where $\nu = \frac{N}{b}$ takes the role of the observability coefficient for this law.

Multiplying (6.26) by the term $\frac{R}{\dot{R}}$, we get:

$$\frac{R^2\ddot{\sigma}}{\dot{R}} + 2R\dot{\sigma} = \nu\frac{\dot{\sigma}}{R} \tag{6.27}$$

Using the massless angular momentum, h (6.8), of the pursuer relative to the target, (6.27) takes the form:

$$\frac{dh}{dR} - \frac{\nu}{R^3}h = 0 \tag{6.28}$$

Once again, this is a linear first order ordinary differential equation. Its solution has the form [87]:

$$h = Cexp(\frac{-\nu}{2R^2}) \tag{6.29}$$

where C is an integration constant.

Using the initial conditions (namely $\dot{\sigma} = \dot{\sigma_0}$ when $R = R_0$) as in the additive OPNG, we deduce the closed form expression of the line-of-sight angle rate:

$$\dot{\sigma} = \dot{\sigma_0}exp(\frac{\nu}{2R_0^2})\frac{exp(-\frac{\frac{\nu}{2R_0^2}}{(\frac{R}{R_0})^2})}{(\frac{R}{R_0})^2} \tag{6.30}$$

We replace the expression of $\dot{\sigma}$ into the first equation of motion (6.25):

$$\ddot{R} = R\dot{\sigma}^2 = R_0\dot{\sigma}_0^2exp(\frac{\nu}{R_0^2})\frac{exp(-\frac{\frac{\nu}{R_0^2}}{(\frac{R}{R_0})^2})}{(\frac{R}{R_0})^3} \tag{6.31}$$

By multiplying (6.31) by dr and integrating, we obtain a closed form expression of the range rate:

$$\dot{R}^2 = \dot{R}_0^2 + \frac{R_0^4\dot{\sigma}_0^2}{\nu}\left\{exp(\frac{\nu}{R_0^2}\left[1 - \frac{1}{(\frac{R}{R_0})^2}\right]) - 1\right\} \tag{6.32}$$

Lemma 6.2 *When implemented in conjunction with the extended Kalman filter, and a passive seeker providing bearing-only-measurements corrupted with thermal noise only, the multiplicative observable proportional navigation guidance law defined by (6.22) and applied to the two-dimensional pursuer-target intercept problem defined by (6.25, 6.26), has closed form solutions in (6.30) and (6.32).*

6.3.2 Characteristics

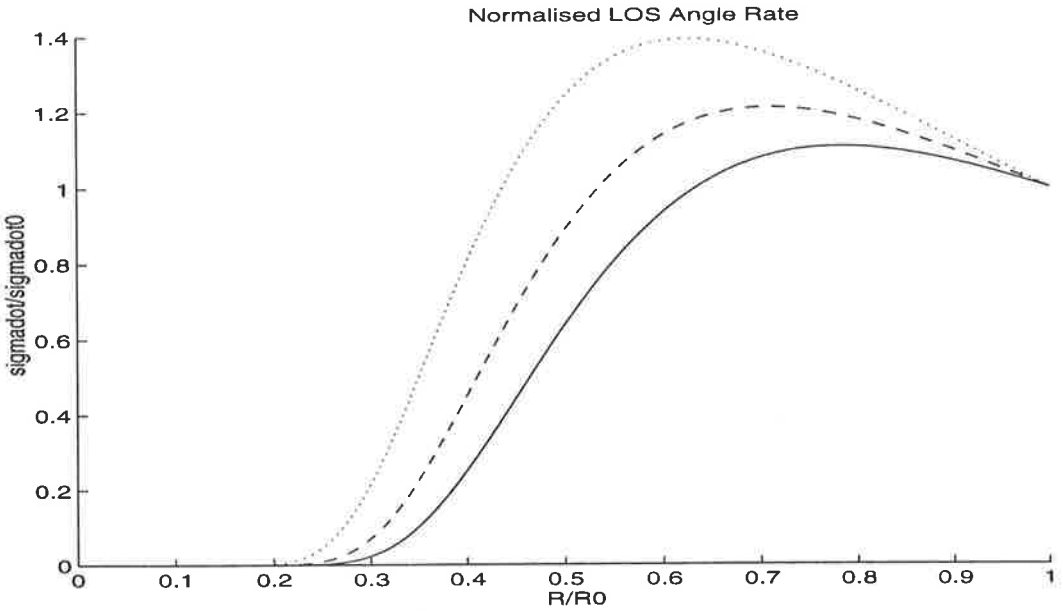

Figure 6.11: Line-of-sight angle rate vs range for increasing values of ν

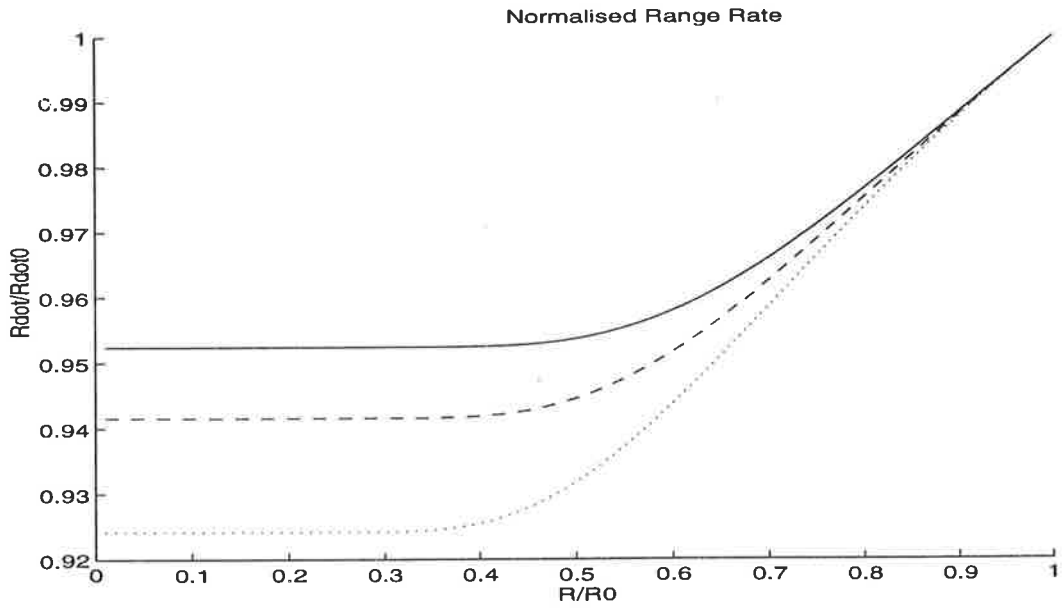

Figure 6.12: Range rate vs range for increasing values of ν

From the closed form solution given in (6.30), it is readily possible to determine that the line-of-sight rate approaches zero when the range approaches zero. On the other hand, it is possible to verify that the range rate approaches the following limit at the end of pursuit:

$$\dot{R} = \dot{R}_0 \sqrt{1 - \frac{R_0^4 \dot{\sigma}_0^2}{\nu \dot{R}_0^2}} \tag{6.33}$$

If $\dot{R}$ is a real number, it would have the same sign as the original range rate. Assuming that the initial range rate is negative, we conclude that intercept can occur "with a finite acceleration and with a finite time of duration" [101]. The condition for the range rate to be a real number becomes a condition for effective intercept, namely:

$$\nu \geq \frac{R_0^4 \dot{\sigma}_0^2}{\dot{R}_0^2} = \frac{R_0^2}{A^2} \tag{6.34}$$

where $A = \frac{\dot{R}_0}{R_0 \dot{\sigma}_0}$ as defined in [104].

In order to observe the behaviour of the line-of-sight rate and the range rate, (6.30) and (6.32) are plotted in terms of the range, as shown in Figures 6.11 and 6.12, respectively. We can see that while in proportional navigation (PNG) the line-of-sight rate approaches zero following a straight line [35], this line-of-sight approaches zero along a curved line oscillating around the PNG straight line. This is a characteristic feature of observability-enhanced guidance laws including the dual control guidance law [40]. On the other hand, the behaviour of the range rate as portrayed in (6.32) proves to be reminiscent of true proportional navigation [104], i.e., the range rate reaches a steady state value after an initial decrease.

6.3.3 Simulation

A comparative simulation study was conducted to test the characteristics of the multiplicative observable proportional navigation (MOPNG) against those of true proportional navigation. Fifty Monte-Carlo runs were carried out on a two-dimensional guidance system for which the initial distance between pursuer and target was fixed at 3000 ft. The same scenarios described in Table 6.1 were considered. In these scenarios, the pursuer and target speeds as well as the target heading angles were constant. The state estimator used was the extended Kalman filter and the noise

Scenario	ν_{min} (R_0^2)	ν (R_0^2)
1	.18	.29
2	.31	.43
3	.48	.5

Table 6.4: Observability coefficients and their necessary minimum bounds for the three different scenarios

associated with the line-of-sight angle was considered of thermal nature only, having a spectral density of the form outlined in (6.23), where the thermal coefficient b is given by:

$$b = 56.25 \times 10^{-8} rad^2 \ s \tag{6.35}$$

The navigation constant was taken to be $N = 3$, while the minimum values of the observability coefficients, ν, were deduced from equation (6.34). The necessary condition on the observability coefficients proved, in practice, to be very useful in adopting the values of these coefficients for all three scenarios. The minimum values, as well as the adopted ones are listed in Table 6.4.

On one hand, we have recorded the estimated final miss-distances attained by each guidance law, as well as the times-to-go it took each law to achieve intercept. These data are listed in Table 6.5. They clearly show an advantage for MOPNG over PNG in terms of final miss-distance and predictability of the estimation errors. The shorter miss-distances are traded off, however, by slightly longer times-to-go for each of the considered scenarios; a trend that characterises guidance laws induced with observability criteria [41].

On the other hand, we have plotted the filter estimation errors in position, speed and target acceleration, as defined by (6.22).

As shown by the plots corresponding to the three scenarios considered (Figure 6.13 — Figure 6.15), the estimation errors, especially in the position, were noted to

Scenario	Multiplicative OPNG		True PNG	
	$\hat{R}_f\ (ft)$	$\hat{t}_f\ (s)$	$\hat{R}_f\ (ft)$	$\hat{t}_f\ (s)$
1	88.39	3.97	415.95	3.58
2	136.59	4.04	352.71	3.32
3	135.36	5.05	303.41	4.72

Table 6.5: Comparative miss-distances and times-to-go for PNG and multiplicative observable PNG

be lower for MOPNG than for PNG; a clear indication of the mutual interaction between guidance law and state estimator. The corresponding trajectory plots (Figure 6.16 — Figure 6.18) show that multiplicative proportional navigation leads the pursuer to *maneuver around the target*, instead of approaching it directly as is the case with PNG.

Figures 6.19 and 6.20 show respectively the estimation errors and the trajectories corresponding to the case of the maneuvering target outlined in section 6.2.4. It is seen that MOPNG outperforms PNG for this maneuvering target although, as for the case of AOPNG, no necessary bound on the observability coefficient was determined.

6.4 Summary

The new *observable proportional navigation guidance law* (OPNG), presented in this chapter, aims at blending the goal of proportional navigation guidance to that of maximum information guidance by attempting to maintain the same information on observability while nulling the line-of-sight rate. Since the deterioration of the Kalman filter observability does not occur until the final stage of the intercept, the new law reacts to any change in filter observability captured through the rate of an observability measure.

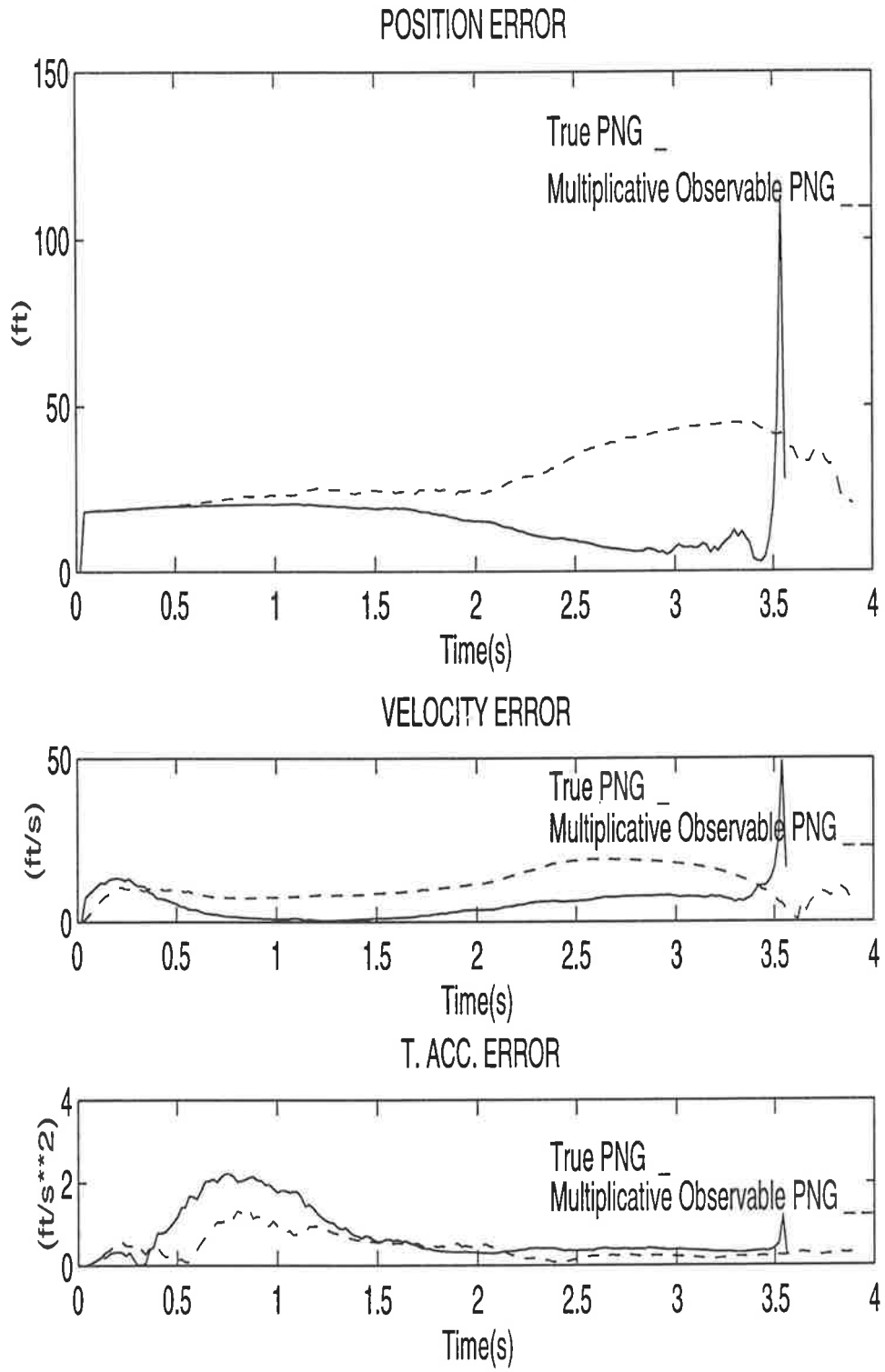

Figure 6.13: Estimation errors for scenario 1

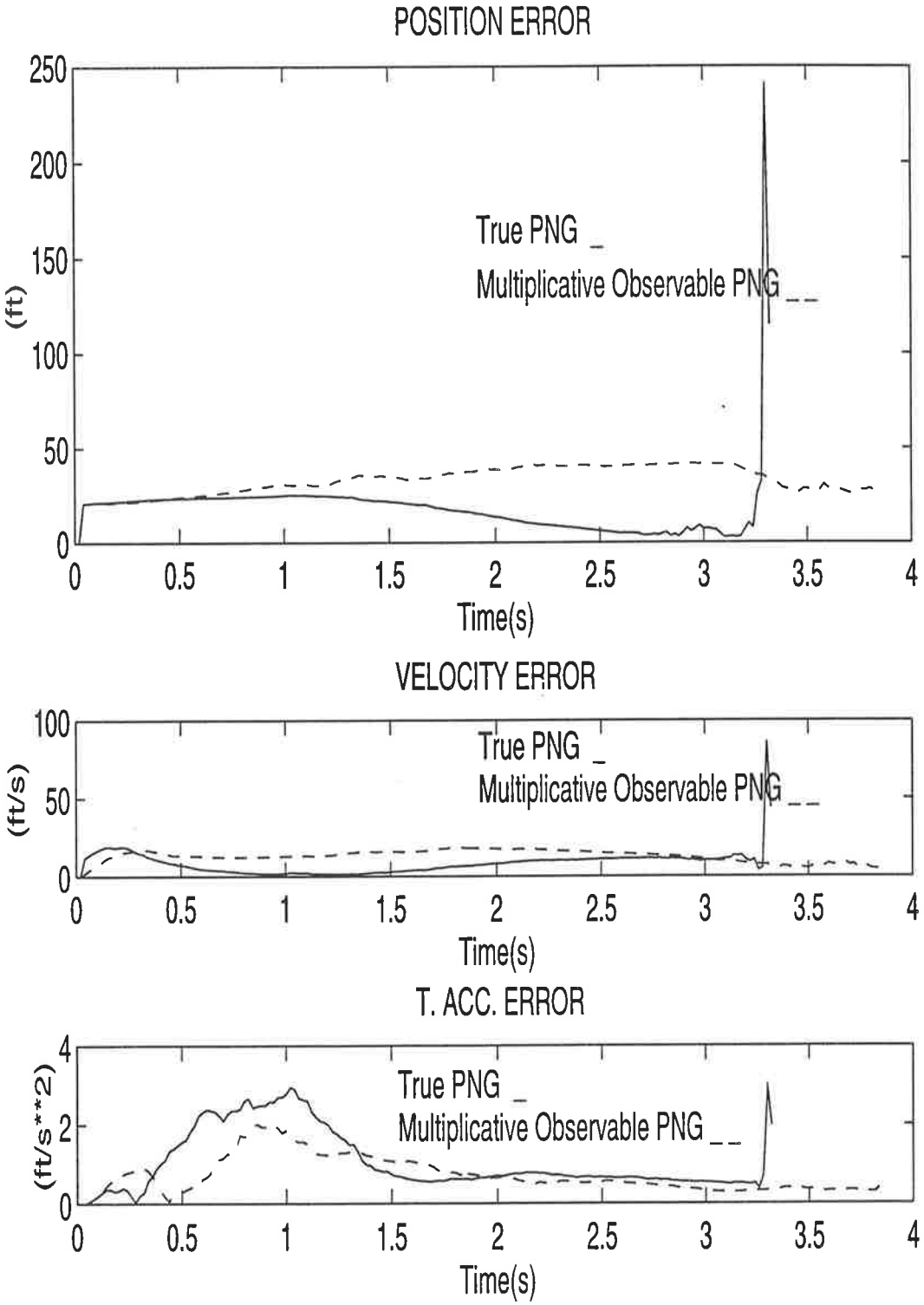

Figure 6.14: Estimation errors for scenario 2

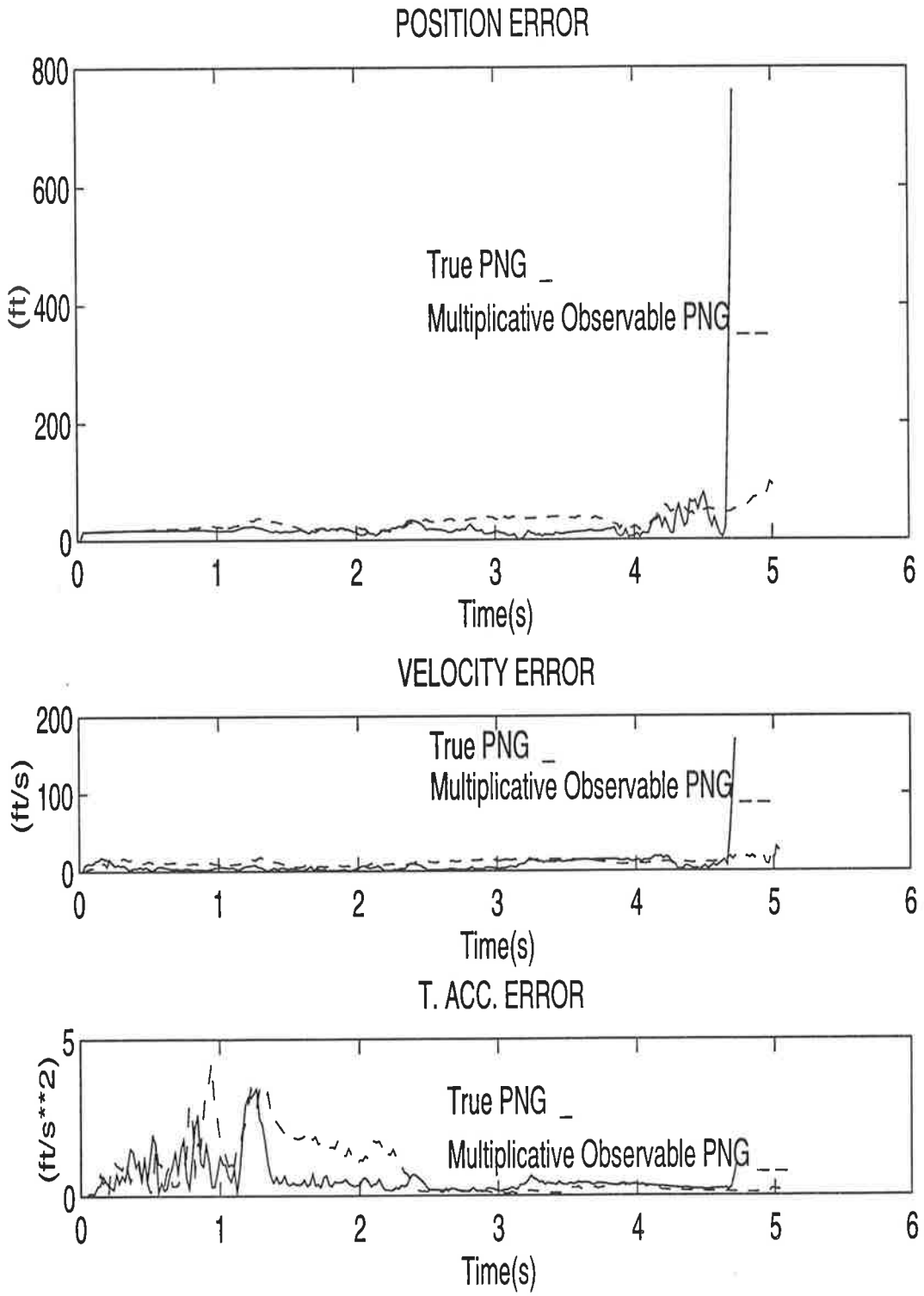

Figure 6.15: Estimation errors for scenario 3

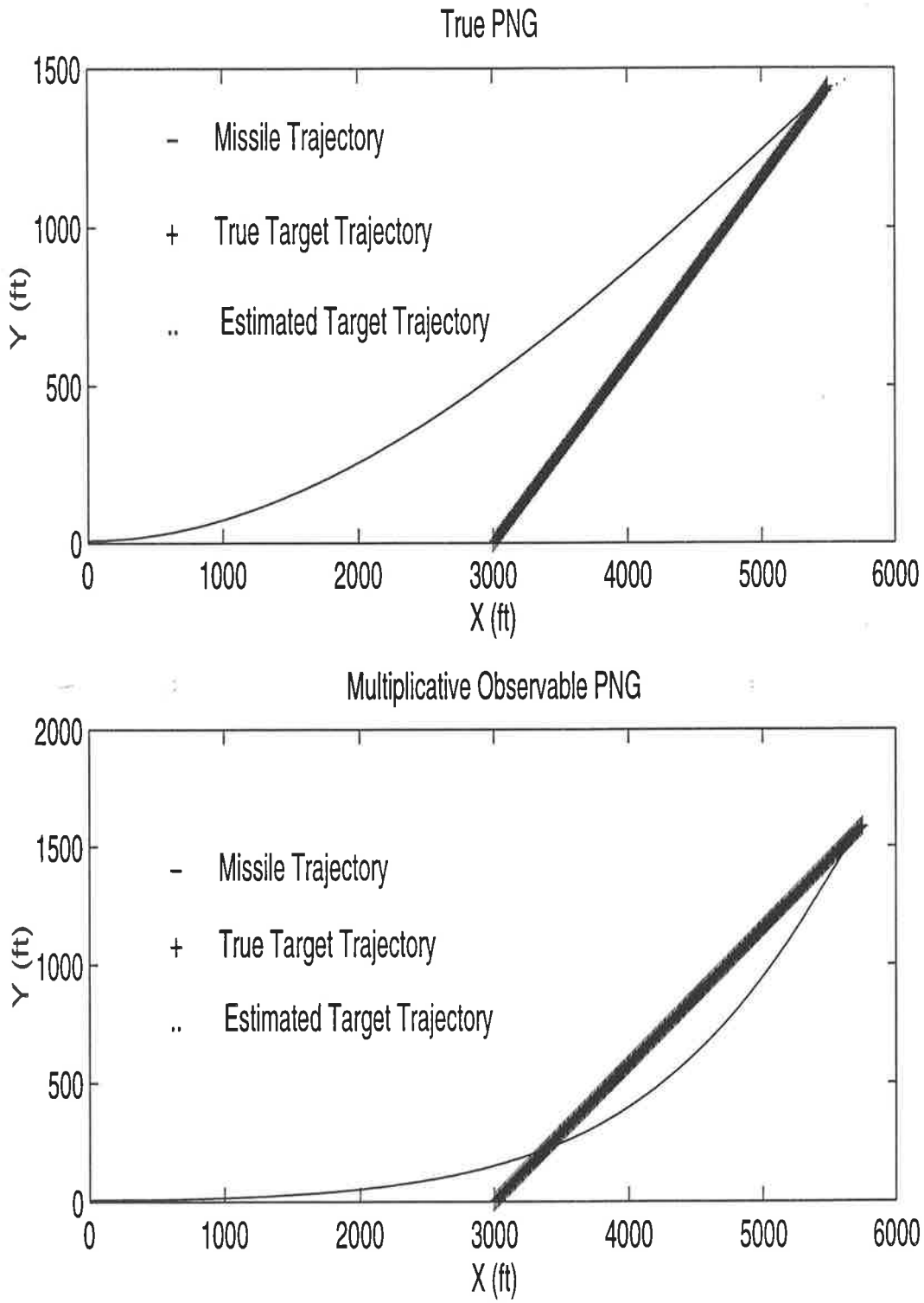

Figure 6.16: Pursuer and target trajectories for scenario 1

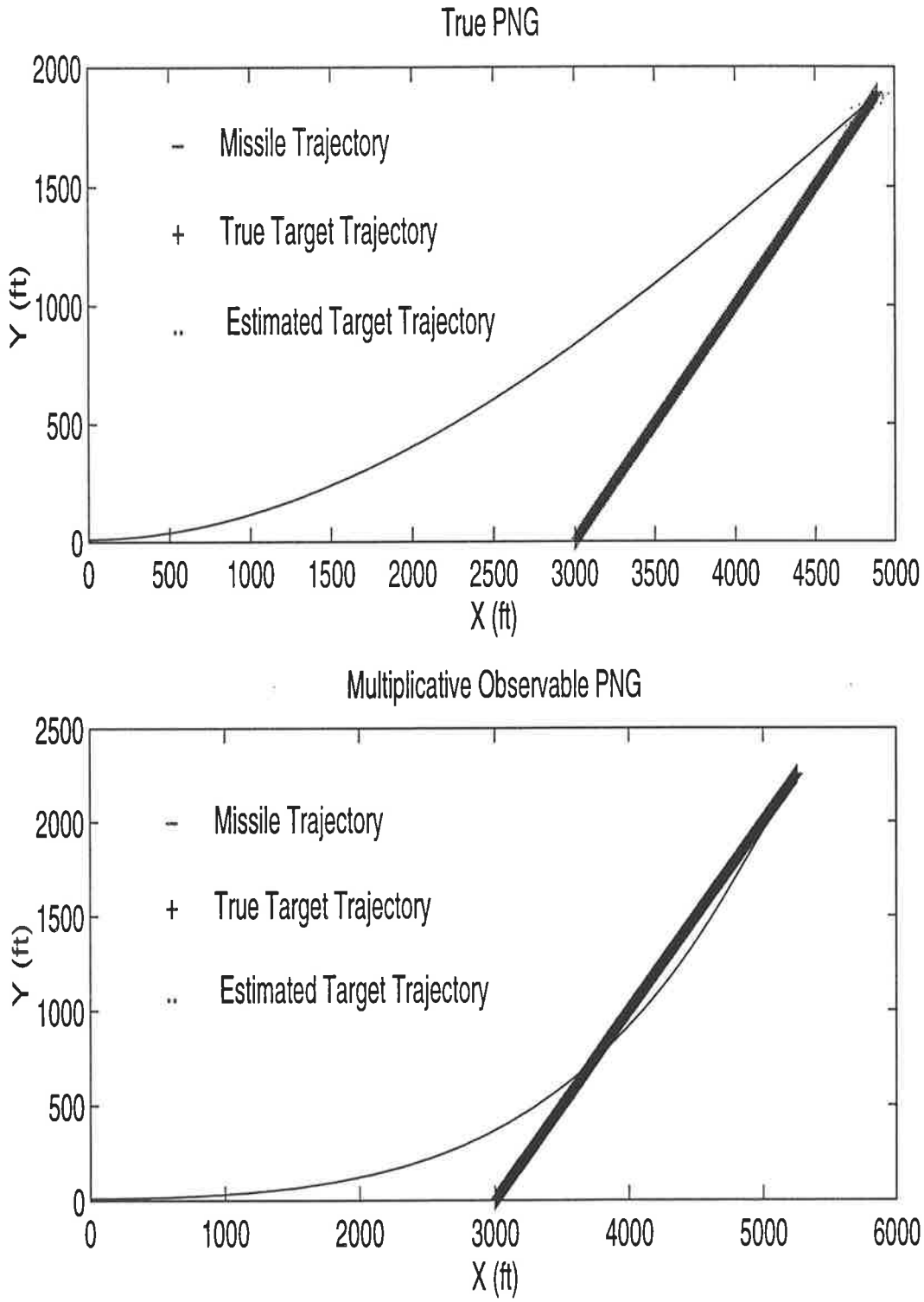

Figure 6.17: Pursuer and target trajectories for scenario 2

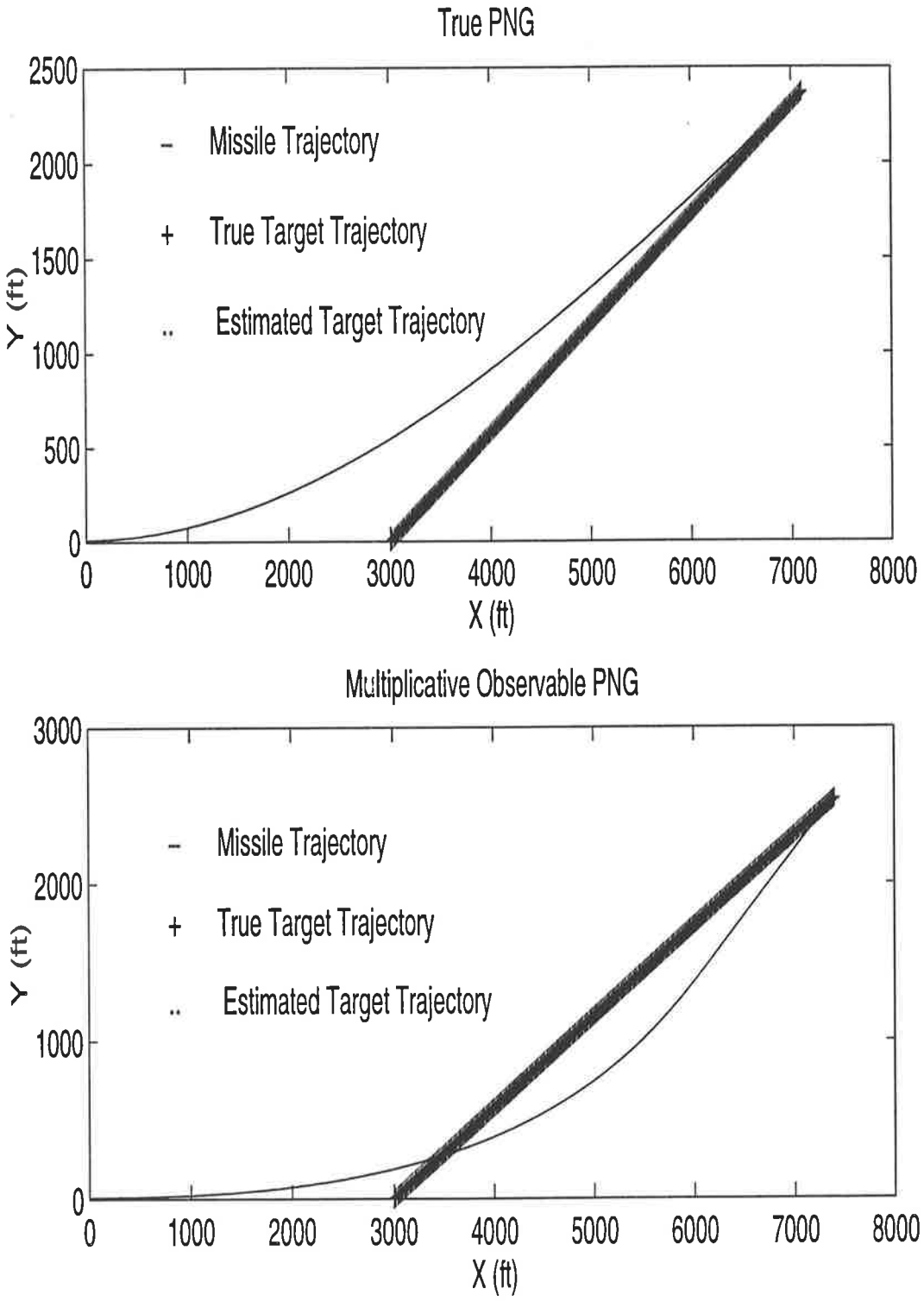

Figure 6.18: Pursuer and target trajectories for scenario 3

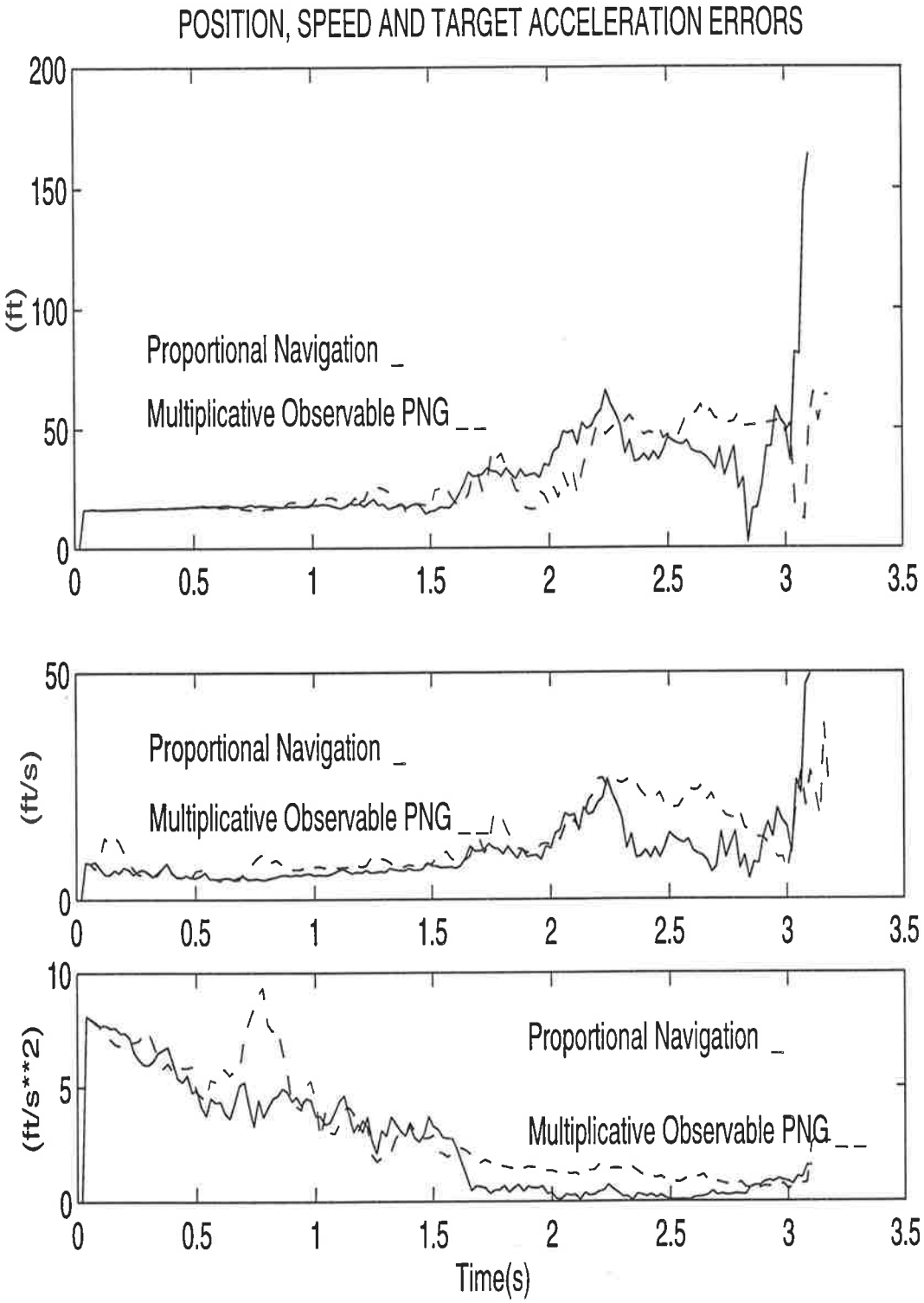

Figure 6.19: Estimation errors for the maneuvering target case - Multiplicative observable PNG

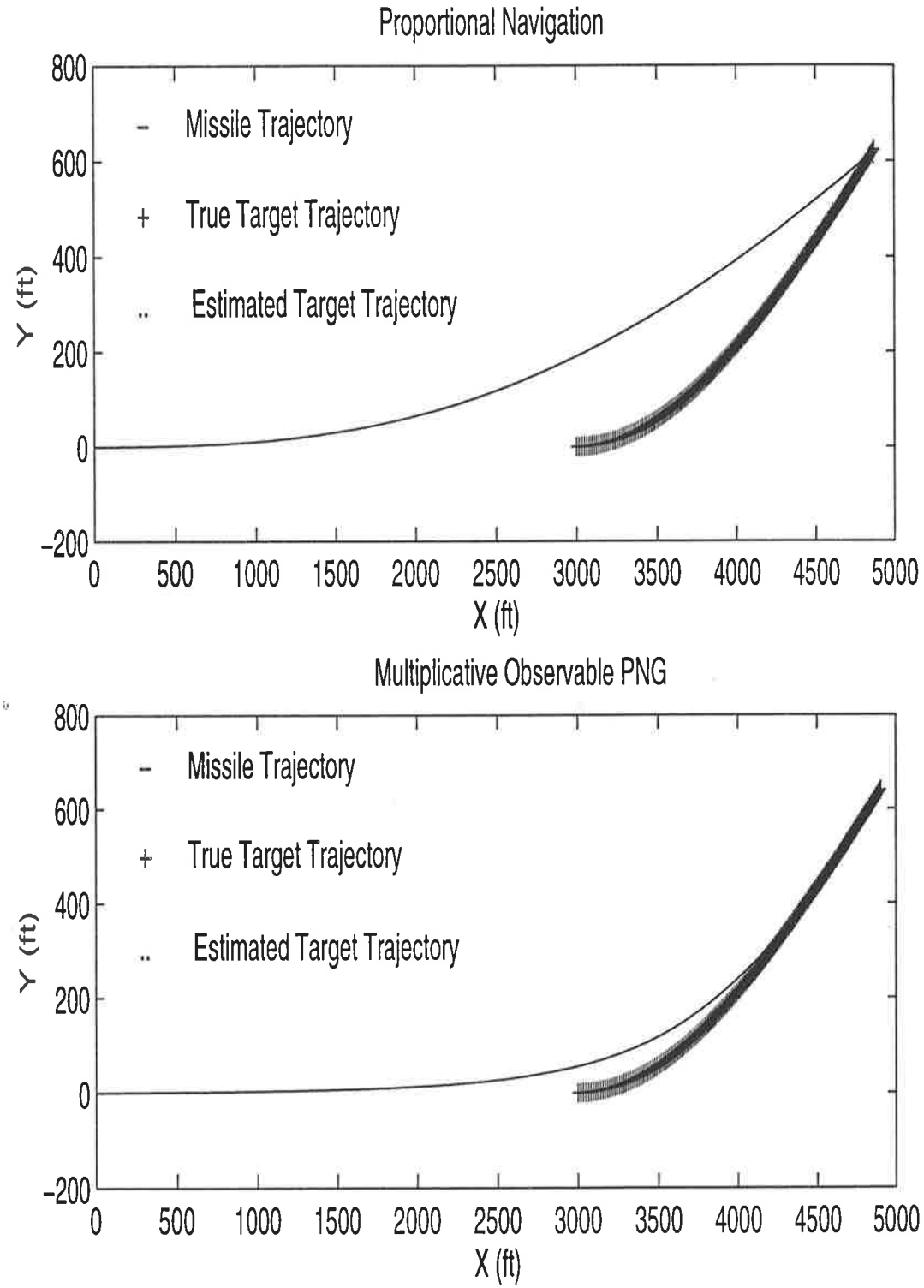

Figure 6.20: Pursuer and target trajectories for the maneuvering target case - Multiplicative observable PNG

Two forms of OPNG were considered. In the additive observable proportional navigation guidance (AOPNG), a term proportional to the rate of the trace of the Fisher information matrix is added to the normal acceleration prescribed by proportional navigation. This form was defined for use along the modified gain extended Kalman filter and for measurements induced with glint noise only. The associated closed form solution showed that the line-of-sight rate is nulled at the end of the engagement, as is the case with proportional navigation, but while this rate is a linear function of the range with PNG, it is nonlinear with AOPNG. From an engineering point of view, the nulling of the line-of-sight rate in AOPNG is not as predictable as with PNG, and the pursuer does not enter the collision triangle until later in the pursuit, delaying the situation where it is being guided with a null control variable.

In the second form of OPNG, the multiplicative observable proportional navigation guidance (MOPNG) multiplies the normal acceleration prescribed by proportional navigation, with the trace of the Fisher information matrix. MOPNG was defined for use along the extended Kalman filter and for measurements induced with thermal noise only. The simple, multiplicative nature of this law allowed it in turn to be solved in closed form, paving the way for the derivation of a necessary bound on the observability coefficient, as is the case with AOPNG. The nonlinear function along which the line-of-sight function is nulled, although different in shape from that of the AOPNG, has the same effect of modulating the pursuer trajectory modifying consequently the time when the pursuer and target are on a collision course. In both cases however, the profile of the range rate is reminiscent of that corresponding to PNG.

Simulation studies performed for several scenarios showed that the proposed law offers a lower final miss-distance and a smaller estimation error compared with proportional navigation, at the expense of a longer time-to-go, as is the case with DCGL.

However, OPNG addresses the limitations of the dual control guidance law by excluding the use of any estimation of the time-to-go and by making use of the

derived necessary bound on the observability coefficient, reducing therefore the extent of trial and error involved in its selection. In addition, this new law offers the possibility of using a wider choice of observability measures (besides the trace of the information matrix) unrestricted by their form (quadratic and symmetric in the case of DCGL).

Chapter 7

Conclusion

7.1 Summary

The main thrust of this study was the design of an alternative way to handle the divergence problem suffered by the extended Kalman filter, when used along the proportional navigation guidance trajectory, given a low cost seeker. The ensuing analysis and design problem was approached sequentially, starting from the problem definition, examining other solutions explored in the past and ending with the proposed solution.

The nature of the problem and a brief historical background were presented in the first chapter, highlighting the three main issues which play an important role in the definition of the guidance problem: guidance law, state estimator, and control strategy. Proportional navigation was introduced as one of the most popular guidance laws currently used, and the extended Kalman filter was presented as a widely used state estimator. It was also pointed out that the separation principle constitutes an accepted control strategy, but that it is at the origin of the divergence problem. Most existing control strategies are based on the separation principle, in that an optimal controller joined in cascade with an optimal estimator would provide an optimal overall guidance strategy. A different approach, called dual control has focused on the relationship between controller and estimator. A brief outline of this

approach was given, but it was pointed out that, as far as our study project was concerned, we basically focused on the fact that the performance of the guidance law is significantly affected by that of the estimator and vice-versa, and therefore it helps to design a guidance law with the estimator performance in mind.

The focus of the second chapter was on proportional navigation. Several variants of proportional navigation were explored. The simplified PNG permitted us, in particular, to deduce some of the main characteristics of proportional navigation, especially the allowable range of the navigation constant, as a function of the acceptable force and torques applied to the pursuer. Also, the *optimal* form of proportional navigation played a remarkable role since it allowed for easy extension, and could be implemented numerically using the control parametrisation method. A brief description of this method showed that by subdividing the continuous control effort over a set of predefined knots, it is possible to reduce the problem to a standard mathematical programming problem. Several simulations showed the effectiveness of proportional navigation, in a noise-free environment, as a first approach.

In the same noise-free environment, the third chapter presented an alternative to proportional navigation: maximum information guidance. Instead of minimising control effort and final position, as is done in optimal PNG, maximum information optimises a measure on the observability of the state estimator. In doing so, maximum information guidance defies the separation principle, by implementing in the guidance law, an objective related to the state estimator, thus blending the optimality of guidance and estimation. Several forms of the measure of observability were explored and it was shown that the trace of the Fisher information matrix, can adequately accommodate the maximum information guidance law, as it is implemented by the control parametrisation method. In addition, by simulating the maximum information guidance law, several characteristics of this law were apparent, namely a shorter miss-distance, a longer time-to-go, and oscillatory behaviours of the pursuer trajectory and its normal acceleration.

The fourth chapter treated the guidance problem from a stochastic point of view, assuming that the measurements are not only nonlinear but also noisy. In order

to handle the noise and the nonlinearity, the extended Kalman filter was analysed, based on the existence of a nominal trajectory sufficiently close to the true trajectory and satisfying the system dynamic equation. A Taylor's series expansion of the measurements equation allowed it to be linearised reducing the problem to one similar in form to the standard Kalman filter. In addition, the measurements satisfied a feature called *modifiability* and the problem was simplified further, giving rise to the modified gain extended Kalman filter. Other types of filters, the iterative filters, were also considered, based on the execution of several local iterations of the extended Kalman filter algorithm. The simulations of the two-dimensional problem, with the filter in the loop, illustrated the divergence problem of the extended Kalman filter near the end of the trajectory, when proportional navigation was used to derive the nominal trajectory.

One existing solution to the filter divergence problem was explored in Chapter 5, through the dual control guidance law (DCGL). While keeping the same rationale of the maximum information guidance studied in Chapter 3, the dual control guidance was *mechanised* along with the state estimator in the loop. Since DCGL was implemented by extending the linear quadratic guidance law (LQGL), this latter law was first analysed and derived in closed form. It was shown that for a particular value of a design coefficient, the LQGL reduces to proportional navigation. On the other hand, DCGL was formulated by adding to the performance index of LQGL, a measure on observability similar to the measure used in maximum information. In a similar fashion, a solution to the DCGL problem was obtained and implemented. Simulation studies showed that DCGL enhances the performance of the extended Kalman filter, which in turn reflects on the final miss-distance and the behaviour of the control history.

In the last chapter, the observable proportional navigation guidance (OPNG) law was presented. As in the case of DCGL, OPNG utilises a measure of observability based on the Fisher information matrix, but instead of maximising it, OPNG aims to maintain it throughout the flight path. This idea is based on the assumption that the target observability is initially adequate, and on the fact that the divergence of the state estimator occurs towards the end of the intercept. Two variants of the

observable proportional navigation were explored and solved in closed form; the additive OPNG consisted of adding to the normal acceleration prescribed by PNG another factor based on the Fisher information matrix, while the multiplicative OPNG multiplied the normal acceleration prescribed by PNG by an additional factor reflecting the observability of the system. The two forms depend on the type of state estimator used in the control loop, as well as on the nature of the noise. Two types of state estimators (EKF and MGEKF) and two types of noise (glint and thermal) were used in the two considered variants of OPNG, respectively. The simulation results and characteristics of this law suggest that it retains the main features of maximum information and dual control guidance, namely better filter performance, shorter miss-distance, longer time-to-go and modulated pursuer trajectory around the trajectory prescribed by proportional navigation.

7.2 Contributions

The observable proportional navigation guidance law offered several advantages over existing guidance laws belonging to the same school of thought (i.e., dual control guidance law). As in the case of DCGL the *duality* between guidance and estimation was introduced via the *measure of observability*, while the separation principle was still formally used to *mechanise* the guidance law within the guidance loop. But in addition to improving the convergence features of the state estimator, leading to better intercept characteristics, compared with the conventional PNG (e.g., shorter miss-distance and smaller estimation errors), the new guidance law offered the following advantages over existing "dual control" guidance laws:

- Closed form solutions to both variants of the guidance law were given in the form of analytical expressions of the range rate and the line-of-sight rate.
- Necessary conditions to be satisfied by the *coefficient of observability* were established, based on the guidance closed form solutions.

- Simple and easy to implement structure not restricted by the constraints imposed by quadratic optimisation, as is the case with other observability-enhanced guidance laws.

- Sound design rationale, eliminating the need to estimate the time-to-go, which can adversely affect the overall guidance performance.

In addition to the above, this research study could be considered to provide the foundation of a well rounded introductory knowledge-base in guidance systems. It offers a platform for the analysis and design of guidance systems, as they apply to bearing-only-measurements. As well as the guidance law and the state estimator, the guidance loop contains the measurement seeker and the relative dynamics, among other building blocks. Each of these blocks was examined in this study with varying degrees of depth, and several analysis and design approaches received special consideration:

- The maximum information guidance law was analysed and applied to a two-dimensional guidance problem. Its features were verified through an open loop involving only the guidance law and the problem dynamics.

- Control parametrisation was adopted as a computational method for the calculation of the relative interceptor-target trajectory, as opposed to the shooting method adopted in previous studies. The features of control parametrisation could then be readily compared to those of the shooting method, as they applied to the problem at hand.

- A new, more comprehensive measure of observability was proposed instead of the trace of the Fisher information matrix. Although complex and difficult to use in an open loop formulation, the new measure could well be used in a closed loop setting.

- An extended Kalman filter (EKF) was implemented to estimate six state variables. The EKF was analysed starting from the standard Kalman filter, carrying out the linearisation procedures, hinging on the linearisation issues

and arriving at the notion of *modifiable measurements* and the modified gain extended Kalman filter.

- Several variants of the EKF were applied to our bearing-only-measurement guidance problem, and their performance compared to that of the EKF. Among those variants were the iterated extended Kalman filter and the iterative linear filter-smoother. Noticeable improvements in the guidance performance resulted directly from the use of iterations in the filter algorithm.

Among the useful contributions of this study, we can also count the fact that it succeeded in closing the guidance loop, by designing a guidance law that is "mechanisable", allowing for on-line interaction between the different building blocks of the guidance system.

7.3 Future Work

This research project dealt with several guidance issues at the same time. The possibility of extending it could therefore take several directions.

The central theme of the study, observability, can be refined through the selection of a more adequate measure of observability combining completeness (representation of all combinations of the state variables), ease of manipulation (closed form expression of the control variables), and effectiveness (lower estimation errors). Three different measures of observability were presented in this study, all of them were related to the Fisher information matrix: the trace, the Hilbert norm, and the b-norm. Due to its simple form and its adaptability to the adopted control parametrisation method, only the trace was used. Other measures could be used as well and the resulting guidance performance compared to that corresponding to the trace. Their computational complexity would surely be compensated for by the benefits they would provide. The main criteria to be fulfilled by a measure of observability, based on the Fisher information matrix, is that it should be a norm of that matrix.

Another area that could be explored is the case of noisy systems, in addition to noisy

measurements. In our case, the engagement system was supposed to be noise-free. This resulted in a simple form of the observability gramian equal to the inverse of the estimation error covariance matrix. It would be interesting, however, to identify a variable upon which measures of observability could be based, in the case of noisy systems, such as those with modelling errors or system uncertainties.

Evidently, there are several areas where one could extend the present study without drastically changing its main focus. Since only a necessary limit on the coefficient of observability is determined, work could be undertaken to define a sufficient limit also, further reducing the uncertainty of the problem. The trace of the Fisher information matrix could be extended to include not only the position component but also the speed and target acceleration components, rendering the analysis more comprehensive. In addition, the form of the guidance law could be diversified to include not only additive and multiplicative observability measures, but other forms as well, as long as the general features of observability-enhanced guidance laws are retained. On the other hand, since the solution to the observable navigation guidance depends on the type of state estimator and the measurement noise, one could attempt to solve the problem with state estimators other than the ones used in this study (i.e., the iterative extended Kalman filters), and noise types other than glint or thermal noise.

More important modifications could be implemented in the bearing-only-measurement problem. Alternative performance indices, such as the exponential cost criterion [70], could serve as a starting base of the study instead of the linear cost criterion adopted in the linear quadratic guidance law. A generalised guidance law [100] or the generalised proportional navigation [102] could also serve as the starting point of the analysis, instead of the true, pure, or optimal form of proportional navigation, and then extended to cover the observability question.

Towards the same objective, variable pursuer and target speeds and more realistic forms of target maneuvering could also be considered. It is true that, in our case, the filter model allowed for the maneuverability of the target according to a Gaussian acceleration model, but it is possible to extend this situation to cover many

realistic target maneuver strategies [43]. One future project could therefore consist of considering a realistic target maneuver model in both the guidance equations of motion and the filter model. For this purpose, the circular models presented in [37] and [86] might provide a good start. When this type of modification takes place, the form of the transition matrix of the system changes accordingly and sometimes becomes difficult to derive in closed form, which increases the complexity of the problem.

For such problems where complexity is not negligible, one possible approach is the dual control as developed by Feldbaum [22]. As stated in the introduction, this approach is based on the theory of probabilities and the stochastic dynamic programming theory [6, 13] and instead of relying on the separation principle by dealing with the optimisation and the estimation problems separately, this approach handles the guidance problem as a stochastic optimal control theory problem [79], in which it is proposed to find the optimal control sequence and the optimal probability densities which minimise the *average risk* function. The *curse of dimensionality* associated with this approach has been tackled by several authors [11, 20, 95], whose work constitutes a good starting point and offers several ideas that deserve to be pursued.

APPENDICES

Appendix A

A.1 Trace of the Fisher Information Matrix

The Fisher information matrix (FIM) is defined by (3.39), namely:

$$I = \int_{t_0}^{t_f} \Phi' H' V^{-1} H \Phi d\tau \tag{A.1}$$

where Φ is the transition matrix,

H the measurement gradient vector, and

V the spectral density of the measurement noise.

By using the definition of the transition matrix (Appendix B), then partitioning the FIM into three different parts corresponding to the relative position, relative speed and target acceleration, and taking only the part that corresponds to the relative position, we could write the performance index as:

$$I_p = I_{11} + I_{22} \tag{A.2}$$

where

$$\begin{aligned} I_{11} &= \int_{t_0}^{t_f} H_1 V^{-1} H_1 d\tau \\ I_{22} &= \int_{t_0}^{t_f} H_2 V^{-1} H_2 d\tau \end{aligned}$$

$$\begin{aligned} H_1 &= -\frac{Y_r}{X_r^2+Y_r^2} \\ H_2 &= \frac{X_r}{X_r^2+Y_r^2} \\ V &= \frac{a}{X_r^2+Y_r^2}+b \end{aligned} \tag{A.3}$$

and a and b are two constants characterising the measurement noise.

It is possible to use the relations (A.3) in the expression of I_p (A.2) to reduce it to the following form:

$$I_p = \int_{t_0}^{t_f} \frac{1}{a+b(X_r^2+Y_r^2)} d\tau$$

which, for the purpose of minimisation, is equivalent to the form:

$$I_p \propto \int_{t_0}^{t_f} \frac{1}{1+\kappa(X_r^2+Y_r^2)} d\tau$$

where

$$\kappa = \frac{b}{a}$$

A.2 Definition of the b-norm

Let us consider the following $n \times n$ matrix:

$$A = \begin{bmatrix} a_{11} & a_{12} & \cdots & a_{1n} \\ a_{21} & a_{22} & \cdots & a_{2n} \\ \vdots & \cdots & \ddots & \vdots \\ a_{n1} & a_{n2} & \cdots & a_{nn} \end{bmatrix} \tag{A.4}$$

A *norm* of A is defined as a non-negative number denoted by $\|A\|$ and satisfying the following properties [61]:

1. $\|A\| > 0$ for $A \neq 0$, $\|A\| = 0$ implies $A = 0$.

2. $\|kA\| = \mid k \mid \|A\|$ for any scalar k.

3. $\|A + B\| \leq \|A\| + \|B\|$.

4. $\|AB\| \leq \|A\| \cdot \|B\|$.

In the following, we consider the sum of the absolute values of all the elements of A (denoted hereinafter as the "SAVAE" for brevity) and we verify that it is a norm of the matrix A.

1. Non-negativity

If $A \neq 0$, at least one of its elements is non-zero. Since the absolute value is always positive and since the sum of two or more positive numbers is positive itself we deduce that $SAVAE(A)$ is positive for $A \neq 0$.

On the other hand, $SAVAE(A) = 0$ means that the sum of all the absolute values of the elements of A is zero. This clearly indicates that all the elements of A are zeros, which in other terms means that $A = 0$.

2. Distributivity with the product by a scalar

Let us consider:

$$kA = \begin{bmatrix} ka_{11} & ka_{12} & \cdots & ka_{1n} \\ ka_{21} & ka_{22} & \cdots & ka_{2n} \\ \vdots & \cdots & \ddots & \vdots \\ ka_{n1} & ka_{n2} & \cdots & ka_{nn} \end{bmatrix} \tag{A.5}$$

We calculate:

$$\begin{aligned} SAVAE(kA) &= \mid ka_{11} \mid + \mid ka_{12} \mid + \cdots + \mid ka_{1n} \mid \\ &\quad + \mid ka_{21} \mid + \mid ka_{22} \mid + \cdots + \mid ka_{2n} \mid \end{aligned}$$

$$+\cdots+\mid ka_{n1}\mid+\mid ka_{n2}\mid+\cdots+\mid ka_{nn}\mid \qquad (A.6)$$

Since in general:

$$\mid ka_{ij}\mid=\mid k\mid\ \mid a_{ij}\mid \qquad (A.7)$$

$\forall i$ and j, we conclude that:

$$\begin{aligned} SAVAE(kA) &= \mid k\mid\ \ (\mid a_{11}\mid+\mid a_{12}\mid+\cdots+\mid a_{1n}\mid \\ &= \mid a_{21}\mid+\mid a_{22}\mid+\cdots+\mid a_{2n}\mid \\ &= \mid a_{n1}\mid+\mid a_{n2}\mid+\cdots+\mid a_{nn}\mid) \end{aligned} \qquad (A.8)$$

which means that:

$$SAVAE(kA)=\mid k\mid\quad SAVAE(A) \qquad (A.9)$$

3. Associativity with the addition operation

Let us consider 2 matrices A and B whose elements are a_{ij} and b_{ij} respectively. We could write:

$$\begin{aligned} SAVAE(A+B) &= \sum_{i=1}^{n}\mid a_{ij}+b_{ij}\mid \\ &\leq \sum_{i=1}^{n}\mid a_{ij}\mid\ \ \mid b_{ij}\mid \end{aligned} \qquad (A.10)$$

This is true because, in general:

$$\mid a_{ij}+b_{ij}\mid\ \leq\ \mid a_{ij}\mid+\mid b_{ij}\mid \qquad (A.11)$$

From (A.10) we deduce that:

$$SAVAE(A+B) \leq SAVAE(A) + SAVAE(B) \tag{A.12}$$

4. Associativity with the product operation

Using the two matrices A and B seen in the previous section, we write:

$$\begin{aligned} SAVAE(AB) &= \sum_{i,j=1}^{n} \mid \sum_{k=1}^{n} a_{ik} b_{kj} \mid \\ &\leq \sum_{i,j=1}^{n} \sum_{k=1}^{n} \mid a_{ik} b_{kj} \mid \end{aligned} \tag{A.13}$$

The last inequality is valid since the absolute value of the sum of two numbers is smaller or equal to the sum of the absolute values of these numbers. Going one step further, we could also take advantage of the fact that the absolute value of the product of two numbers is smaller or equal to the product of their absolute values:

$$SAVAE(AB) \leq \sum_{i,j,k=1}^{n} \mid a_{ik} \mid \ \mid b_{kj} \mid \tag{A.14}$$

On the other hand, by definition:

$$\begin{aligned} SAVAE(A) \cdot SAVAE(B) &= \sum_{i,j=1}^{n} \mid a_{ij} \mid \cdot \sum_{l,m=1}^{n} \mid b_{lm} \mid \\ &= \sum_{i,j,l,m=1}^{n} \mid a_{ij} \mid \ \mid b_{lm} \mid \end{aligned} \tag{A.15}$$

By examining the above expression we could subdivide it into two different positive sums:

$$SAVAE(A) \cdot SAVAE(B) = \sum_{i,j,k=1}^{n} \mid a_{ik} \mid \ \mid b_{kj} \mid + \sum_{i,j,l,m}^{j \neq l} \mid a_{ij} \mid \ \mid b_{lm} \mid \tag{A.16}$$

By comparing (A.14) to (A.16) we deduce:

$$SAVAE(AB) \leq SAVAE(A) \cdot SAVAE(B) \tag{A.17}$$

Conclusion

In view of the definition of the norm [61] it is concluded that the function called so far "SAVAE" is a norm defined on the set of real matrices. This norm will be called *"the b-norm"*:

$$\|A\|_b \equiv SAVAE(A) \tag{A.18}$$

A.3 B-norm of the Information Matrix

We can develop (3.45) which defines the (symmetric) information matrix I, using (3.46), (3.47), (3.41) and (3.49) and assuming that $t_0 = 0$ and $\lambda = 1$. The following expressions of the elements P_{ij} of the integrand matrix of I, are obtained:

$$\begin{aligned}
P_{11} &= \frac{Y_r^2}{[X_r^2 + Y_r^2][a + b(X_r^2 + Y_r^2)]} \\
P_{22} &= \frac{X_r^2}{[X_r^2 + Y_r^2][a + b(X_r^2 + Y_r^2)]} \\
P_{33} &= \frac{Y_r^2 t^2}{[X_r^2 + Y_r^2][a + b(X_r^2 + Y_r^2)]} \\
P_{44} &= \frac{X_r^2 t^2}{[X_r^2 + Y_r^2][a + b(X_r^2 + Y_r^2)]} \\
P_{55} &= \frac{Y_r^2 (e^{-t} + t - 1)^2}{[X_r^2 + Y_r^2][a + b(X_r^2 + Y_r^2)]} \\
P_{66} &= \frac{X_r^2 (e^{-t} + t - 1)^2}{[X_r^2 + Y_r^2][a + b(X_r^2 + Y_r^2)]} \\
P_{12} &= -\frac{X_r Y_r}{[X_r^2 + Y_r^2][a + b(X_r^2 + Y_r^2)]} \\
P_{13} &= \frac{Y_r^2 t}{[X_r^2 + Y_r^2][a + b(X_r^2 + Y_r^2)]}
\end{aligned}$$

$$
\begin{aligned}
P_{14} &= -\frac{X_r Y_r t}{[X_r^2+Y_r^2][a+b(X_r^2+Y_r^2)]} \\
P_{15} &= \frac{Y_r^2(e^{-t}+t-1)}{[X_r^2+Y_r^2][a+b(X_r^2+Y_r^2)]} \\
P_{16} &= \frac{-X_r Y_r(e^{-t}+t-1)}{[X_r^2+Y_r^2][a+b(X_r^2+Y_r^2)]} \\
P_{23} &= P_{14} \\
P_{24} &= \frac{X_r^2 t}{[X_r^2+Y_r^2][a+b(X_r^2+Y_r^2)]} \\
P_{25} &= -\frac{X_r Y_r(e^{-t}+t-1)}{[X_r^2+Y_r^2][a+b(X_r^2+Y_r^2)]} \\
P_{26} &= \frac{X_r^2(e^{-t}+t-1)}{[X_r^2+Y_r^2][a+b(X_r^2+Y_r^2)]} \\
P_{34} &= -\frac{X_r Y_r t^2}{[X_r^2+Y_r^2][a+b(X_r^2+Y_r^2)]} \\
P_{35} &= \frac{Y_r^2 t(e^{-t}+t-1)}{[X_r^2+Y_r^2][a+b(X_r^2+Y_r^2)]} \\
P_{36} &= -\frac{X_r Y_r t(e^{-t}+t-1)}{[X_r^2+Y_r^2][a+b(X_r^2+Y_r^2)]} \\
P_{45} &= P_{16} \\
P_{46} &= \frac{X_r^2 t(e^{-t}+t-1)}{[X_r^2+Y_r^2][a+b(X_r^2+Y_r^2)]} \\
P_{56} &= -\frac{X_r Y_r(e^{-t}+t-1)^2}{[X_r^2+Y_r^2][a+b(X_r^2+Y_r^2)]}
\end{aligned}
\tag{A.19}
$$

In order to calculate the b-norm of the information matrix integrand, we proceed to calculate the sums of the absolute values of its elements, one row at a time:

- Sum, S_1, of the absolute values of the first row:

$$S_1 = \frac{(Y_r^2 + \mid X_r Y_r \mid)(1 + t + \mid e^{-t} + t - 1 \mid)}{[X_r^2+Y_r^2][a+b(X_r^2+Y_r^2)]}$$

- Sum, S_2, of the absolute values of the second row:

$$S_2 = \frac{(X_r^2 + \mid X_r Y_r \mid)(1 + t + \mid e^{-t} + t - 1 \mid)}{[X_r^2+Y_r^2][a+b(X_r^2+Y_r^2)]}$$

- Sum, S_3, of the absolute values of the third row:

$$S_3 = \frac{t(Y_r^2 + \mid X_r Y_r \mid)(1 + t + \mid e^{-t} + t - 1 \mid)}{[X_r^2+Y_r^2][a+b(X_r^2+Y_r^2)]}$$

- Sum, S_4, of the absolute values of the fourth row:

$$S_4 = \frac{t(X_r^2 + \mid X_r Y_r \mid)(1 + t + \mid e^{-t} + t - 1 \mid)}{[X_r^2 + Y_r^2][a + b(X_r^2 + Y_r^2)]}$$

- Sum, S_5, of the absolute values of the fifth row:

$$S_5 = \frac{(Y_r^2 + \mid X_r Y_r \mid)(\mid e^{-t} + t - 1 \mid)(1 + t + \mid e^{-t} + t - 1 \mid)}{[X_r^2 + Y_r^2][a + b(X_r^2 + Y_r^2)]}$$

- Sum, S_6, of the absolute values of the sixth row:

$$S_6 = \frac{(X_r^2 + \mid X_r Y_r \mid)(\mid e^{-t} + t - 1 \mid)(1 + t + \mid e^{-t} + t - 1 \mid)}{[X_r^2 + Y_r^2][a + b(X_r^2 + Y_r^2)]}$$

The b-norm of the integrand of the information matrix is obtained by adding up the sums S_1 through S_6. Also, since the b-norm operation consists of the sums of absolute values, it is interchangeable with the integral operation. The b-norm of the information matrix is therefore the integral of the b-norm of the information matrix integrand:

$$J_I = \int_{t_0}^{t_f} \frac{(1 + \frac{2|X_r Y_r|}{R^2})(1 + t + \mid e^{-t} + t - 1 \mid)^2}{a + bR^2} dt \tag{A.20}$$

where: $R^2 = X_r^2 + Y_r^2$.

Appendix B

B.1 Calculation of the Transition Matrix

Given the filter dynamics matrix (4.34) where the target acceleration components are considered equal in the X and Y directions:

$$A = \begin{bmatrix} 0 & 0 & 1 & 0 & 0 & 0 \\ 0 & 0 & 0 & 1 & 0 & 0 \\ 0 & 0 & 0 & 0 & 1 & 0 \\ 0 & 0 & 0 & 0 & 0 & 1 \\ 0 & 0 & 0 & 0 & -\lambda & 0 \\ 0 & 0 & 0 & 0 & 0 & -\lambda \end{bmatrix} \tag{B.1}$$

It is proposed to calculate the filter transition matrix Φ by *back substitution* [83].

Let us consider the following simplified version of the filter model:

$$\dot{X}(t) = AX(t) \tag{B.2}$$

The solution to the system above is given by:

$$X(t) = \Phi(t, t_0)X_0 \tag{B.3}$$

where t_0 is the initial time and X_0 the initial state vector.

If we derive (B.3) and equate to (B.2), we get:

$$\dot{\Phi} = A\Phi \tag{B.4}$$

Let Φ_{ij} where $i, j = 1$ to 6 be the elements of Φ. Equation (B.4) allows us to write the following sets of equations:

$$\begin{array}{lll}
\dot{\Phi}_{11} = \Phi_{31} & \dot{\Phi}_{12} = \Phi_{32} & \dot{\Phi}_{16} = \Phi_{36} \\
\dot{\Phi}_{21} = \Phi_{41} & \dot{\Phi}_{22} = \Phi_{42} & \dot{\Phi}_{26} = \Phi_{46} \\
\dot{\Phi}_{31} = \Phi_{51} & \dot{\Phi}_{32} = \Phi_{52} & \dot{\Phi}_{36} = \Phi_{56} \\
\dot{\Phi}_{41} = \Phi_{61} & \dot{\Phi}_{42} = \Phi_{62} & \dot{\Phi}_{46} = \Phi_{66} \\
\dot{\Phi}_{51} = -\lambda\Phi_{51} & \dot{\Phi}_{52} = -\lambda\Phi_{52} & \dot{\Phi}_{56} = -\lambda\Phi_{56} \\
\dot{\Phi}_{61} = -\lambda\Phi_{61} & \dot{\Phi}_{62} = -\lambda\Phi_{62} & \dot{\Phi}_{66} = -\lambda\Phi_{66}
\end{array} \quad \cdots \tag{B.5}$$

Noting that one of the properties of a transition matrix is:

$$\Phi(t_0, t_0) = I_n \tag{B.6}$$

where I_n is the n-dimensional identity matrix (here $n = 6$), we could solve (B.5), starting with the last equation and working our way backwards.

$$\begin{aligned}
\dot{\Phi}_{66} &= -\lambda\Phi_{66} \Rightarrow \Phi_{66} = e^{-\lambda f_1} \equiv f_2 \\
\dot{\Phi}_{56} &= -\lambda\Phi_{56} \Rightarrow \Phi_{56} = 0 \\
\dot{\Phi}_{46} &= \Phi_{66} = e^{-\lambda\Delta t} \Rightarrow \Phi_{46} = \frac{1}{\lambda}(1 - f_2) \equiv f_3 \\
\dot{\Phi}_{36} &= \Phi_{56} = 0 \Rightarrow \Phi_{36} = 0 \\
\dot{\Phi}_{26} &= \Phi_{46} = f_3 \Rightarrow \Phi_{26} = \frac{1}{\lambda^2}(f_2 + \lambda f_1 - 1) \equiv f_4
\end{aligned} \tag{B.7}$$

where

$$f_1 = t_{k+1} - t_k$$

$$\Delta t = t_{k+1} - \tau$$

and τ is the integration variable.

If we continue solving (B.5) backwards, we finally get:

$$\Phi(t_{k+1}, t_k) = \begin{bmatrix} 1 & 0 & f_1 & 0 & f_4 & 0 \\ 0 & 1 & 0 & f_1 & 0 & f_4 \\ 0 & 0 & 1 & 0 & f_3 & 0 \\ 0 & 0 & 0 & 1 & 0 & f_3 \\ 0 & 0 & 0 & 0 & f_2 & 0 \\ 0 & 0 & 0 & 0 & 0 & f_2 \end{bmatrix} \tag{B.8}$$

where f_1, f_2, f_3 and f_4 are defined in (B.7).

B.2 Calculation of the Matrix Γ

The matrix Γ is defined in (4.11) as:

$$\Gamma(k+1, k) = \int_k^{k+1} \Phi(t_{k+1}, \tau) B(\tau) d\tau \tag{B.9}$$

where the transition matrix is defined by (B.8), and the input matrix is given by:

$$B = \begin{bmatrix} 0 & 0 \\ 0 & 0 \\ -1 & 0 \\ 0 & -1 \\ 0 & 0 \\ 0 & 0 \end{bmatrix} \tag{B.10}$$

Multiplying the transition matrix (B.8) by the input matrix, we get:

$$\Phi(t_{k+1},\tau)\cdot B = \begin{bmatrix} -(t_{k+1}-\tau) & 0 \\ 0 & -(t_{k+1}-\tau) \\ -1 & 0 \\ 0 & -1 \\ 0 & 0 \\ 0 & 0 \end{bmatrix} \tag{B.11}$$

The problem of finding Γ amounts, hence, to the problem of integrating the term $(t_{k+1}-\tau)$ between times t_k and t_{k+1}:

$$\int_{t_k}^{t_{k+1}} -(t_{k+1}-\tau)d\tau = -\frac{(t_{k+1}-t_k)^2}{2} \tag{B.12}$$

Γ could then be written as:

$$\Gamma = \begin{bmatrix} -\frac{(t_{k+1}-t_k)^2}{2} & 0 \\ 0 & -\frac{(t_{k+1}-t_k)^2}{2} \\ t_k - t_{k+1} & 0 \\ 0 & t_k - t_{k+1} \\ 0 & 0 \\ 0 & 0 \end{bmatrix} \tag{B.13}$$

B.3 Models Equivalence

In attempting to find the conditions under which the guidance model (2.1) is equivalent to the Kalman filter model (4.32), one first step is to realise that the target acceleration components in the guidance model are null. And since we are considering that the noise is only present in the measurements, we could write the solutions to the two differential equations of the target accelerations as:

$$A_{T_X} = A_{T_{X_0}} e^{-\lambda t}$$

$$A_{T_Y} = A_{T_{Y0}} e^{-\lambda t}$$

In order to guarantee zero acceleration components over all the time of the engagement, it is necessary to take:

$$A_{T_{X0}} = 0$$
$$A_{T_{Y0}} = 0$$

These conditions simplify the differential equations of the velocity components in the filter model. If we, then, equate those equations with their counterparts derived from the guidance model by taking the derivatives of the positions differential equations, we get:

$$A_{M_X} = -A_n cos\theta$$
$$A_{M_Y} = A_n sin\theta$$

Note that these two equations could be obtained directly through geometric considerations.

Finally if we integrate and equate the relative accelerations and relative speeds components respectively, we deduce the remaining initial conditions to be satisfied, namely:

$\dot{X}_r^g = \dot{X}_r^f$ if $U_r^g(0) = U_r^f(0)$ and
$\dot{Y}_r^g = \dot{Y}_r^f$ if $V_r^g(0) = V_r^f(0)$

This can be interpreted as:

$$U_r^f(0) = V_T cos\phi - V_M cos\theta_0$$
$$V_r^f(0) = V_T sin\phi - V_M sin\theta_0$$

In a similar fashion, it is possible to write:

$X_r^g = X_r^f$ if $X_r^g(0) = X_r^f(0)$ and
$Y_r^g = Y_r^f$ if $Y_r^g(0) = Y_r^f(0)$

These are the equations to be satisfied, in order for the guidance and filter models to be equivalent.

Appendix C

C.1 Solution of the LQGL Problem

Let us assume first that the matrix P could be written as follows:

$$P = \begin{bmatrix} P_1 & P_2 & P_3 \\ P_4 & P_5 & P_6 \\ P_7 & P_8 & P_9 \end{bmatrix} \tag{C.1}$$

As a result, equation (5.22) could be developed in terms of the nine elements of P, taking into consideration that $Q = 0$. If the following coordinate transformation is adopted:

$$\tau = t_f - t \tag{C.2}$$

we obtain the following nine differential equations along with their initial conditions:

$$\dot{P}_1 = \quad 0 \qquad P_1(0) = \frac{c}{2} \tag{C.3}$$

$$\dot{P}_2 = \quad 0 \qquad P_2(0) = 0 \tag{C.4}$$

$$\dot{P}_3 = \quad 0 \qquad P_3(0) = 0 \tag{C.5}$$

$$\dot{P}_4 = \quad P_1 \qquad P_4(0) = 0 \tag{C.6}$$

$$\dot{P}_5 = \quad P_2 \qquad P_5(0) = 0 \tag{C.7}$$

$$\dot{P}_6 = P_3 \qquad P_6(0) = 0 \tag{C.8}$$

$$\dot{P}_7 = P_4 - \lambda P_7 \qquad P_7(0) = 0 \tag{C.9}$$

$$\dot{P}_8 = P_5 - \lambda P_8 \qquad P_8(0) = 0 \tag{C.10}$$

$$\dot{P}_9 = P_6 - \lambda P_9 \qquad P_9(0) = 0 \tag{C.11}$$

By simple examination, we could easily obtain the solutions to most of the above equations. The differential equation in P_7 has probably the only non-trivial solution. This equation could be written under the form:

$$\frac{dy}{dx} + f(x)y = g(x) \tag{C.12}$$

the solution of which could be given by [87]:

$$y = e^{-\int f dx}\left(\int g e^{\int f dx} dx + k\right) \tag{C.13}$$

where k is the integration constant.

Solving for P_7, we can write the matrix P as:

$$P = \begin{bmatrix} \frac{c}{2} & 0 & 0 \\ \frac{c\tau}{2} & 0 & 0 \\ \frac{c}{2\lambda^2}(e^{-\lambda\tau} + \lambda\tau - 1) & 0 & 0 \end{bmatrix} \tag{C.14}$$

On the other hand, if we let the matrix L be equal to:

$$L = \begin{bmatrix} L_1 & L_2 & L_3 \\ L_4 & L_5 & L_6 \\ L_7 & L_8 & L_9 \end{bmatrix} \tag{C.15}$$

since the elements of P are available, it is possible to develop the differential equation (5.23) at the element level. If, in addition, we adopt the coordinate transformation defined by (C.2) we could write:

$$\dot{L}_1 = -L_4 \qquad L_1(0) = 1 \tag{C.16}$$

$$\dot{L}_2 = -L_5 \qquad L_2(0) = 0 \tag{C.17}$$

$$\dot{L}_3 = -L_6 \qquad L_3(0) = 0 \tag{C.18}$$

$$\dot{L}_4 = c\tau - L_7 \qquad L_4(0) = 0 \tag{C.19}$$

$$\dot{L}_5 = -L_8 \qquad L_5(0) = 1 \tag{C.20}$$

$$\dot{L}_6 = -L_9 \qquad L_6(0) = 0 \tag{C.21}$$

$$\dot{L}_7 = \lambda L_7 \qquad L_7(0) = 0 \tag{C.22}$$

$$\dot{L}_8 = \lambda L_8 \qquad L_8(0) = 0 \tag{C.23}$$

$$\dot{L}_9 = \lambda L_9 \qquad L_9(0) = 1 \tag{C.24}$$

We could readily solve the above equations backwards to obtain:

$$L = \begin{bmatrix} 1 - \frac{c\tau^3}{6} & -\tau & \frac{1}{\lambda^2}(e^{\lambda\tau} - \lambda\tau - 1) \\ \frac{c\tau^2}{2} & 1 & \frac{1}{\lambda}(1 - e^{\lambda\tau}) \\ 0 & 0 & e^{\lambda\tau} \end{bmatrix} \tag{C.25}$$

The inverse of the matrix L could then be obtained in closed form. In addition, due to the form of B_s (5.13) and P (C.1), only the first row of the inverse of L^{-1} is needed:

$$\{L^{-1}\}_1 = \frac{3}{3 + c\tau^3} \tag{C.26}$$

$$\{L^{-1}\}_2 = \frac{3\tau}{3 + c\tau^3} \tag{C.27}$$

$$\{L^{-1}\}_3 = \frac{3(e^{-\lambda\tau} + \lambda\tau - 1)}{\lambda^2(3 + c\tau^3)} \tag{C.28}$$

At this stage, (5.24) could simply be deduced from (5.18), given (5.21), (C.1) and the needed elements of L^{-1}.

C.2 Solution of the DCGL Problem

As suggested in section 5.2.3, the solution to this problem follows the same procedure carried out to solve the LQGL problem. the only difference is that, in this case, the expression of Q is not null. We first simplify the performance index (5.37) by the factor of $\frac{1}{2}$ which figures in all its elements. We then designate the elements of the matrices P and L in (5.22) and (5.23) as in (C.1) and (C.15) respectively. Applying, subsequently equation (5.22) and the coordinate transformation (C.2) we obtain the following:

$$\dot{P}_1 = -\omega L_1 \qquad P_1(0) = c \tag{C.29}$$

$$\dot{P}_2 = -\omega L_2 \qquad P_2(0) = 0 \tag{C.30}$$

$$\dot{P}_3 = -\omega L_3 \qquad P_3(0) = 0 \tag{C.31}$$

$$\dot{P}_4 = P_1 \qquad P_4(0) = 0 \tag{C.32}$$

$$\dot{P}_5 = P_2 \qquad P_5(0) = 0 \tag{C.33}$$

$$\dot{P}_6 = P_3 \qquad P_6(0) = 0 \tag{C.34}$$

$$\dot{P}_7 = P_4 - \lambda P_7 \qquad P_7(0) = 0 \tag{C.35}$$

$$\dot{P}_8 = P_5 - \lambda P_8 \qquad P_8(0) = 0 \tag{C.36}$$

$$\dot{P}_9 = P_6 - \lambda P_9 \qquad P_9(0) = 0 \tag{C.37}$$

On the other hand, if we apply (5.23) we get:

$$\dot{L}_1 = -L_4 \qquad L_1(0) = 1 \tag{C.38}$$

$$\dot{L}_2 = -L_5 \qquad L_2(0) = 0 \tag{C.39}$$

$$\dot{L}_3 = -L_6 \qquad L_3(0) = 0 \tag{C.40}$$

$$\dot{L}_4 = -L_7 + P_4 \qquad L_4(0) = 0 \tag{C.41}$$

$$\dot{L}_5 = -L_8 + P_5 \qquad L_5(0) = 1 \tag{C.42}$$

$$\dot{L}_6 = -L_9 + P_6 \qquad L_6(0) = 0 \tag{C.43}$$

$$\dot{L}_7 = \lambda L_7 \qquad L_7(0) = 0 \tag{C.44}$$

$$\dot{L}_8 = \lambda L_8 \qquad L_8(0) = 0 \tag{C.45}$$

$$\dot{L}_9 = \lambda L_9 \qquad L_9(0) = 1 \tag{C.46}$$

The solution to the above equations is presented in [40] and worked out here in more details:

First, we solve equations (C.44), (C.45) and (C.46):

$$L_7 = 0 \tag{C.47}$$

$$L_8 = 0 \tag{C.48}$$

$$L_9 = e^{\lambda\tau} \tag{C.49}$$

Next, we manipulate equations (C.40), (C.43), (C.31) and (C.34). From (C.40) and (C.43) we write:

$$\ddot{L}_3 = L_9 - P_6 \tag{C.50}$$

On the other hand, equations (C.31) and (C.34) imply:

$$\ddot{P}_6 = -\omega L_3 \tag{C.51}$$

Combining (C.50), (C.51) and (C.49), we obtain the following differential equation:

$$L_3^{(4)} - \omega L_3 = \ddot{L}_9 = \lambda^2 e^{\lambda\tau} \tag{C.52}$$

The solution to this equation could be separated into a homogeneous solution and a particular one. The solution to the homogeneous equation has the following form:

$$L_3 = ae^{\alpha\tau} \tag{C.53}$$

where a and α are integration constants.

It could readily be shown that the constant α can take 4 different forms: $\alpha = \omega^{\frac{1}{4}}$, $\alpha = -\omega^{\frac{1}{4}}$, $\alpha = j\omega^{\frac{1}{4}}$, $\alpha = -j\omega^{\frac{1}{4}}$, where $j^2 = -1$. If on the other hand we seek a particular solution of the form:

$$L_3 = \beta e^{\lambda\tau} \tag{C.54}$$

the value of the constant β could be easily derived. Combining the homogeneous and particular solutions, we can finally write:

$$L_3 = a_1 e^{k\tau} + a_2 e^{-k\tau} + b_1 cos(k\tau) + b_2 sin(k\tau) + \beta e^{\lambda\tau} \tag{C.55}$$

where $k = \omega^{\frac{1}{4}}$, $\beta = \frac{\lambda^2}{\lambda^4 - \omega}$.

The expressions of the constants a_1, a_2, b_1, and b_2 as well as the solutions to equations (C.43), (C.34), and (C.31) could be obtained by using the expression of (C.55) in those equations and solving the initial conditions of the 4 resulting equations simultaneously.

On the other hand, equations (C.38), (C.41), (C.29) and (C.32) could be manipulated in a similar fashion to the way equations (C.40), (C.43), (C.31) and (C.34) were handled. The same is also true for equations (C.39), (C.42), (C.30) and (C.33), respectively. The only remaining needed expression is that of P_6. It is obtained from equation (C.34) by simple integration. Following is a list of all the needed elements of P:

$$P_4 = \frac{c_1}{k} e^{k\tau} - \frac{c_2}{k} e^{-k\tau} - \frac{d_2}{k} cos(k\tau) + \frac{d_1}{k} sin(k\tau) \tag{C.56}$$

$$P_5 = -e_1 k^2 e^{k\tau} - e_2 k^2 e^{-k\tau} + f k^2 sin(k\tau) \tag{C.57}$$

$$P_6 = -a_1 k^2 e^{k\tau} - a_2 k^2 e^{-k\tau} + b_1 k^2 cos(k\tau) + b_2 k^2 sin(k\tau) - \frac{w}{\lambda^2} \beta e^{\lambda\tau} \tag{C.58}$$

and here is a list of all the elements of L:

$$L_1 = -\frac{c_1}{k^3}e^{k\tau} + \frac{c_2}{k^3}e^{-k\tau} - \frac{d_2}{k^3}cos(k\tau) + \frac{d_1}{k^3}sin(k\tau) \quad (C.59)$$

$$L_2 = e_1e^{k\tau} + e_2e^{-k\tau} + fsin(k\tau) \quad (C.60)$$

$$L_3 = a_1e^{k\tau} + a_2e^{-k\tau} + b_1cos(k\tau) + b_2sin(k\tau) + \beta e^{\lambda\tau} \quad (C.61)$$

$$L_4 = \frac{c_1}{k^2}e^{k\tau} + \frac{c_2}{k^2}e^{-k\tau} - \frac{d_1}{k^2}cos(k\tau) - \frac{d_2}{k^2}sin(k\tau) \quad (C.62)$$

$$L_5 = -e_1ke^{k\tau} + e_2ke^{-k\tau} - fkcos(k\tau) \quad (C.63)$$

$$L_6 = -a_1ke^{k\tau} + a_2ke^{-k\tau} + b_1ksin(k\tau) - b_2kcos(k\tau) - \lambda\beta e^{\lambda\tau} \quad (C.64)$$

$$L_7 = 0 \quad (C.65)$$

$$L_8 = 0 \quad (C.66)$$

$$L_9 = e^{\lambda\tau} \quad (C.67)$$

The coefficients of the above equations are as follows:

$$k = \omega^{\frac{1}{4}} \quad (C.68)$$

$$\beta = \frac{\lambda^2}{\lambda^4 - \omega} \quad (C.69)$$

$$a_1 = -\frac{(\lambda + k)(\lambda^2 + k^2)}{4k(\lambda^4 - \omega)} \quad (C.70)$$

$$a_2 = -\frac{(\lambda - k)(\lambda^2 + k^2)}{4k(\lambda^4 - \omega)} \quad (C.71)$$

$$b_1 = \frac{\omega^{\frac{1}{2}} - \lambda^2}{2(\lambda^4 - \omega)} \quad (C.72)$$

$$b_2 = -\frac{\lambda(\omega - \lambda^2k^2)}{2k^3(\lambda^4 - \omega)} \quad (C.73)$$

$$c_1 = \frac{1}{4}(c - \frac{\omega}{k}) \quad (C.74)$$

$$c_2 = \frac{1}{4}(c + \frac{\omega}{k}) \quad (C.75)$$

$$d_1 = \frac{c}{2} \quad (C.76)$$

$$d_2 = -\frac{\omega}{2k} \quad (C.77)$$

$$f = -\frac{1}{2k} \quad (C.78)$$

$$e_1 = -\frac{1}{4k} \quad (C.79)$$

$$e_2 = \frac{1}{4k} \quad (C.80)$$

Bibliography

[1] F. Adler. Missile guidance by three dimensional proportional navigation. *Journal of Applied Physics*, 27:500–507, May 1956.

[2] Vincent J. Aidala. Kalman filter behavior in bearings-only tracking applications. *IEEE Transactions on Aerospace and Electronic Systems*, AES-15(1):29–39, January 1979.

[3] Vincent J. Aidala and Sherry E. Hammel. Utilization of modified polar coordinates for bearings-only tracking. *IEEE Transactions on Automatic Control*, AC-28(3):283–294, March 1983.

[4] Vincent J. Aidala and Steven C. Nardone. Biased estimation properties of the pseudolinear tracking filter. *IEEE Transactions on Aerospace and Electronic Systems*, AES-18(4):432–441, July 1982.

[5] G.M. Anderson. A near optimal closed-loop solution method for nonsingular zero-sum differential games. *Journal of Optimisation Theory and Applications*, 13(3):303–318, 1974.

[6] A Aoki. *Optimisation of Stochastic Systems.* Academic Press, New York, 1967.

[7] Karl J. Åström and Björn Wittenmark. *Computer Controlled Systems Theory and Design.* Prentice Hall, Inc., Englewood Cliffs, N.J., 2nd edition, 1990.

[8] S. N. Balakrishnan and J. L. Speyer. Assumed density filter with application to homing missile guidance. *Journal of Guidance*, 12(1):4–12, January-February 1989.

[9] S. N. Balakrishnan and Jason L. Speyer. Coordinate transformation-based filter for improved target tracking. *Journal of Guidance*, 9(6):704–709, November-December 1986.

[10] Y. Bar-Shalom and E. Tse. Dual effect, certainty equivalence, and separation in stochastic control. *IEEE Transactions on Automatic Control*, AC-19:494–500, Oct 1974.

[11] Y. Bar-Shalom and E. Tse. Adaptive dual control for stochastic non-linear systems with free end time. *IEEE Transactions on Automatic Control*, AC-20:670–675, Oct 1975.

[12] Richard Bellman. *Dynamic Programming.* Inoizdat, 1960.

[13] Richard Bellman. *Adaptive Control Processes: A Guided Tour.* Princeton University Press, Princeton, New Jersey, 1961.

[14] S. M. Brainin. Optimal biased proportional navigation. *IEEE Transactions on Automatic Control*, pages 440–442, August 1968.

[15] Robert G. Brown and Patrick Y. Hwang. *Introduction to Random Signals and Applied Kalman Filtering.* John Wiley, New York, 2nd edition, 1992.

[16] Arthur E. Bryson and Yu-Chi Ho. *Applied Optimal Control.* Ginn and Company, Waltham, Massachussets, 1969.

[17] Richard James Casler Jr. Dual control guidance strategy for homing interception taking angle-only measurements. *Journal of Guidance and Control*, 1(1):63–70, Jan-Feb 1978.

[18] C.S. Chang. A terminal guidance theory using dynamic programming formulation. *Proceedings of the AIAA Guidance and Control Conference*, pages 912–916, May 1970.

[19] Walter F. Denham and Samuel Pines. Sequential estimation when measurement function nonlinearity is comparable to measurement error. *AIAA Journal*, 4(6):1071–1076, June 1966.

[20] J.L. Doob. *Stochastic Processes.* Wiley, New York, 1953.

[21] Svein Fagerlund. Target tracking based on bearing only measurements. Technical Report LIDS-R-1003, Massachussetts Institute of Technology, Cambridge, MA, June 1980.

[22] A. Feldbaum. *Optimal Control Systems*, volume 22 of *Mathematics in Science and Engineering.* Academic Press, 1965. Translated by A. Kraiman.

[23] I. Forte and J. Shinar. Improved guidance law design based on the mixed-strategy concept. *Journal of Guidance*, 12(5):739–745, September-October 1989. Technion-Israel Institute of Technology, Haifa, Israel.

[24] Bernard Friedland. *Control System Design, An Introduction to State Space Methods.* McGraw-Hill Book Company, Sydney, 1986.

[25] Bernard Friedland. *Control System Design - An Introduction to State- Space Methods.* McGraw-Hill Book Company, 1987.

[26] Peggy J. Galkowski and Mohammed A. Islam. An alternative derivation of the modified gain function of Song and Speyer. *IEEE Transactions on Automatic Control*, 36(11):1323–1326, November 1991.

[27] M. Guelman. A qualitative study of proportional navigation. *IEEE Transactions on Aerospace and Electronic Systems*, pages 337–343, July 1971.

[28] Mauricio Guelman. Proportional navigation with a maneuvering target. *IEEE Transactions on Aerospace and Electronic Systems*, AES-8(3):364–371, May 1972.

[29] Mauricio Guelman. The closed-form solution of true proportional navigation. *IEEE Transactions on Aerospace and Electronic Systems*, AES-12(4):472–482, July 1976.

[30] S. E. Hammel and V. J. Aidala. Observability requirements for three-dimensional tracking via angle measurements. *IEEE Transactions on Aerospace and Electronic Systems*, AES-21:200–207, March 1985.

[31] G. E. Hassoun and C. C. Lim. Maximum information guidance in bearing-only-measurement systems. Technical Report CTRL 94-1, The University of Adelaide, Dpt. of Electrical and Electronic Engineering, March 1994.

[32] G. E. Hassoun and C. C. Lim. Observable proportional navigation for homing missiles with bearing-only-measurements. Technical Report CTRL 94-3, The University of Adelaide, Dpt. of Electrical and Electronic Engineering, August 1994.

[33] George E. Hassoun and Cheng Chew Lim. Maximum information and measurement modifiability in homing missile guidance. In 20^{th} *TTCP WTP-5 Symposium*, DSTO, Salisbury, April 1992.

[34] George E. Hassoun and Cheng Chew Lim. A study of the extended kalman filter performance in bearing-only-measurement problems. In *TTCP WTP-5 Meeting*, DSTO, Salisbury, June 1993.

[35] George E. Hassoun and Cheng Chew Lim. Advanced guidance control system design for homing missiles with bearing-only-measurements. In *IEEE International Conference on Industrial Technology*, Guangzhou, China, December 1994.

[36] Stephan A. R. Hepner and Hans P. Geering. Observability analysis for target maneuver estimation via bearing-only and bearing-rate-only measurements. *Journal of Guidance*, 13(6):977–983, Nov-Dec 1990.

[37] D.G. Hill, P.C. Kite, and J.L. Speyer. New target models for homing missile guidance. *Proceedings of the AIAA Guidance and Control Conference*, pages 22–29, 1983.

[38] Y. C. Ho, A. E. Bryson, and S. Baron. Differential games and optimal pursuit-evasion strategies. *IEEE Transactions on Automatic Control*, AC-10(4):385–389, October 1965.

[39] D. G. Hull, J. L. Speyer, and D. B. Burris. A linear-quadratic guidance law for dual control of homing missiles. Technical Report 87-2381, American Institute

of Aeronautics and Astronautics, Inc., Department of Aerospace Engineering and Engineering Mechanics, University of Texas, Austin, Texas, 1987.

[40] D. G. Hull, J. L. Speyer, and D. B. Burris. Linear-quadratic guidance law for dual control of homing missiles. *Journal of Guidance*, 13(1):137–144, Jan-Feb 1990.

[41] D. G. Hull, J. L. Speyer, and C. Y. Tseng. Maximum information guidance for homing missiles. *Journal of Guidance*, 8(4):494–497, July-August 1985.

[42] T. L. Gunckel II and Gene F. Franklin. A general solution for linear sampled data control. *Transactions of the ASME, Journal of Basic Engineering*, 85D:197–203, June 1963.

[43] Fumiako Imado and Susumu Miwa. Fighter evasive maneuvers against proportional navigation missile. *Journal of Aircraft*, 23(11):825–830, November 1986.

[44] Andrew H. Jazwinski. *Stochastic Processes and Filtering Theory.* Academic Press, New York, NY, 1970.

[45] L. S. Jennings, M. E. Fisher, K. L. Teo, and C. G Goh. *MISER3 Optimal Control Software.* version 1.0. EMCOSS Pty Ltd, Carine, WA, 1990.

[46] P. D. Joseph and J. T. Tou. On linear control theory. *Transactions of the AIEE*, Volume 80, pt. 2(3):193–196, September 1961.

[47] R. E. Kalman. Contributions to the theory of optimal control. *Bol. Soc. Mat. Mexicana 5*, pages 102-119, 1960.

[48] R. E. Kalman. A new approach to linear filtering and prediction problems. *Transactions of the ASME, Journal of Basic Engineering*, 82D(1):35–45, March 1960.

[49] R. E. Kalman. On the general theory of control systems. *Proc. IFAC Congress, 1st*, pages 481–491, 1961.

[50] R. E. Kalman and R. S. Bucy. New results in linear filtering and prediction theory. *Transactions of the ASME, Journal of Basic Engineering*, pages 95–108, March 1961. Series 83D.

[51] Ching-Fang Lin. *Modern Navigation Guidance and Control Processing*, volume 2 of *Advanced Navigation, Guidance and Control*. Prentice Hall, Englewood Cliffs, New Jersey, 1991.

[52] Ching-Fang Lin and Marc W. Shafroth. A missile control strategy for maneuvering targets. In *American Control Conference*, pages 1084–1089, San Francisco, June 1983.

[53] Allen G. Lindgren and Kai F. Gong. Position and velocity estimation via bearing observations. *IEEE Transactions on Aerospace and Electronic Systems*, AES-14(4):564–577, July 1978.

[54] Raman K. Mehra. A comparison of several nonlinear filters for reentry vehicle tracking. *IEEE Transactions on Automatic Control*, AC-16(4):307–319, August 1971.

[55] Raman K. Mehra. Optimal input signals for parameter estimation in dynamic systems - survey and new results. *IEEE Transactions on Automatic Control*, AC-19(6):753–768, December 1974.

[56] D. Middleton. *An Introduction to Statistical Communication Theory*. McGraw-Hill Book Company, New York, 1960.

[57] Stephen A. Murtaugh and Harry E. Criel. Fundamentals of proportional navigation. *IEEE Spectrum*, pages 75–85, December 1966.

[58] Steven C. Nardone and Vincent J. Aidala. Observability criteria for bearings-only target motion analysis. *IEEE Transactions on Aerospace and Electronic Systems*, AES-17(2):162–166, March 1981.

[59] F. W. Nesline. Missile guidance for low altitude air defense. *Journal of Guidance and Control*, pages 283–289, July-August 1979.

[60] H.E. Newell. Guided missile kinematics. Technical Report R-2538, Naval Research Laboratory, Washington, D.C., May 1945.

[61] Ben Noble. *Applied Linear Algebra.* Prentice Hall, Inc., Englewood Cliffs, New Jersey, 1969.

[62] H.L. Pastrick, S.M. Seltzer, and M.E. Warren. Guidance laws for short range tactical missiles. *Journal of Guidance and Control*, 4(2):98–108, January 1979.

[63] Anthony N. Payne. The observability problem for the bearings-only tracking. Technical Report UCRL–91435, Lawrence Livermore National Laboratory, University of California, Livermore, California, August 1987.

[64] Anthony N. Payne. Observability conditions for angles-only tracking. Technical Report UCRL–99979 and DE89 004045, Lawrence Livermore National Laboratory, University of California, Livermore, California, 1989.

[65] C. Pfeiffer. A successive approximation technique for constructing a near-optimum guidance law. In *International Astronautical Conference, Astrodynamics, Guidance and Control, Miscellanea*, pages 285–291, 1967.

[66] R.A. Poulter and G.M. Anderson. A guidance concept for air-to-air missiles based on nonlinear differential game theory. In *National Aerospace Electronics Conference*, pages 605–609, 1976.

[67] Allen E. Puckett and Simon Ramo, editors. *Guided Missile Engineering.* McGraw-Hill Book Company, Inc., 1959.

[68] V.S. Pugachev. *Theory of Random Functions and its Application to Automatic Control Problems.* Fizmatgiz, 1960.

[69] Sanford M. Roberts and Jerome S. Shipman. *Two-Point Boundary Value Problems: Shooting Methods*, volume 31 of *Modern Analytic and Computational Methods in Science and Mathematics.* American Elsevier Publishing Company, Inc., New York, 1972.

[70] Ilan Rusnak. Guidance law based on an exponential cost criterion for high order missile and maneuvering target. In *American Control Conference*, pages 2386–2390, 1992.

[71] Ilan Rusnak and Levi Meir. Optimal guidance for high-order and acceleration constrained missile. *Journal of Guidance*, 14(3):589–596, May-June 1991.

[72] M. G. Safonov and M. Athans. Robustness and computational aspects of nonlinear stochastic estimators and regulators. *IEEE Transactions on Automatic Control*, AC-23, August 1978.

[73] L. Schwartz and E. Steer. A computation comparison of several nonlinear filters. *IEEE Transactions on Automatic Control*, pages 83–86, February 1968.

[74] H. A. Simon. Dynamic programming under uncertainty with a quadratic criterion function. *Econometrica*, 24:74–81, 1956.

[75] Robert A. Singer. Estimating optimal tracking filter performance for manned maneuvering targets. *IEEE Transactions on Aerospace and Electronic Systems*, AES-6(4):473–483, July 1970.

[76] Taec L. Song and Jason L. Speyer. A stochastic analysis of a modified gain extended Kalman filter with applications to estimation with bearings only measurements. *IEEE Transactions on Automatic Control*, AC-30(10):940 – 949, October 1985.

[77] H. W. Sorenson. Least-squares estimation: From Gauss to Kalman. *IEEE Spectrum*, pages 63–68, July 1970.

[78] Harold W. Sorenson, editor. *Kalman Filtering - Theory and Application.* IEEE PRESS, New York, NY, 1985.

[79] J. L. Speyer and Y. Hahn. Asymptotic series solutions to a class of stochastic dual control problems. In *American Control Conference*, pages 164–169, Atlanta, June 1988.

[80] J. L. Speyer, D. G. Hull, C. Y. Tseng, and S. W. Larson. Estimation enhancement by trajectory modulation for homing missiles. *Journal of Guidance*, 7(2):167 - 174, March-April 1984.

[81] J. L. Speyer and T. L. Song. A comparison between pseudomeasurement and extended Kalman observers. *20th IEEE Conference on Decision and Control*, Dec 1981.

[82] Jason L. Speyer, William M. Greenwell, and David G. Hull. Adaptive noise estimation and guidance for homing missiles. In *Proceedings of the AIAA Guidance and Control Conference*, pages 48–56, 1982.

[83] Jason L. Speyer, David F. Hull, and William P. Bernard. Performance of the modified-gain extended Kalman filter along an enhanced information path of a homing missile. In *Proceedings of the AIAA Guidance and Control Conference*, Williamsburg, Virginia, August 1986.

[84] Jason L. Speyer and David G. Hull, editors. *Comparison of Several Extended Kalman Filter Formulations for Homing Missile Guidance*, Danvers, Mass., August 1980. Proceedings of the AIAA Guidance and Control Conference.

[85] Jason L. Speyer and David G. Hull. Advanced guidance algorithms for homing missiles with bearings-only measurements. Technical Report AFOSR-TR-87-1962, The University of Texas at Austin, November 1987. Final Technical Report, Grant AFOSR-84-0371.

[86] Jayson L. Speyer, Kevin D. Kim, and Minjea Tahk. Passive homing missile guidance law based on new target maneuver model. *Journal of Guidance*, 13(5):803–812, Sept-Oct 1990.

[87] Murray R. Spiegel. *Mathematical Handbook*. Schaum's Outline Series In Mathematics. McGraw-Hill Book Company, 1968.

[88] H. Spits. Partial navigation courses for a guided missile attacking a constant velocity target. Technical Report R-2790, Naval Research Laboratory, Washington, D.C., March 1946.

[89] A.R. Stubberud. Theory of pitch steering for ascent guidance. In *National Space Navigation Meeting*, pages 136–160, March 1967.

[90] T. J. Tarn and Y. Rasis. Observers for nonlinear stochastic systems. *IEEE Transactions on Automatic Control*, AC-21, August 1976.

[91] Robert R. Tenney, Ralph S. Hebbert, and Nils R. Sandell. A tracking filter for maneuvering sources. *IEEE Transactions on Automatic Control*, AC-22(4):246–251, April 1977.

[92] K. L. Teo, C. G. Goh, and K. H. Wong. *A Unified Computational Approach for Optimal Control Problems.* Longman Scientific and Technical, 1991.

[93] Thomas L. Ting. On developing a robust missile guidance algorithm. In *American Control Conference*, pages 2380–2385, 1992.

[94] E. Tse and Y. Bar-Shalom. An actively adaptive control for linear systems with random parameters via the dual control approach. *IEEE Transactions on Automatic Control*, AC-18(2):109–117, April 1973.

[95] Edison Tse, Yaakov Bar-Shalom, and III Lewis Meier. Wide-sense adaptive dual control for nonlinear stochastic systems. *IEEE Transactions on Automatic Control*, AC-18(2):98–106, April 1973.

[96] Ching-Yeh Tseng. *A Study of Maximum Infomation Trajectories for Homing Missile Guidance.* PhD thesis, University of Texas at Austin, 1983.

[97] J.H.J.M. Vriends. *Systems and Control Encyclopedia*, volume 5, chapter Missile Guidance and Control, pages 3006–3012. Pergamon Press, Oxford, Great Britain, 1987.

[98] H. Weiss and J. B. Moore. Improved extended Kalman filter for passive tracking. *IEEE Transactions on Automatic Control*, AC-25(4):807–811, August 1980.

[99] W. M. Wonham. On the separation theorem of stochastic control. *SIAM Journal on Control*, 6(2):312–326, 1968.

[100] Ciann-Dong Yang, F. B. Hsiao, and Fang-Bo Yeh. Generalised guidance law for homing missiles. *IEEE Transactions on Aerospace and Electronic Systems*, AES-25(2):197–211, March 1989.

[101] Ciann-Dong Yang and Fang-Bo Yeh. Closed form solution for a class of guidance laws. *Journal of Guidance*, 10(4):412–415, July-August 1987.

[102] Ciann-Dong Yang, Fang-Bo Yeh, and Jen-Heng Chen. The closed form solution of generalised proportional navigation. *Journal of Guidance*, 10(2):216–218, March-April 1987.

[103] Pin-Jar Yuan and Jeng-Shing Chern. Analytic study of biased proportional navigation. *Journal of Guidance*, 15(1):185–190, Jan-Feb 1992.

[104] Pin-Jar Yuan and Jeng-Shing Chern. Solutions of true proportional navigation for maneuvering and nonmaneuvering targets. *Journal of Guidance*, 15(1):268–271, Jan-Feb 1992.

[105] Paul Zarchan. *Tactical and Strategic Missile Guidance*, volume 124 of *AIAA Tactical Missile*. Progress in Astronautics and Aeronautics, 1990.